



Measuring the Anomalous Magnetic Moment of the Muon

Joseph Price, University of Liverpool
On Behalf of the Muon $g-2$ Collaboration
PASCOS, Manchester UK
July 3rd, 2019



UNIVERSITY OF
LIVERPOOL

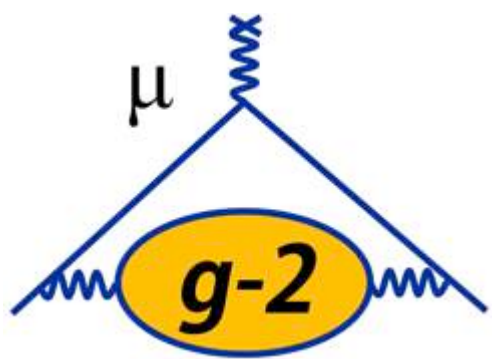


Outline



- Introducing the anomaly
- Standard Model contributions
- Theoretical status and prospects
- Fermilab Muon $g-2$ experiment
 - Measurement principle
 - Analysis methods
 - Current status and prospects
- Conclusions

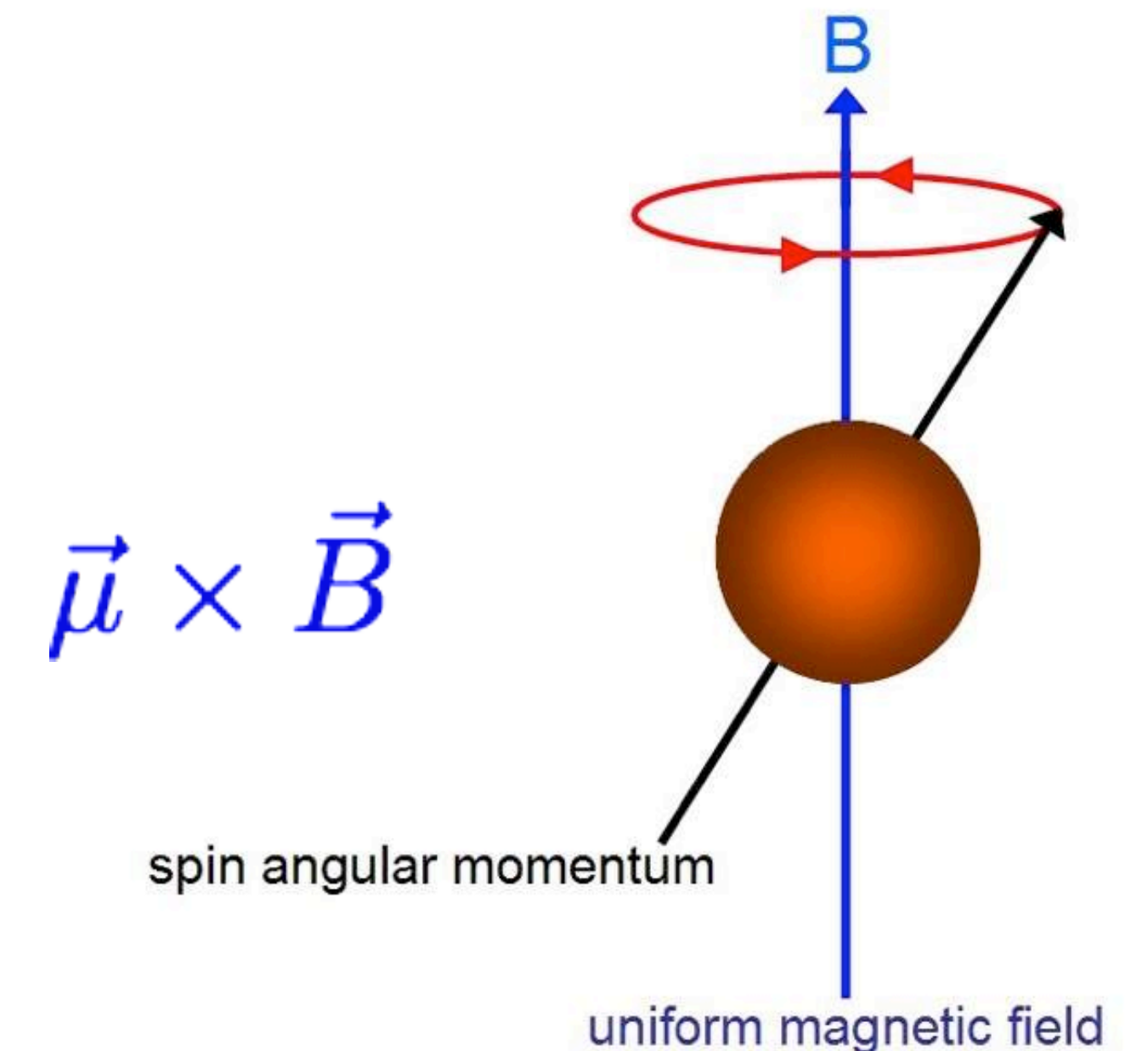
Muon Magnetic Moment



- The muon has an intrinsic magnetic moment that is coupled to its spin via the gyromagnetic ratio g :

$$\vec{\mu} = g \frac{e}{2m_{\mu}} \vec{S}$$

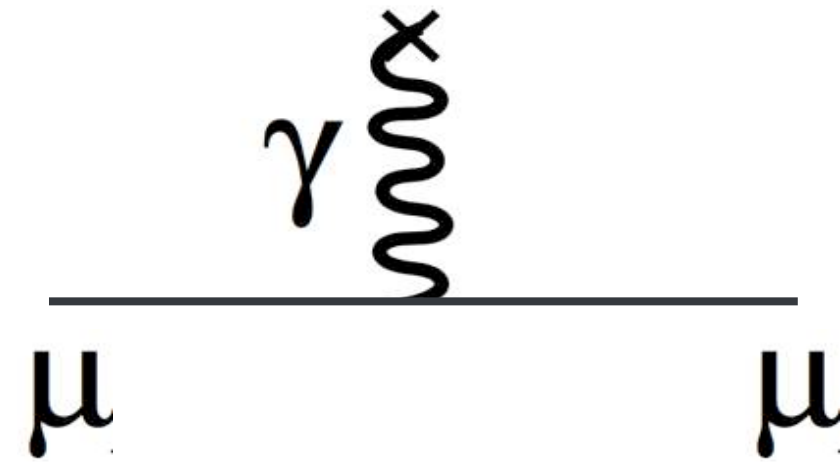
- Magnetic moment (spin) interacts with external B-fields
- Makes spin precess at frequency determined by g



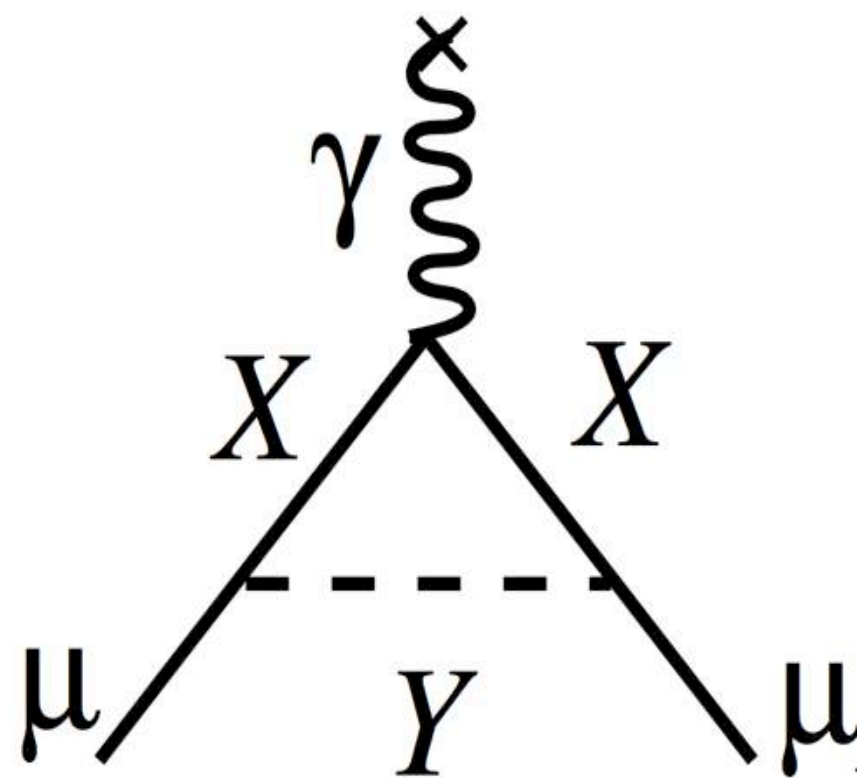
Magnetic Moment & Virtual Loops



- For a pure Dirac spin- $1/2$ charged fermion, g is exactly 2



- Interactions between the muon and virtual loops change the value - X & Y particles could be SM or new physics:

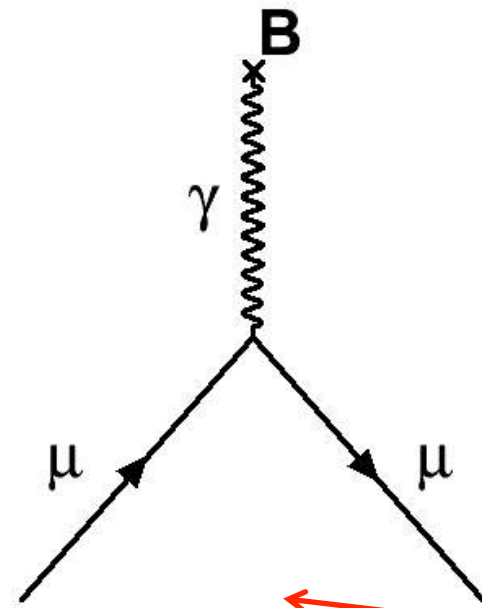
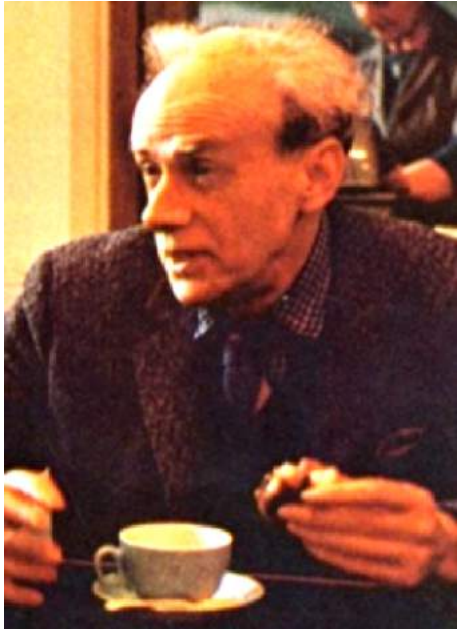


Standard Model Components of $g-2$



Dirac

Charged,
spin $\frac{1}{2}$ particle



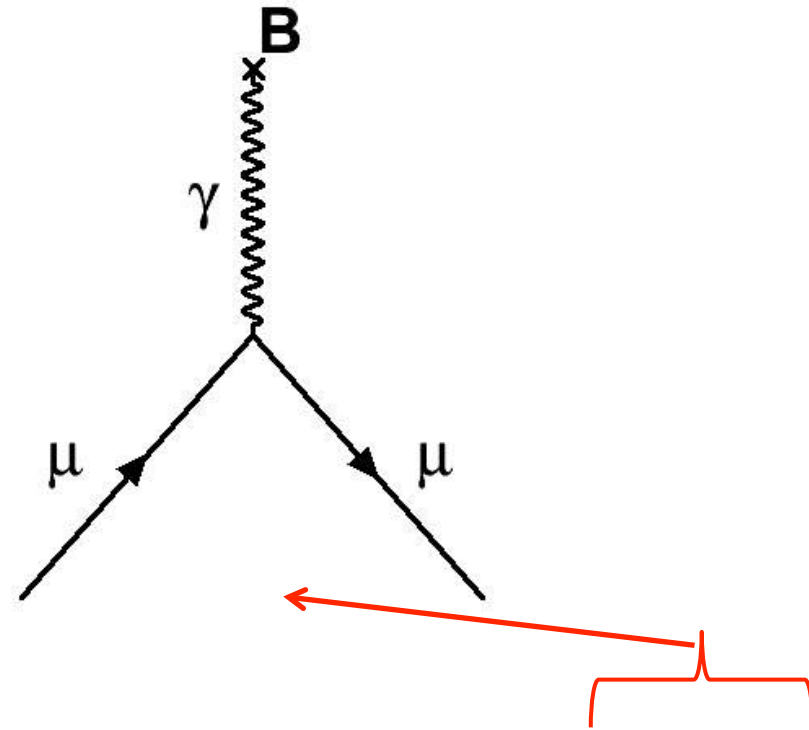
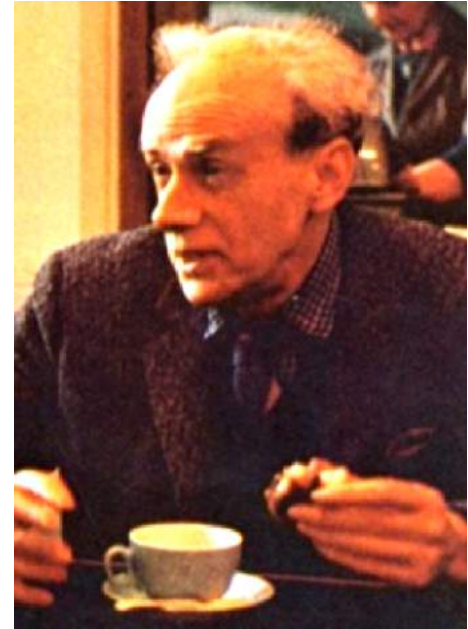
$$g_{\mu} = 2$$

Standard Model Components of $g-2$



Dirac

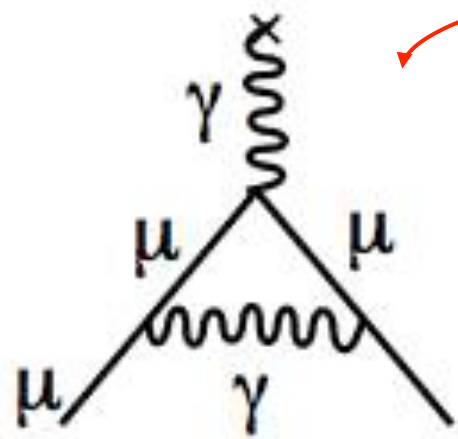
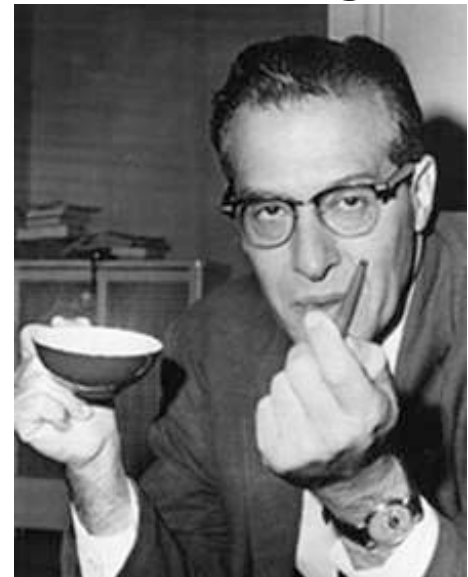
Charged,
spin 1/2 particle



g_{μ}

$= 2$

Schwinger



1st Order QED

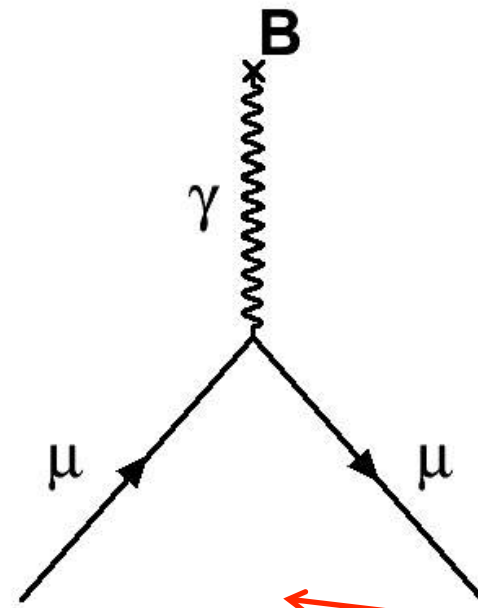
$$\frac{\alpha}{2\pi} = 0.00232$$

Standard Model Components of g-2



Dirac

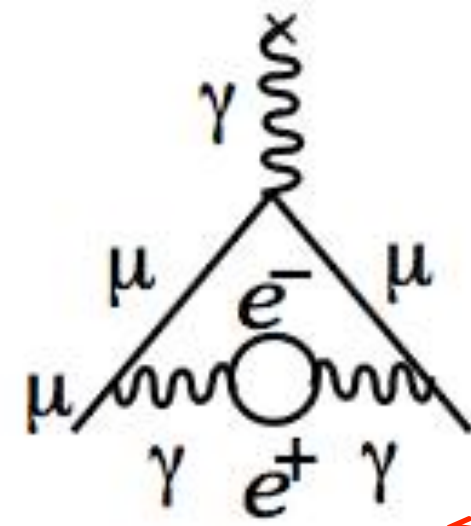
Charged,
spin 1/2 particle



Kinoshita

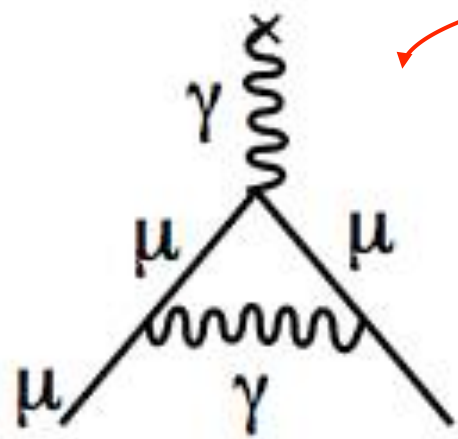
Up to 10th
Order QED

+12671
diagrams



$$g_{\mu} = 2.0$$

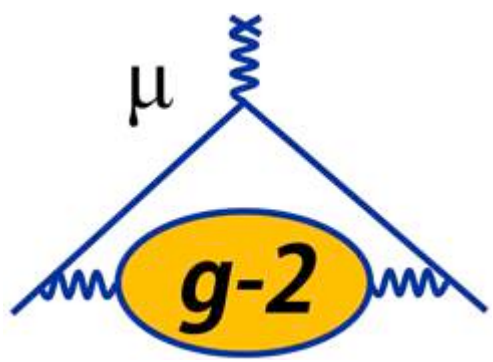
Schwinger



1st Order QED

$$\frac{\alpha}{2\pi} = 0.00232$$

Standard Model Components of g-2



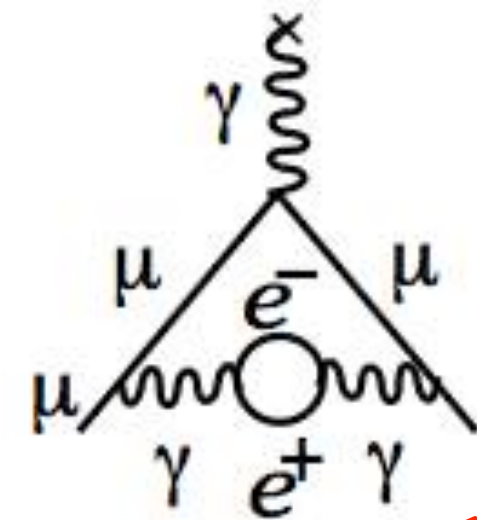
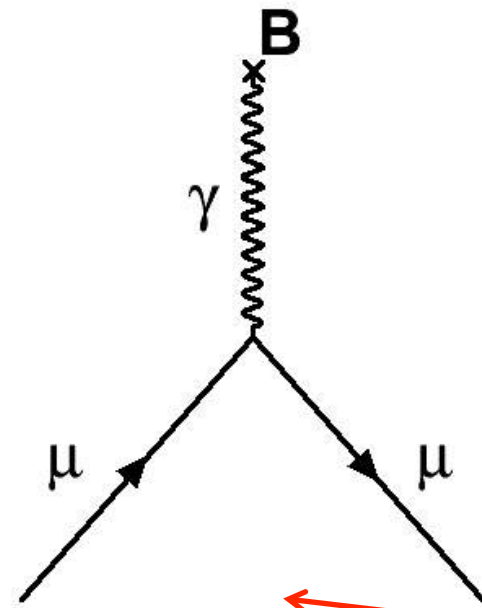
Dirac

Charged, spin $\frac{1}{2}$ particle

Kinoshita

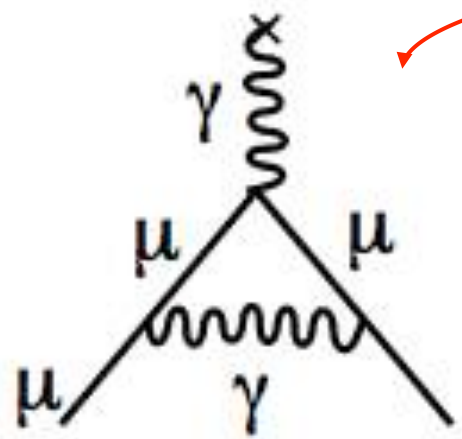
Up to 10th Order QED

+12671 diagrams



$$g_{\mu} = 2.0$$

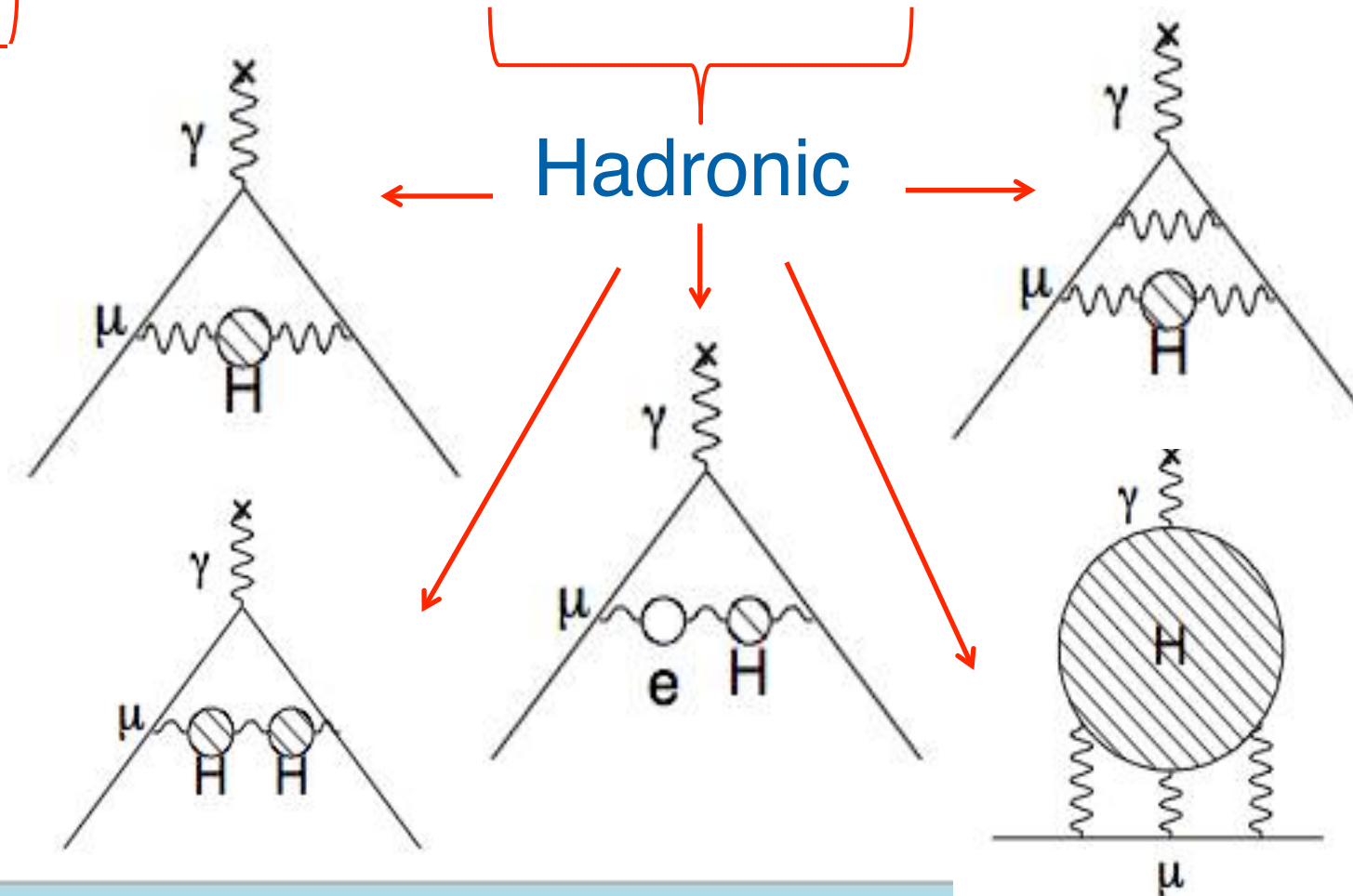
Schwinger



1st Order QED

$$\frac{\alpha}{2\pi} = 0.00232$$

Hadronic



Standard Model Components of g-2



Dirac

Charged, spin 1/2 particle

Kinoshita

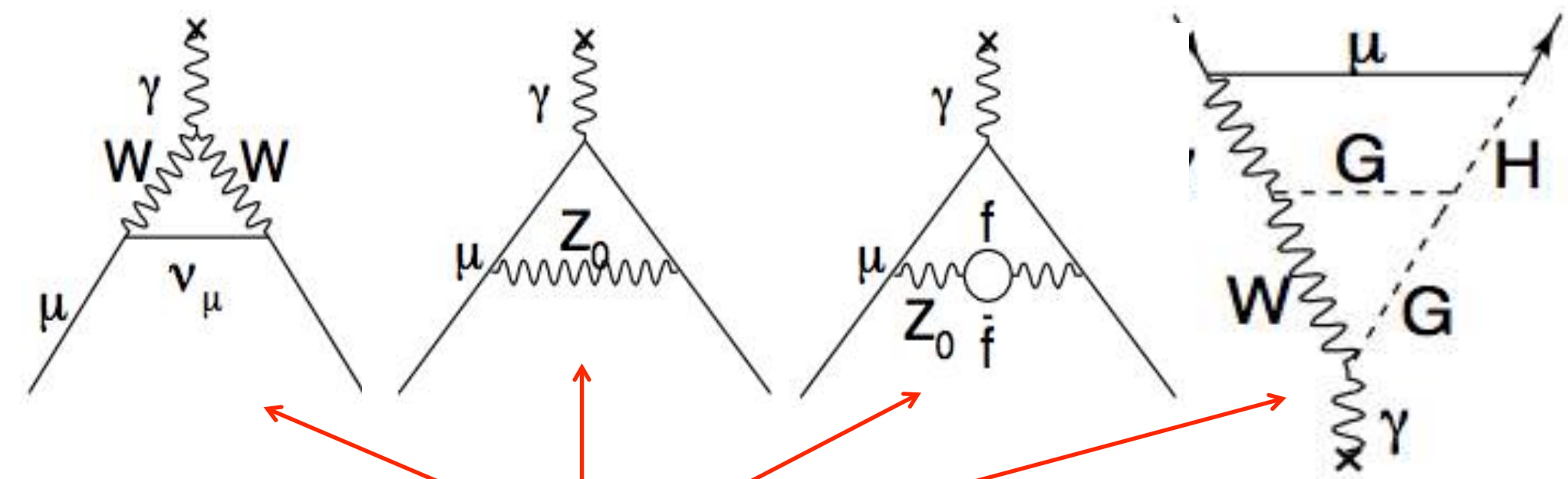
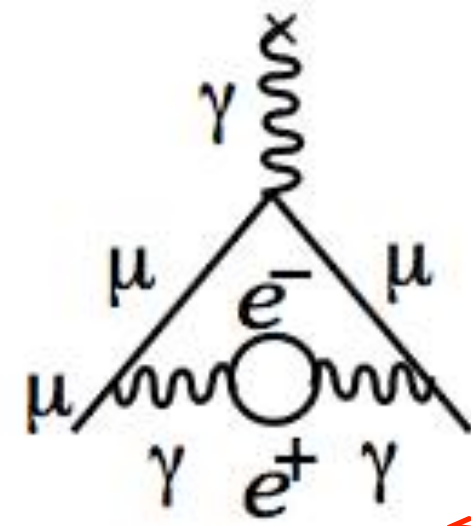
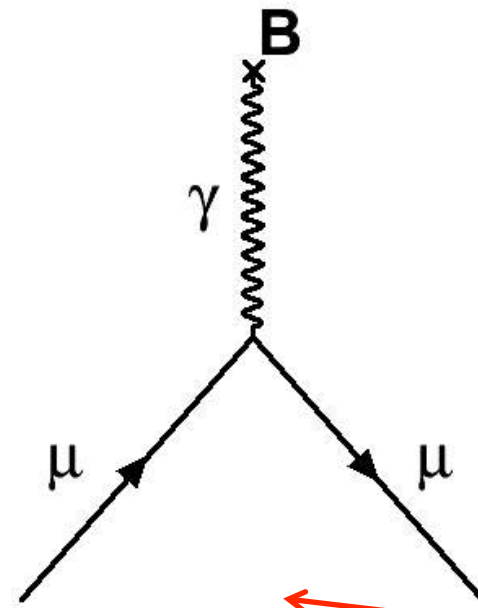
Up to 10th Order QED

+12671 diagrams

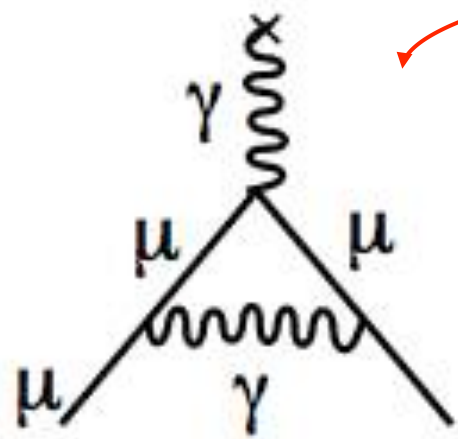
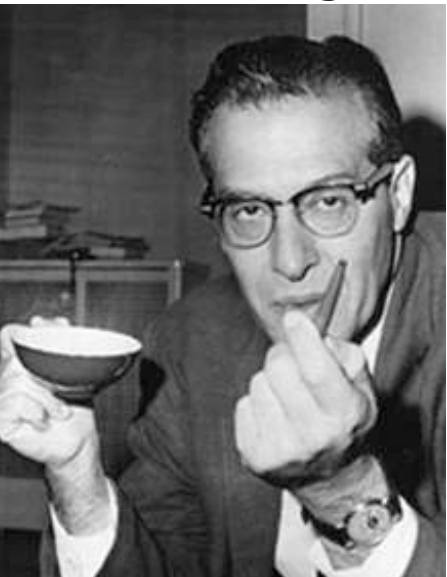
Electroweak

Hadronic

$$g_\mu = 2.002\,331\,841\,7$$

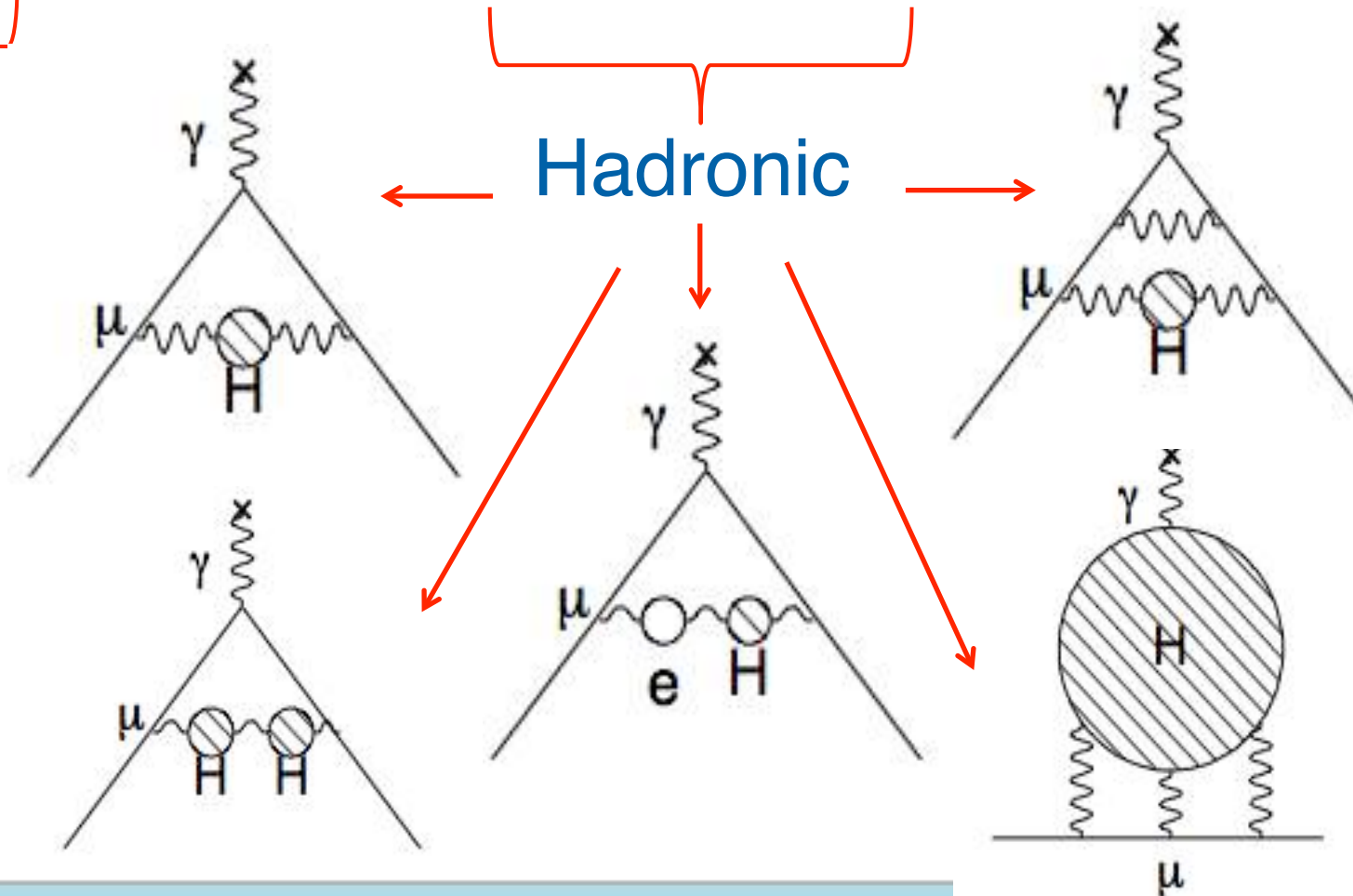


Schwinger



1st Order QED

$$\frac{\alpha}{2\pi} = 0.00232$$



Standard Model Components of g-2



Dirac

Charged, spin 1/2 particle

Kinoshita

Up to 10th Order QED

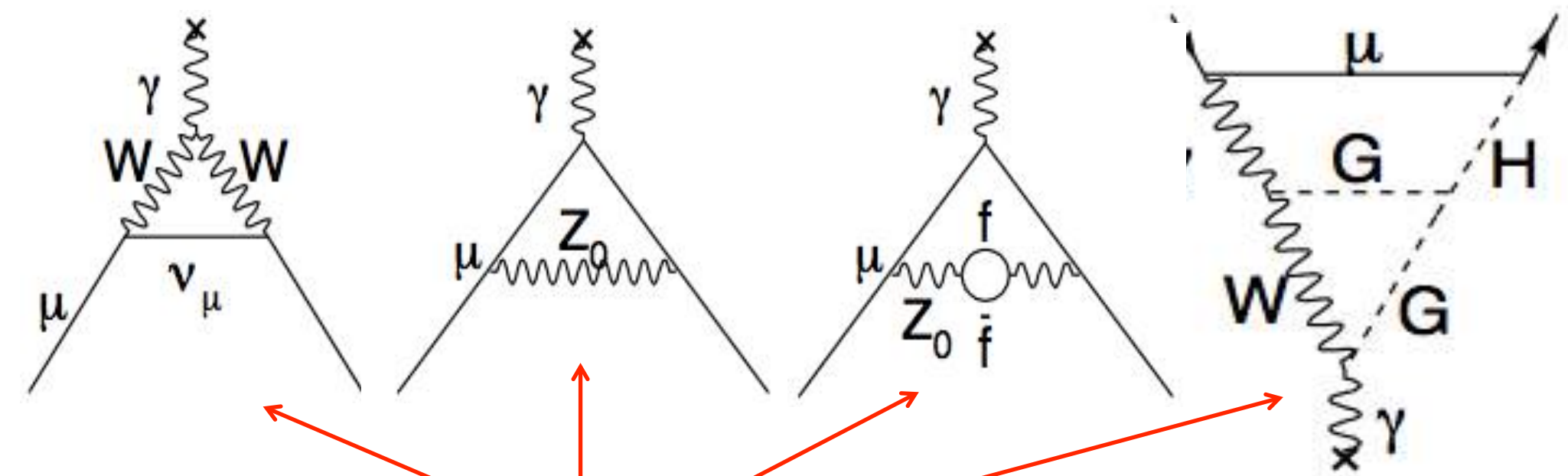
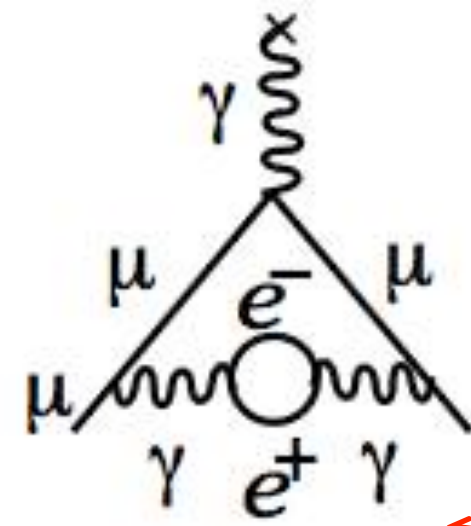
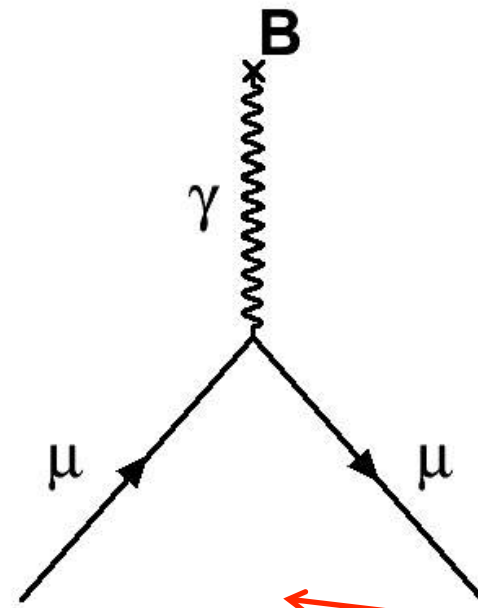
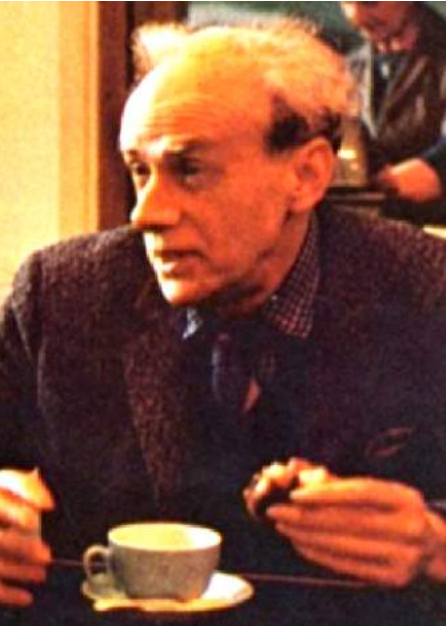
+12671 diagrams

Electroweak

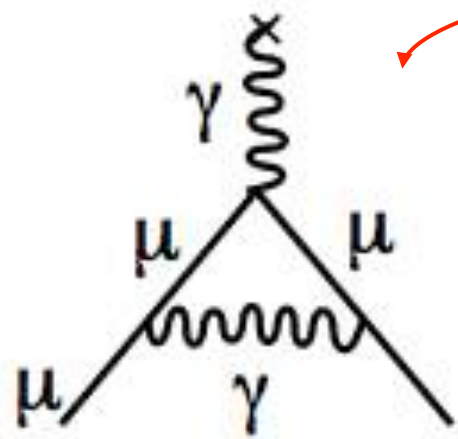
Hadronic

BSM?

$$g_\mu = 2.002\ 331\ 841\ 78(126)$$

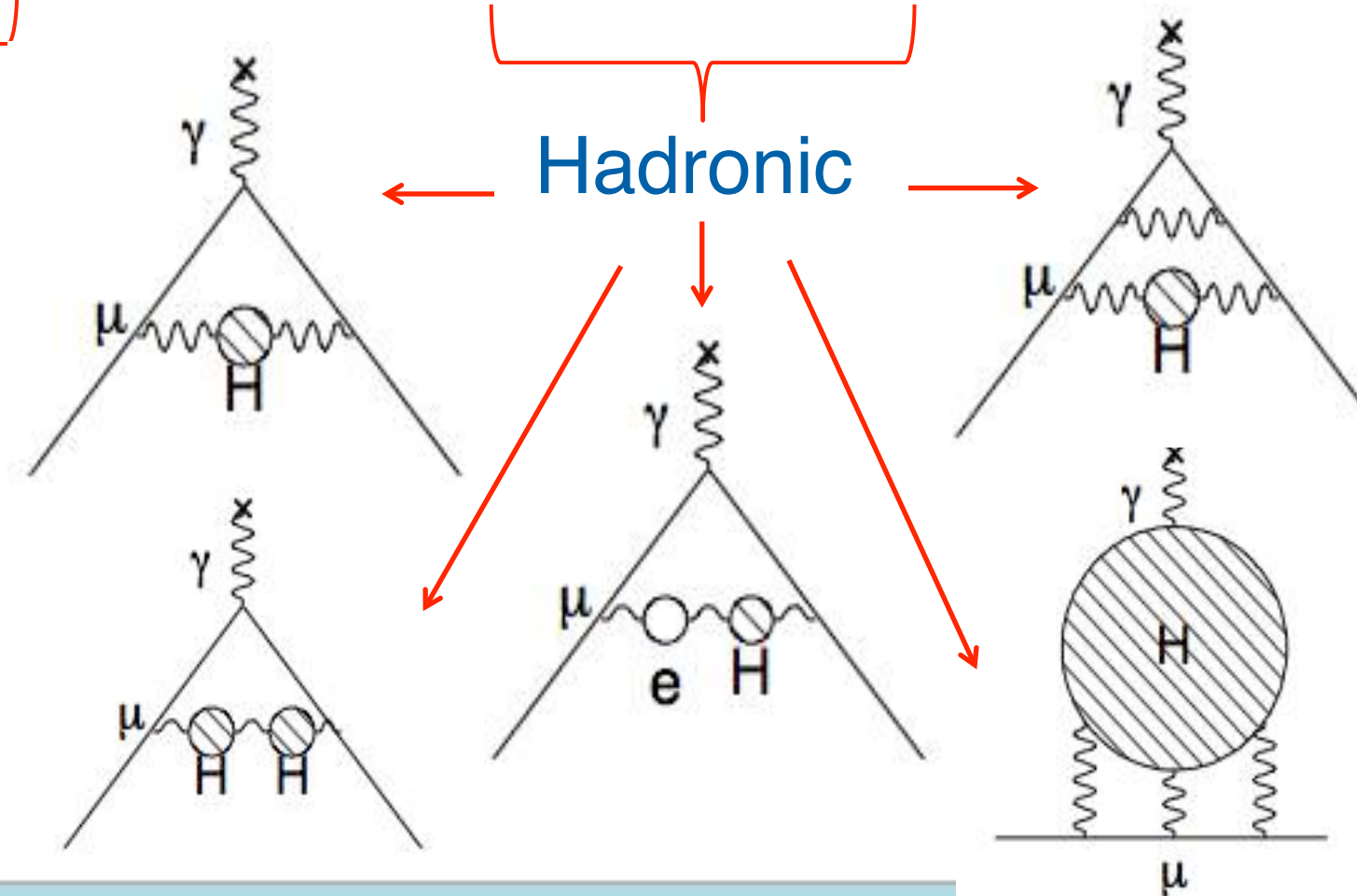


Schwinger

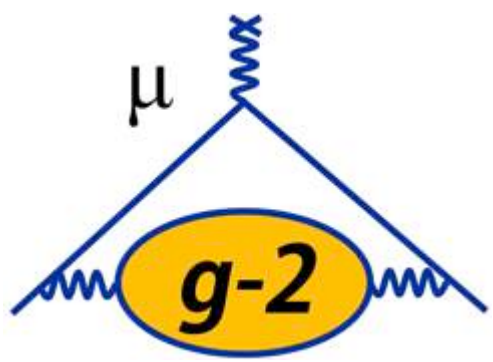


1st Order QED

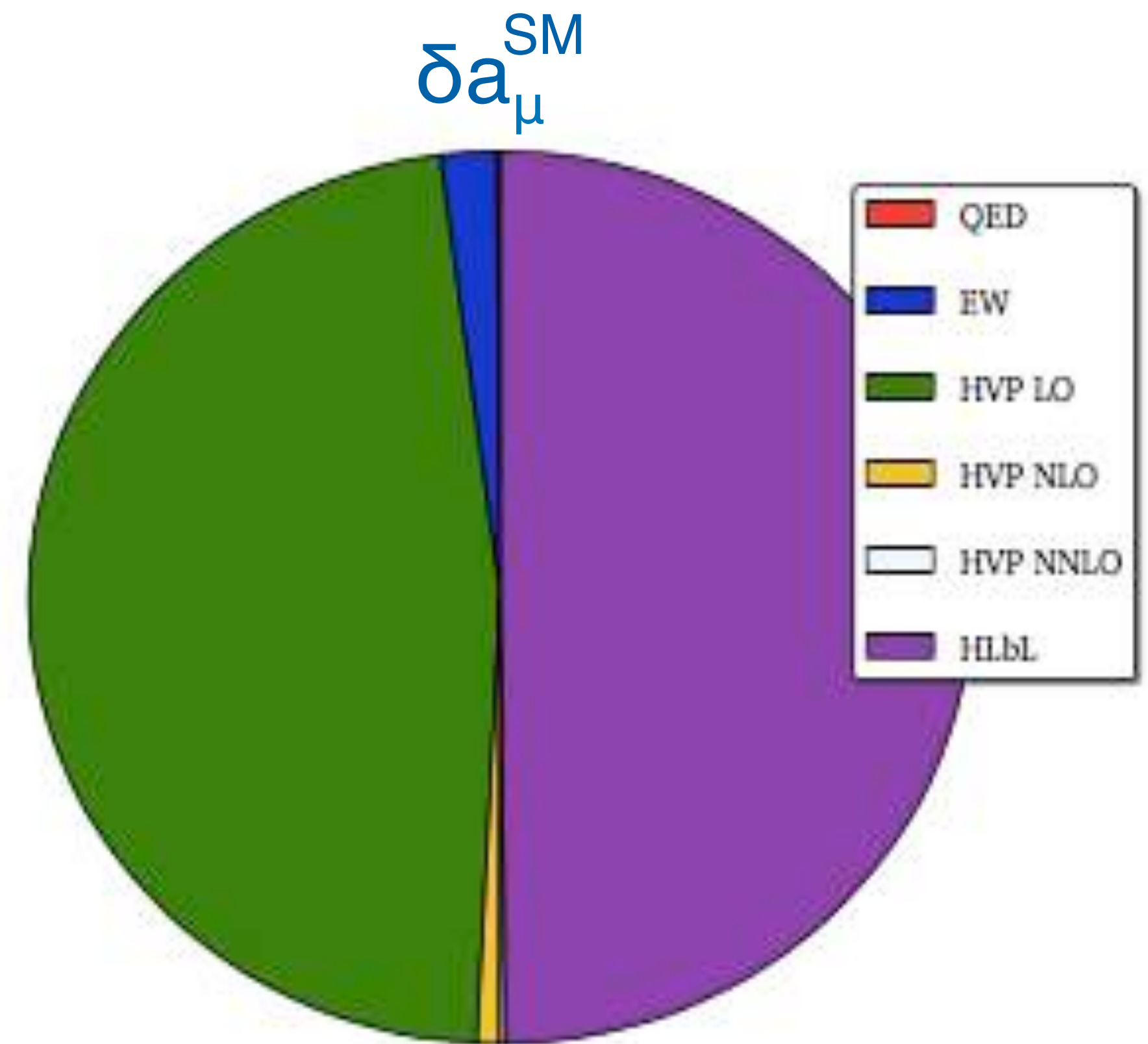
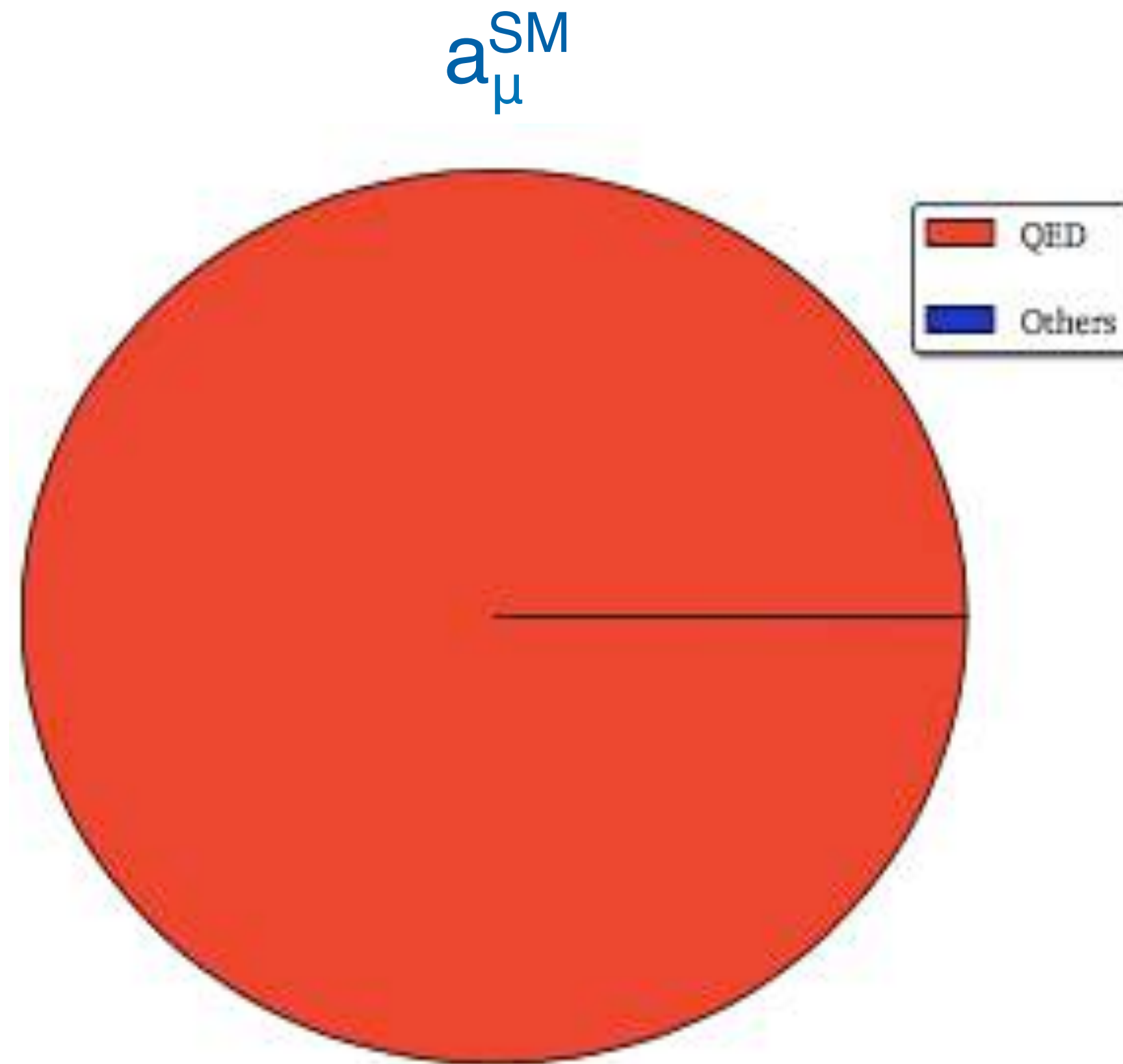
$$\frac{\alpha}{2\pi} = 0.00232$$



Standard Model Uncertainties



$$a_\mu = \frac{g_\mu - 2}{2}$$



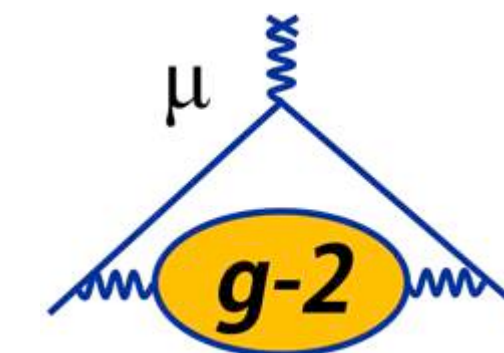
- The SM value of a_μ is dominated by QED
- But its uncertainty is dominated by Hadronic contributions
- Split into Hadronic Vacuum Polarisation (HVP) & Hadronic Light by Light (HLbL)

a_μ Theoretical Status



Contribution	Value (x 10 ⁻¹¹)	Reference
QED	116 584 718.95 \pm 0.08	PRL 109 111808 (2012)
EW	153.6 \pm 1.0	PRD 88 053005 (2013)

a_μ Theoretical Status



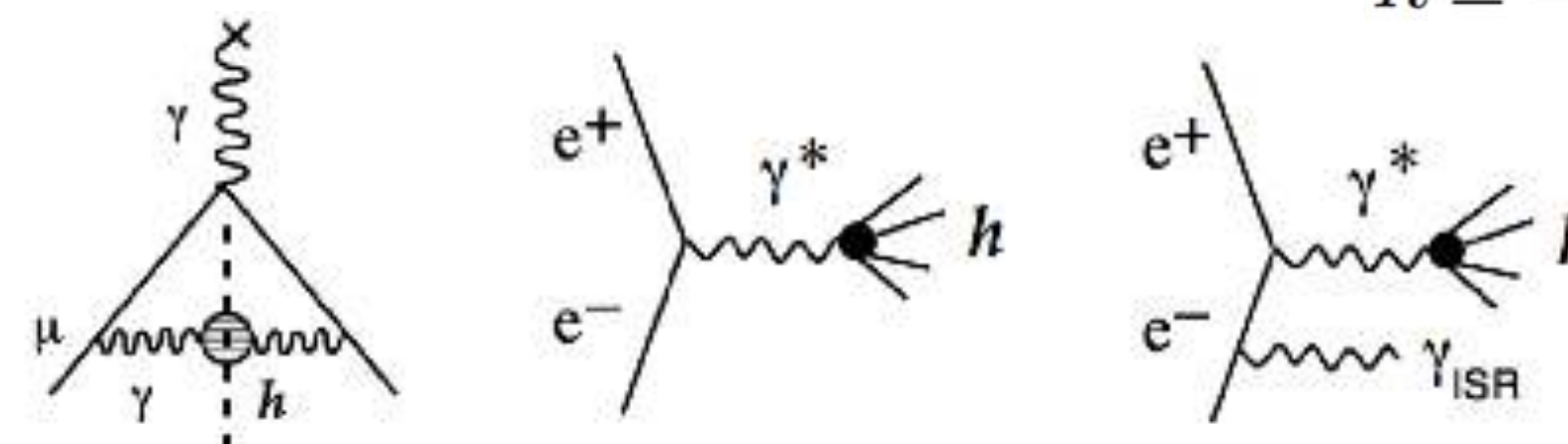
Contribution	Value (x 10 ⁻¹¹)	Reference
QED	116 584 718.95 ± 0.08	PRL 109 111808 (2012)
EW	153.6 ± 1.0	PRD 88 053005 (2013)
HVP (LO)	6931 ± 34	EPJ C 77 827 (2017)
HVP (LO)	6933 ± 25	PRD 97 114025 (2018)

HVP (LO): Lowest-Order Hadronic Vacuum Polarization

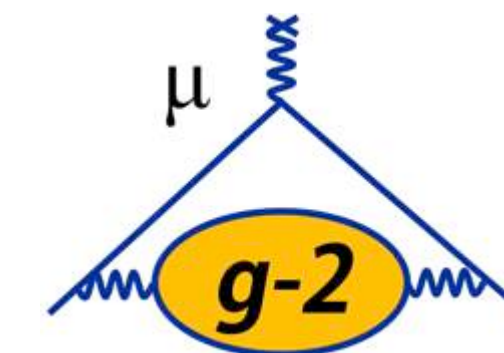
- **Critical input** from e^+e^- colliders (data from SND, CMD3, BaBar, KLOE, Belle, BESIII), $\delta a_\mu^{\text{HVP}} \sim 0.5\%$; extensive physics program in place to reduce $\delta a_\mu^{\text{HVP}}$ to $\sim 0.3\%$ in coming years
- **Progress on the lattice**: Calculations at physical π mass; goal: $\delta a_\mu^{\text{HVP}} \sim 1-2\%$ in a few years (cross-check with e^+e^- data)

$$a_\mu^{\text{had;LO}} = \left(\frac{\alpha m_\mu}{3\pi}\right)^2 \int_{m_\pi^2}^{\infty} \frac{ds}{s^2} K(s) R(s)$$

$$R \equiv \frac{\sigma_{\text{tot}}(e^+e^- \rightarrow \text{hadrons})}{\sigma(e^+e^- \rightarrow \mu^+\mu^-)}$$



a_μ Theoretical Status



Contribution	Value ($\times 10^{-11}$)	Reference
QED	$116\,584\,718.95 \pm 0.08$	PRL 109 111808 (2012)
EW	153.6 ± 1.0	PRD 88 053005 (2013)
HVP (LO)	6931 ± 34	EPJ C 77 827 (2017)
HVP (LO)	6933 ± 25	PRD 97 114025 (2018)
HVP (NLO)	-98.7 ± 0.7	EPJ C 77 827 (2017)
HVP (NLO)	-98.2 ± 0.4	PRD 97 114025 (2018)
HVP (NNLO)	12.4 ± 0.1	PLB 734 144 (2014)

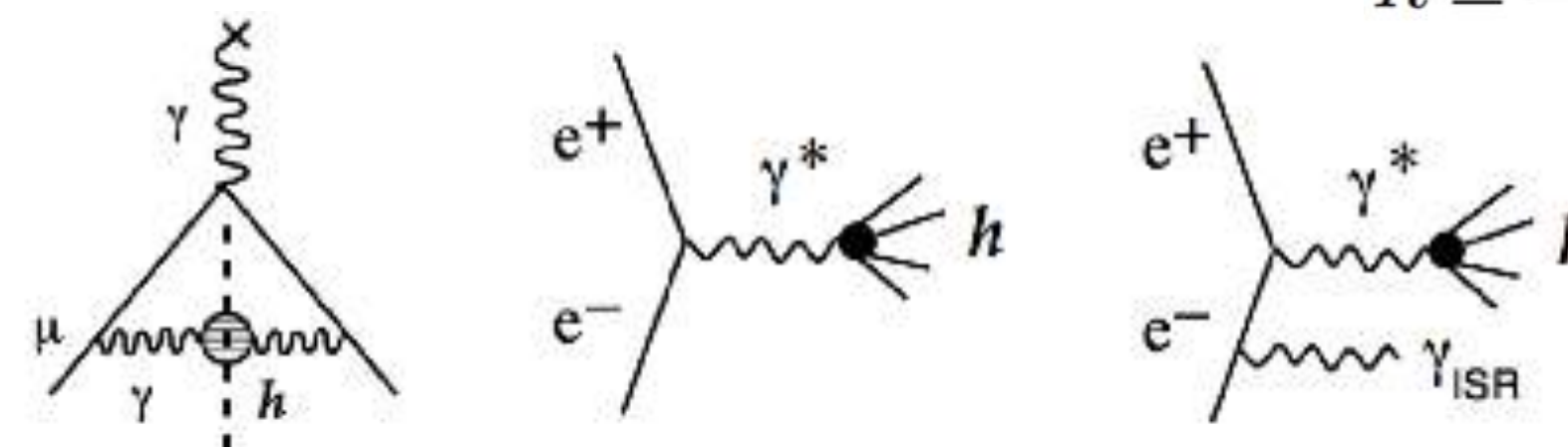
HVP (LO): Lowest-Order Hadronic Vacuum Polarization

- Critical input** from e^+e^- colliders (data from SND, CMD3, BaBar, KLOE, Belle, BESIII), $\delta a_\mu^{\text{HVP}} \sim 0.5\%$; extensive physics program in place to reduce $\delta a_\mu^{\text{HVP}}$ to $\sim 0.3\%$ in coming years

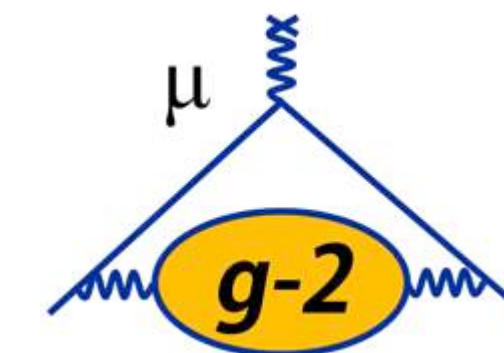
- Progress on the lattice:** Calculations at physical π mass; goal: $\delta a_\mu^{\text{HVP}} \sim 1-2\%$ in a few years (cross-check with e^+e^- data)

$$a_\mu^{\text{had;LO}} = \left(\frac{\alpha m_\mu}{3\pi}\right)^2 \int_{m_\pi^2}^{\infty} \frac{ds}{s^2} K(s) R(s)$$

$$R \equiv \frac{\sigma_{\text{tot}}(e^+e^- \rightarrow \text{hadrons})}{\sigma(e^+e^- \rightarrow \mu^+\mu^-)}$$



a_μ Theoretical Status



New *ab initio* approaches [PRD 98 094503 (2018)] finding consistent result of $(-93 \pm 13) \times 10^{-11}$ — lattice making big strides

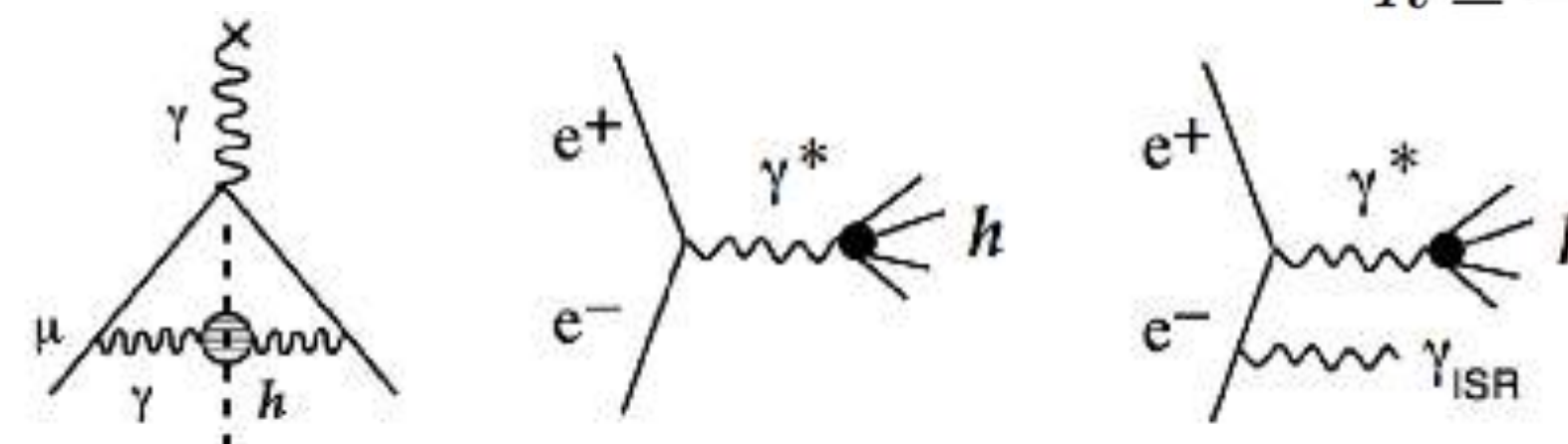
			12)
			13)
			7)
HVP (LO)	6933 ± 25	PRD 97 114025 (2018)	
HVP (NLO)	-98.7 ± 0.7	EPJ C 77 827 (2017)	
HVP (NLO)	-98.2 ± 0.4	PRD 97 114025 (2018)	
HVP (NNLO)	12.4 ± 0.1	PLB 734 144 (2014)	

HVP (LO): Lowest-Order Hadronic Vacuum Polarization

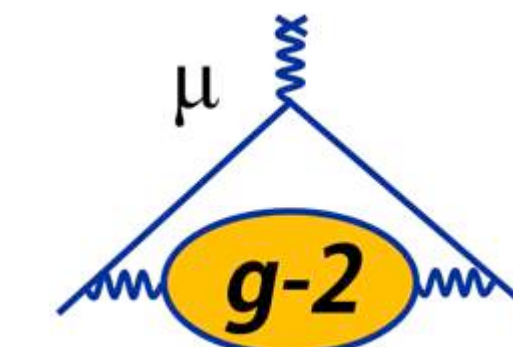
- Critical input** from e^+e^- colliders (data from SND, CMD3, BaBar, KLOE, Belle, BESIII), $\delta a_\mu^{\text{HVP}} \sim 0.5\%$; extensive physics program in place to reduce $\delta a_\mu^{\text{HVP}}$ to $\sim 0.3\%$ in coming years
- Progress on the lattice:** Calculations at physical π mass; goal: $\delta a_\mu^{\text{HVP}} \sim 1-2\%$ in a few years (cross-check with e^+e^- data)

$$a_\mu^{\text{had;LO}} = \left(\frac{\alpha m_\mu}{3\pi} \right)^2 \int_{m_\pi^2}^{\infty} \frac{ds}{s^2} K(s) R(s)$$

$$R \equiv \frac{\sigma_{\text{tot}}(e^+e^- \rightarrow \text{hadrons})}{\sigma(e^+e^- \rightarrow \mu^+\mu^-)}$$



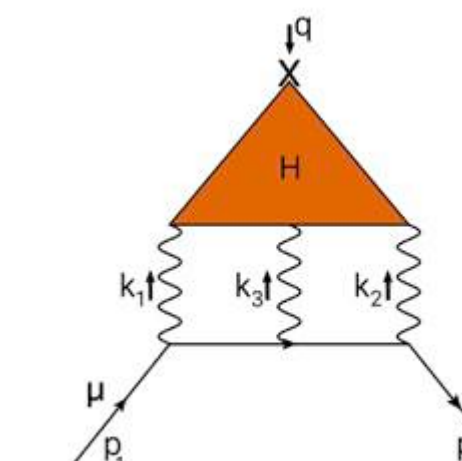
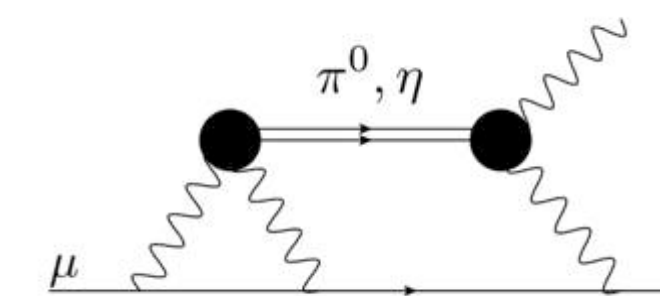
a_μ Theoretical Status



New *ab initio* approaches [PRD 98 094503 (2018)] finding consistent result of $(-93 \pm 13) \times 10^{-11}$ — lattice making big strides

HVP (LO)	6933 ± 25	PRD 97 114025 (2018)
HVP (NLO)	-98.7 ± 0.7	EPJ C 77 827 (2017)
HVP (NLO)	-98.2 ± 0.4	PRD 97 114025 (2018)
HVP (NNLO)	12.4 ± 0.1	PLB 734 144 (2014)
HLbL (LO + NLO)	101 ± 26	PLB 735 90 (2014), EPJ Web Conf 118 01016 (2016)
Total SM	$116\,591\,818 \pm 43$ (368 ppb)	
	$116\,591\,821 \pm 36$ (309 ppb)	

HLbL: Hadronic Light-by-Light



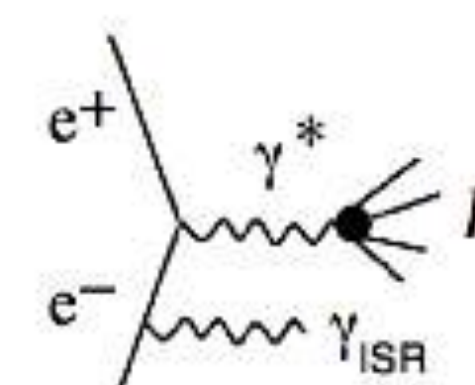
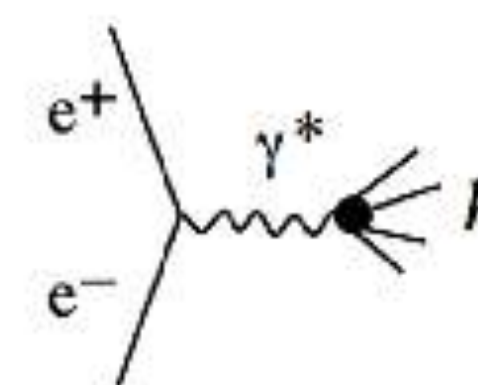
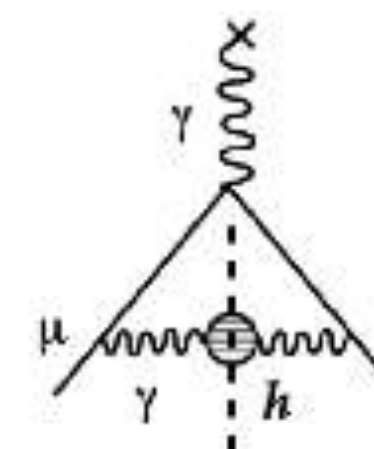
- Model dependent: based on χ PT + short-distance constraints (operator product expansion)
- Difficult to relate to data like HVP (LO); γ^* physics, π^0 data (BESIII, KLOE) important for constraining models
- **Theory Progress:** New dispersive calculation approach; extend the lattice (finite volume, disconnected diagrams); Blum et al. making excellent progress

HVP (LO): Lowest-Order Hadronic Vacuum Polarization

- **Critical input** from e^+e^- colliders (data from SND, CMD3, BaBar, KLOE, Belle, BESIII), $\delta a_\mu^{\text{HVP}} \sim 0.5\%$; extensive physics program in place to reduce $\delta a_\mu^{\text{HVP}}$ to $\sim 0.3\%$ in coming years
- **Progress on the lattice:** Calculations at physical π mass; goal: $\delta a_\mu^{\text{HVP}} \sim 1-2\%$ in a few years (cross-check with e^+e^- data)

$$a_\mu^{\text{had};\text{LO}} = \left(\frac{\alpha m_\mu}{3\pi}\right)^2 \int_{m_\pi^2}^{\infty} \frac{ds}{s^2} K(s) R(s)$$

$$R \equiv \frac{\sigma_{\text{tot}}(e^+e^- \rightarrow \text{hadrons})}{\sigma(e^+e^- \rightarrow \mu^+\mu^-)}$$



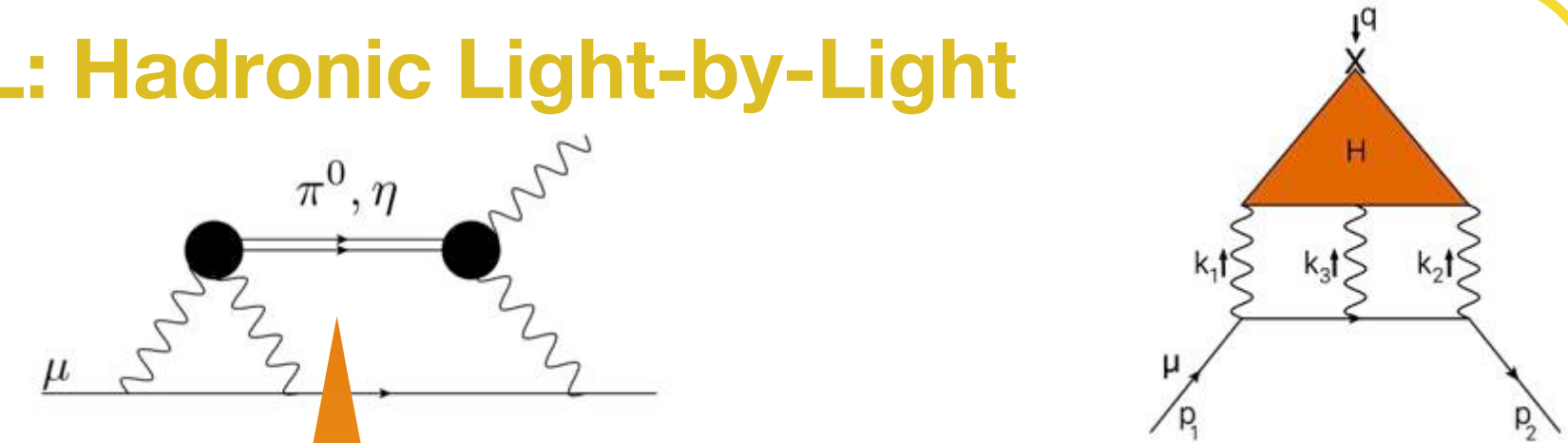
a_μ Theoretical Status



New *ab initio* approaches [PRD 98 094503 (2018)] finding consistent result of $(-93 \pm 13) \times 10^{-11}$ — lattice making big strides

HVP (LO)	6933 ± 25	PRD 97 114025 (2018)
HVP (NLO)	-98.7 ± 0.7	EPJ C 77 827 (2017)
HVP (NLO)	-98.2 ± 0.4	PRD 97 114025 (2018)
HVP (NNLO)	12.4 ± 0.1	PLB 734 144 (2014)
HLbL (LO + NLO)	101 ± 26	PLB 735 90 (2014), EPJ Web Conf 118 01016 (2016)

HLbL: Hadronic Light-by-Light



- Model dependent: based on χ PT + short-distance constraints (operator product expansion)
- Difficult to relate to data like HVP (LO); γ^* physics, π^0 data (BESIII, KLOE) important for constraining models
- **Theory Progress**: new dispersive calculation approach; extend the lattice to finite volume, disconnected diagrams; progress

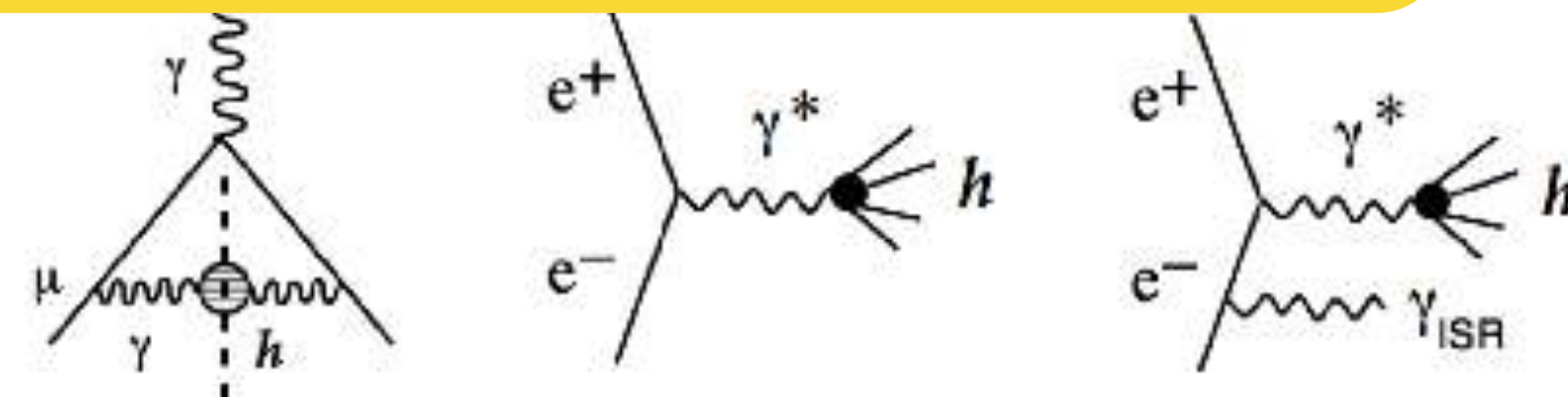
Builds confidence in HLbL term

Recent data-driven calculation [PRL 121 112002 (2018)] for $a_\mu^{\pi^0\text{-pole}}$ is consistent with earlier vector-, lowest-meson dominance calcs [PRD 65 073034 (2002), PRD 94 053006 (2016), EJC 75 586 (2015)]

HVP (LO): Lowest-Order Hadronic Vacuum Polarization

- **Critical input** from e^+e^- colliders (data BaBar, KLOE, Belle, BESIII), $\delta a_\mu^{\text{HVP}} \sim 0.5\%$ program in place to reduce $\delta a_\mu^{\text{HVP}}$ to $\sim 0.3\%$ in coming years
- **Progress on the lattice**: Calculations at physical π mass; goal: $\delta a_\mu^{\text{HVP}} \sim 1-2\%$ in a few years (cross-check with e^+e^- data)

$$R(s) \equiv \frac{\sigma_{\text{tot}}(e^+e^- \rightarrow \text{hadrons})}{\sigma(e^+e^- \rightarrow \mu^+\mu^-)}$$

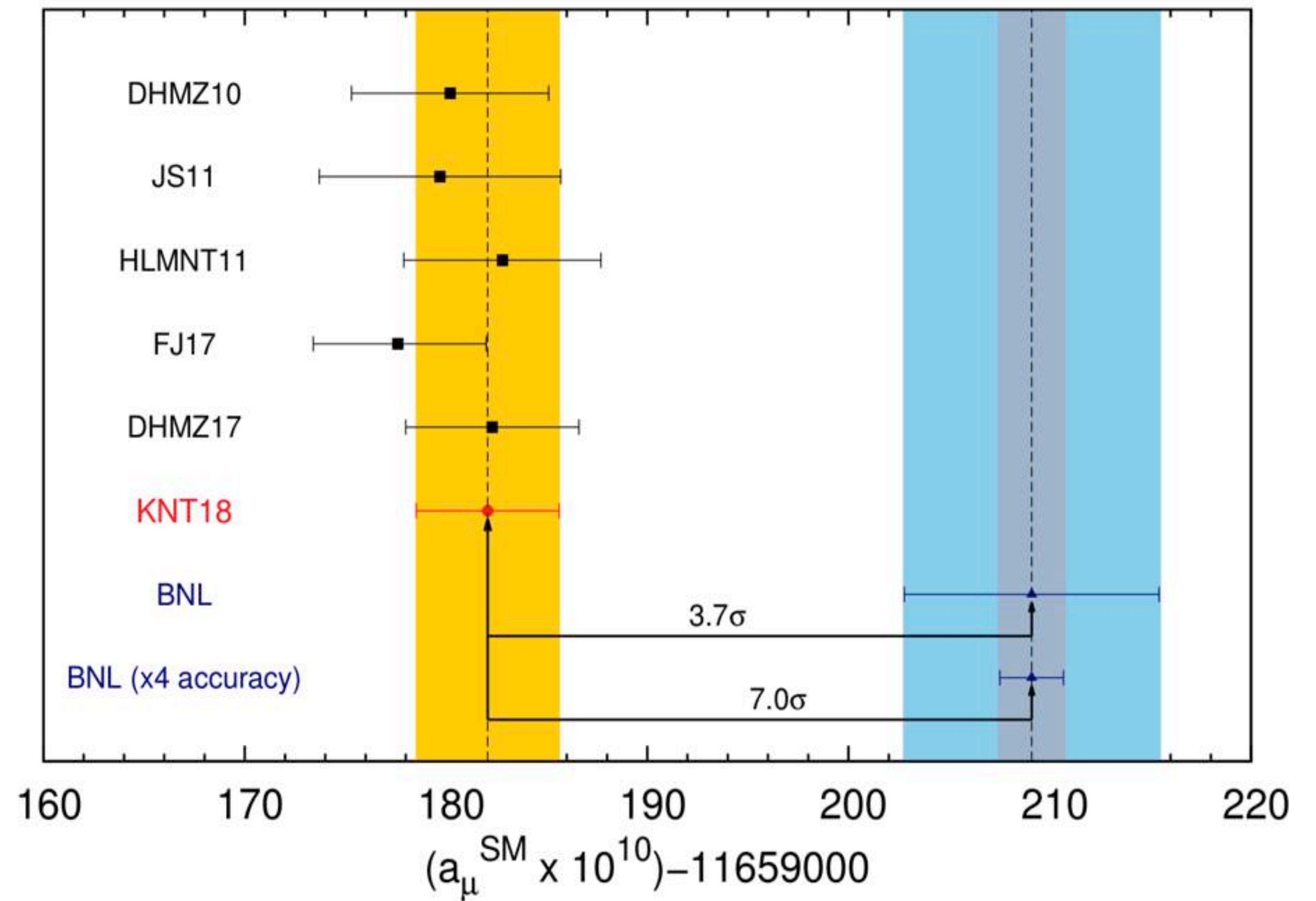


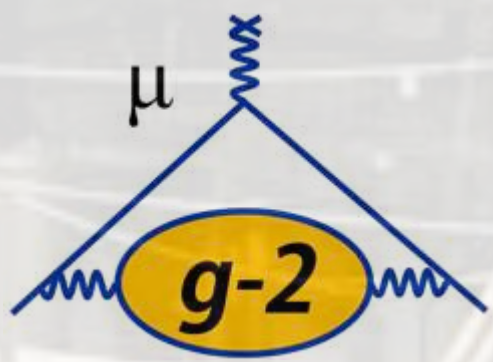
Current status



- New combination (KNT18) has not moved central value significantly, reduced uncertainties
- $> 3.5\sigma$ discrepancy persists
- Theory groups are making progress to achieve competitive uncertainties on same time scale as new FNAL experiment...

PRD **97** 114025 (2018)





The Fermilab Muon $g-2$ Experiment

Muon g-2: 33 Institutions, 7 countries, 203 Members

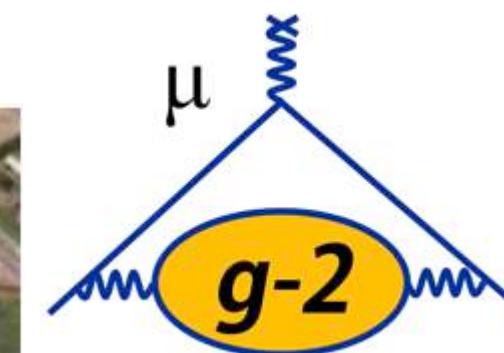
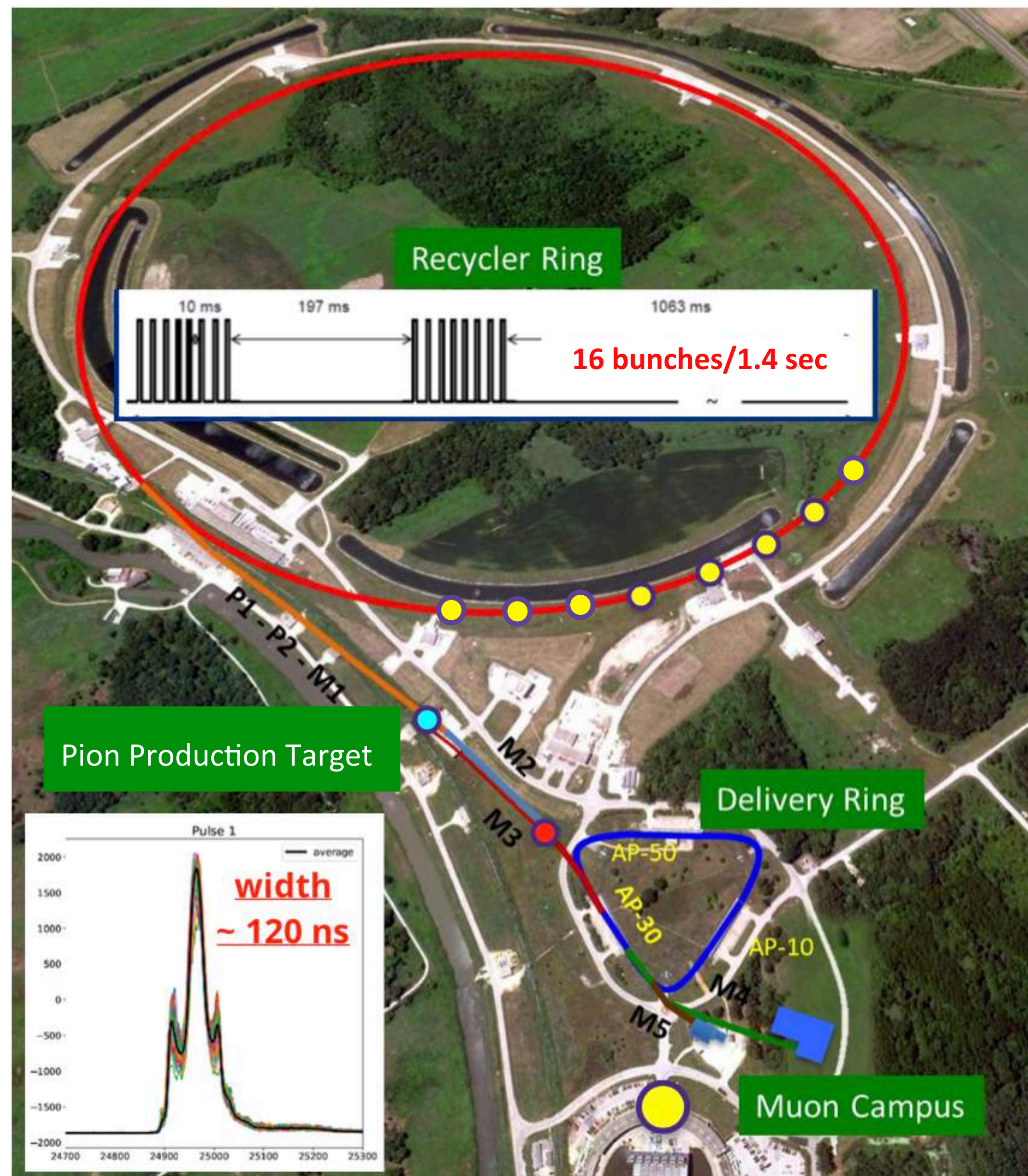


Why Fermilab?

- BNL limited by statistics (540 ppb on 9×10^9 detected e^+)
- E989 goal: Factor of 21 more statistics (2×10^{11} detected e^+)

Fermilab advantages

- Long beam line to collect $\pi^+ \rightarrow \mu^+$
- Much reduced amount of p, π in ring
- 4x higher fill frequency than BNL



Measurement Principle

- Inject polarized muon beam into magnetic storage ring
- Measure **difference** between spin precession and cyclotron frequencies
- If $g = 2$, $\omega_a = 0$
- $g \neq 2$, $\omega_a \approx (e/m_\mu)a_\mu B$



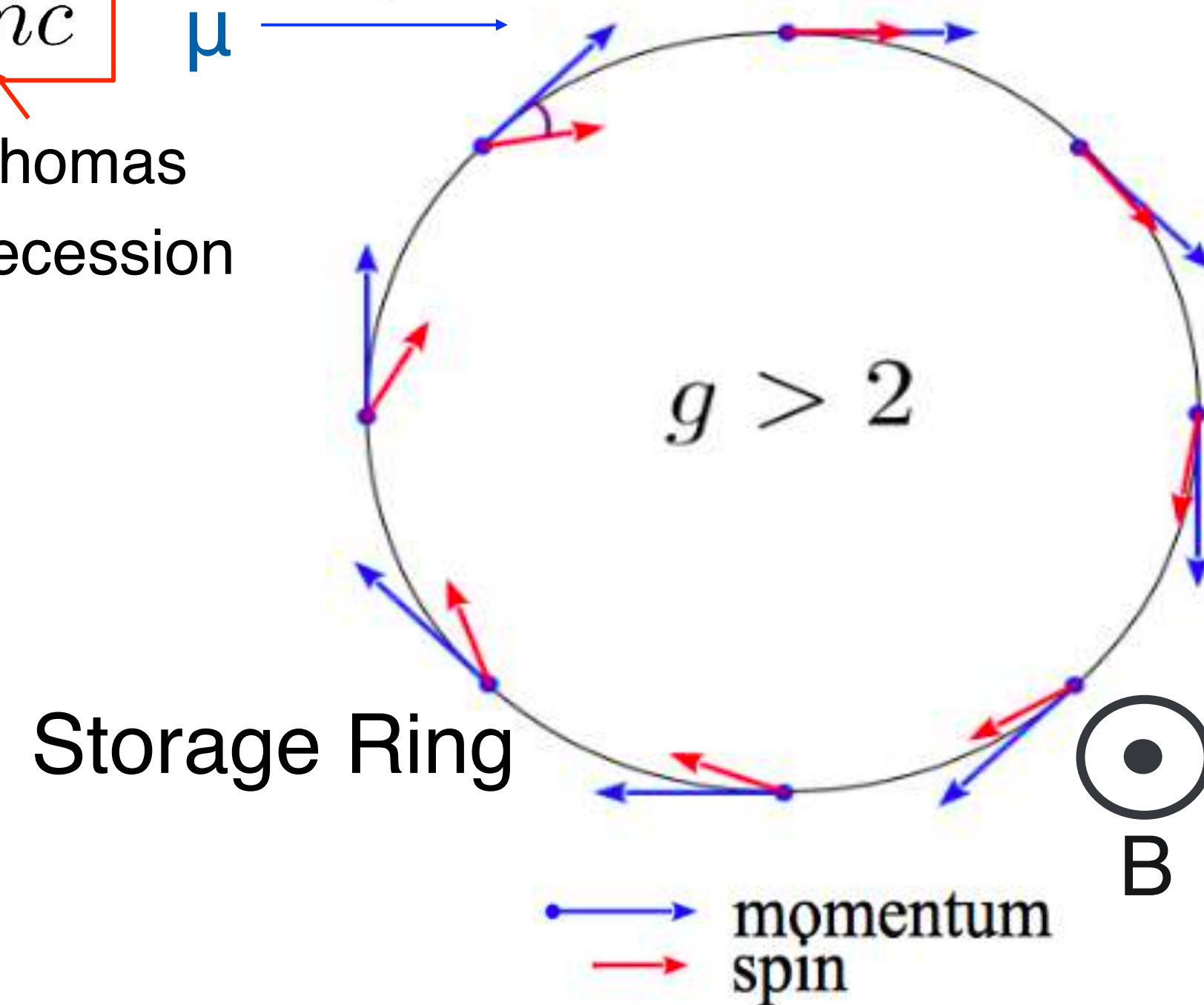
$$\omega_s = \frac{geB}{2mc} + (1 - \gamma) \frac{eB}{\gamma mc}$$

Larmor precession

$$\omega_c = \frac{eB}{\gamma mc}$$

Thomas precession

$$\omega_a = \omega_s - \omega_c = a_\mu \frac{eB}{mc}$$



$$a_\mu = \frac{\omega_a}{\tilde{\omega}_p} \frac{\mu_p}{\mu_e} \frac{m_\mu}{m_e} \frac{g_e}{2}$$

3 ppb

22 ppb

0.3 ppt

Rev. Mod. Phys. 88, 035009 (2016)

- We measure ω_a and ω_p separately
- Aiming for 70 ppb precision on each (systematic)
- **Target: $\delta a_\mu(\text{syst}) = 140$ ppb; factor of 4 improvement over BNL**

Real World Considerations



- Muon beam has a small vertical component
- We need to use Electric fields to focus the beam so we can store the muons

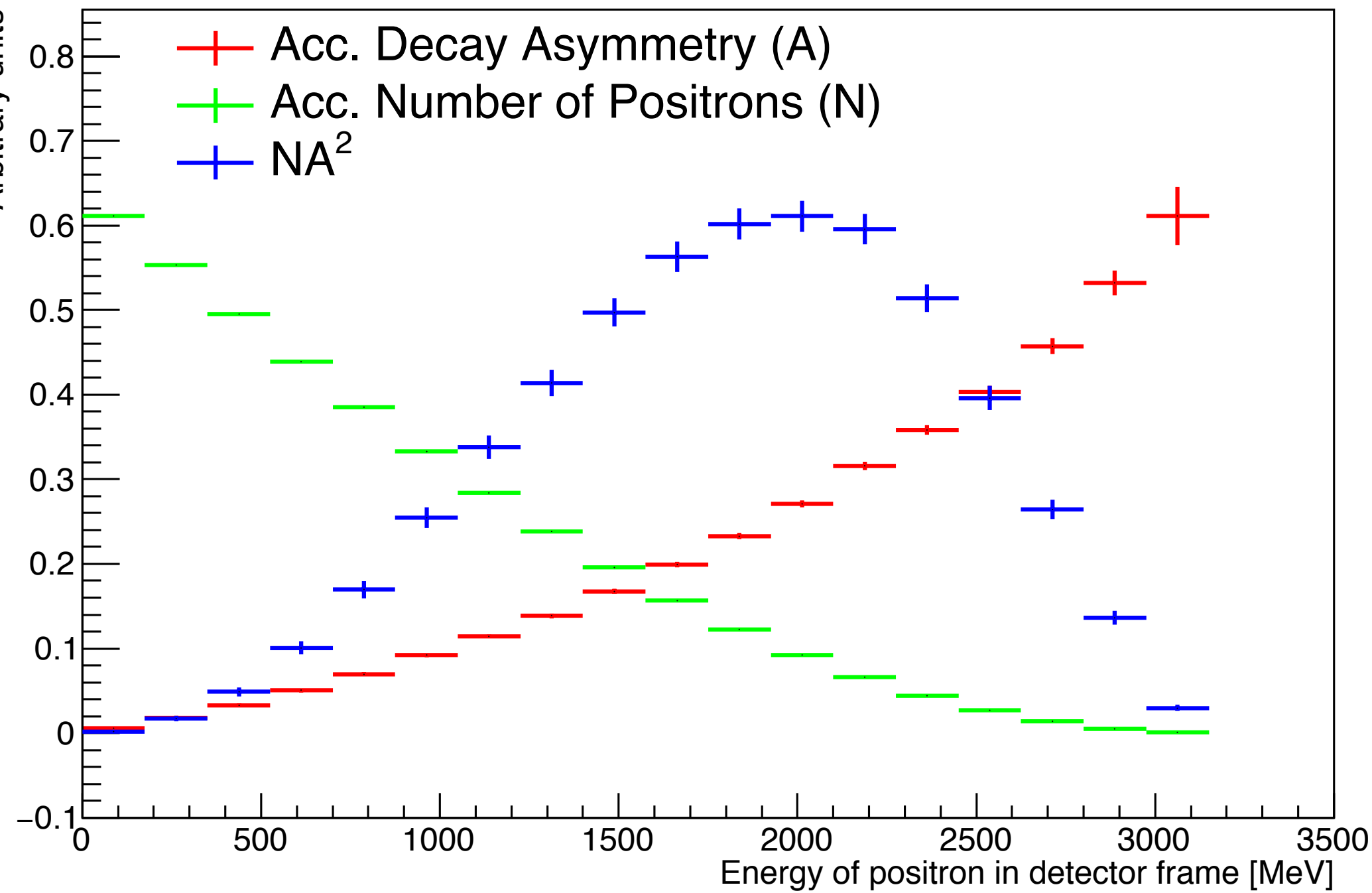
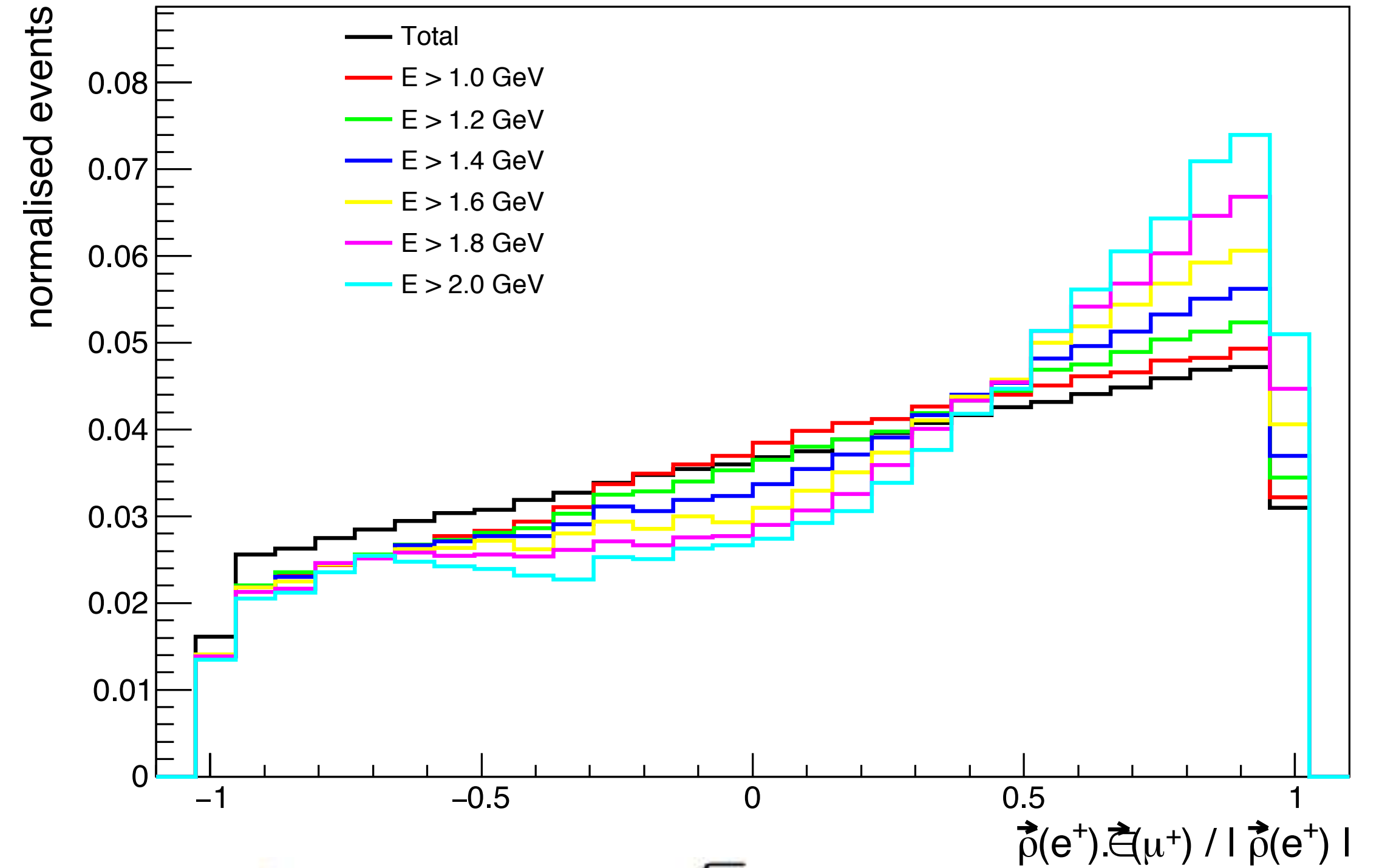
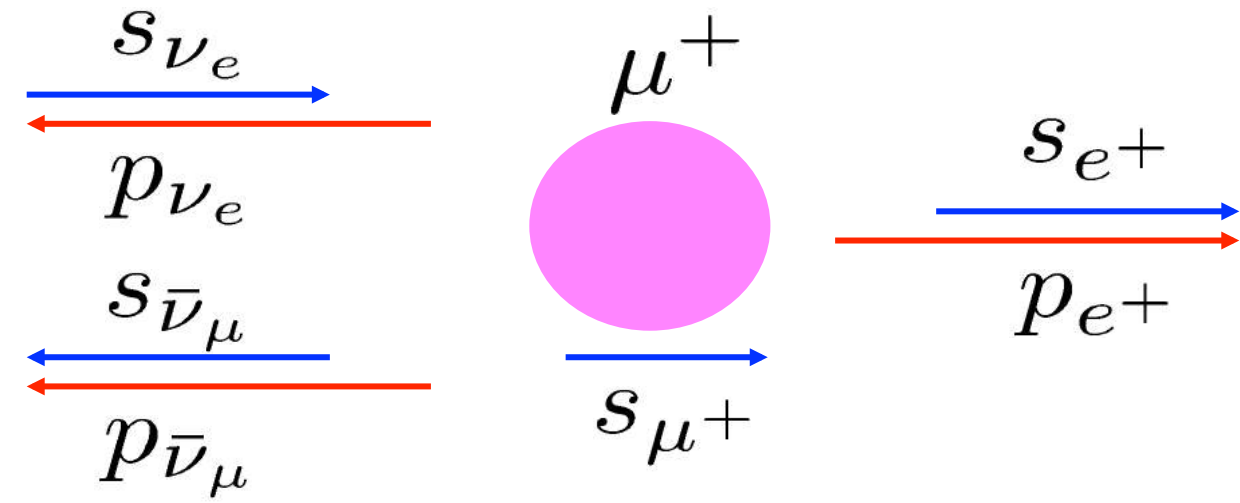
$$\vec{\omega}_a = \frac{e}{mc} \left[a_\mu \vec{B} - \left(a_\mu - \frac{1}{\gamma^2 - 1} \right) \vec{\beta} \times \vec{E} - a_\mu \left(\frac{\gamma}{\gamma + 1} \right) \left(\vec{\beta} \cdot \vec{B} \right) \vec{\beta} \right]$$

- This introduces an unwanted $\beta \times E$ term...
- ...unless $\gamma = 29.3$, then E-field term vanishes: we call this the “magic” momentum (3.094 GeV)
- Leaves 2 effects that we can’t ignore:
 - Not all muons are exactly at magic momentum
 - Some small degree of vertical motion of muons (reduces effective B-field)
- We use tracker and beam dynamics models to calculate the small corrections for these (< 1 ppm)

Measuring the muon spin...



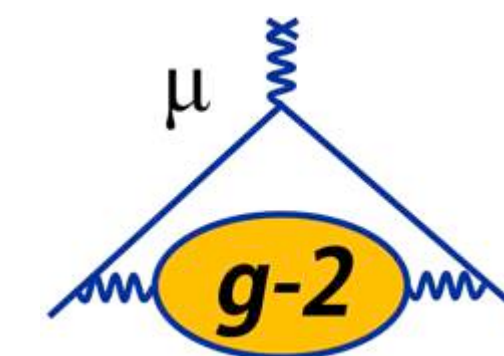
- e^+ preferentially emitted in direction of muon spin



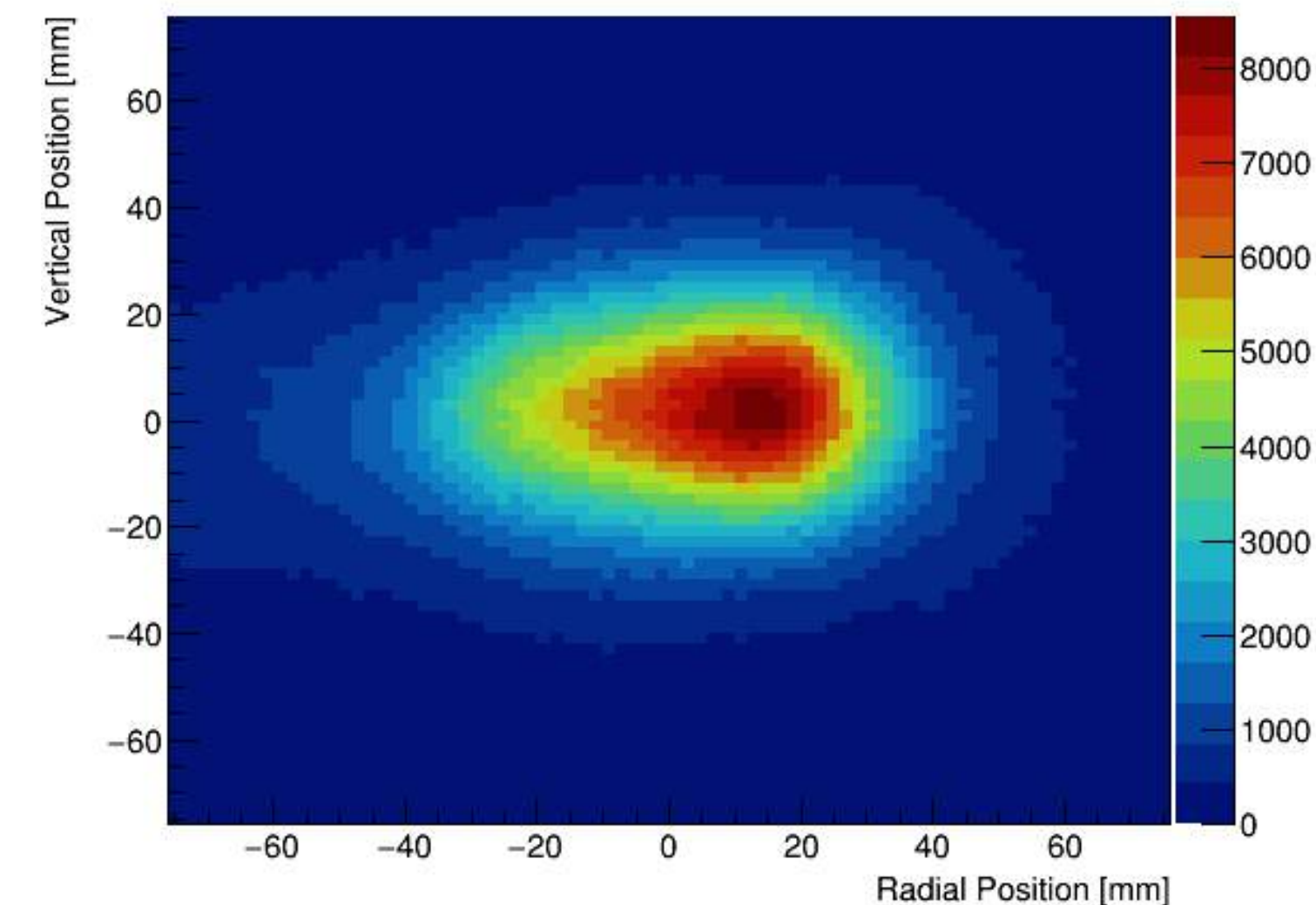
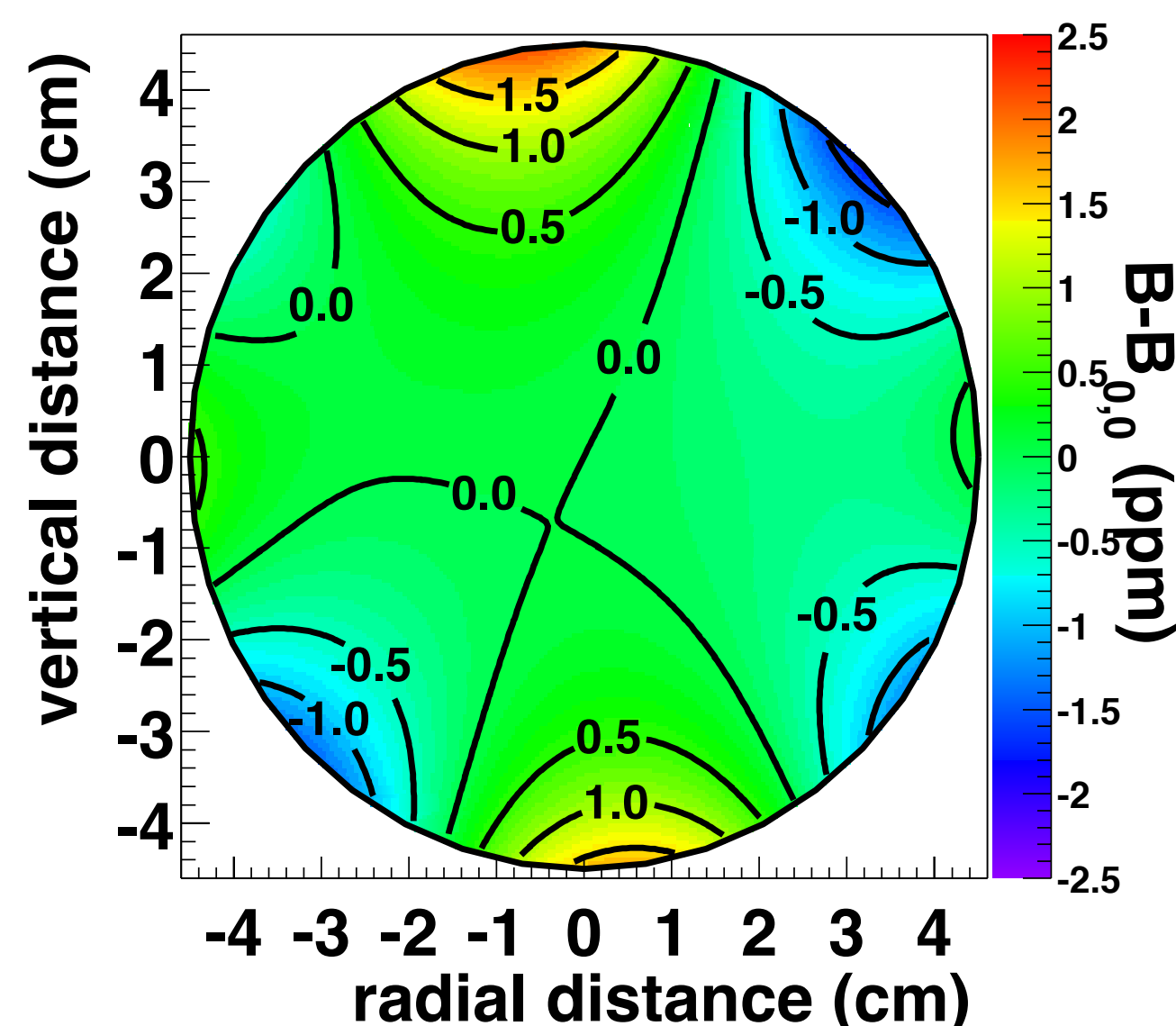
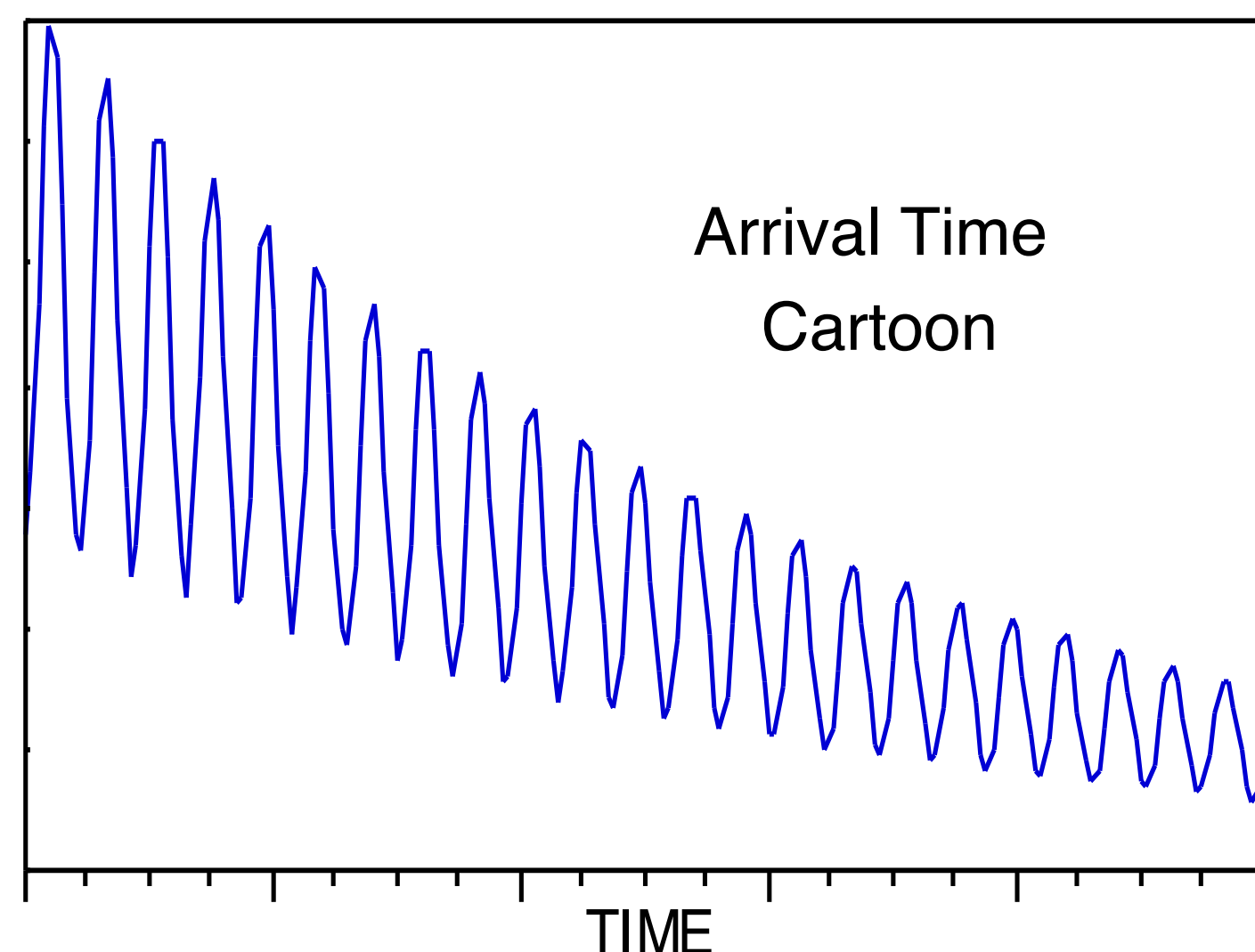
$$\frac{\delta\omega_a}{\omega_a} = \frac{\sqrt{2}}{2\pi f_a \tau_\mu \sqrt{NA^2}}$$

- Asymmetry is larger for high momentum e^+
- Optimal cut at $E \sim 1.8$ GeV

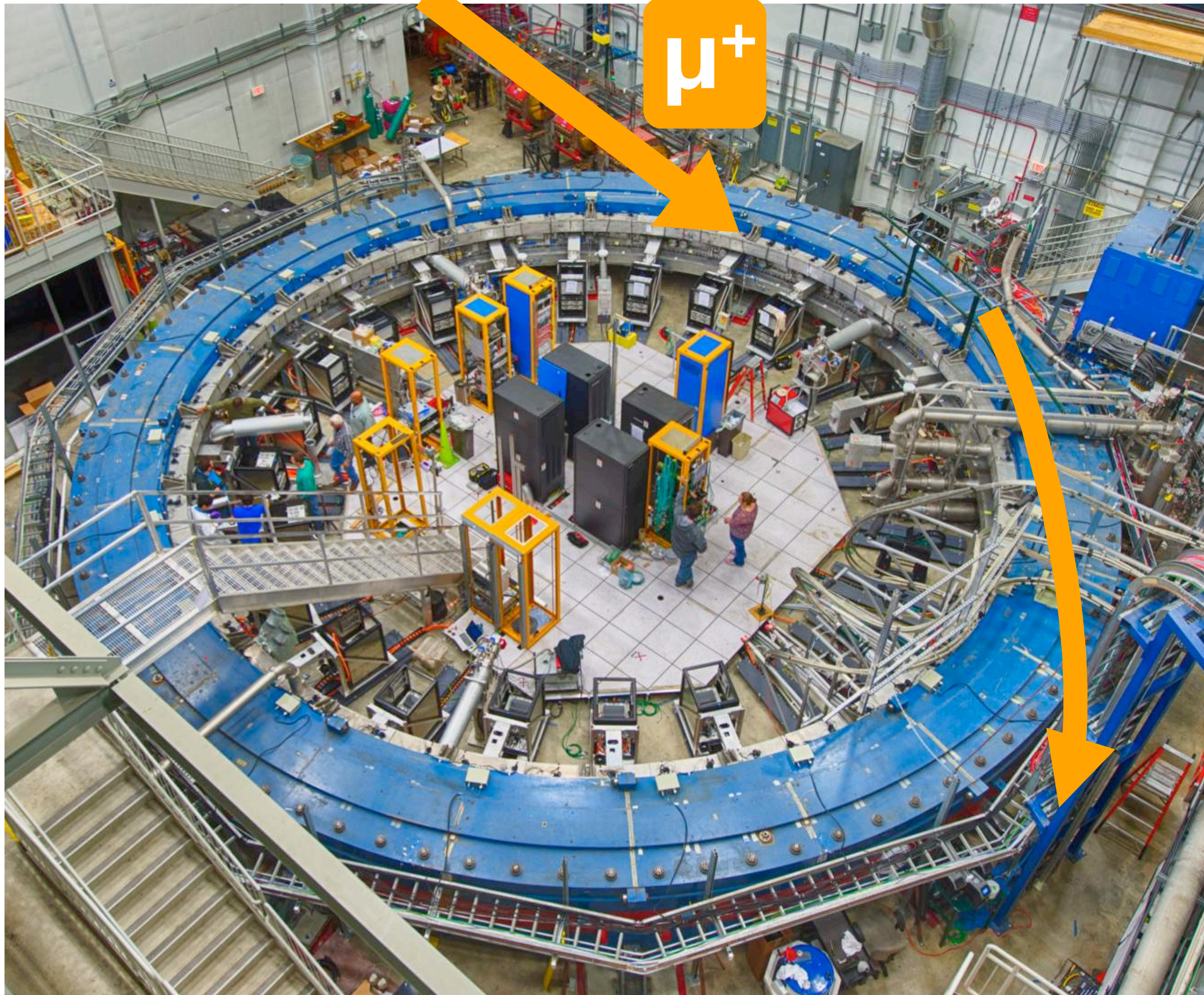
Measurement Principle



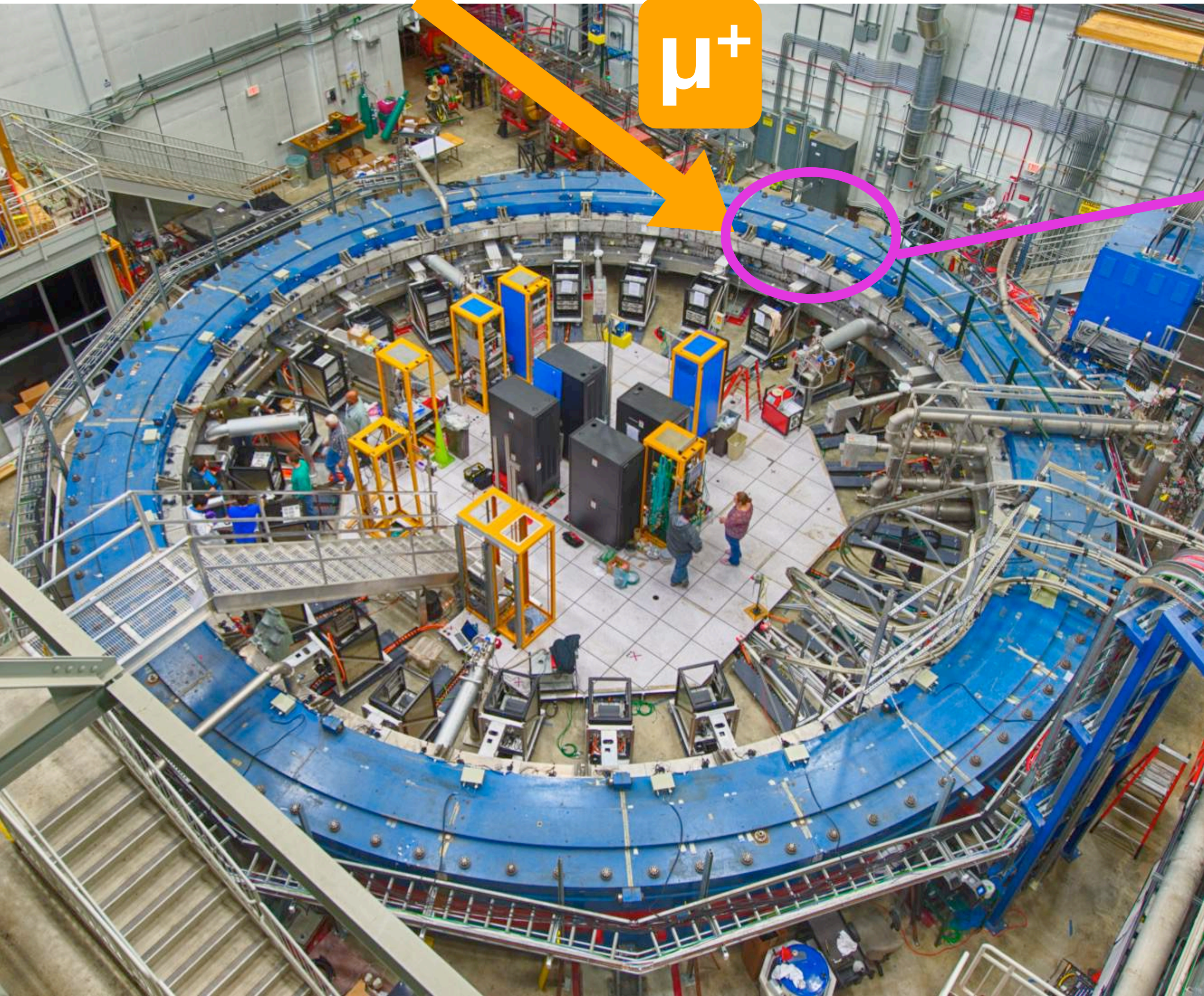
- Three ingredients to measure $a_\mu \sim (\omega_a / \tilde{\omega}_p)$
 - ω_a : Arrival time spectrum of high energy positrons
 - ω_p : Magnetic field in storage region measured by proton NMR
 - $\tilde{\omega}_p$: Muon distribution to get weighted magnetic field frequency



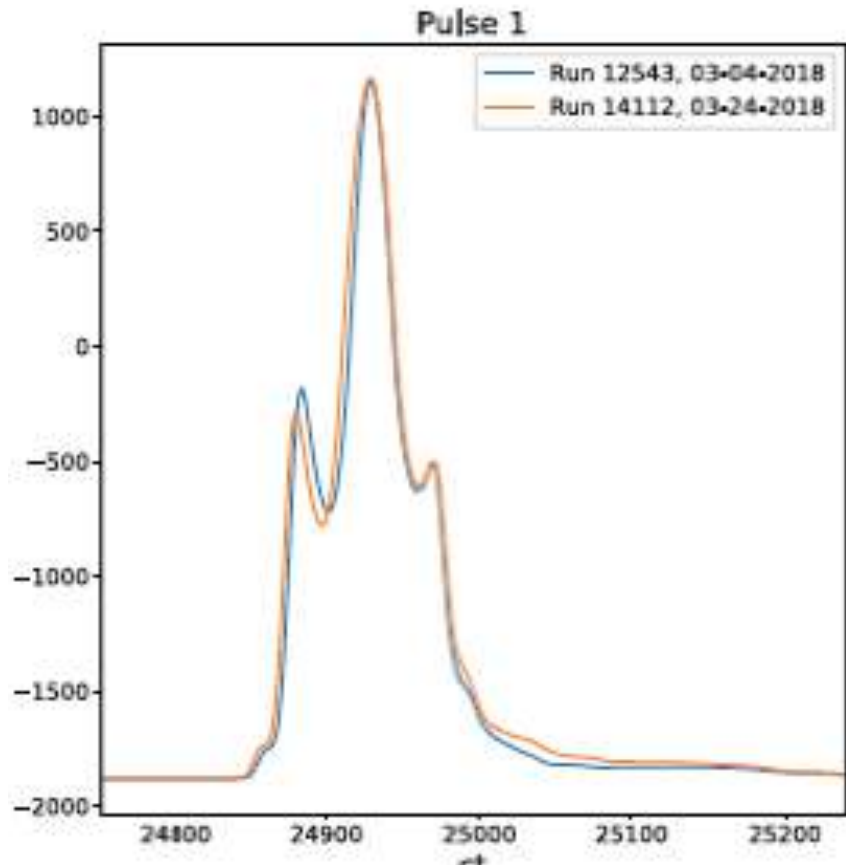
Muon Beam Injection



Muon Beam Injection



- Monitor beam profile before entrance with scintillating X and Y fibres
- Get time profile of beam using scintillating pad
- $\sim 125\text{ns}$ wide

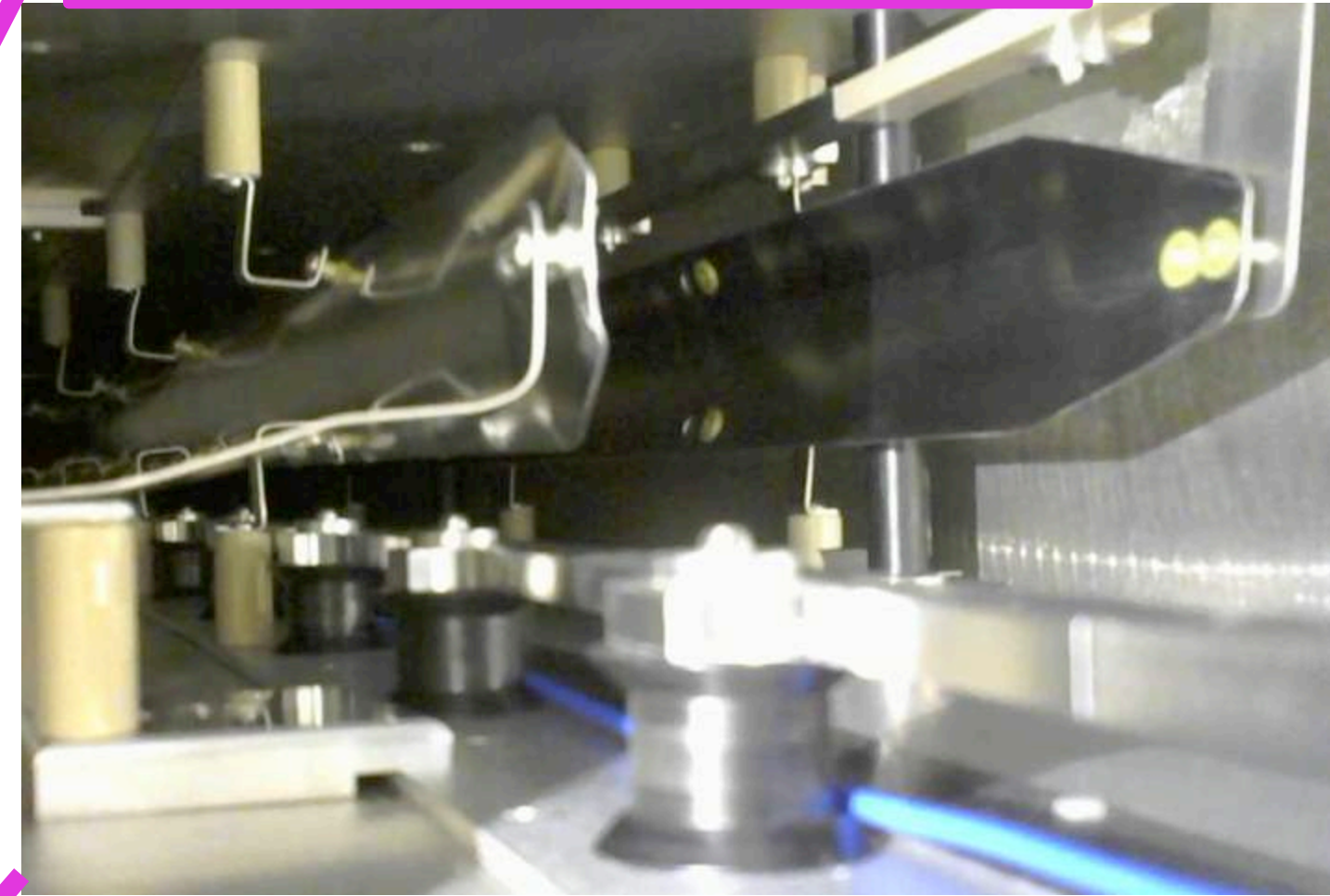


- Cancel B-field during injection using Inflector, so muons can get into the ring

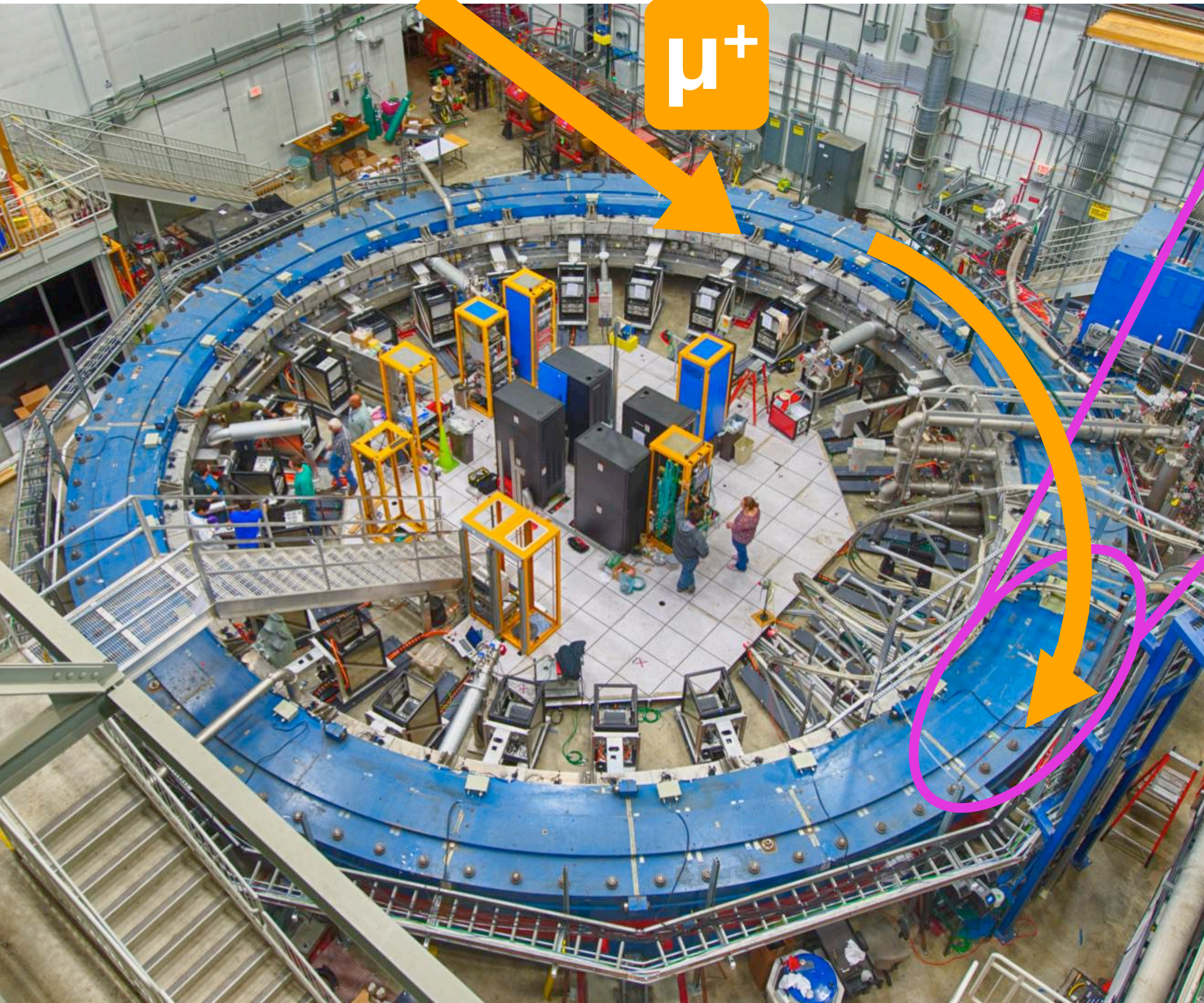
Muon Beam Injection



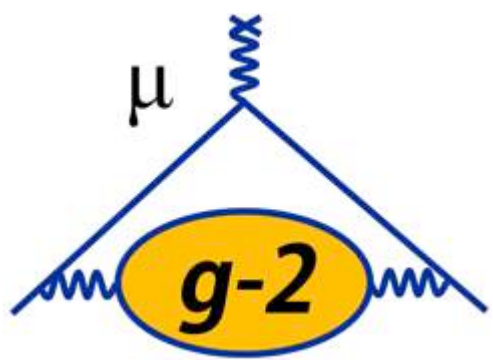
Kicker magnets



- After inflector, muons enter storage region at $r = 77$ mm outside central closed orbit
- Deliver pulse in < 149 ns to muon beam
- Steer muons onto stored orbit

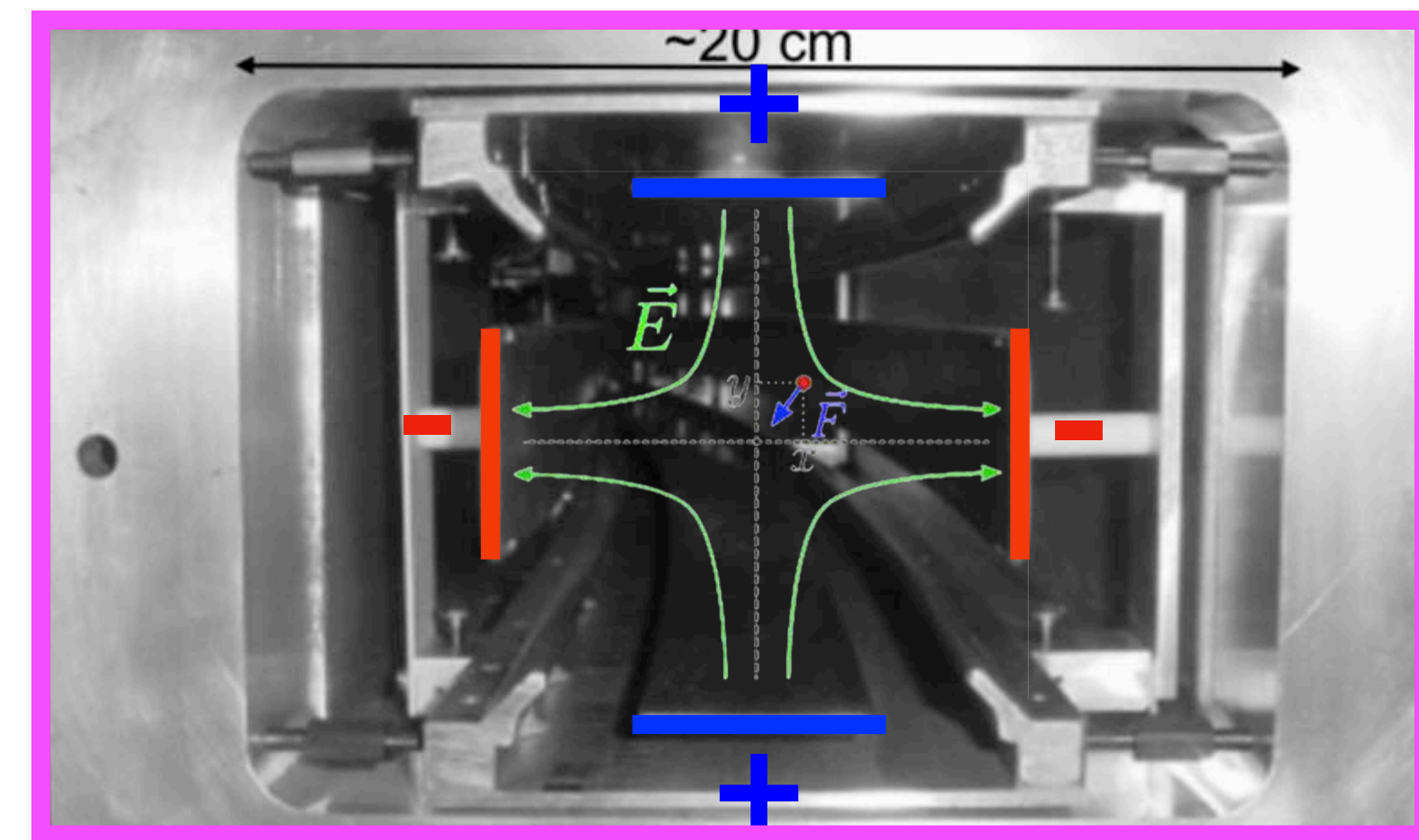


Muon Beam Injection



Electrostatic quadrupoles

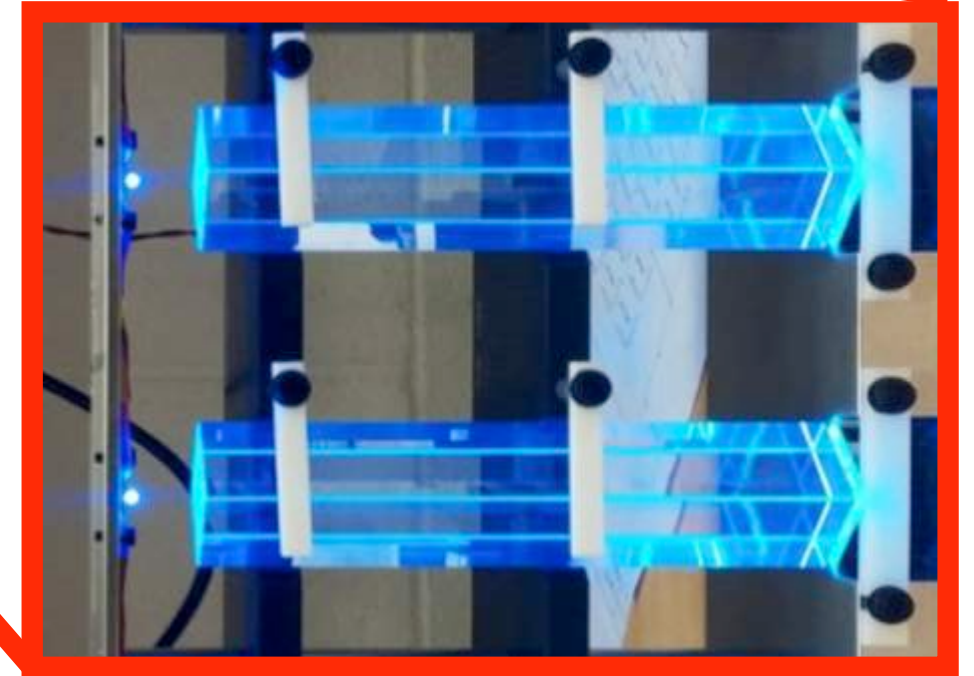
- Drive the muons towards the central part of storage region vertically
- Minimizes beam “breathing”, improves muon orbit stability
- Aluminum electrodes cover $\sim 43\%$ of total circumference



Muon Beam Injection



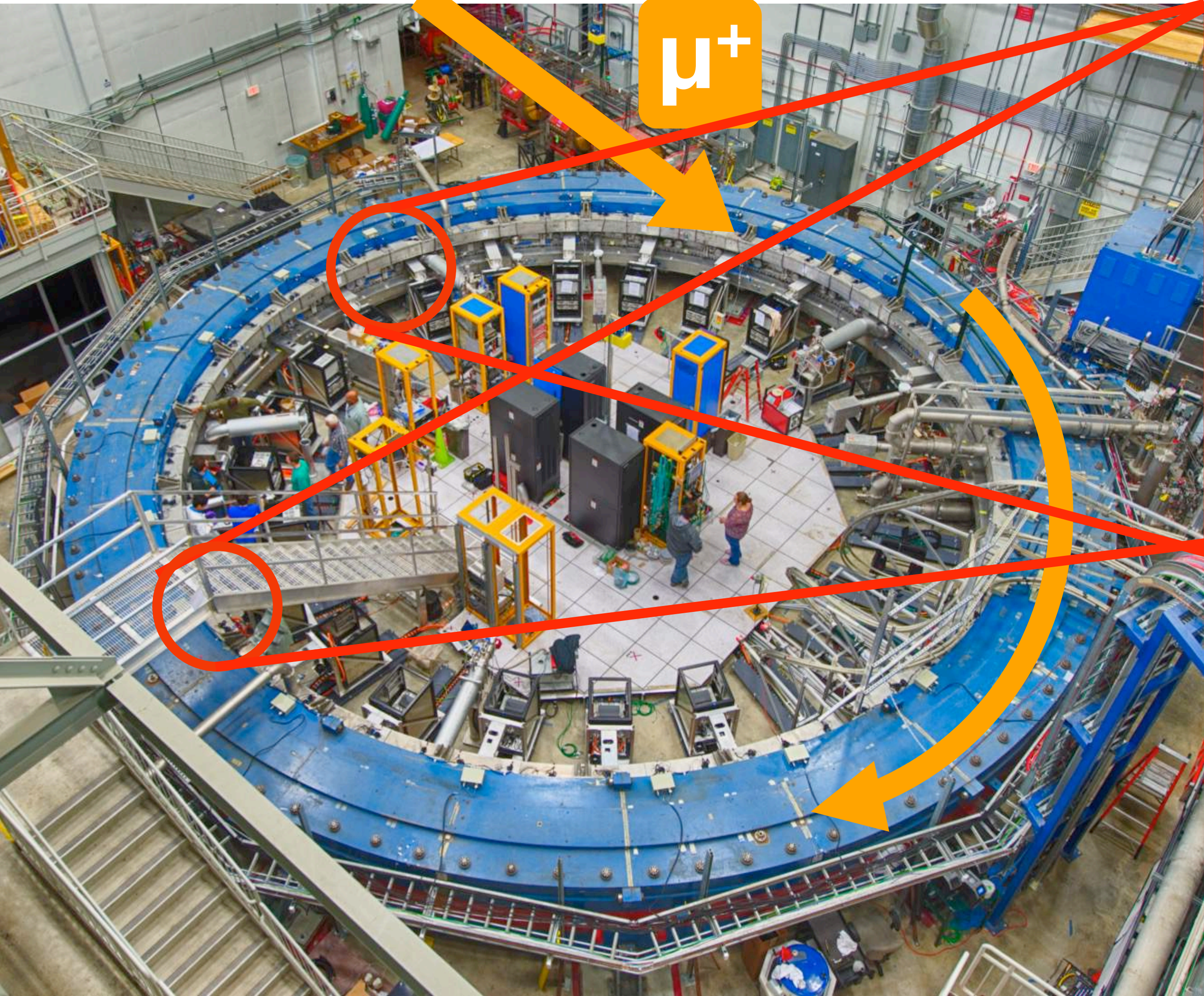
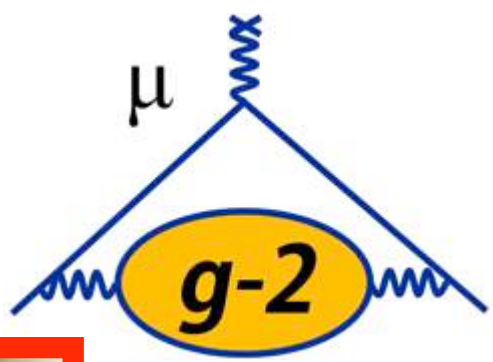
μ^+



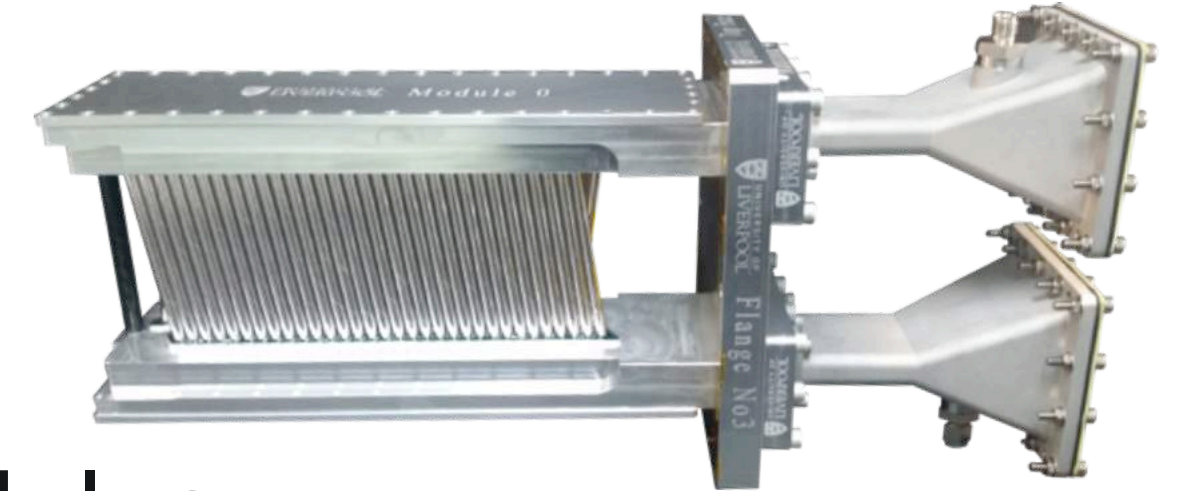
24 segmented PbF₂ crystal calorimeters

- Each crystal array of 6 x 9 PbF₂ crystals - 2.5 x 2.5 cm² x 14 cm (15X₀)
- Readout by SiPMs to 800 MHz WFDs (1296 channels in total)

Muon Beam Injection



2 Tracking stations

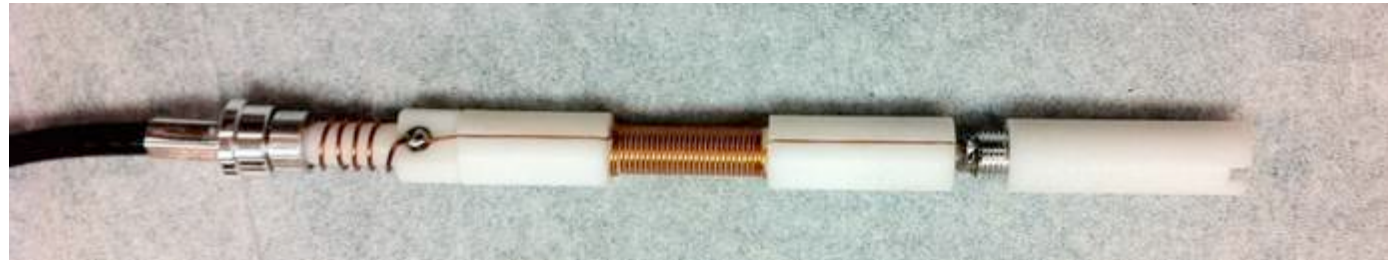


- Each contain 8 modules
- 128 gas filled straws in each module
- Traceback positrons to their decay point

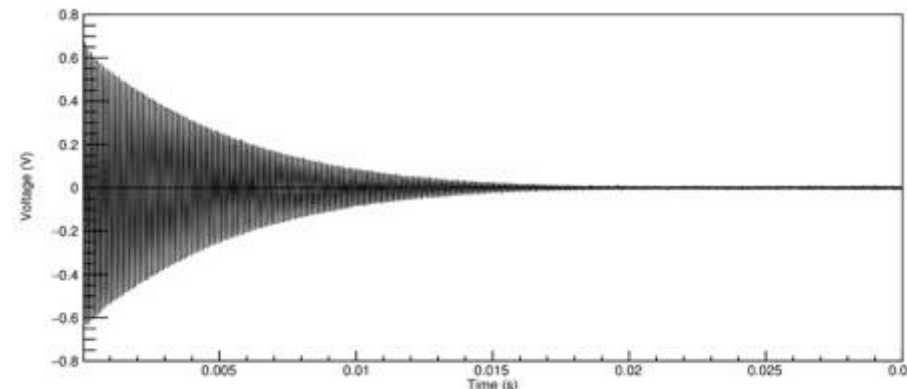
Monitoring and Mapping the Magnetic Field



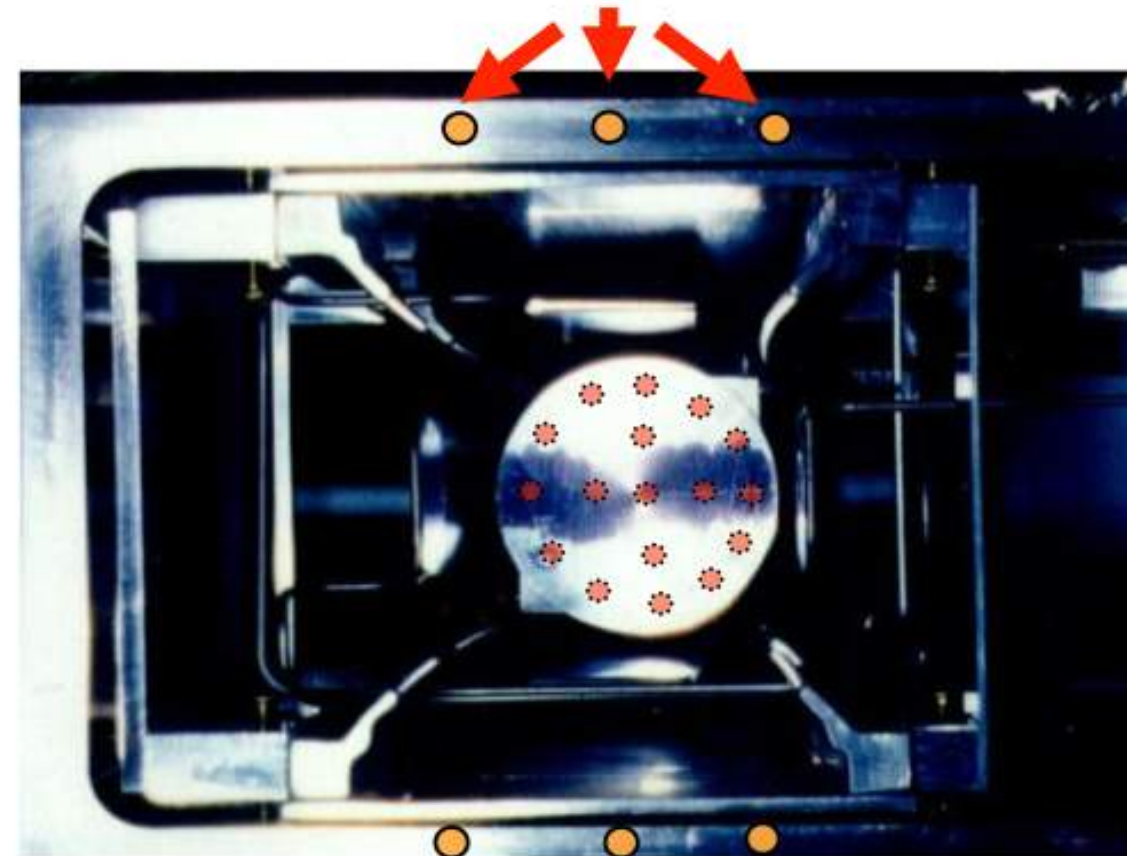
Pulsed NMR



- Deliver $\pi/2$ pulse to probe, induce & record the free-induction decay (FID)
- Extracted frequency precision: 10 ppb/FID



Fixed probes on vacuum chambers



- Measure field while muons are in ring – 378 probes **outside** storage region

Trolley matrix of 17 NMR probes



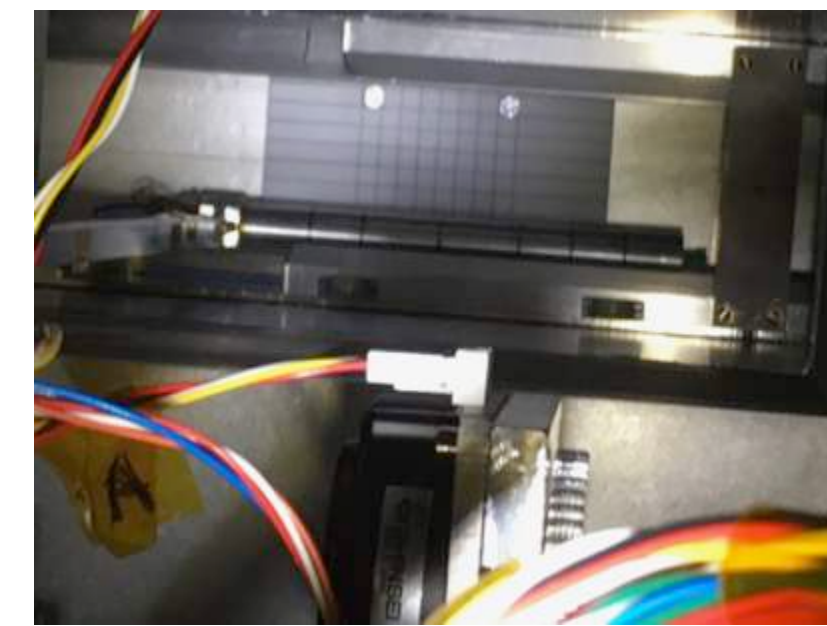
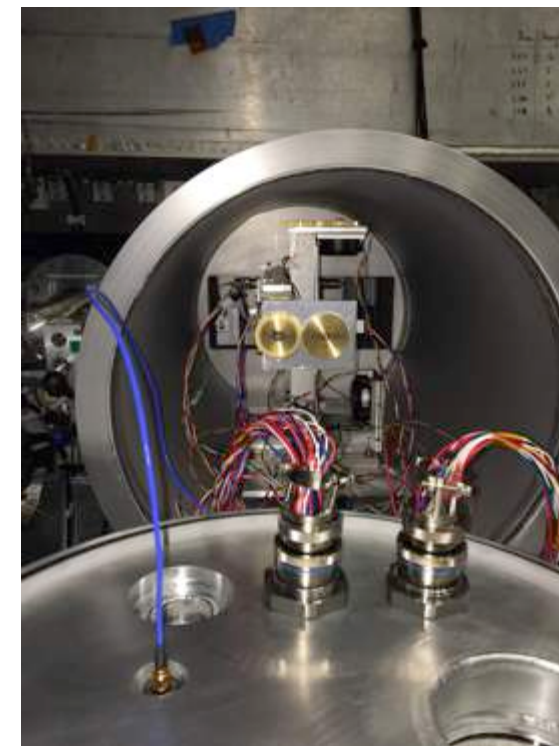
Electronics,
Microcontroller,
Communication

Position of NMR probes

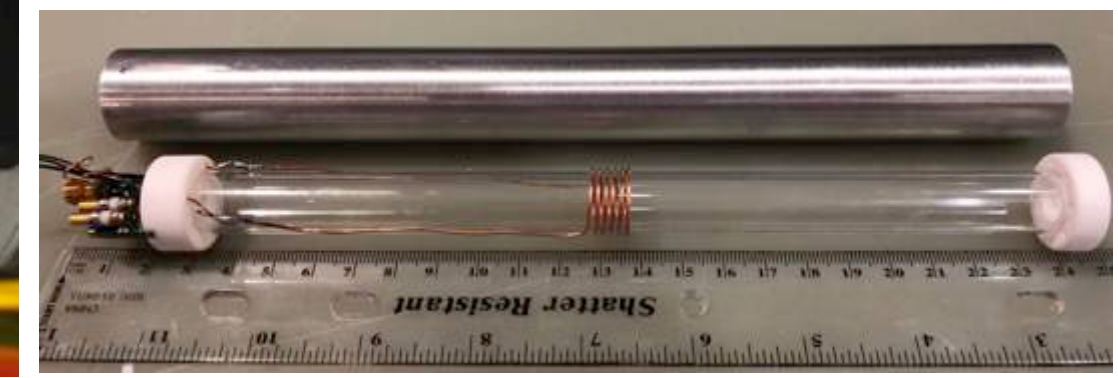
- Measure field in storage region during **specialized runs** when **muons are not being stored**

- **Trolley** probes **calibrated to free-proton Larmor frequency**

- Calibrate trolley probes using a special probe that uses a water sample
- Measurements in specially-shimmed region of ring

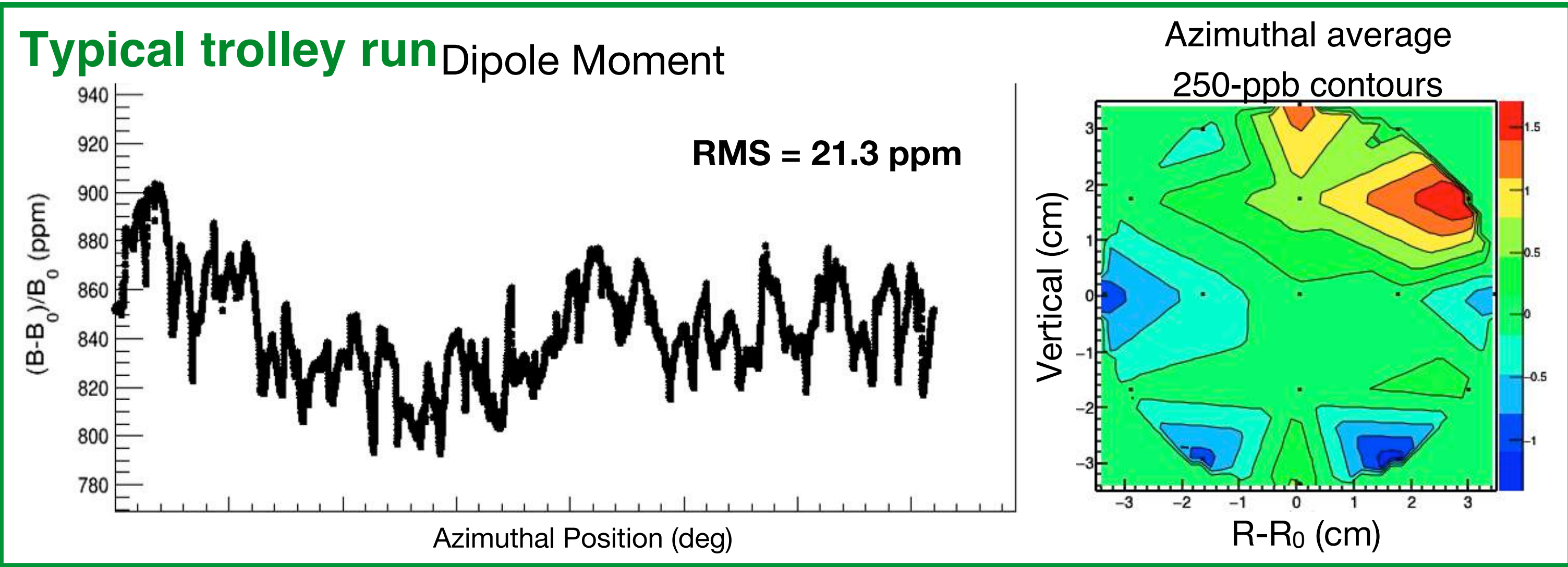
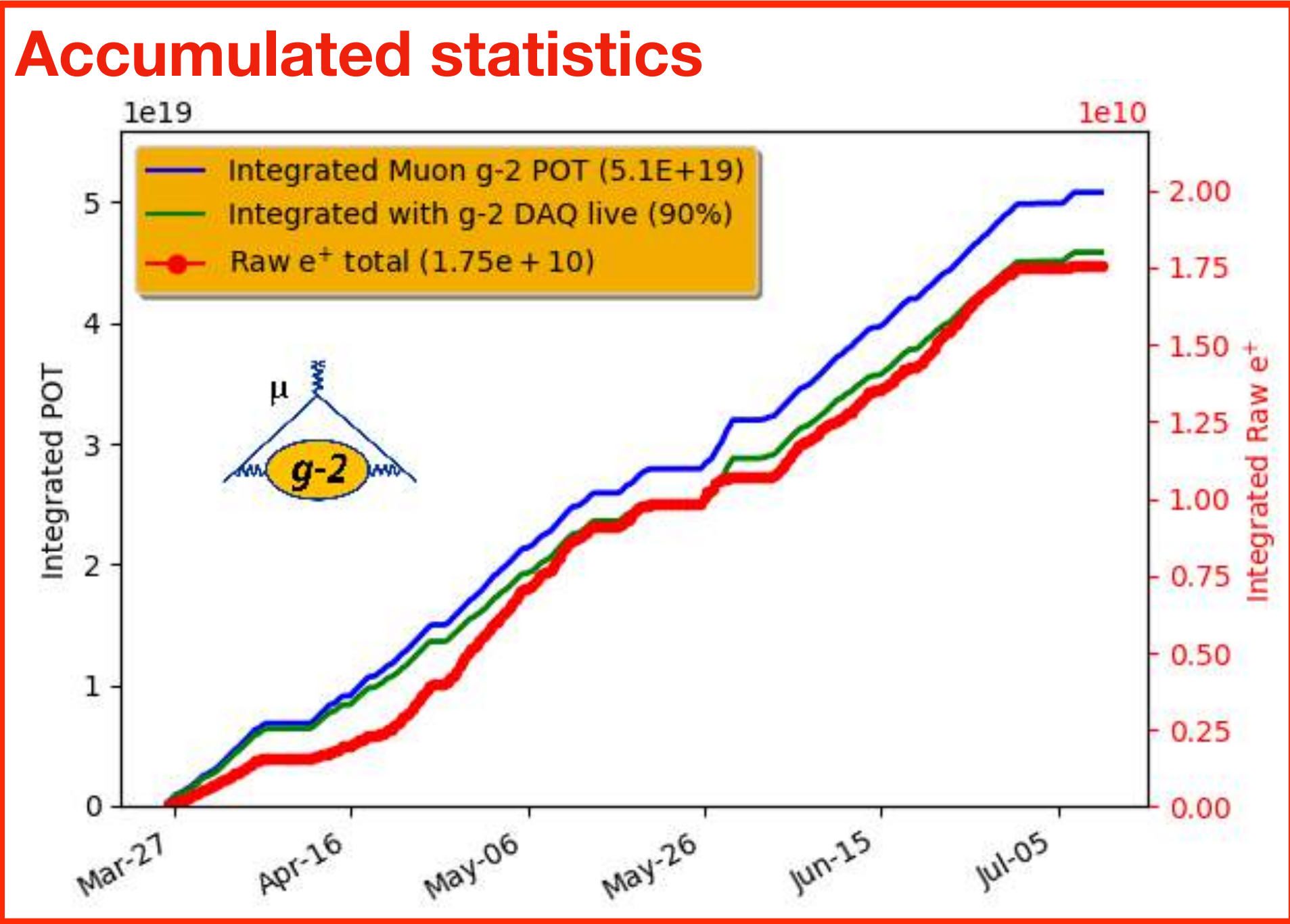


Plunging Probe



Run 1 Overview

- Data taking period: April—July 2018
- Accumulated $\sim 1.4 \times$ BNL statistics (after data quality cuts) — $\delta\omega_a(\text{stat}) \sim 350 \text{ ppb}$
- Field uniformity $\sim 2x$ better than BNL



Systematic Uncertainty Comparison: E821 and E989



$$a_{\mu} = \frac{\omega_a}{\tilde{\omega}_p} \frac{\mu_p}{\mu_e} \frac{m_{\mu}}{m_e} \frac{g_e}{2}$$

- New hardware (calorimeters, trackers, NMR)
- Improved analysis techniques
- Reduce uncertainties by at least a factor of 2.5

ω_a Goal: Factor of 3 Improvement		
Category	E821 (ppb)	E989 Goal (ppb)
Gain Changes	120	20
Lost Muons	90	20
Pileup	80	40
Horizontal CBO	70	< 30
E-field/pitch	110	30
Quadrature Sum	214	70

ω_p Goal: Factor of 2.5 Improvement		
Category	E821 (ppb)	E989 Goal (ppb)
Field Calibration	50	35
Trolley Measurements	50	30
Fixed Probe Interpolation	70	30
Muon Convolution	30	10
Time-Dependent Fields	–	5
Others	100	50
Quadrature Sum	170	70

Run-1 Analysis Status — ω_a

Run 1 Analysis Status: ω_a



- Account for a number of effects that can affect the extraction of ω_a

$$N(t) = N_0 e^{-t/\tau} [1 - A \cos(\omega_a t + \phi)]$$

Detector effects

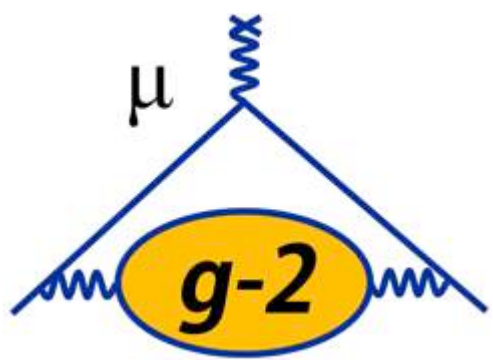
Gain instability

- Gain changes over time in calorimeters affects phase of signal: $N \rightarrow N(t)$, $A \rightarrow A(t)$, $\phi \rightarrow \phi(t)$
- Laser system provides corrections

Event pileup

- Low-energy events can mimic high-energy events in calorimeter
- Spin precession phase varies with energy — apparent high-energy decay carries phase of low-energy decays

Run 1 Analysis Status: ω_a

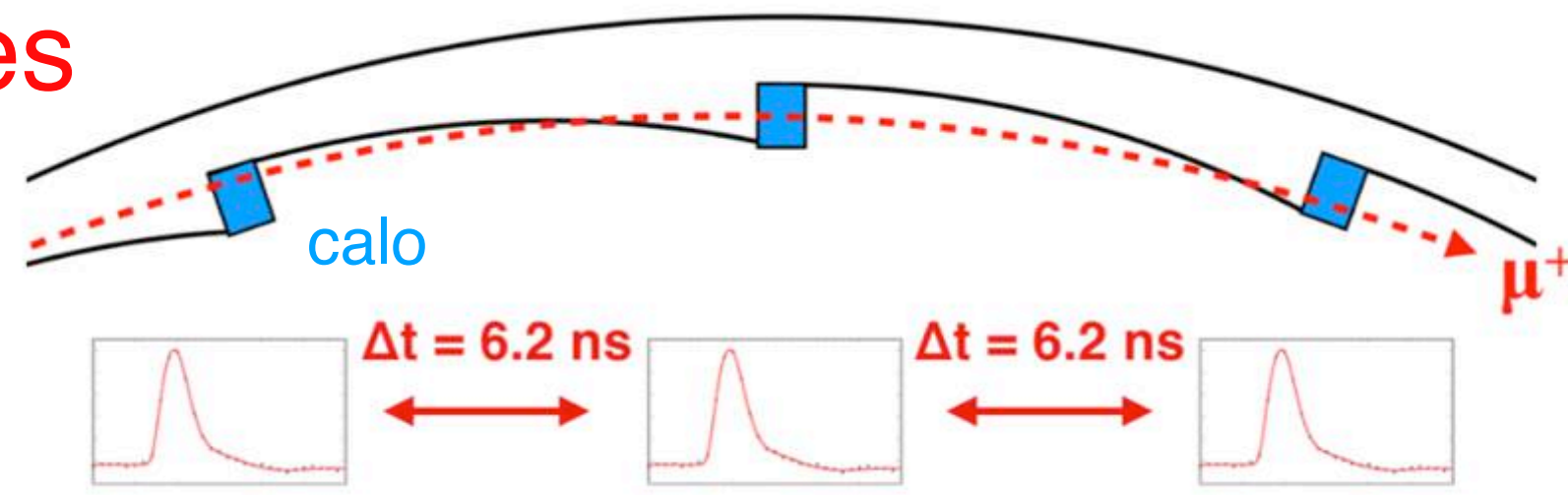


- Account for a number of effects that can affect the extraction of ω_a

$$N(t) = N_0 e^{-t/\tau} [1 - A \cos(\omega_a t + \phi)]$$

Beam dynamics

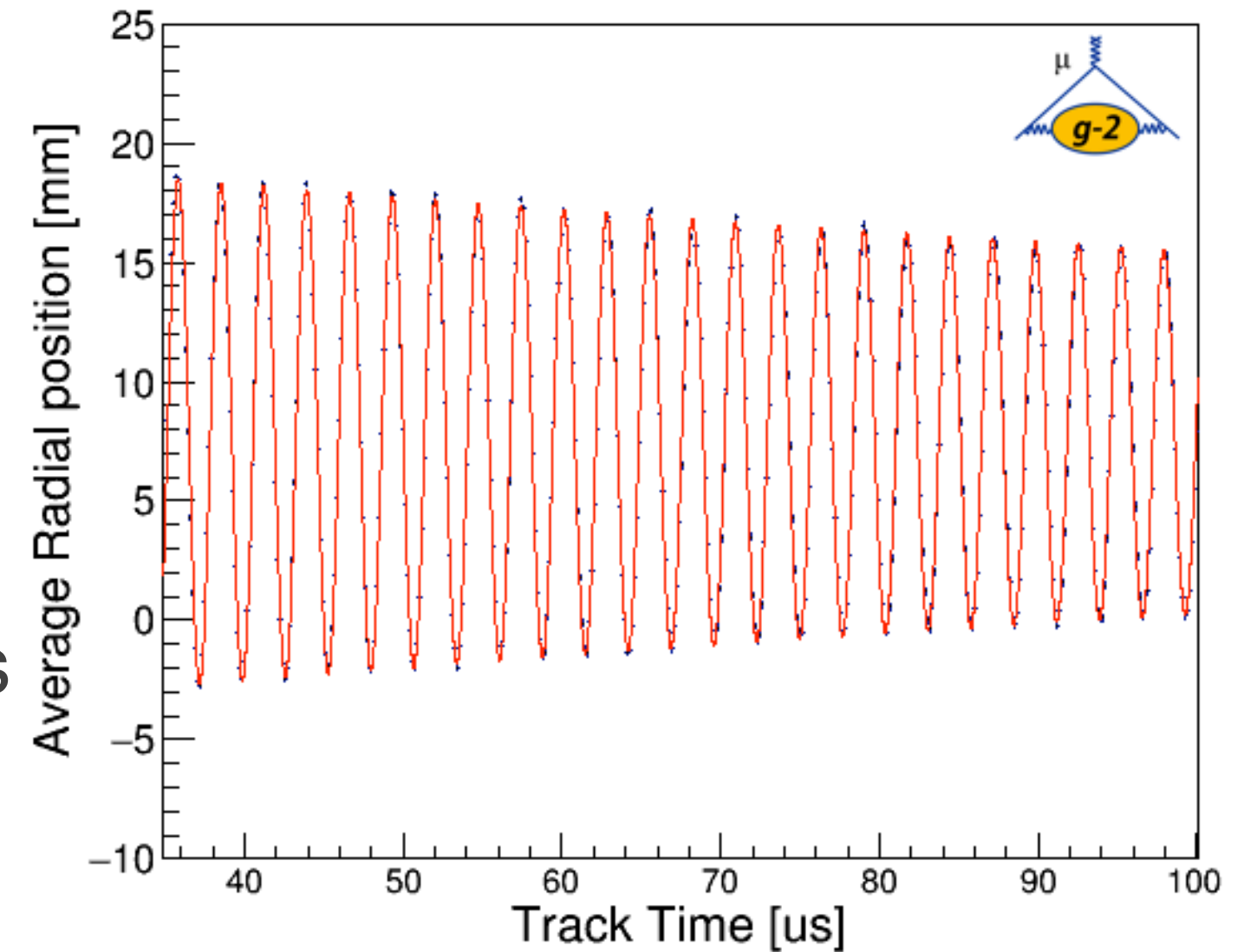
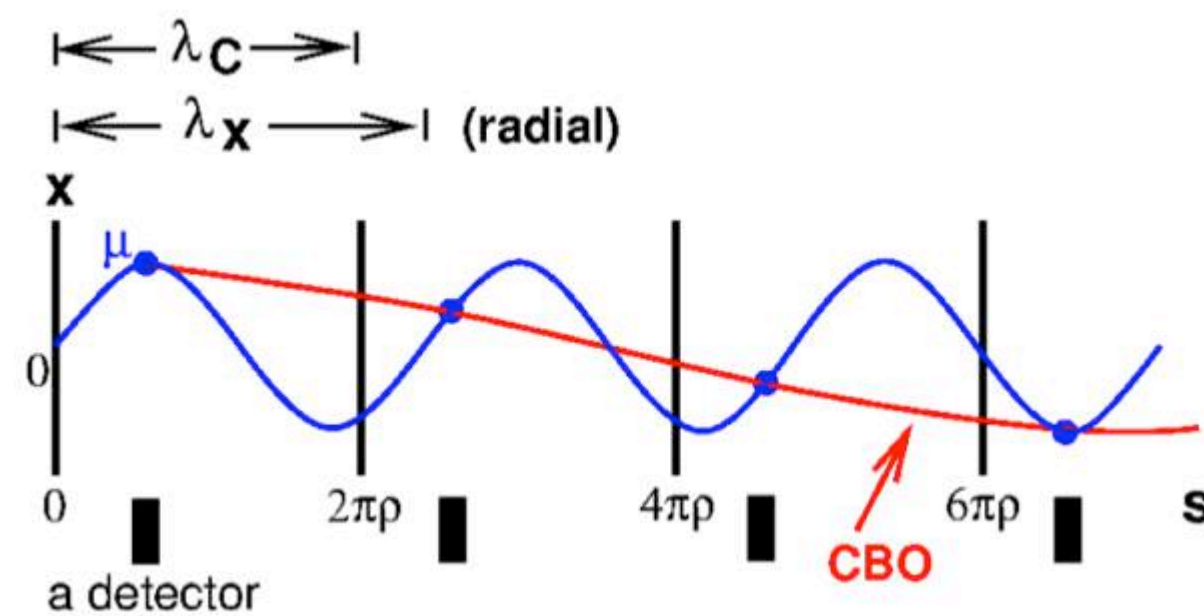
Muon losses



- Muons can leave storage ring by decaying or escaping
- Exhibit specific signature in multiple calorimeters
- Amplitude N_0 scaled by:

$$\Lambda(t) = 1 - K_{\text{loss}} \int_0^t e^{t'/\tau} L(t') dt'$$

Coherent betatron oscillations (CBO)



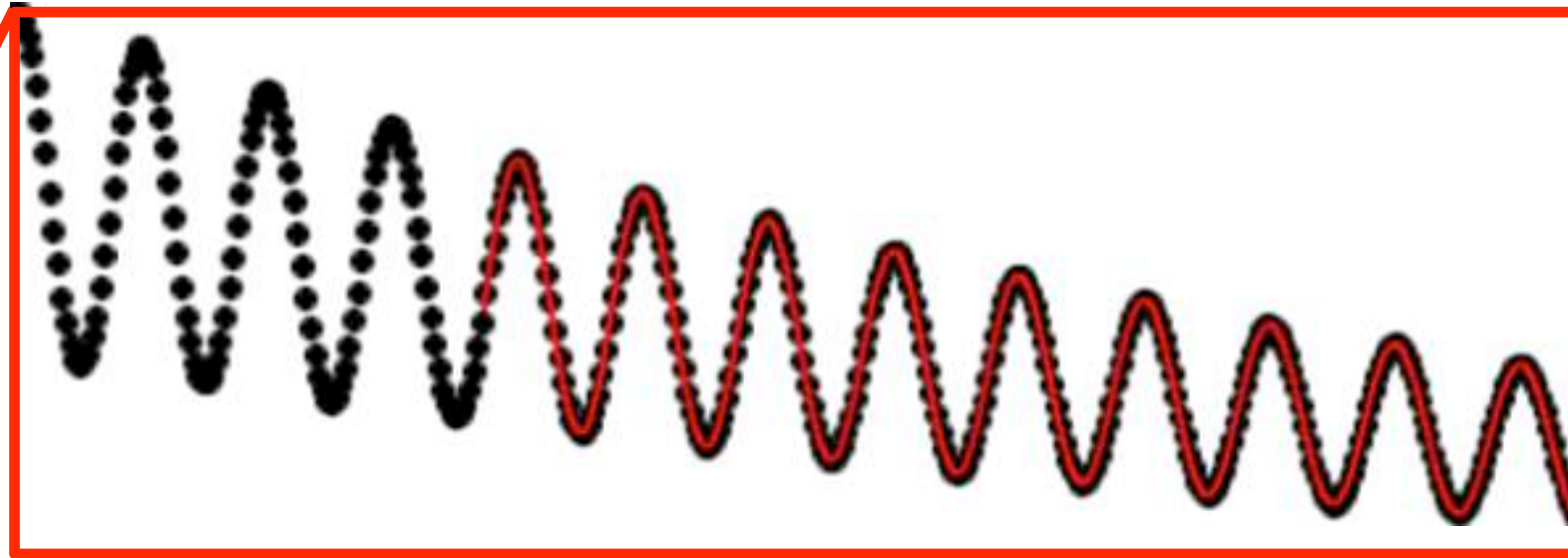
- Acceptance of calorimeters affected by coherent radial beam motion
- Amplitude N_0 scaled by:

$$C(t) = 1 - e^{-t/\tau_{\text{CBO}}} A_1 \cos(\omega_{\text{CBO}} t + \phi_1)$$

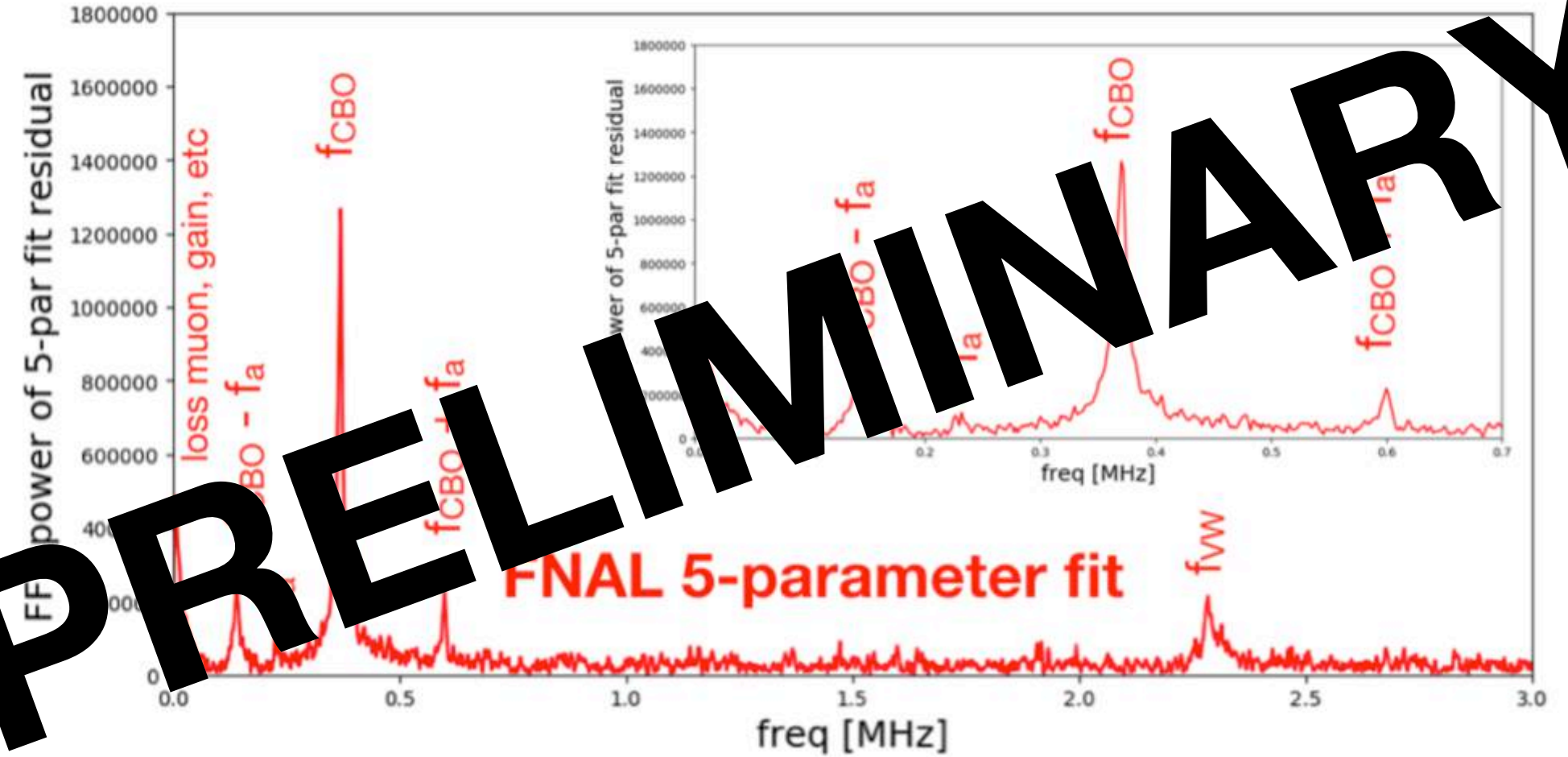
Run 1 Analysis Status: ω_a



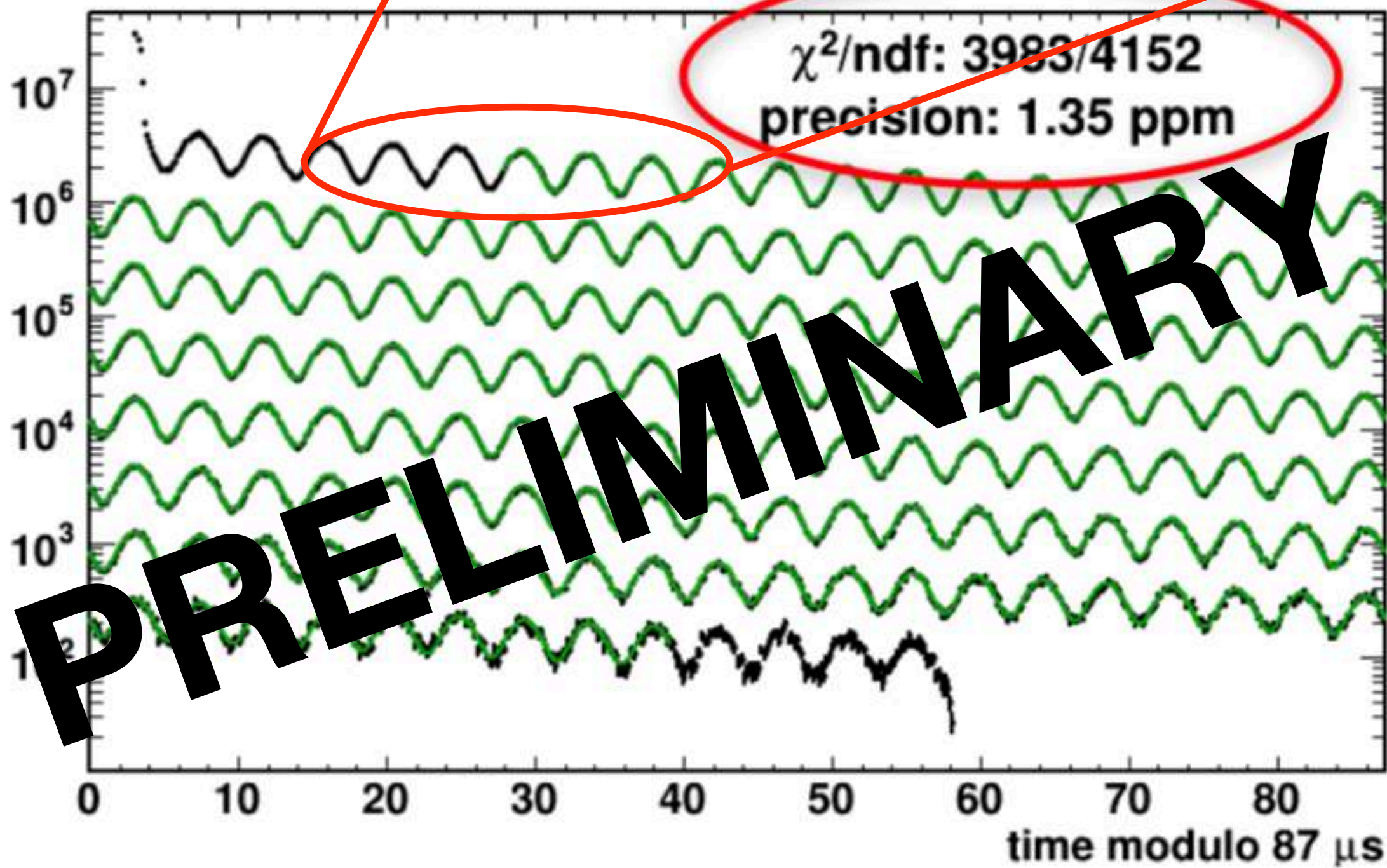
Simple five-parameter fit



FFT of fit residuals

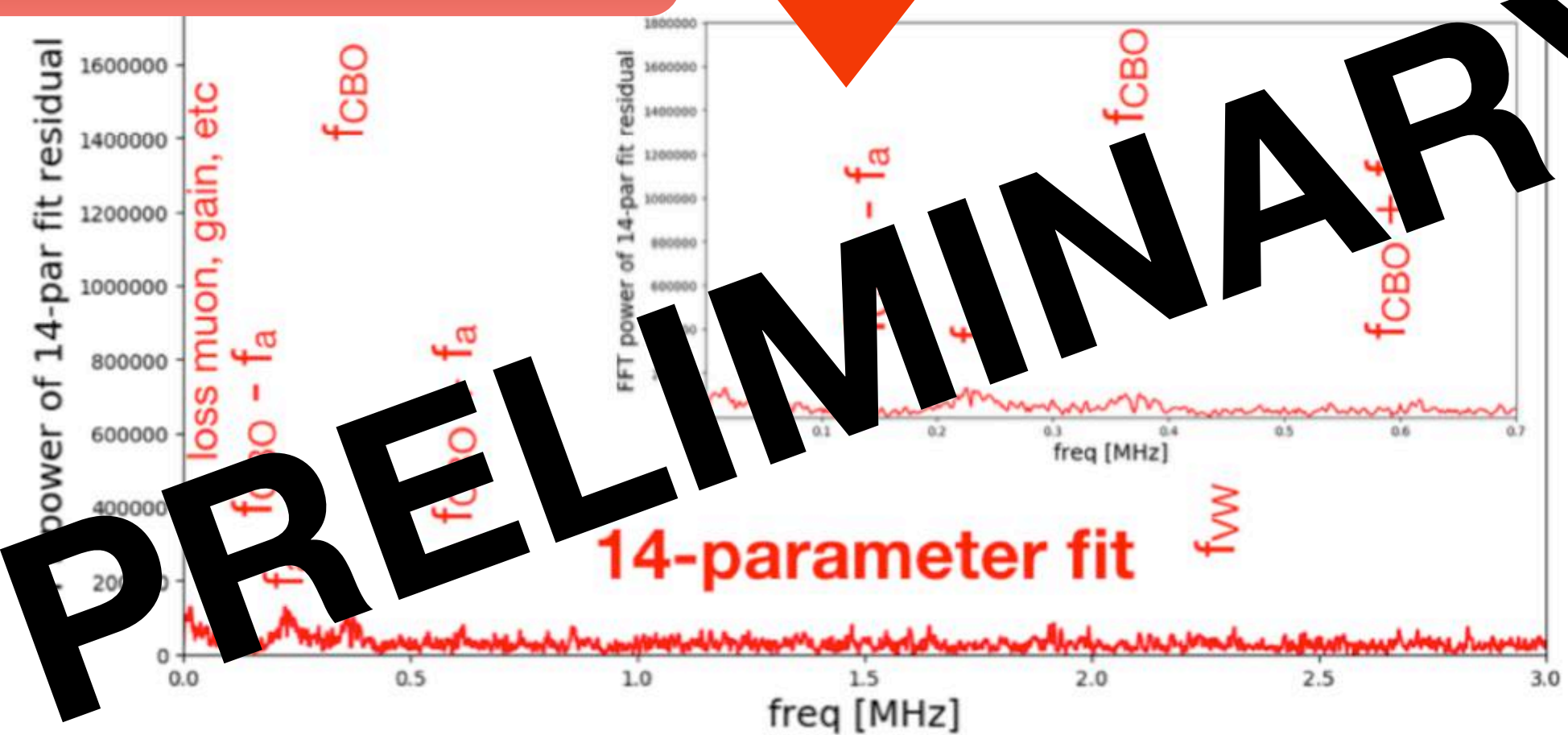


PRELIMINARY



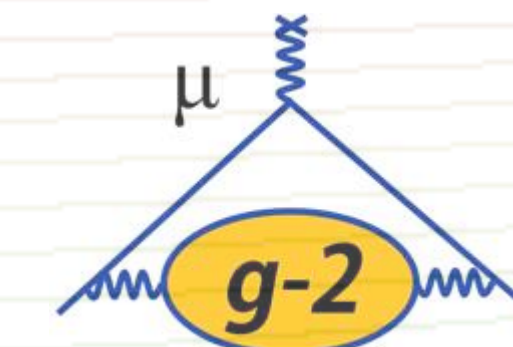
PRELIMINARY

Big improvements when accounting for CBO, lost muons,...

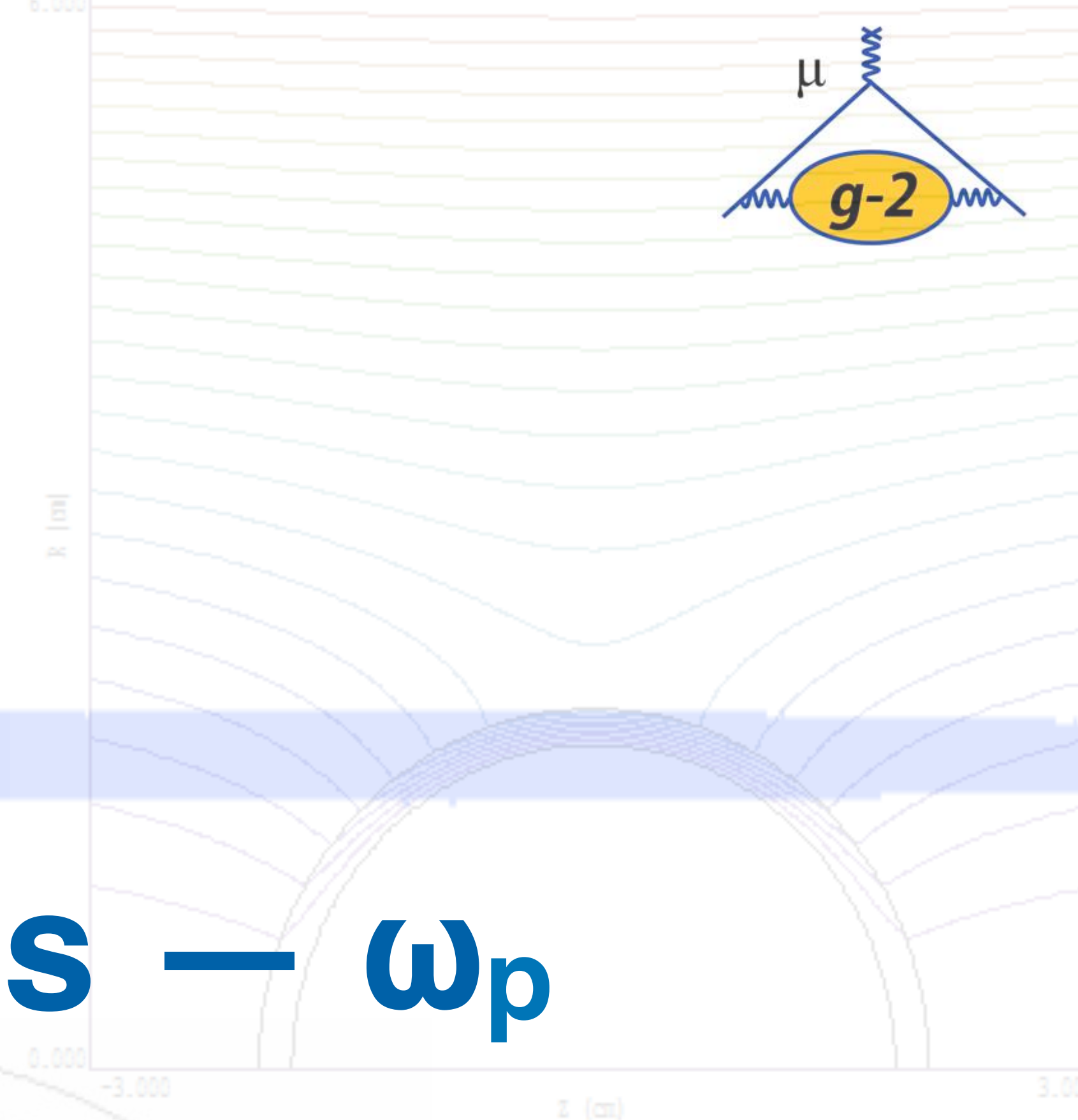
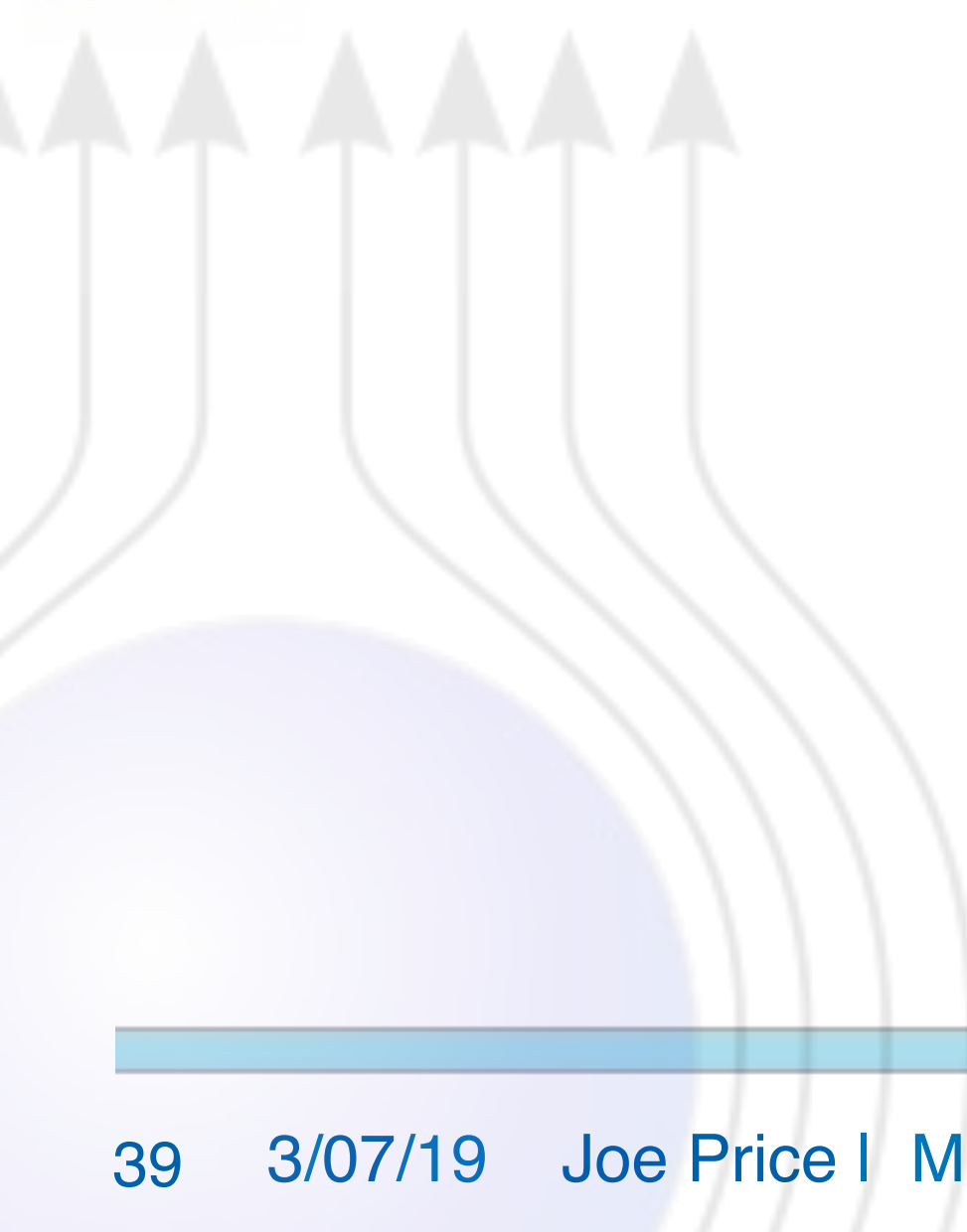


PRELIMINARY

Paramagnetism



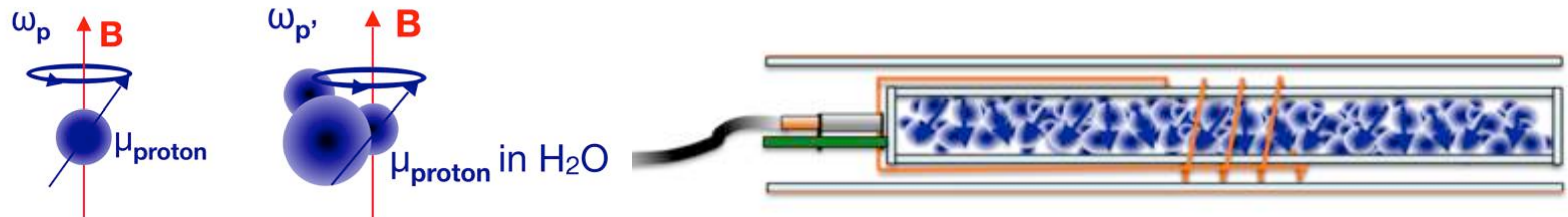
Run-1 Analysis Status — ω_p



Run 1 Analysis Status: ω_p — Field Calibration



- In the experiment, need to extract ω_p ; however, don't have free protons
 - Need a calibration
- Field at the proton differs from the applied field



$$\omega_p^{\text{meas}} = \omega_p^{\text{free}} \left[1 - \sigma(\text{H}_2\text{O}, T) - \left(\epsilon - \frac{4\pi}{3} \right) \chi(\text{H}_2\text{O}, T) - \delta_m \right]$$

Protons in H₂O molecules, diamagnetism of electrons screens protons => local B changes

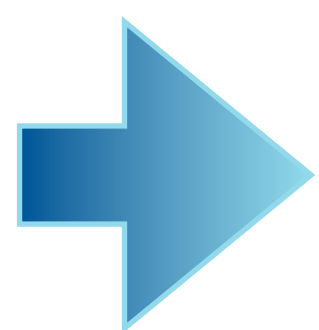
- **Known to 2.5 ppb**

Magnetic susceptibility of water gives shape-dependent perturbation

- $\epsilon = 4\pi/3$ (sphere), 2π (cylinder) when probe is perpendicular to B
- **Known to 5 ppb**

Magnetization of probe materials perturbs the field at site of protons

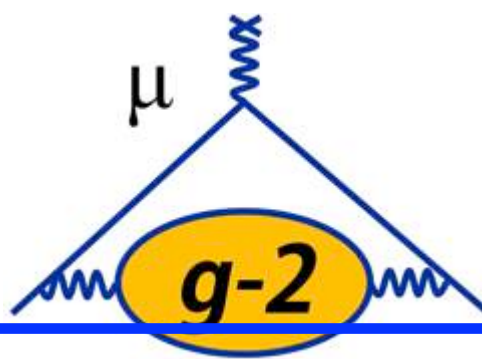
- **Measured to 6.5 ppb**



Goal: Determine total correction to ≤ 35 ppb accuracy

These are **static** corrections; need to worry about **dynamic** ones too (radiation damping, RF coil inhomogeneity, time dependence of gradients, ...)

Run 1 Analysis Status: ω_p — Field Calibration



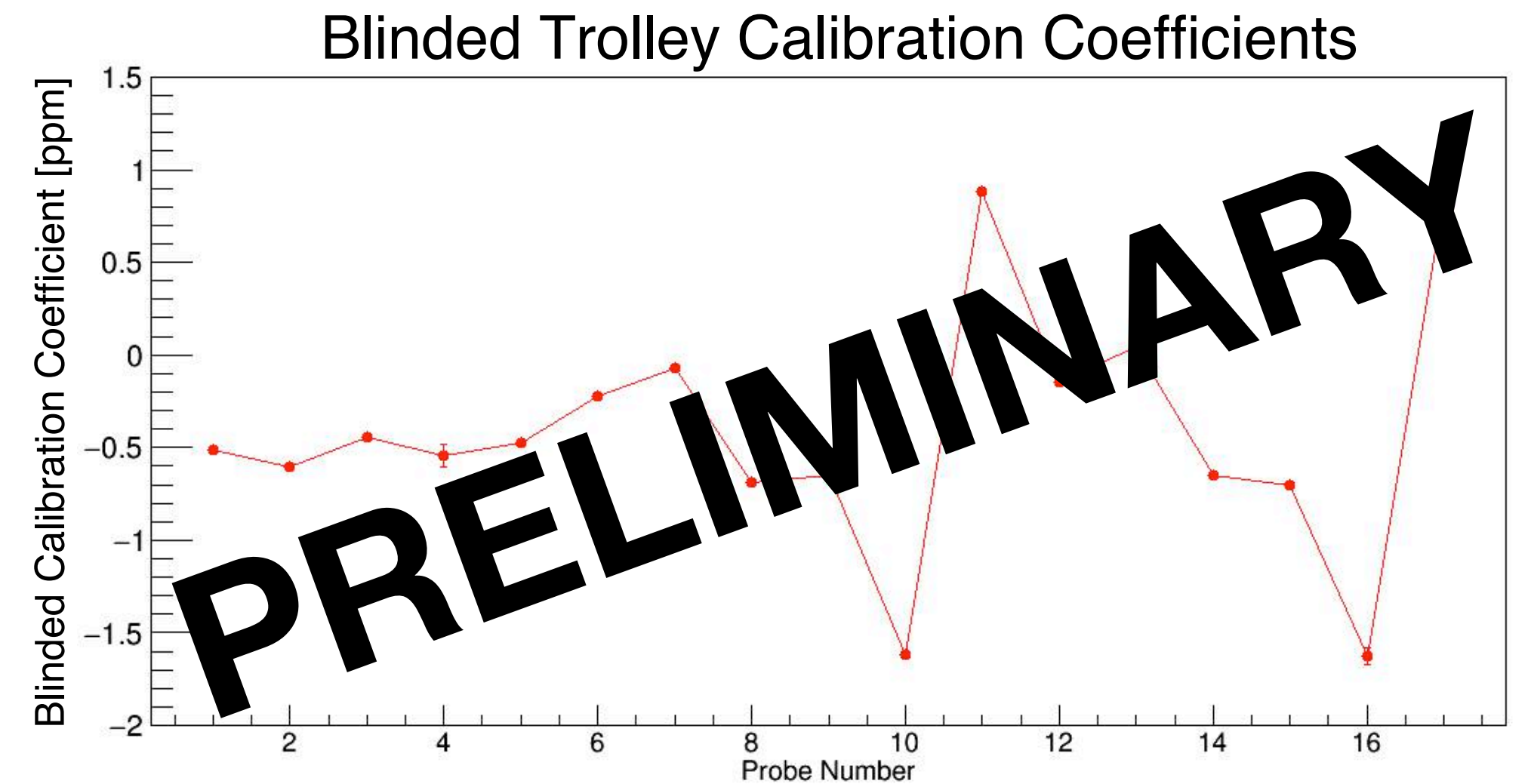
Plunging Probe

- Achieved **small perturbation of plunging probe** $\sim (-5.0 \pm 6.5)$ ppb
- Quantified uncertainties on plunging probe material, dynamic effects — **under budget of 35 ppb**

Plunging Probe Uncertainties	
Effect	Uncertainty (ppb)
Probe Perturbation to Field (includes images)	6.5
Radiation Damping	20
Probe Dipolar Field	2
Oxygen Contamination of Water Sample	< 1
TOTAL	21

Trolley Calibration

- Calibration of trolley probes under control**
- Factor of ≥ 2 improvement on uncertainties for nearly all probes compared to E821
- Uncertainty is ~ 26 ppb on average per probe — **under budget of 30 ppb**

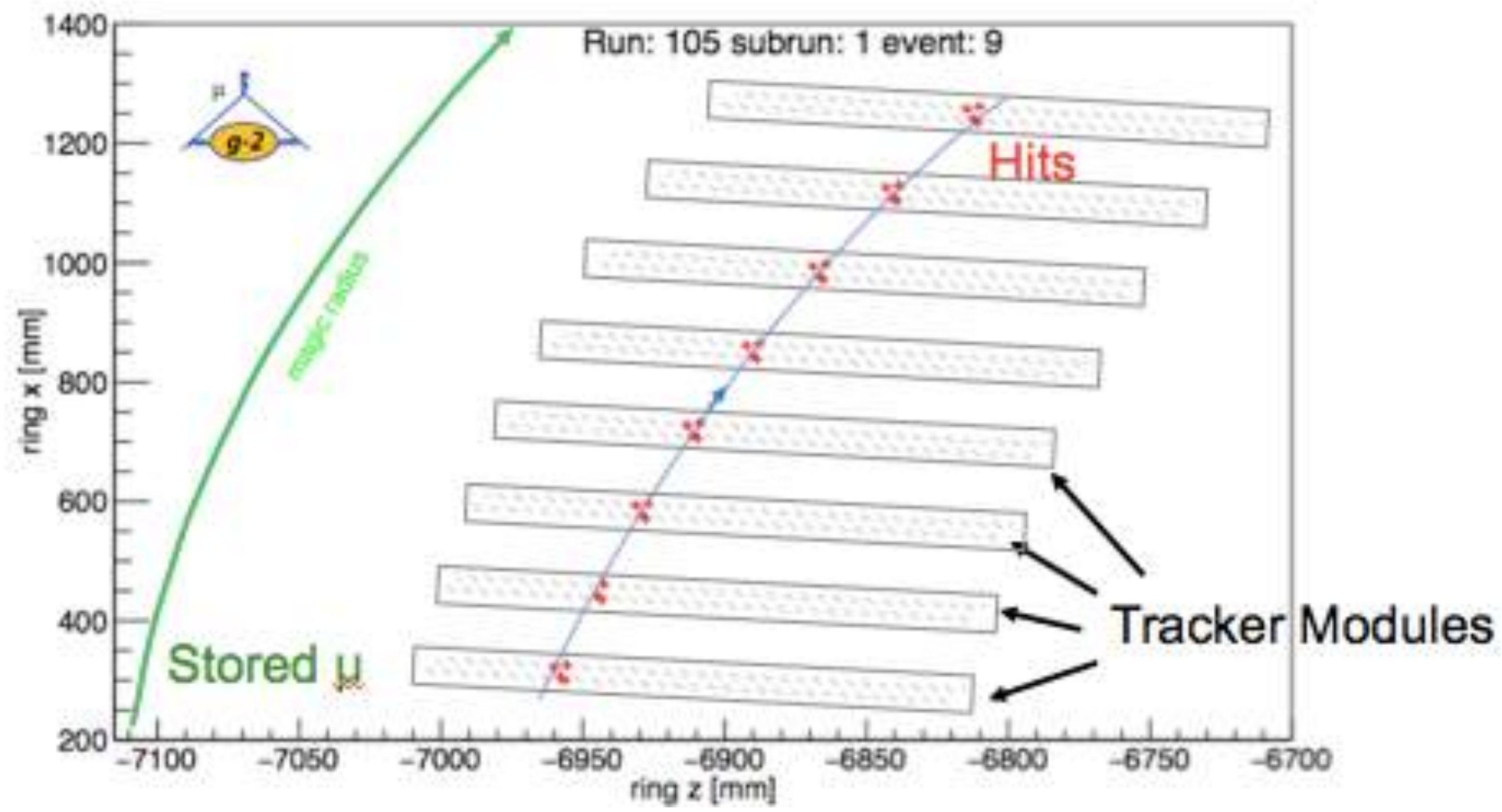
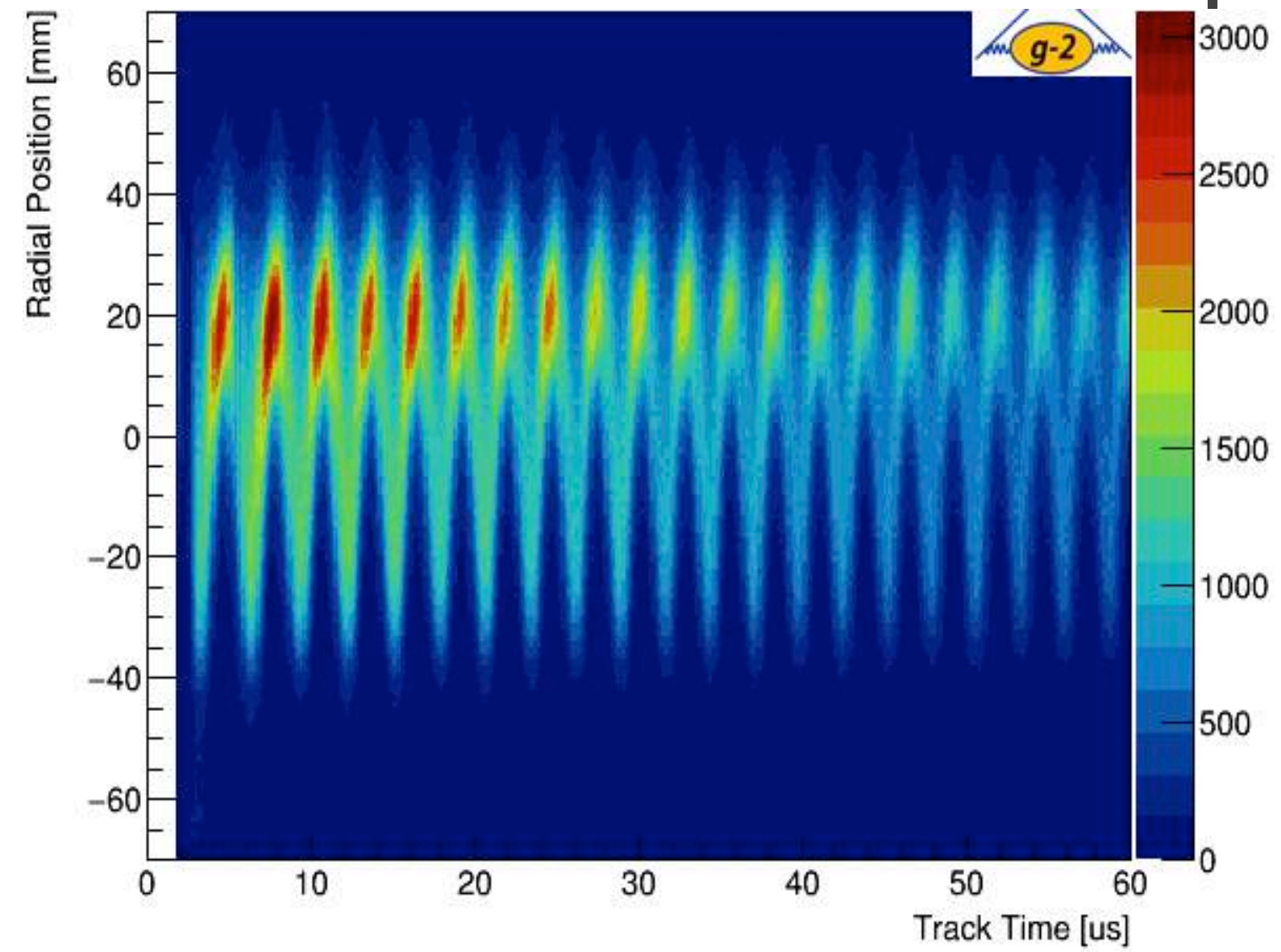


Run-1 Analysis Status — $\tilde{\omega}_p$

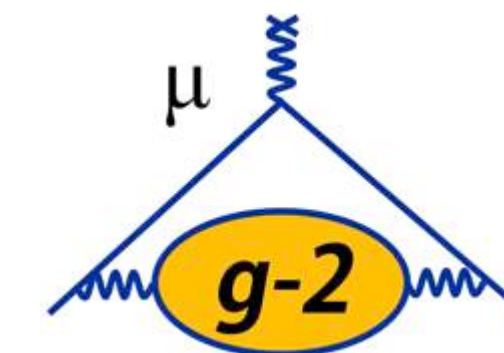
Position of the beam



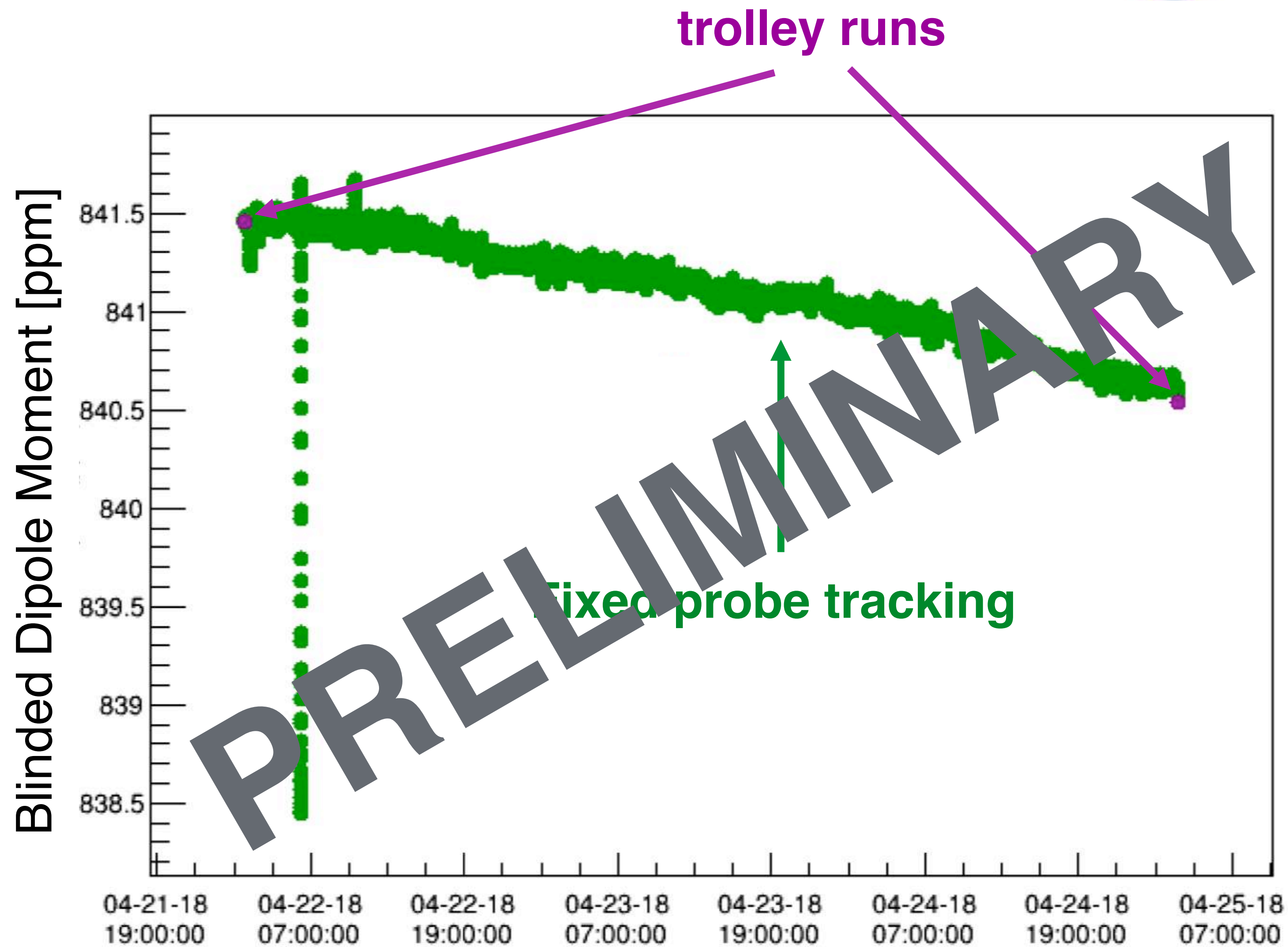
- Use Trackers to measure the beam
- Extrapolate tracks back through B-field to point of radial Tangency
- Observe beam moving in time
- Use Trolley-Fixed probe interpolation to tell us the field at these positions



Run 1 Analysis Status: $\tilde{\omega}_p$ – Field Interpolation

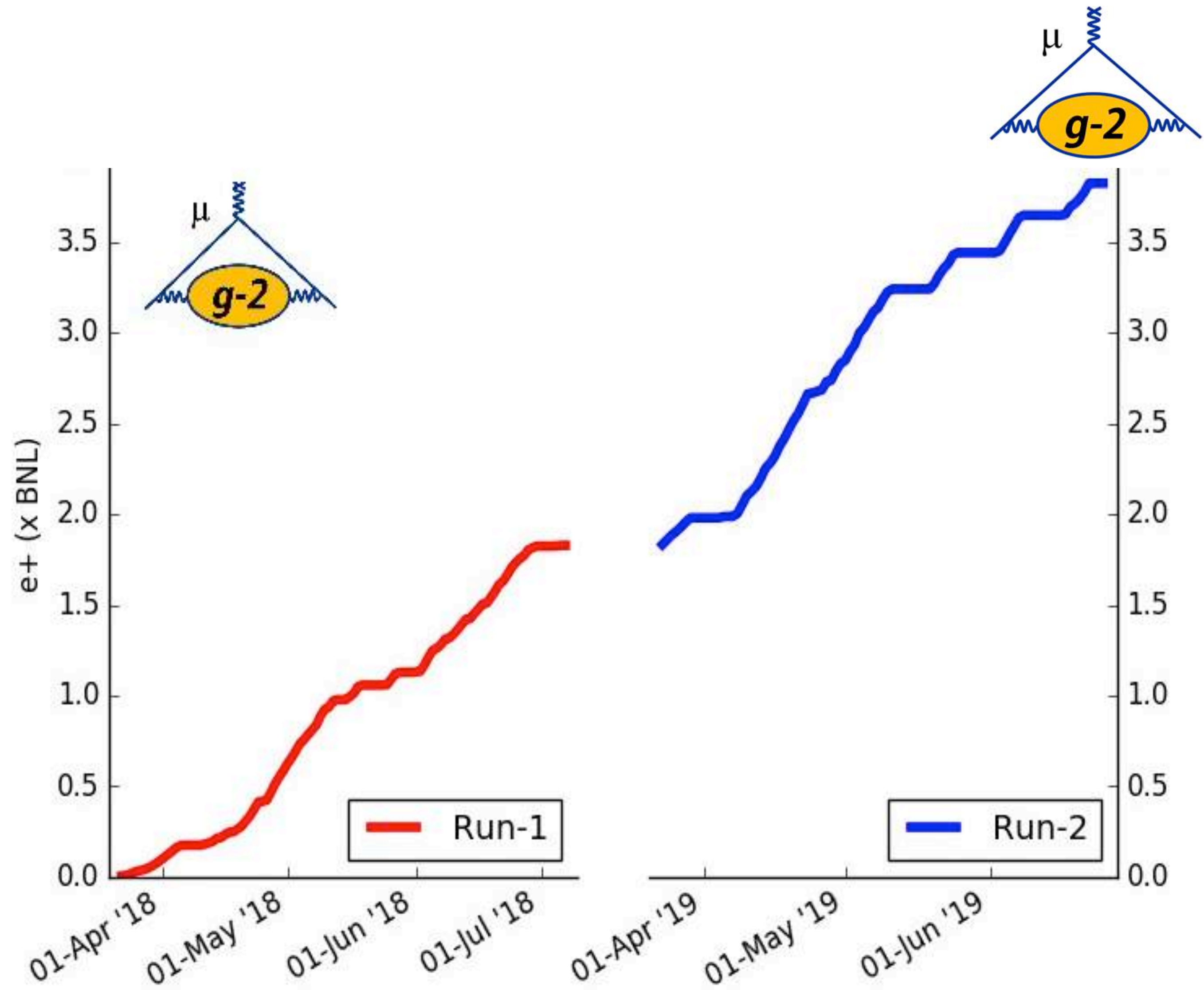
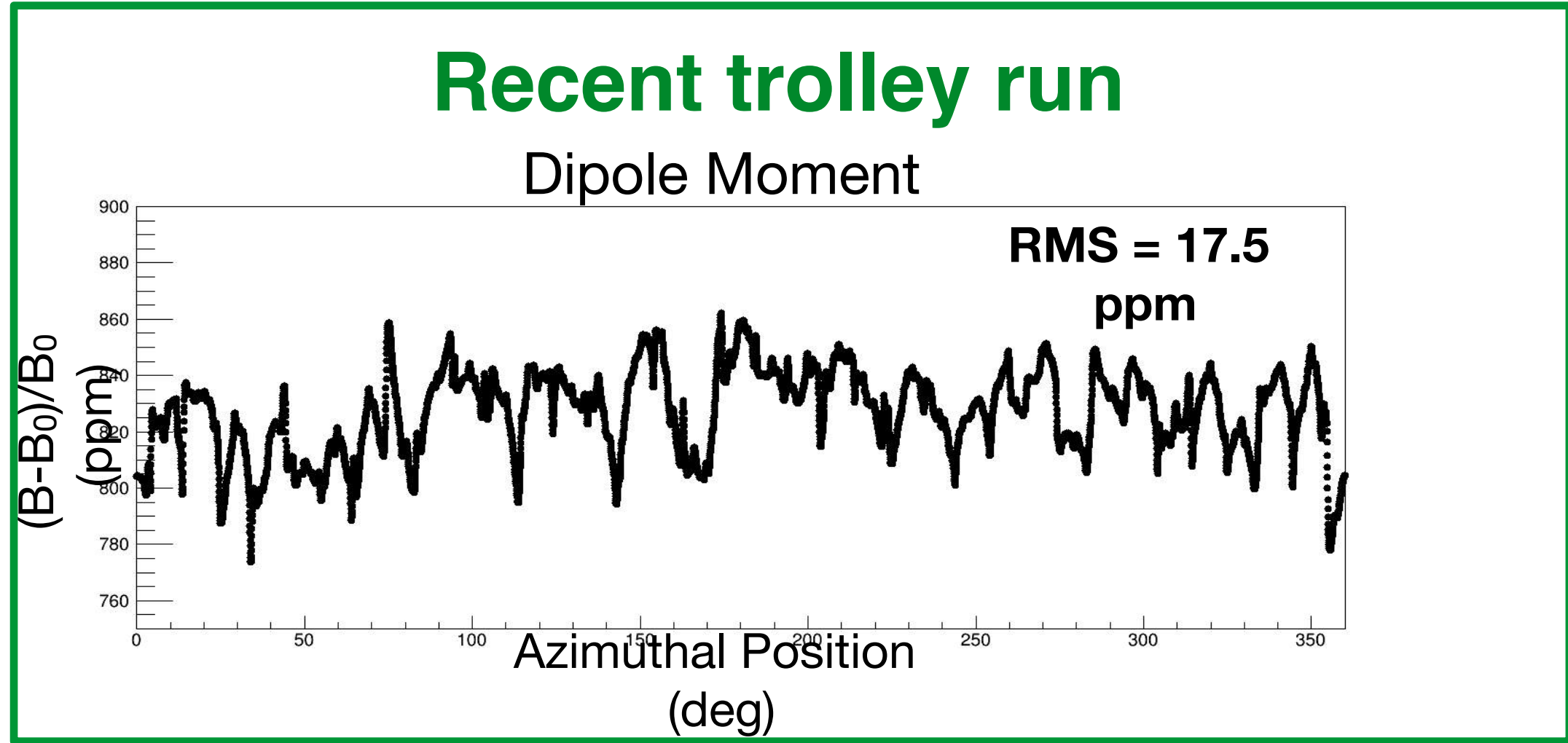
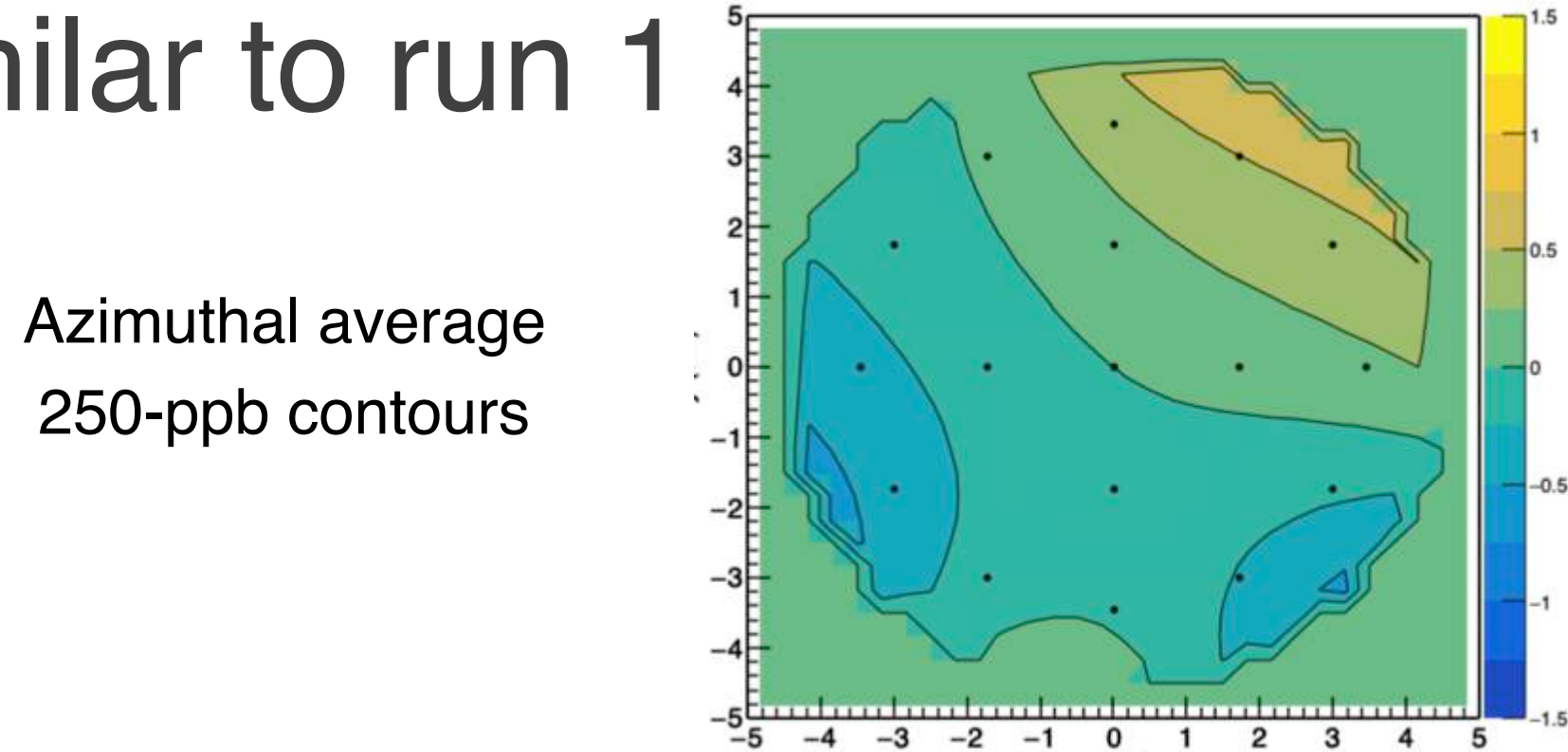


- Need to determine ω_p at all times while storing muons
- Interpolate between trolley maps using fixed probe data
- Tracking algorithms showing good agreement with trolley runs
- Also tracking higher-order multipole moments – important for extracting $\tilde{\omega}_p$



Run 2 Overview

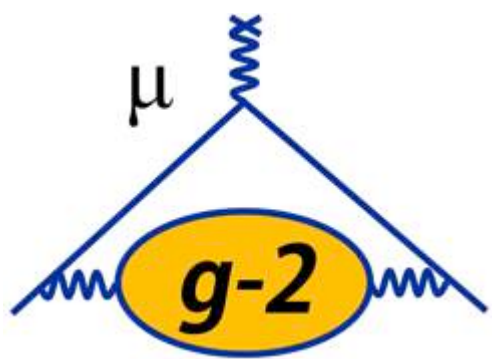
- More data taken during 2019
- Field uniformity expected to be similar to run 1



Can take 5% of a BNL per day!



Summary

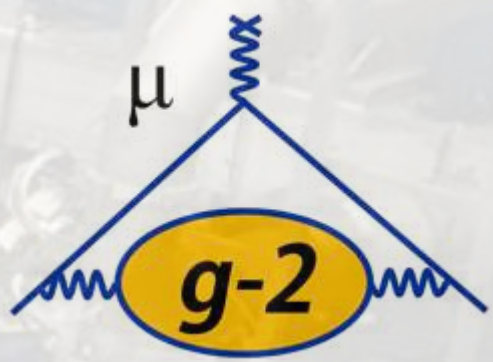


Theoretical calculations

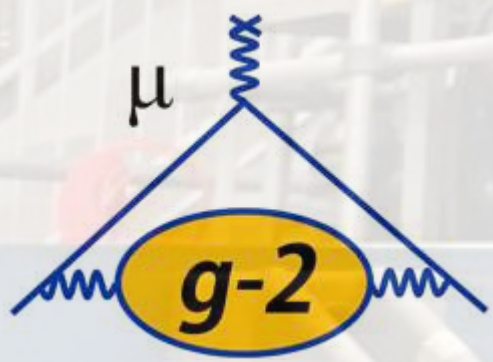
- Highly sensitive test of the SM with discrepancy between theory and experiment at the 3.7σ level
- Improvements in Lattice techniques becoming competitive for HVP uncertainty
- New data for HVP improving uncertainty, and not moving central value
- Data driven methods for HLbL agree with theory, too soon for competitive uncertainties
- On course for improvement on same time scale as Fermilab result

The Fermilab Muon $g-2$ Experiment

- Completed Run 1 in July 2018: result planned for late 2019. Statistic $\sim 1.5 \times$ BNL
- Run 2 nearly complete (this Saturday!) — another $2 \times$ BNL this year
- Taking 5% of a BNL a day, on course for 21 BNLs over next 2 years
- No new systematic uncertainties unearthed, all at or below target level for run 1
- Aiming for $>5\sigma$ result (if central value remains the same as BNL) at end of year

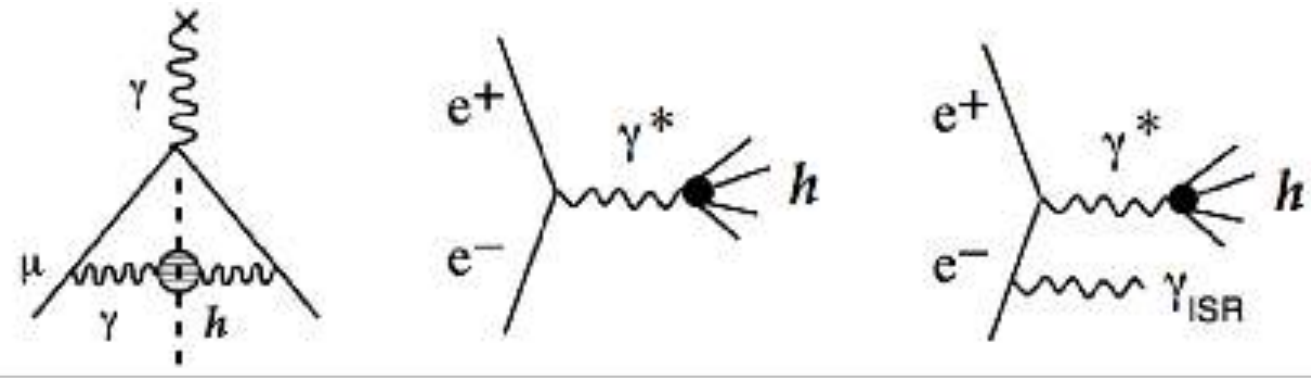


Thank you!



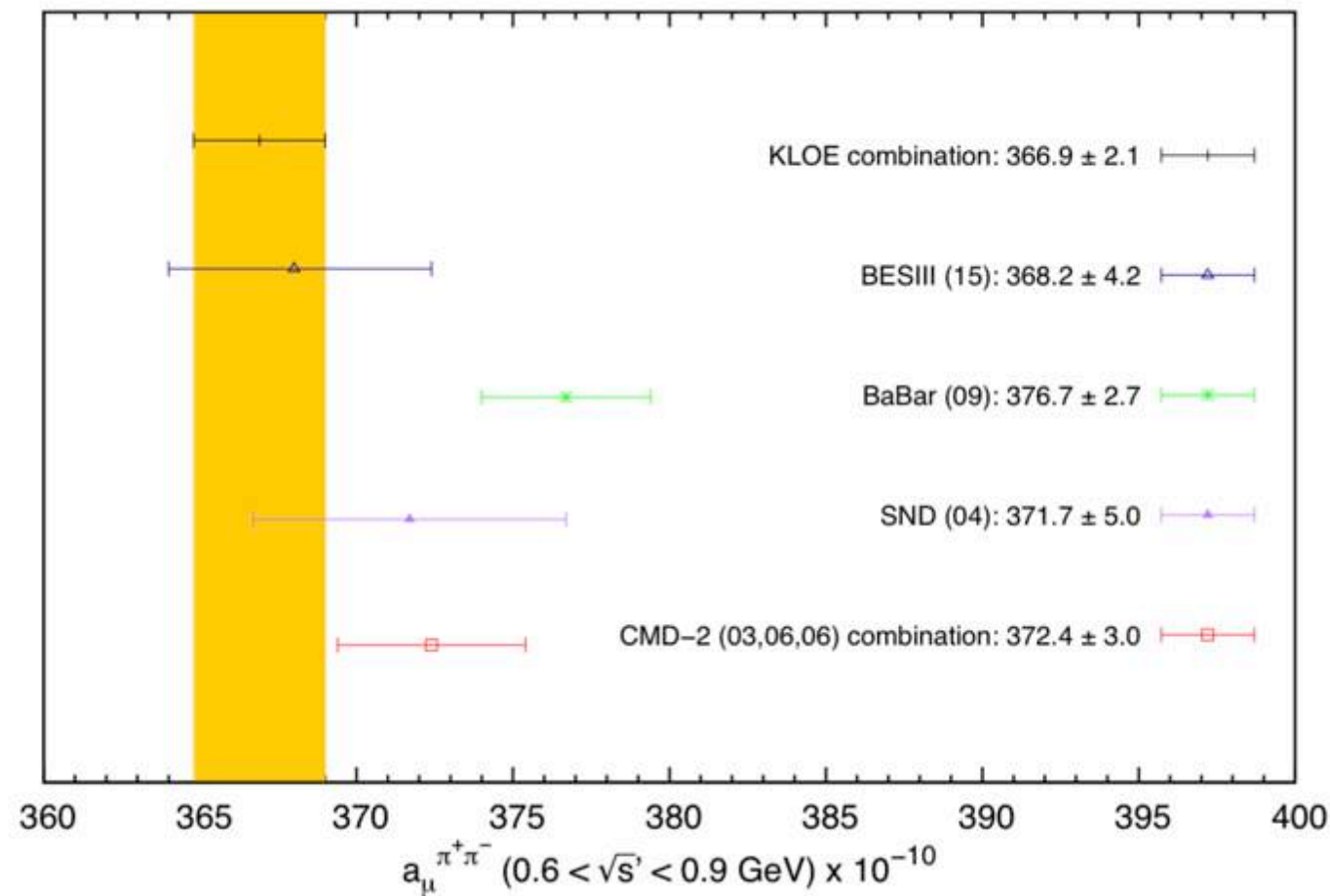
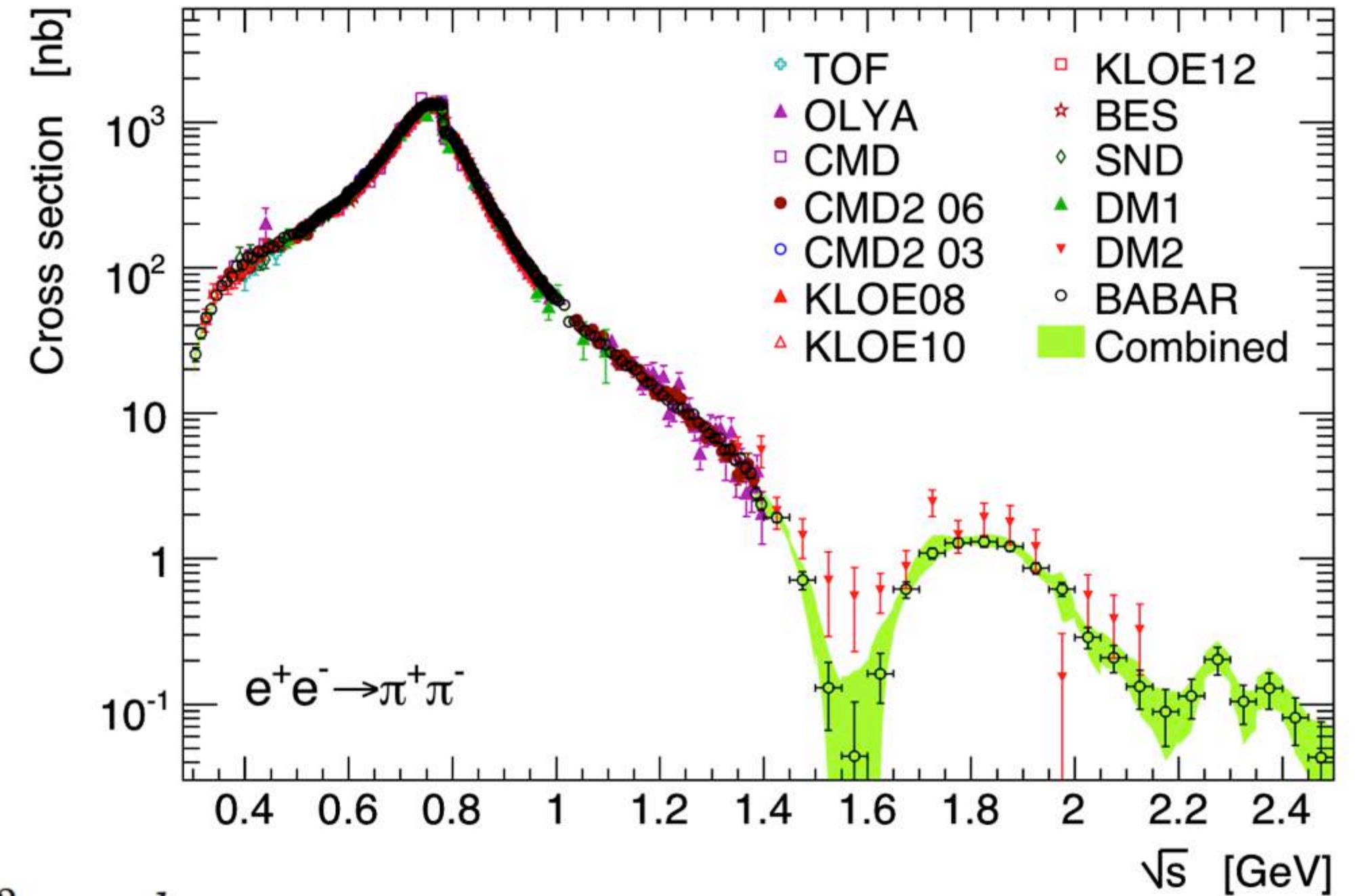
Backup

Hadronic Vacuum Polarization



M. Davier et al., arXiv:1706.09436 [hep-ph]

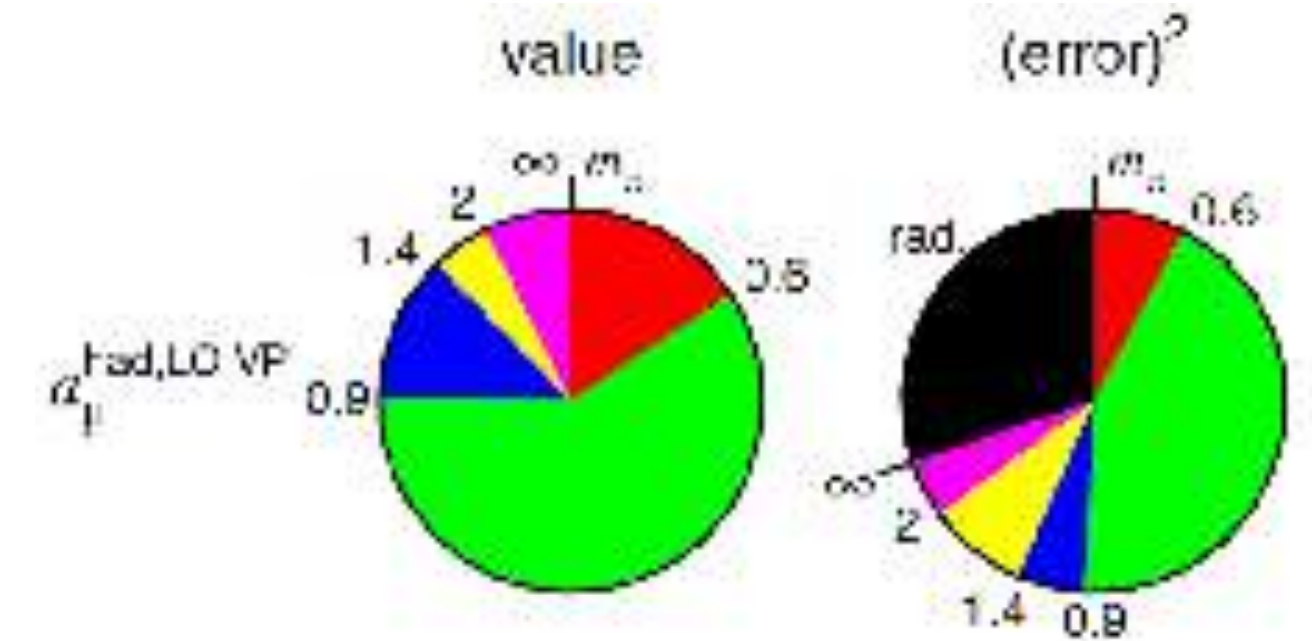
- **Critical input to HVP** from e^+e^- colliders (SND, CMD3, BaBar, KLOE, Belle, BESIII)
- **BESIII**: 3x more data available, luminosity measurement improvements
- **VEPP-2000**: Aiming for 0.3% (fractional) uncertainty; radiative return + energy scan
- **CMD3**: Will measure up to 2 GeV (energy scan, ISR — good cross check)



A. Anastasi et al., arXiv:1711.03085 [hep-ex]

$$a_\mu^{\text{had;LO}} = \left(\frac{\alpha m_\mu}{3\pi}\right)^2 \int_{m_\pi^2}^{\infty} \frac{ds}{s^2} K(s) R(s)$$

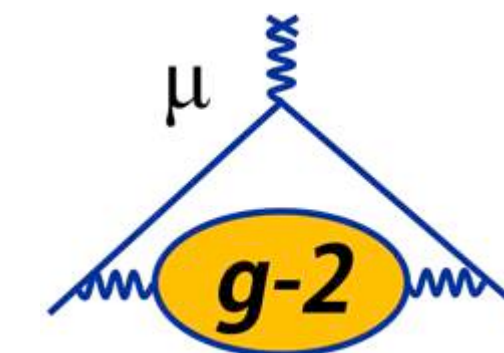
$$R \equiv \frac{\sigma_{\text{tot}}(e^+e^- \rightarrow \text{hadrons})}{\sigma(e^+e^- \rightarrow \mu^+\mu^-)}$$



- **Lattice calculations** of a_μ^{HVP} to 1% possible, 30% for HLbL in 3–5 years

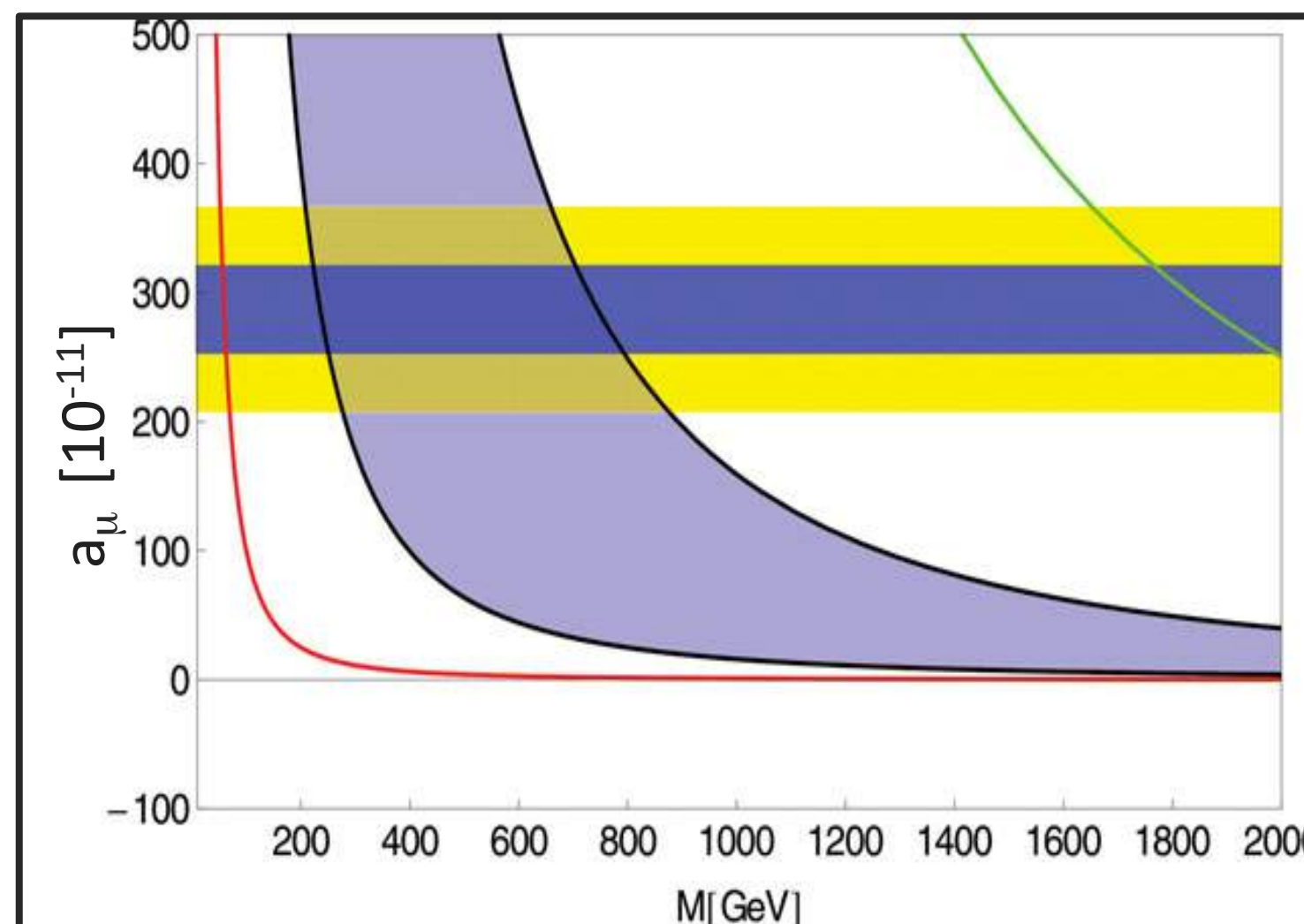


Physics Beyond the Standard Model?



SUSY, TeV-Scale Models

- Higgs measured at the LHC to be ~ 125 GeV
- Theory: Higgs should acquire much heavier mass from loops with heavy SM particles (e.g., top quark)
 - Supersymmetry: new class of particles** that enters such loops and **cancels this contribution**

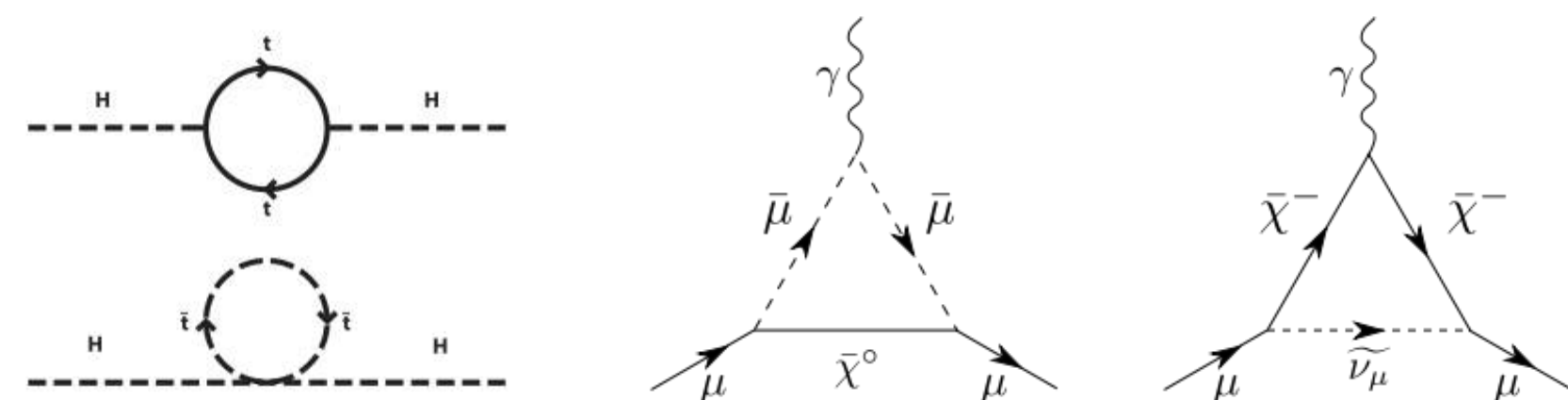


D. Hertzog, Ann. Phys. (Berlin), 2015, courtesy D. Stockinger

- $Z', W', \text{UED, Littlest Higgs}$
 - Assumes typical weak coupling
- Radiative muon mass generation
- Unparticles, Extra Dimension Models, SUSY ($\tan \beta = 5$ to 50)

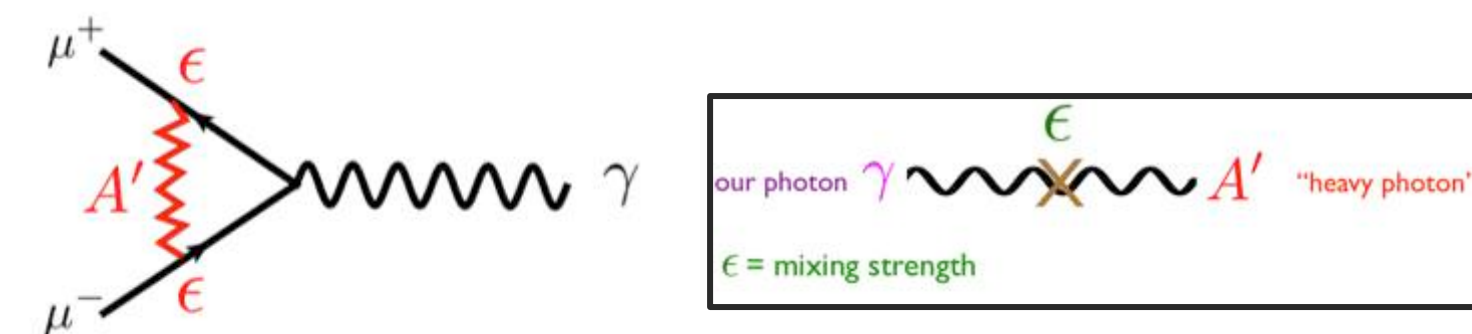
Complementary to direct searches at the LHC

- Sensitivity to $\text{sgn}(\mu), \tan(\beta)$
- Contributions to a_μ arise from charginos, sleptons
- LHC searches sensitive to squarks, gluinos

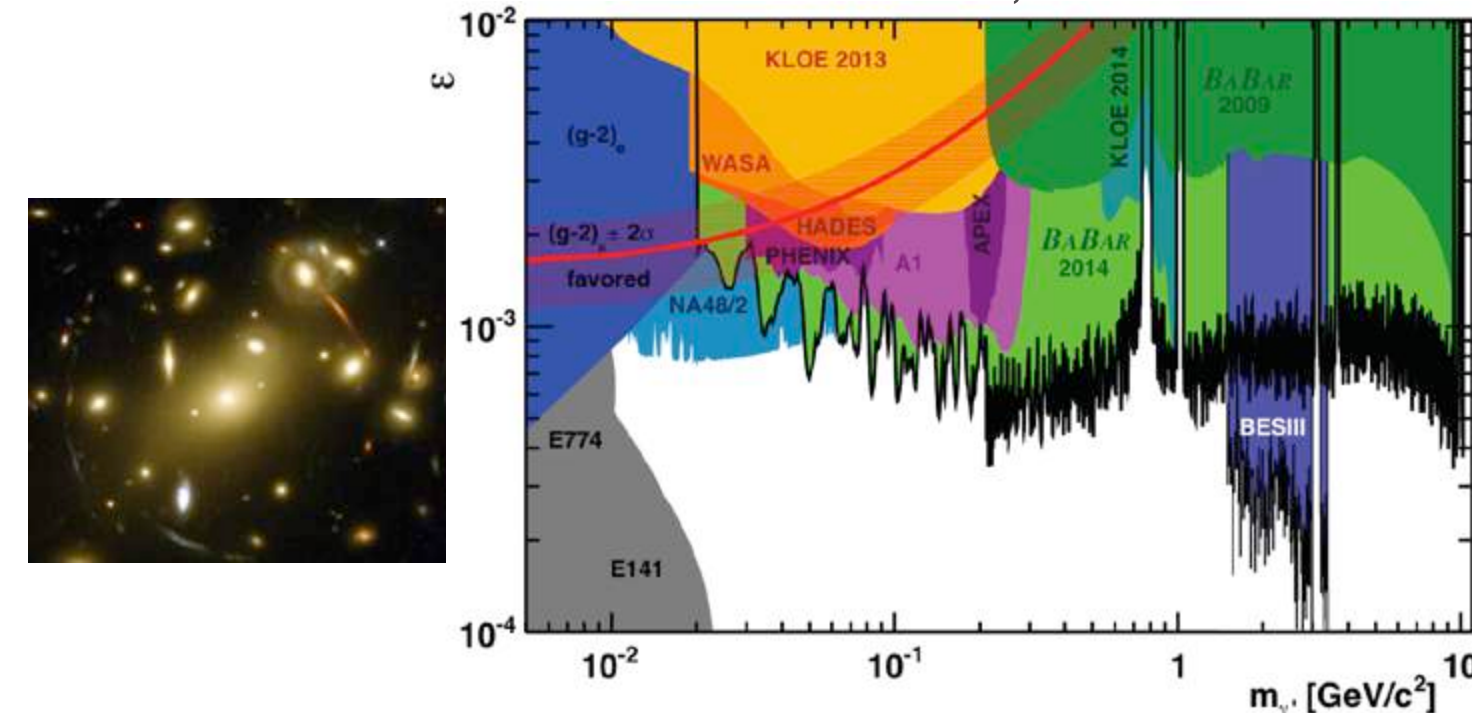


Dark Matter

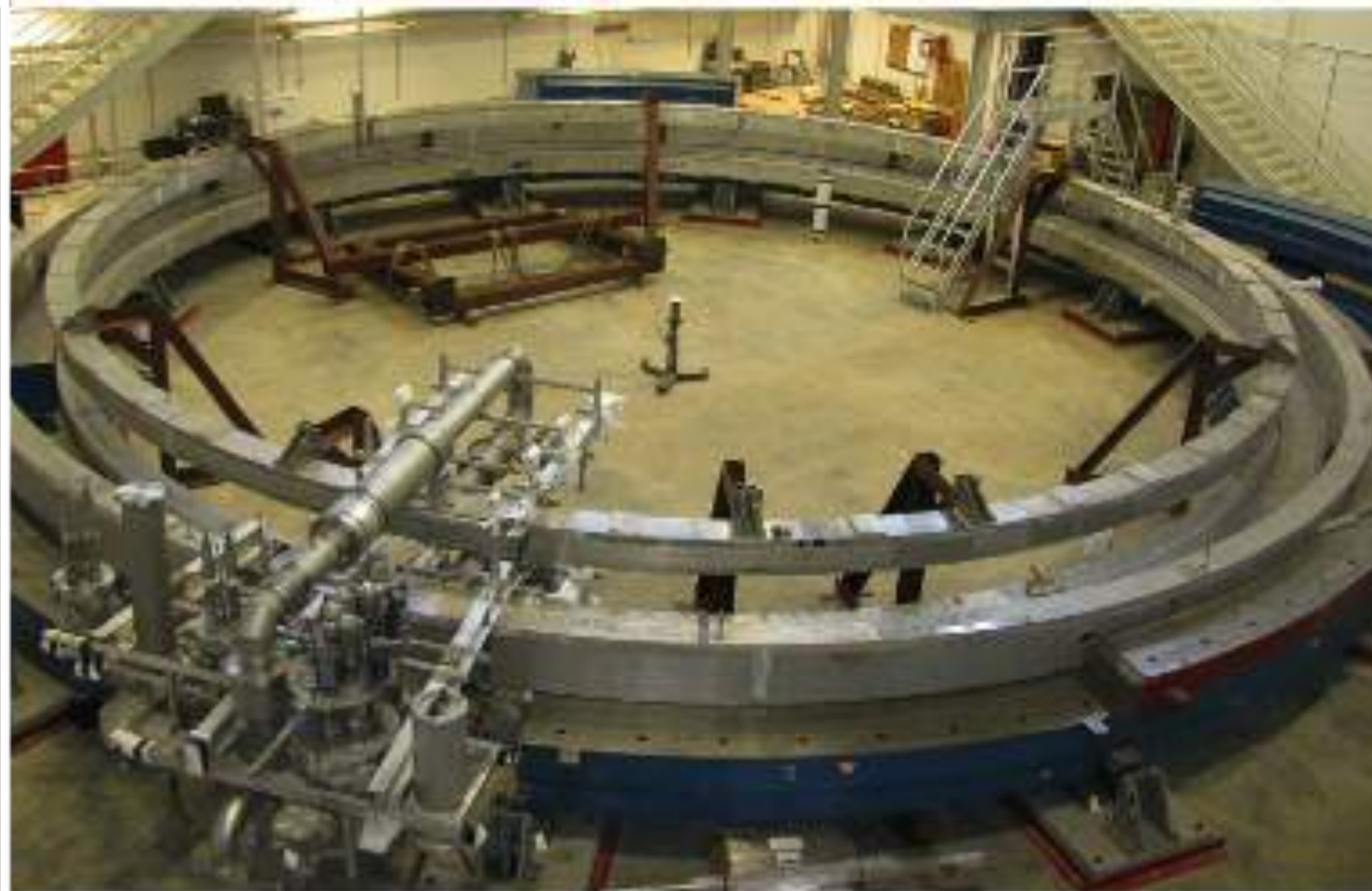
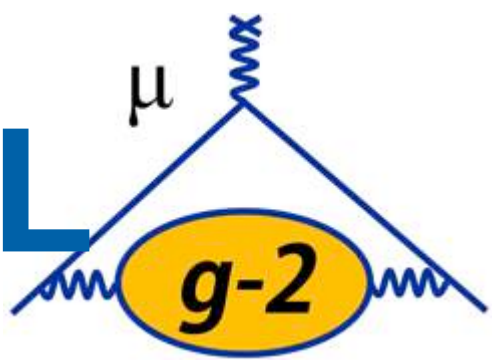
- Cosmological observations** (galaxy rotation curves, lensing) point to much **more mass in the universe** than expected
- Many **theories** to explain dark matter
 - A new $U(1)'$ symmetry: dark photon A'**
 - Could impact the muon's magnetic moment
 - Many direct-detection searches underway



A. Soffer, arXiv:1507.02330



The Big Move: Transporting the Ring from BNL to FNAL

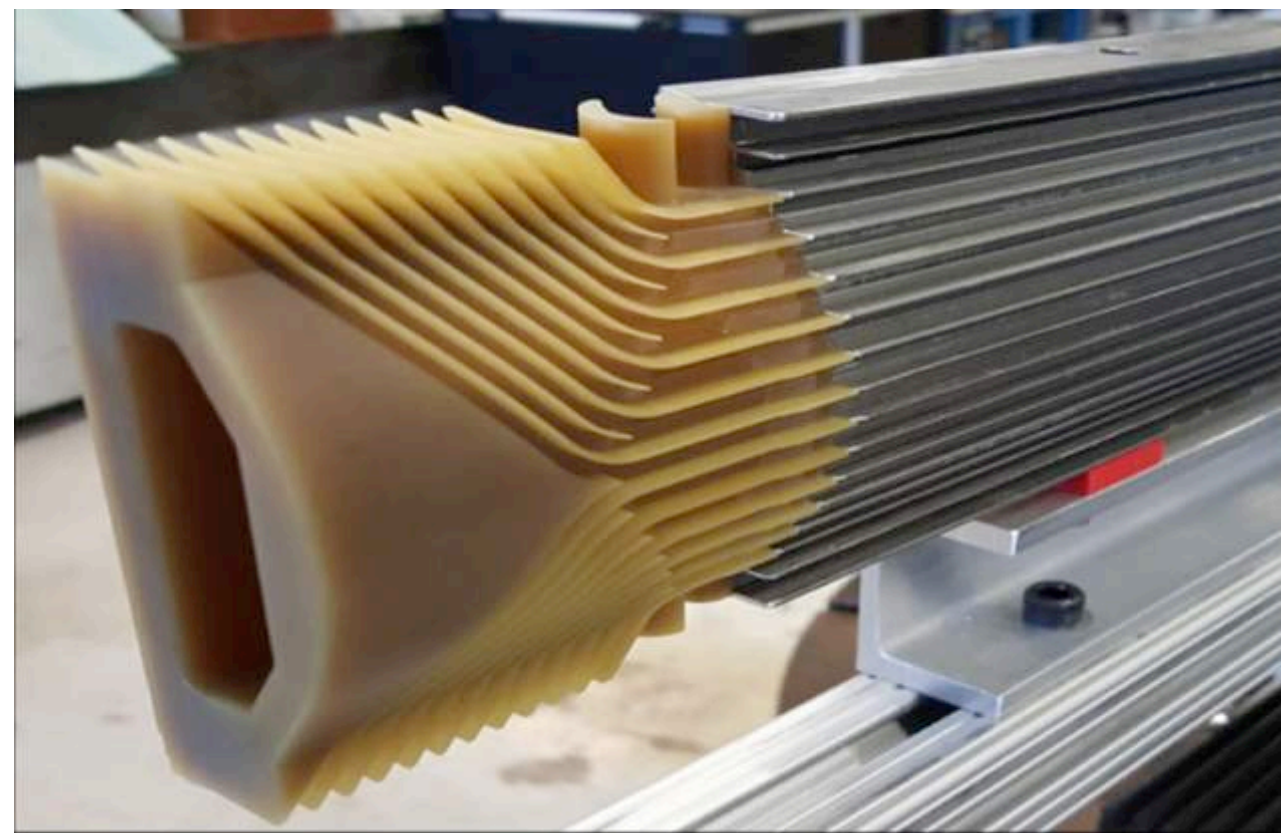
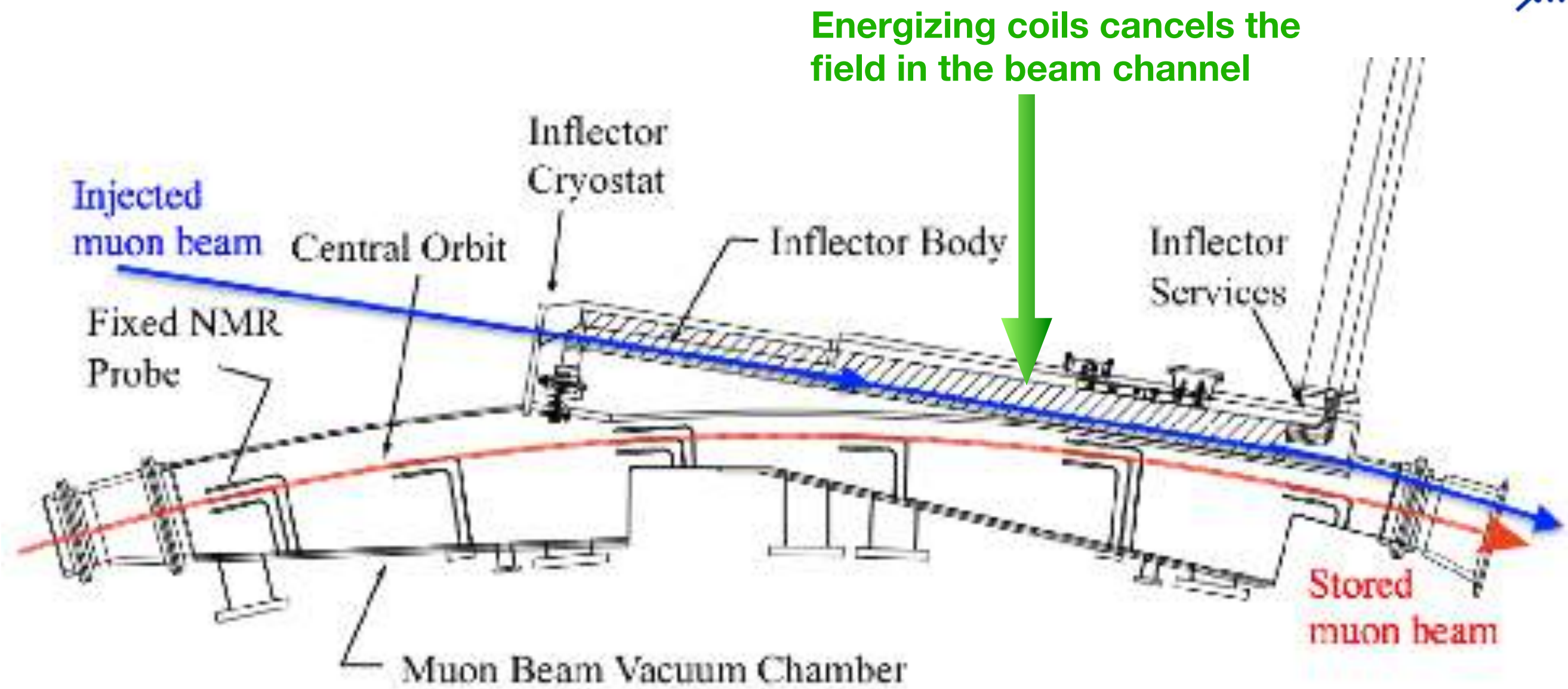


- June 2013—June 2015
- Ring deconstructed at BNL, transported by barge/flatbed trailer
- Reassembled at FNAL
- Ring successfully cooled and powered to 1.45 T in September 2015 — remarkable achievement!

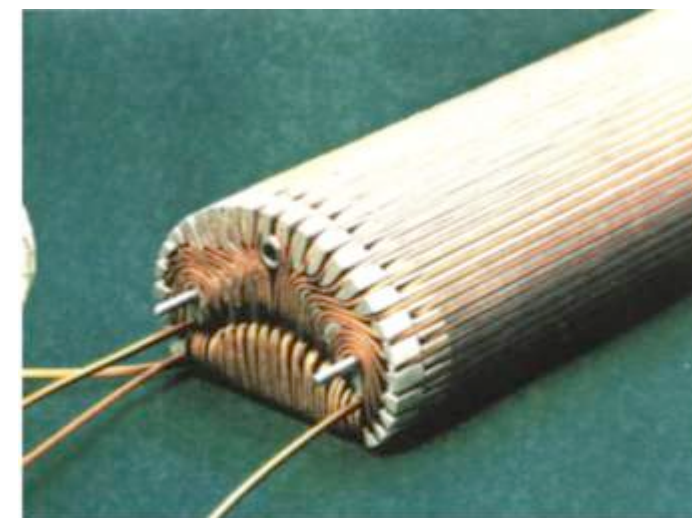
Getting Muons Into the Ring: Inflector Magnet



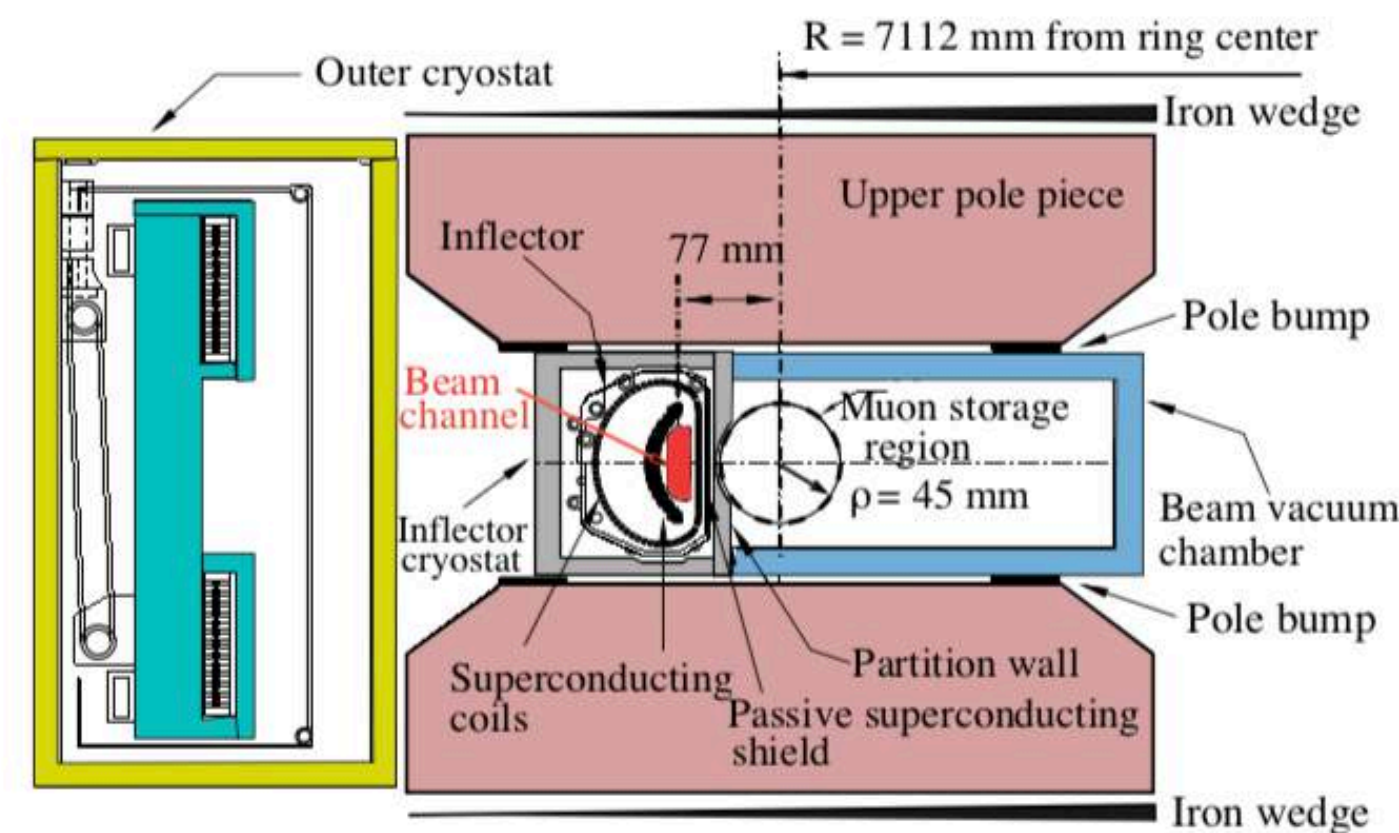
- Outside ring: $B = 0$ T, inside: $B = 1.45$ T
- Need to cancel field in order to get muons in (strong deflection otherwise)
- No perturbation to field outside shield
- New inflector design with higher transmission under development
- **Improve injection by 40%**



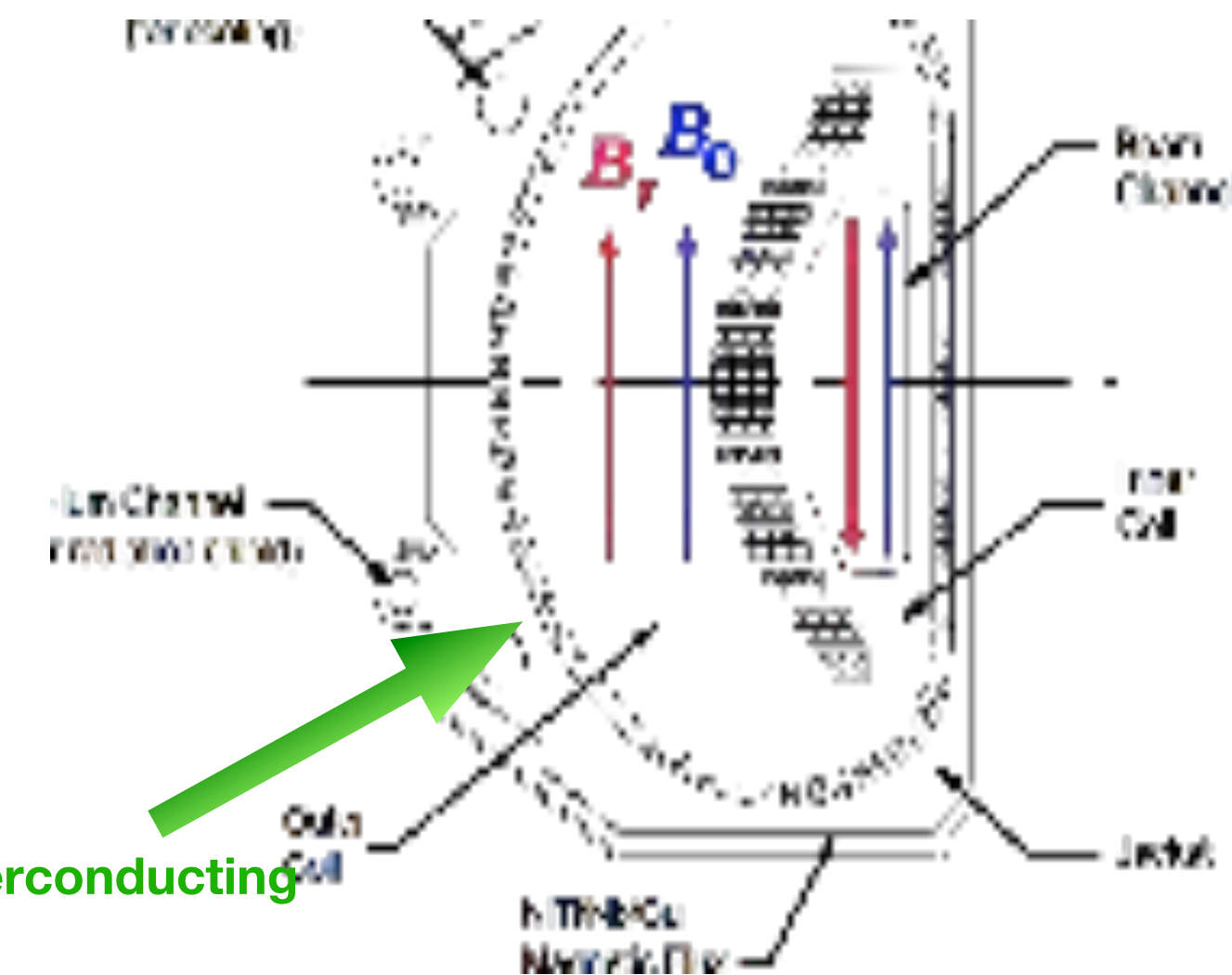
New inflector coil winding mount



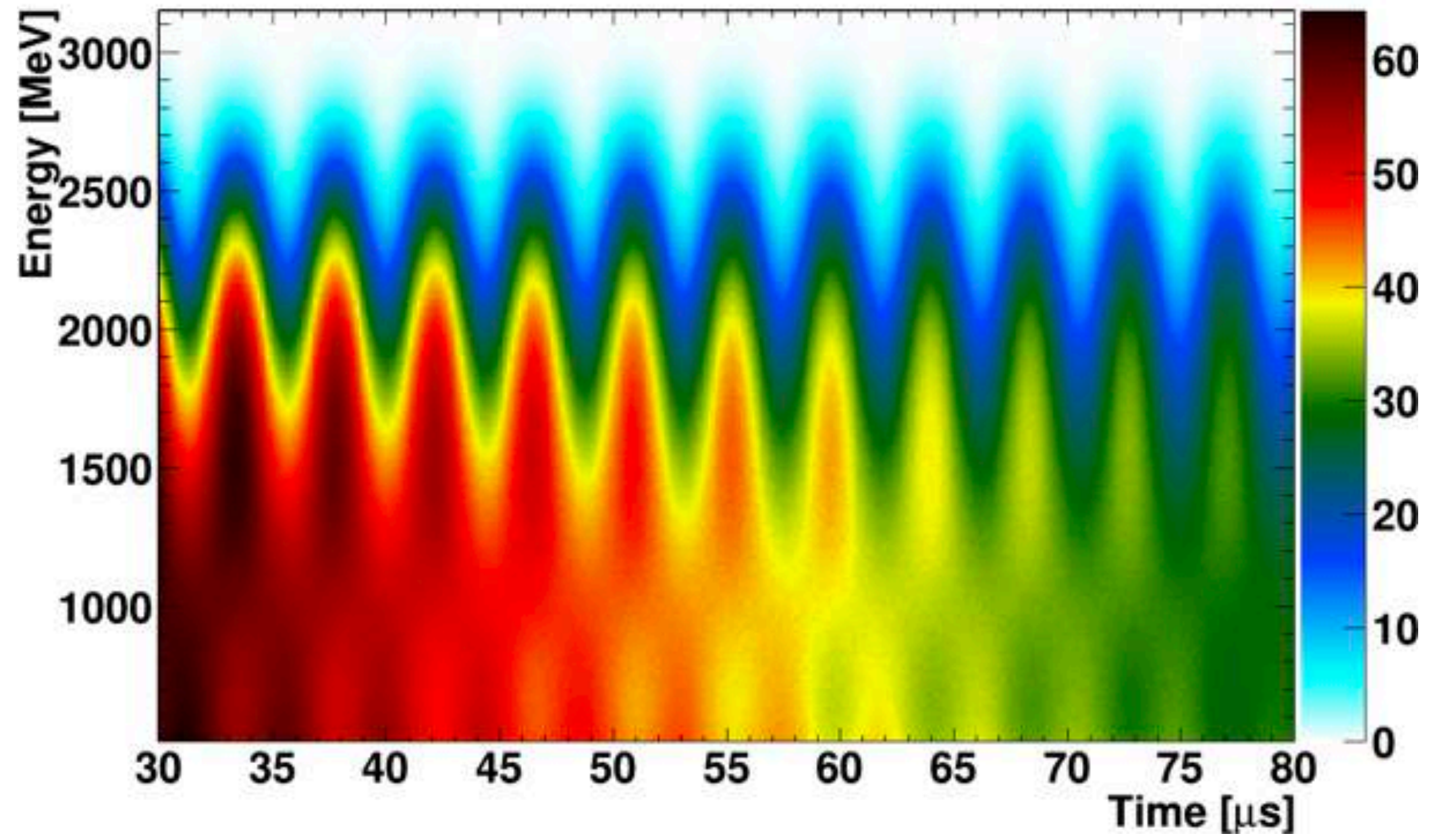
Present inflector



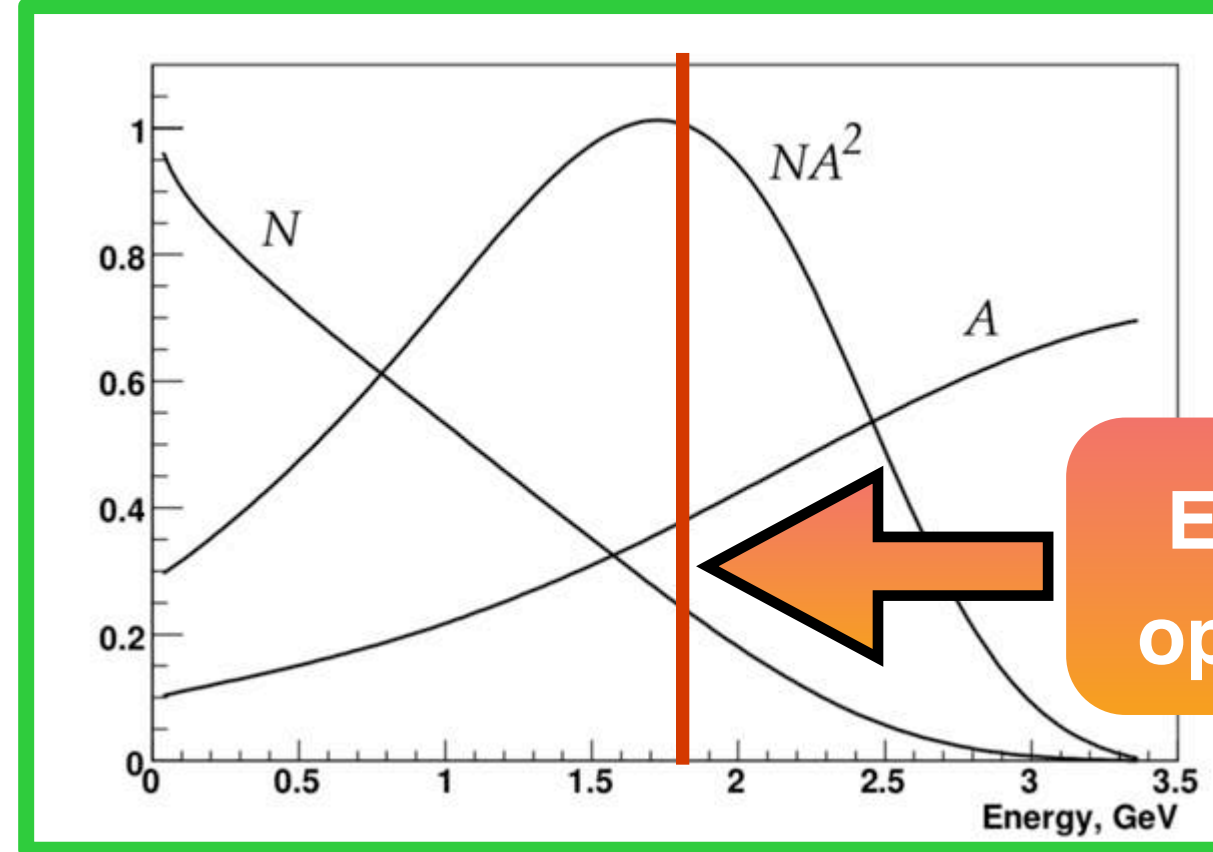
Super currents in passive superconducting shield prevents flux leakage



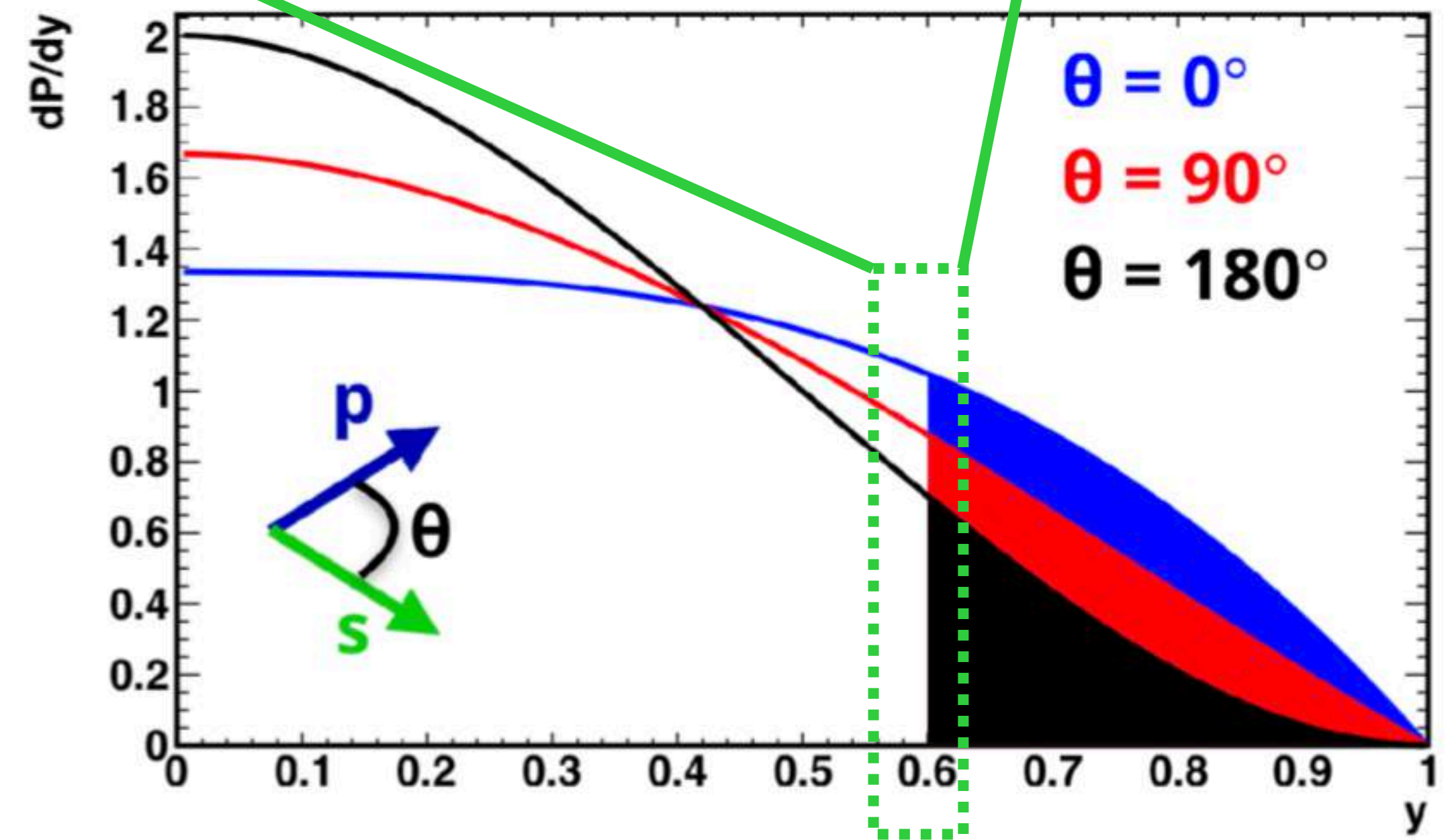
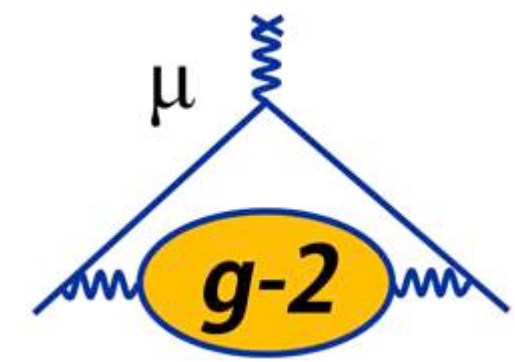
Run 1 Analysis Status: ω_a



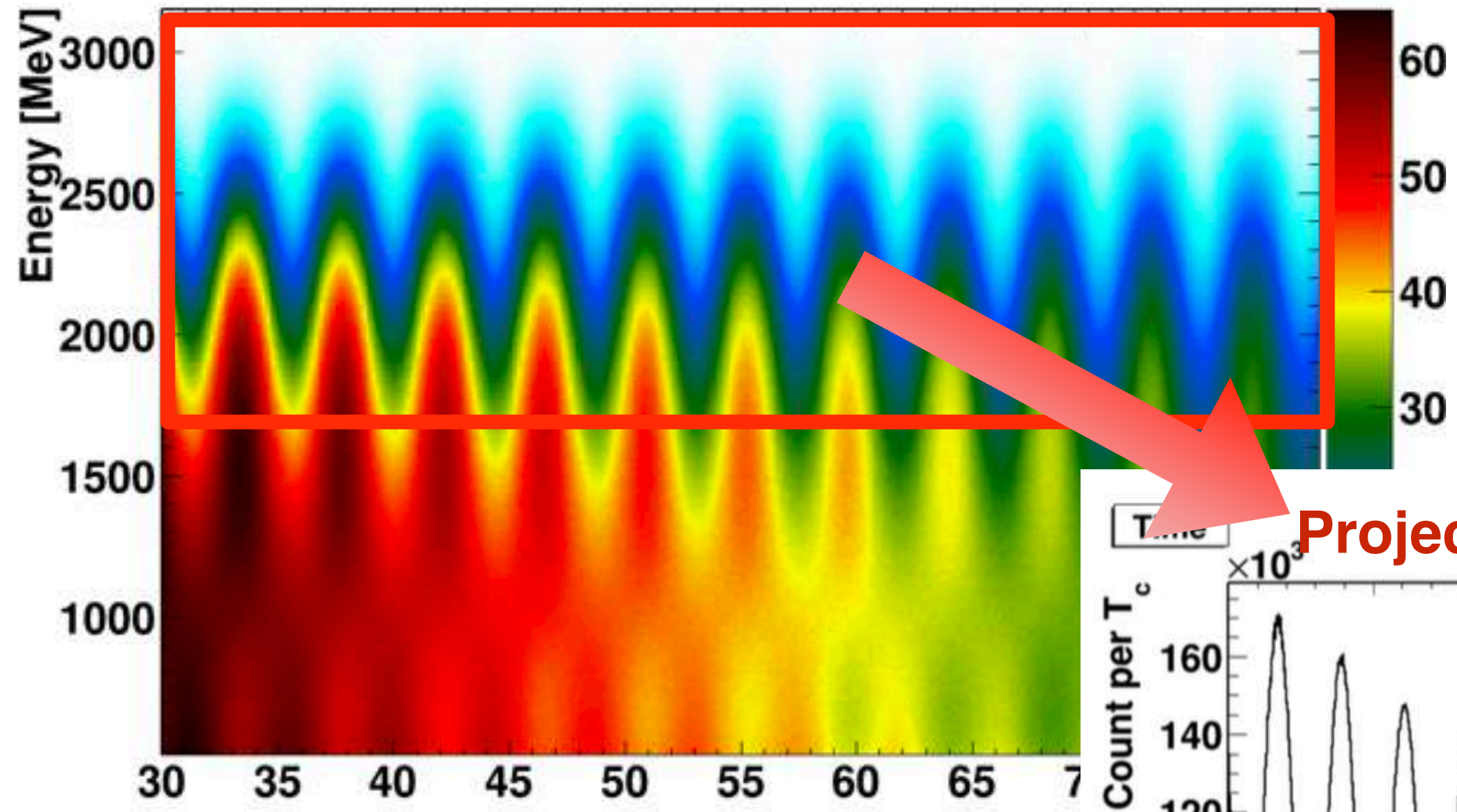
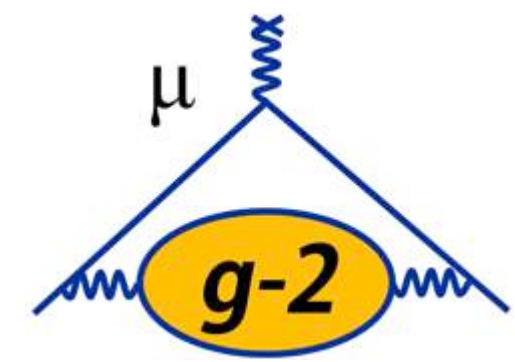
$$\frac{\delta\omega_a}{\omega_a} = \frac{\sqrt{2}}{2\pi f_a \tau_\mu N^{\frac{1}{2}} A}$$



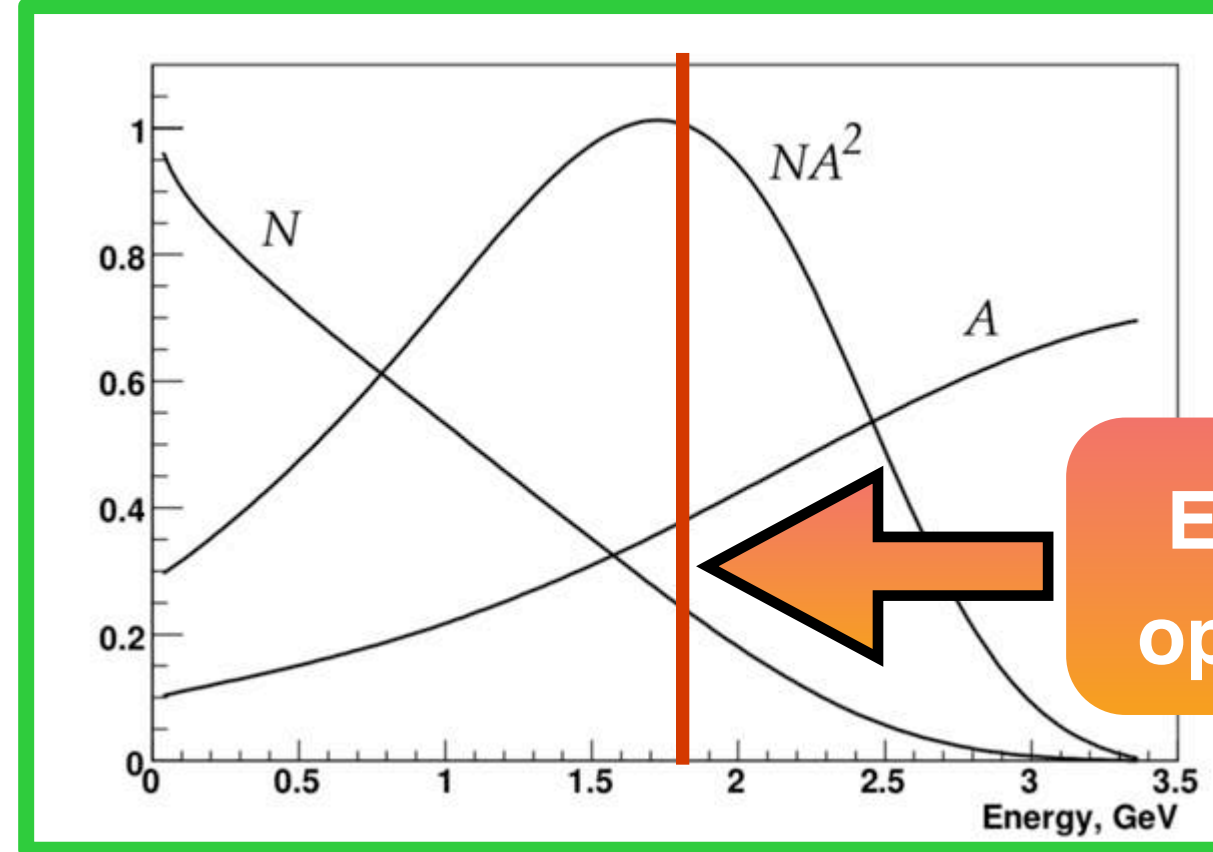
Energy cut chosen to optimize figure-of-merit



Run 1 Analysis Status: ω_a

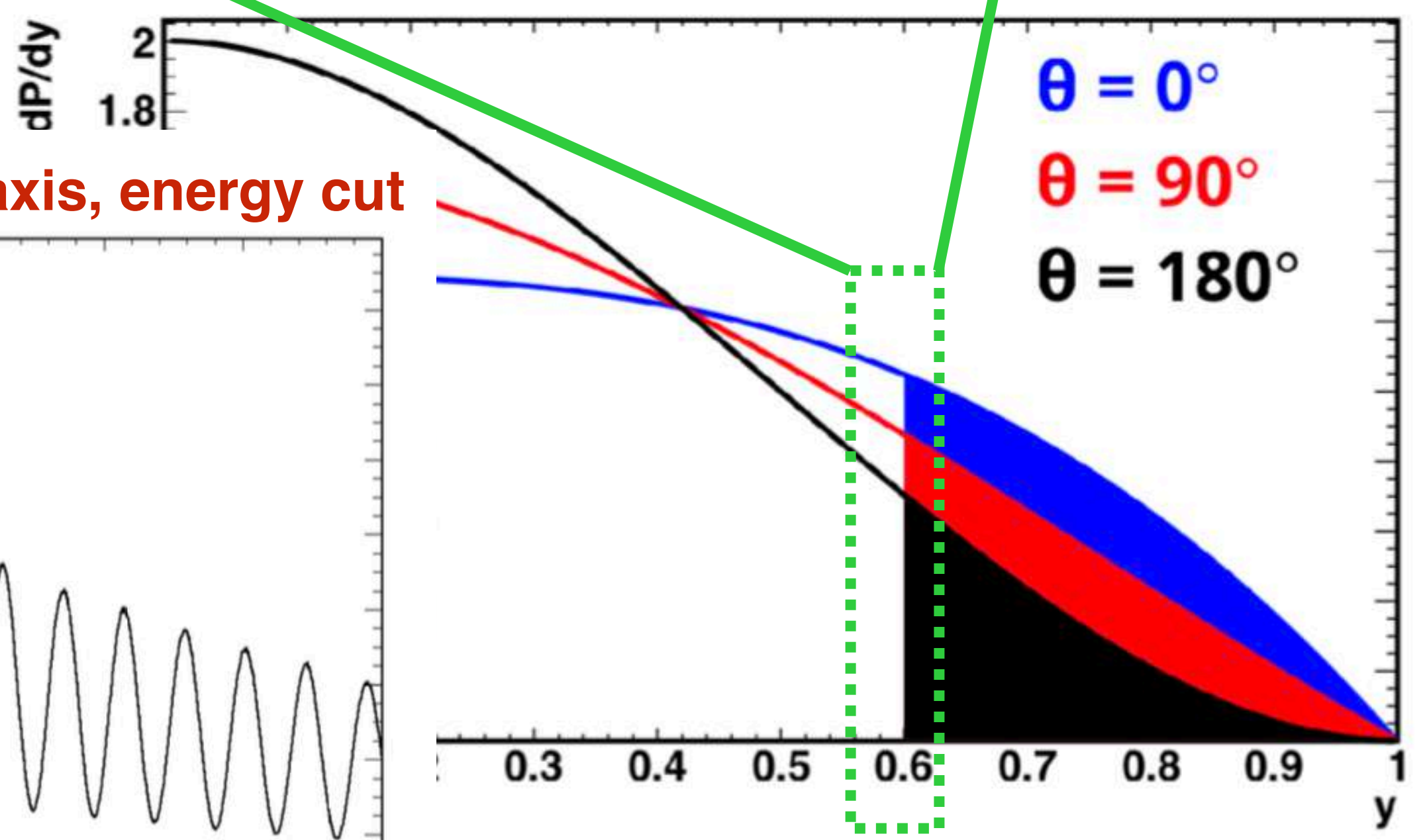
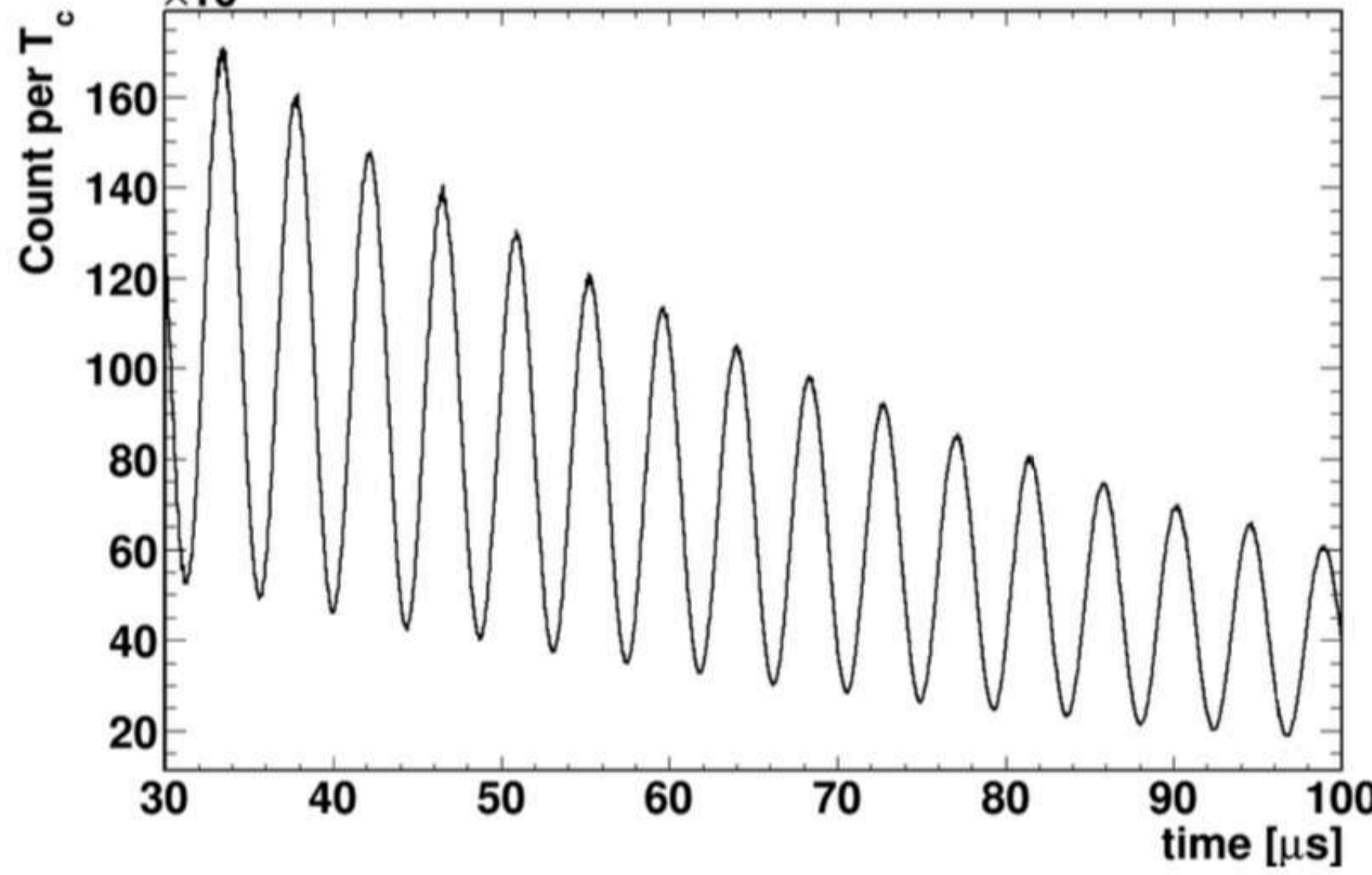


$$\frac{\delta\omega_a}{\omega_a} = \frac{\sqrt{2}}{2\pi f_a \tau_\mu N^{\frac{1}{2}} A}$$

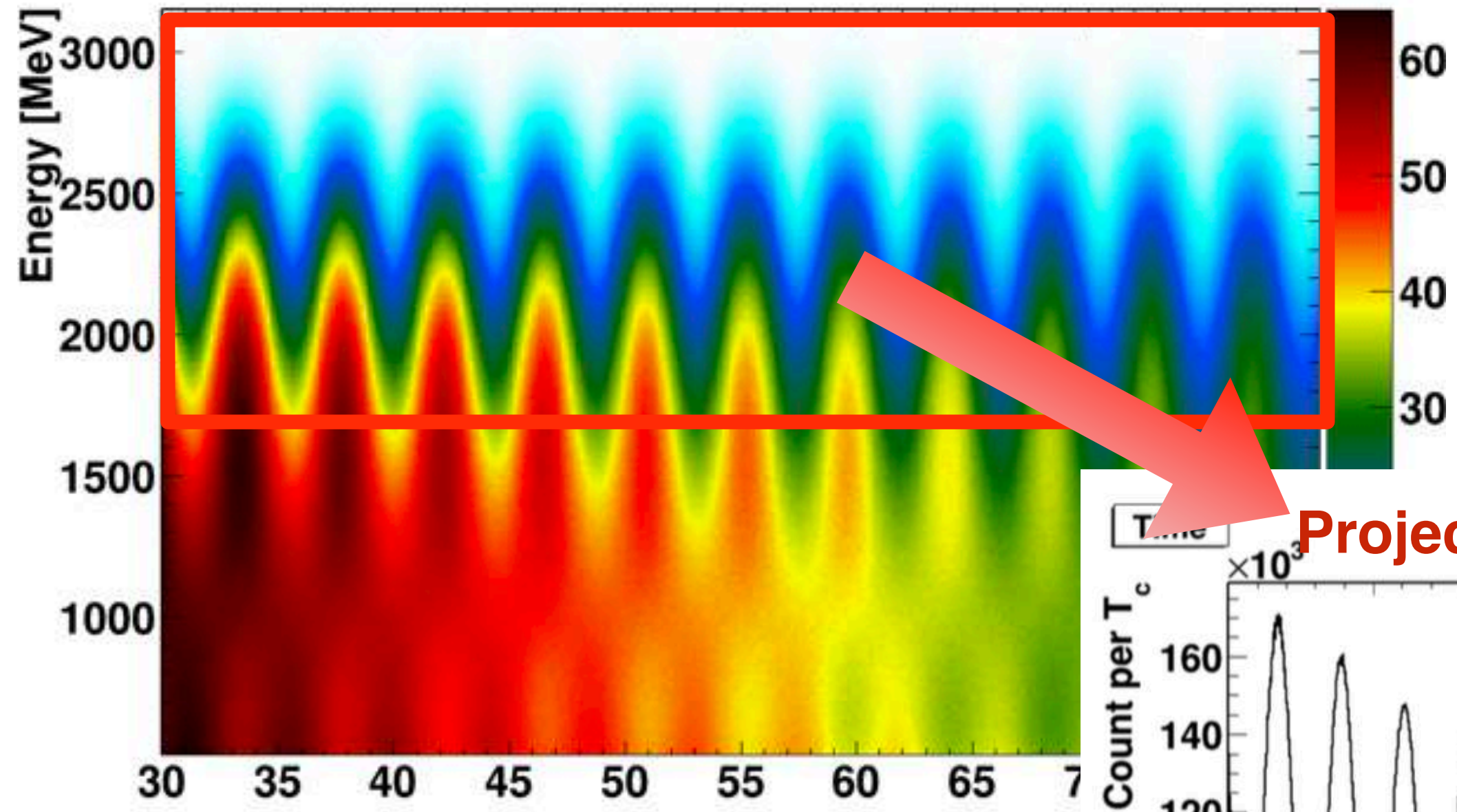
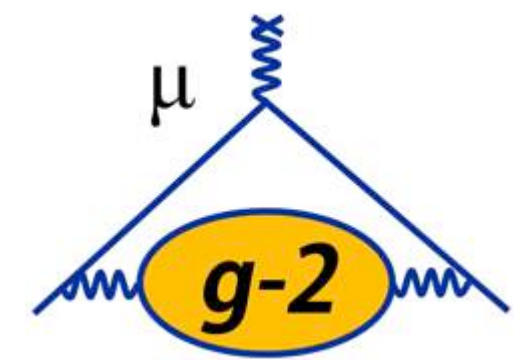


Energy cut chosen to optimize figure-of-merit

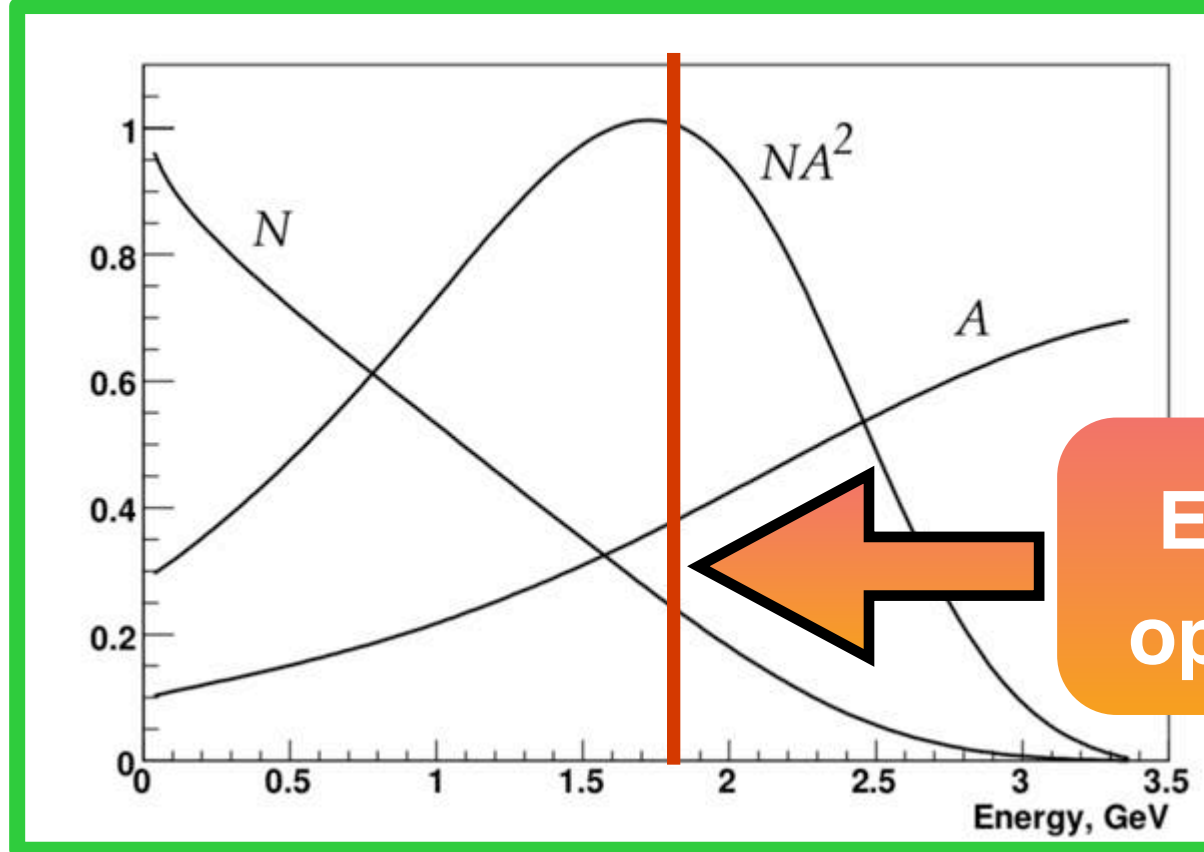
Project along time axis, energy cut



Run 1 Analysis Status: ω_a

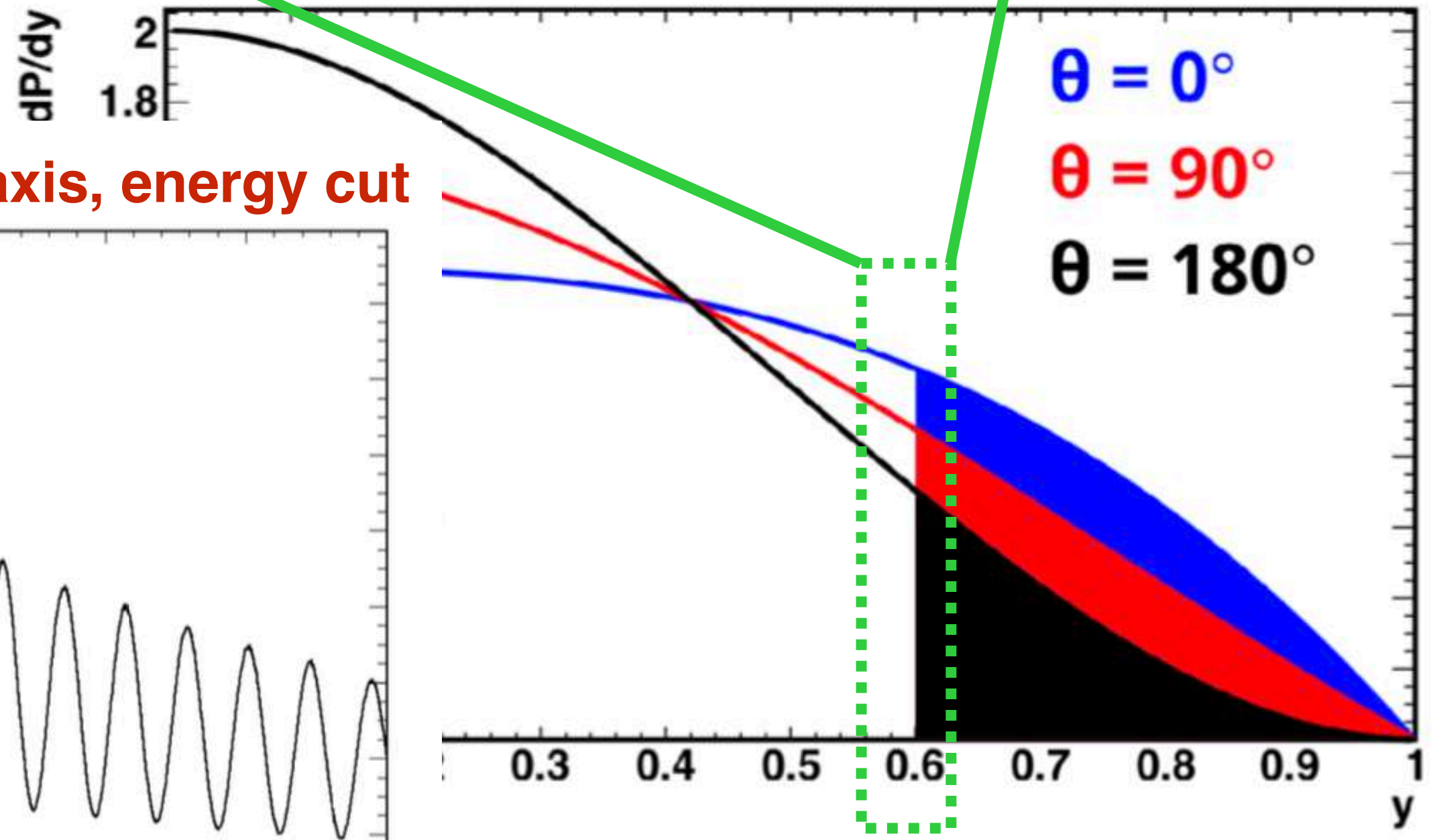
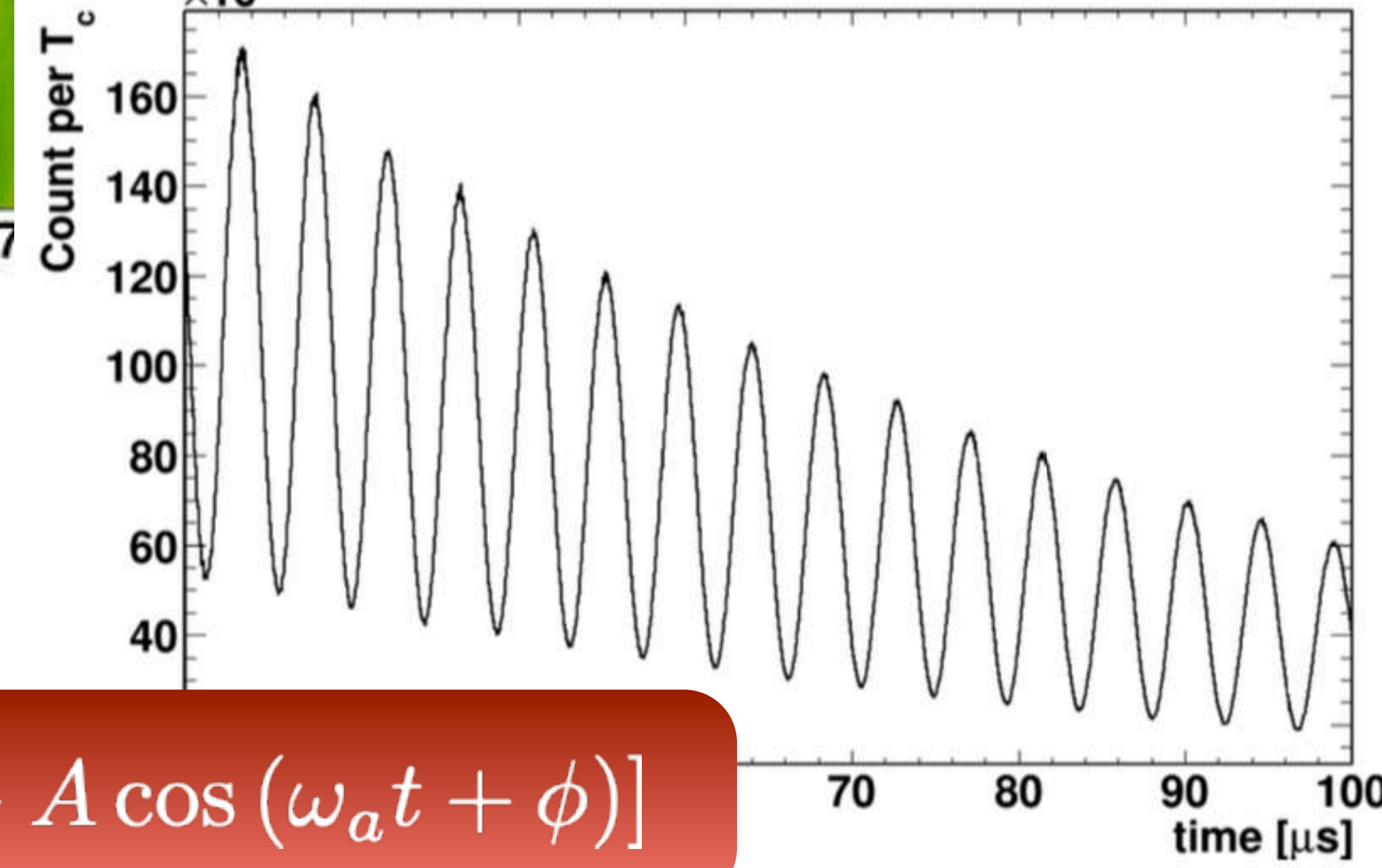


$$\frac{\delta\omega_a}{\omega_a} = \frac{\sqrt{2}}{2\pi f_a \tau_\mu N^{\frac{1}{2}} A}$$



Energy cut chosen to optimize figure-of-merit

Project along time axis, energy cut



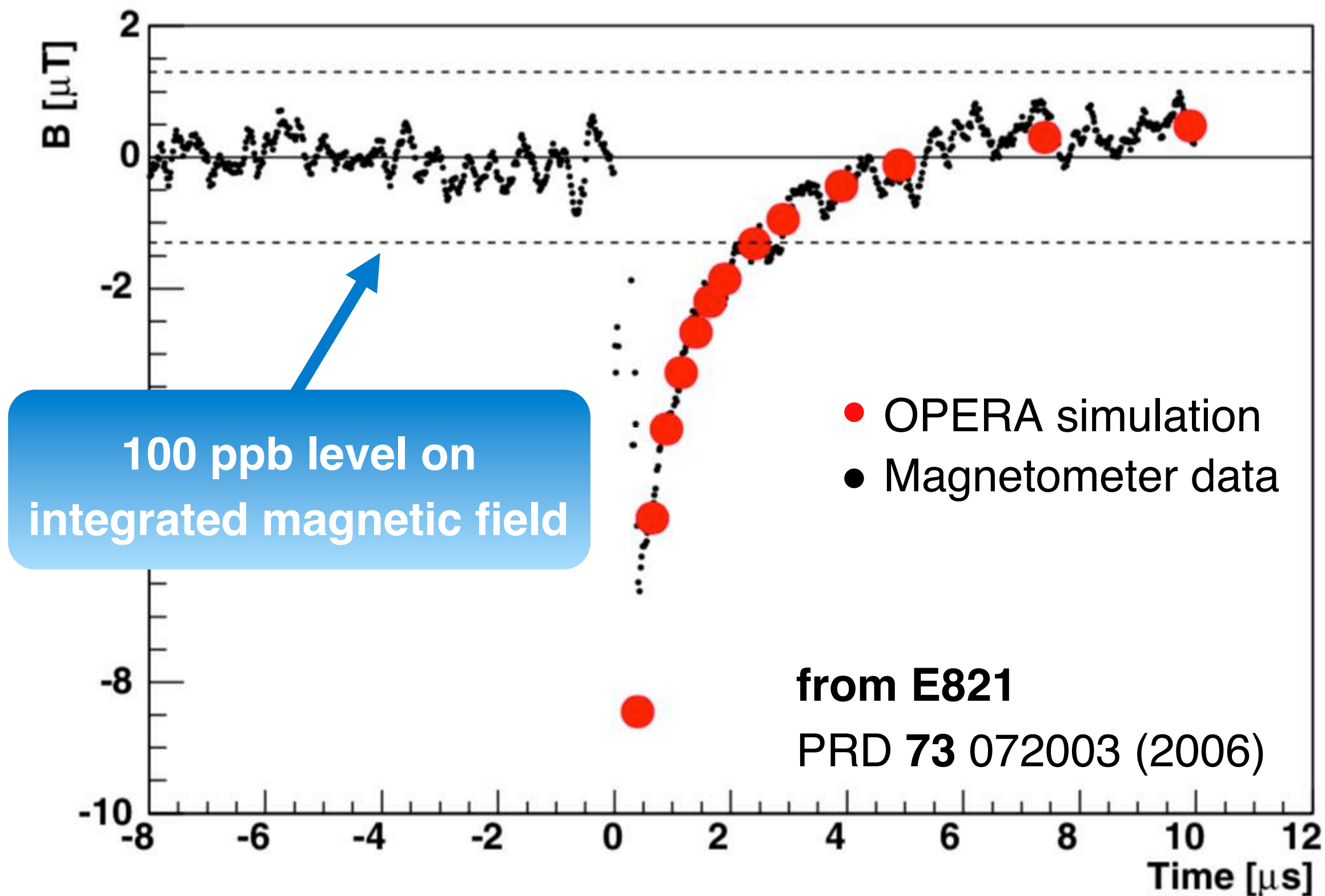
Fit to: $N(t) = N_0 e^{-t/\tau} [1 - A \cos(\omega_a t + \phi)]$

What Drives the ω_a Fit Start Time?

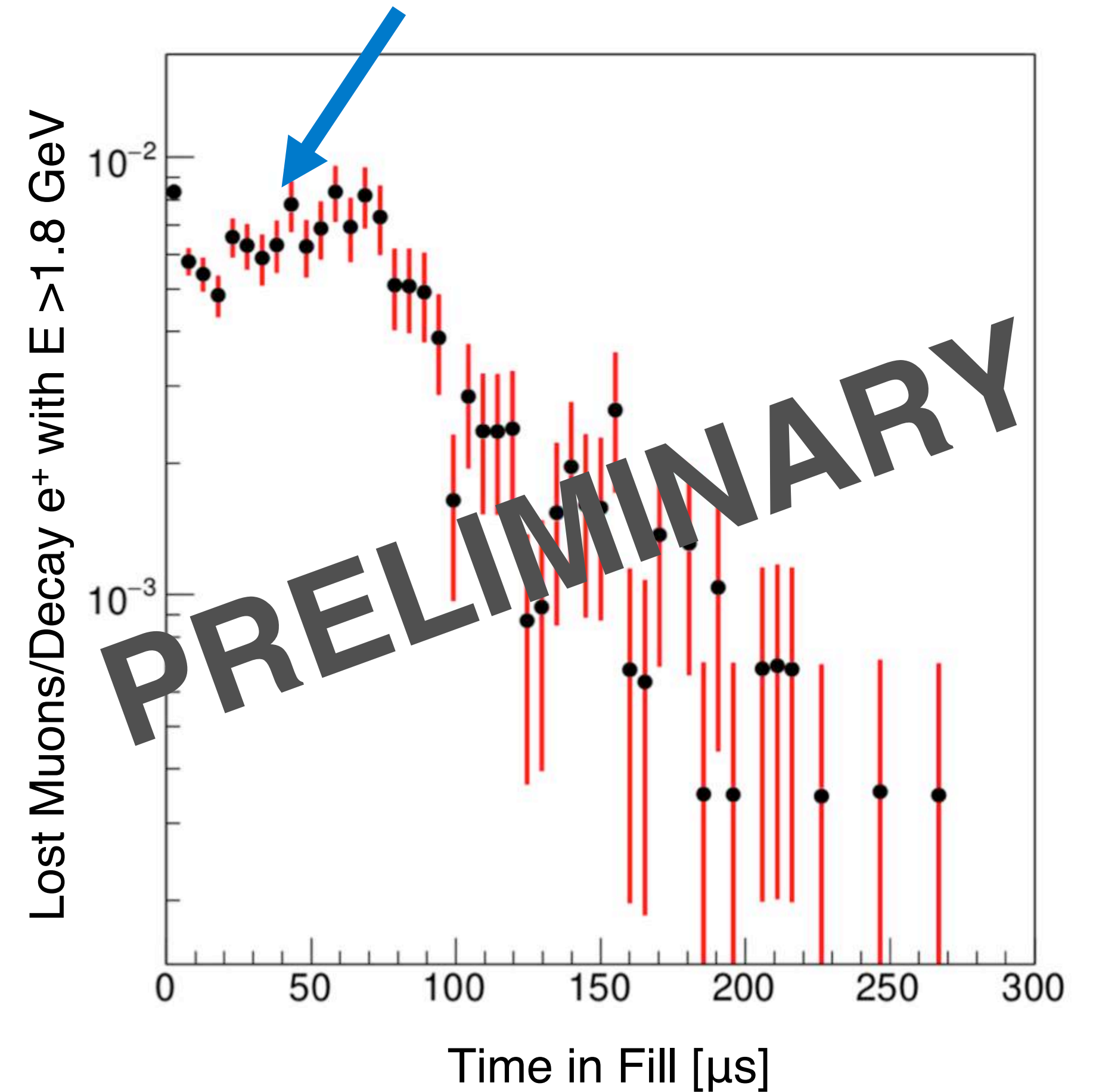


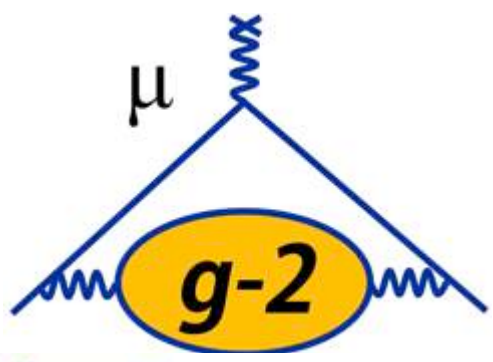
- Start fit window to extract ω_a at $\sim 30 \mu\text{s}$ to avoid:

Kicker eddy currents affect the magnetic field



Quad scraping at early times to reduce losses

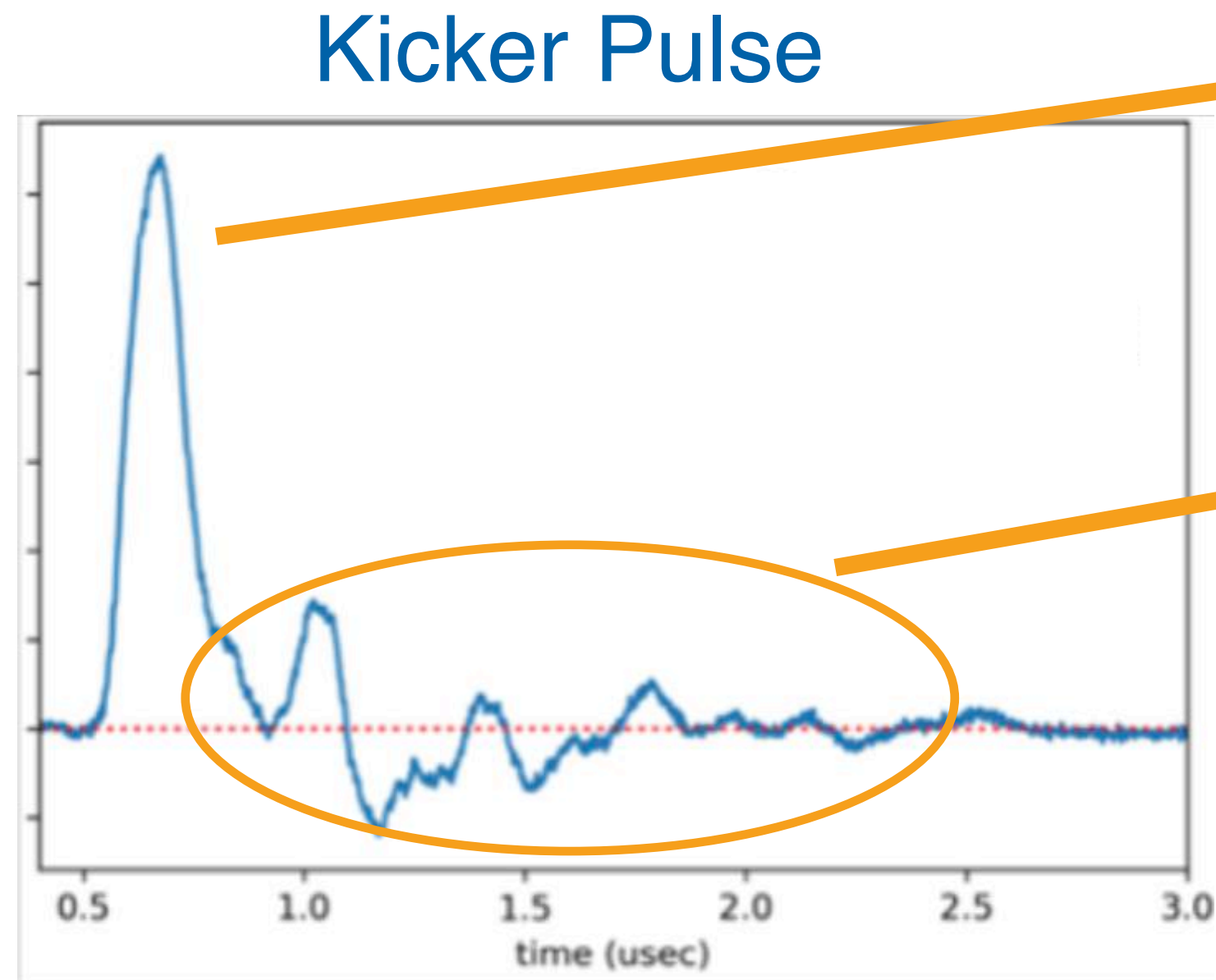




What Affects the Beam Shape?

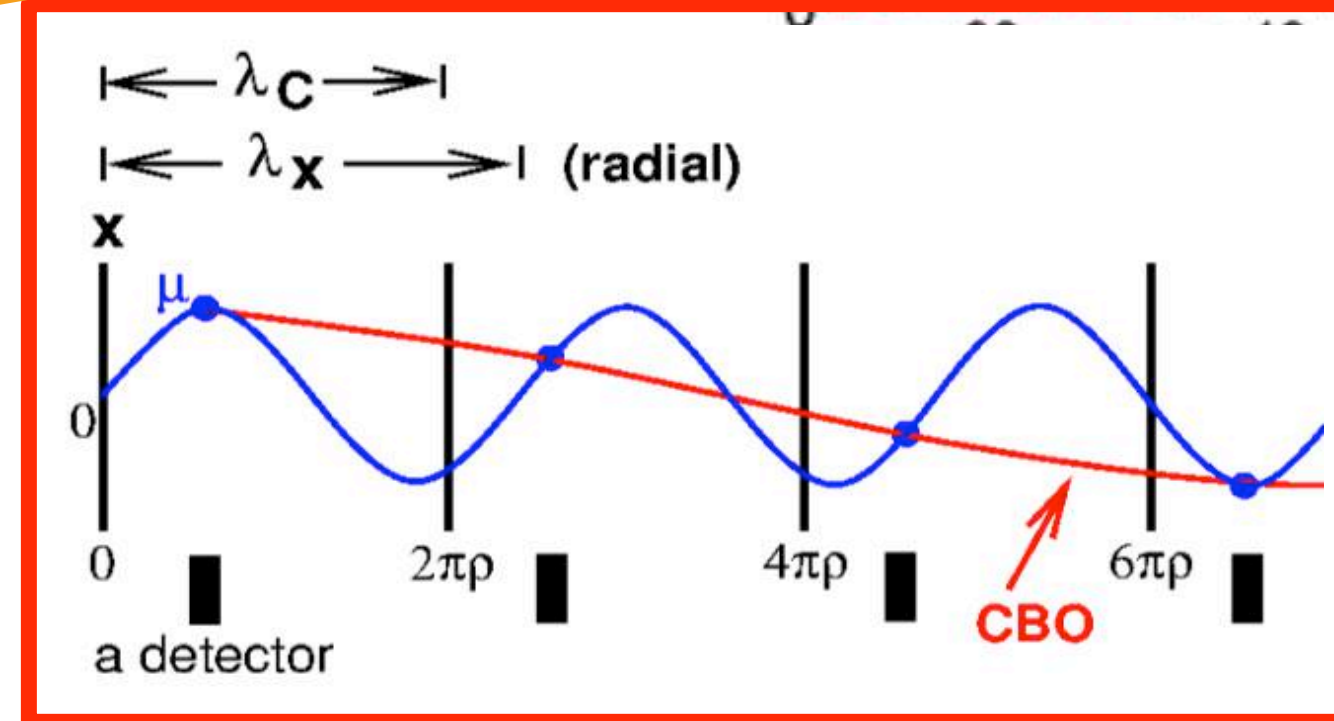
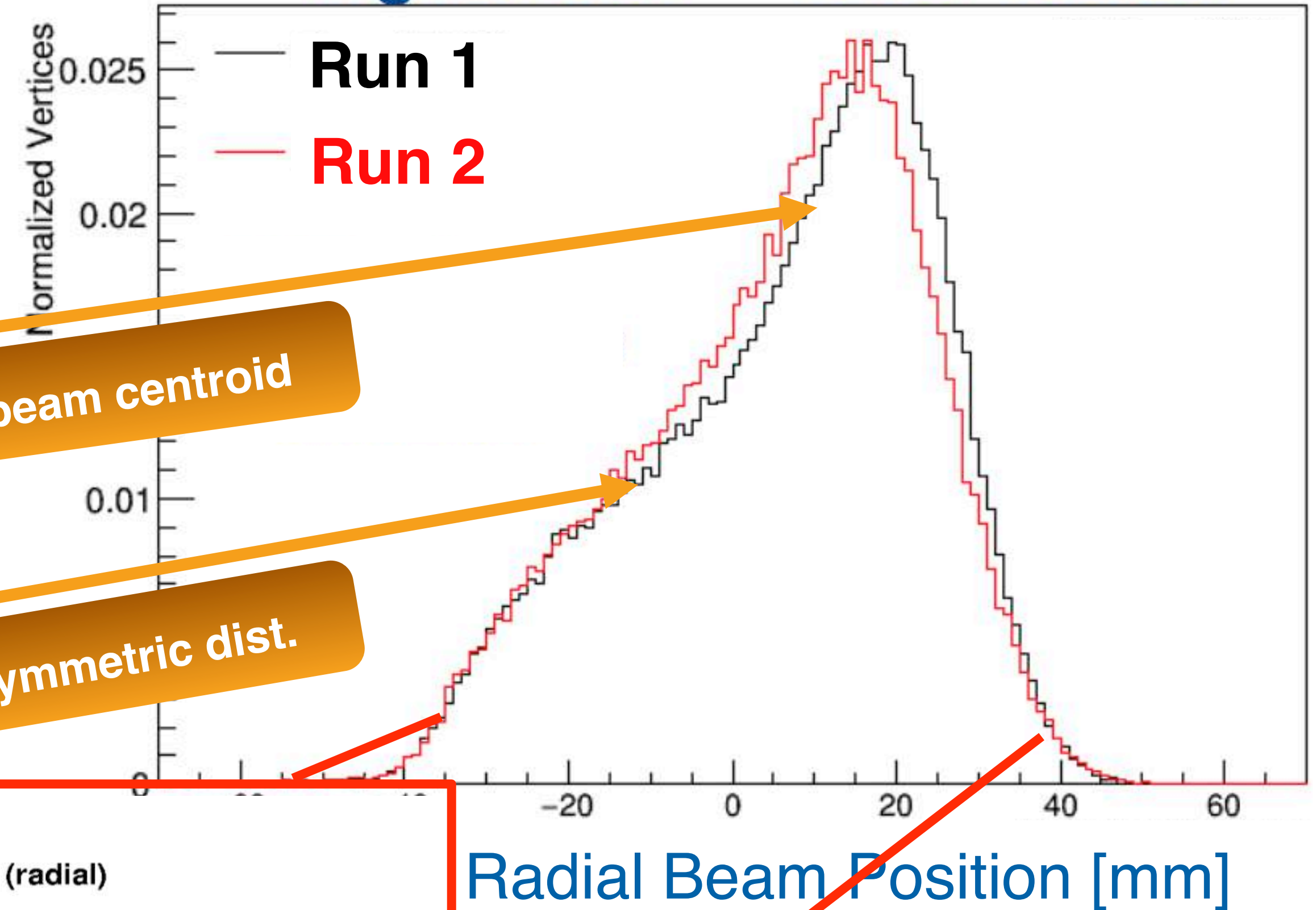
- **Kicker pulse** strength, shape affects structure of beam
- **Beam width** affected by dynamics

Higher kick → lower radius



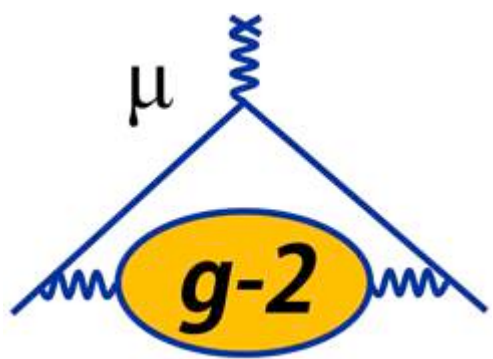
kick strength → beam centroid

ringing kick → asymmetric dist.



CBO → radial width

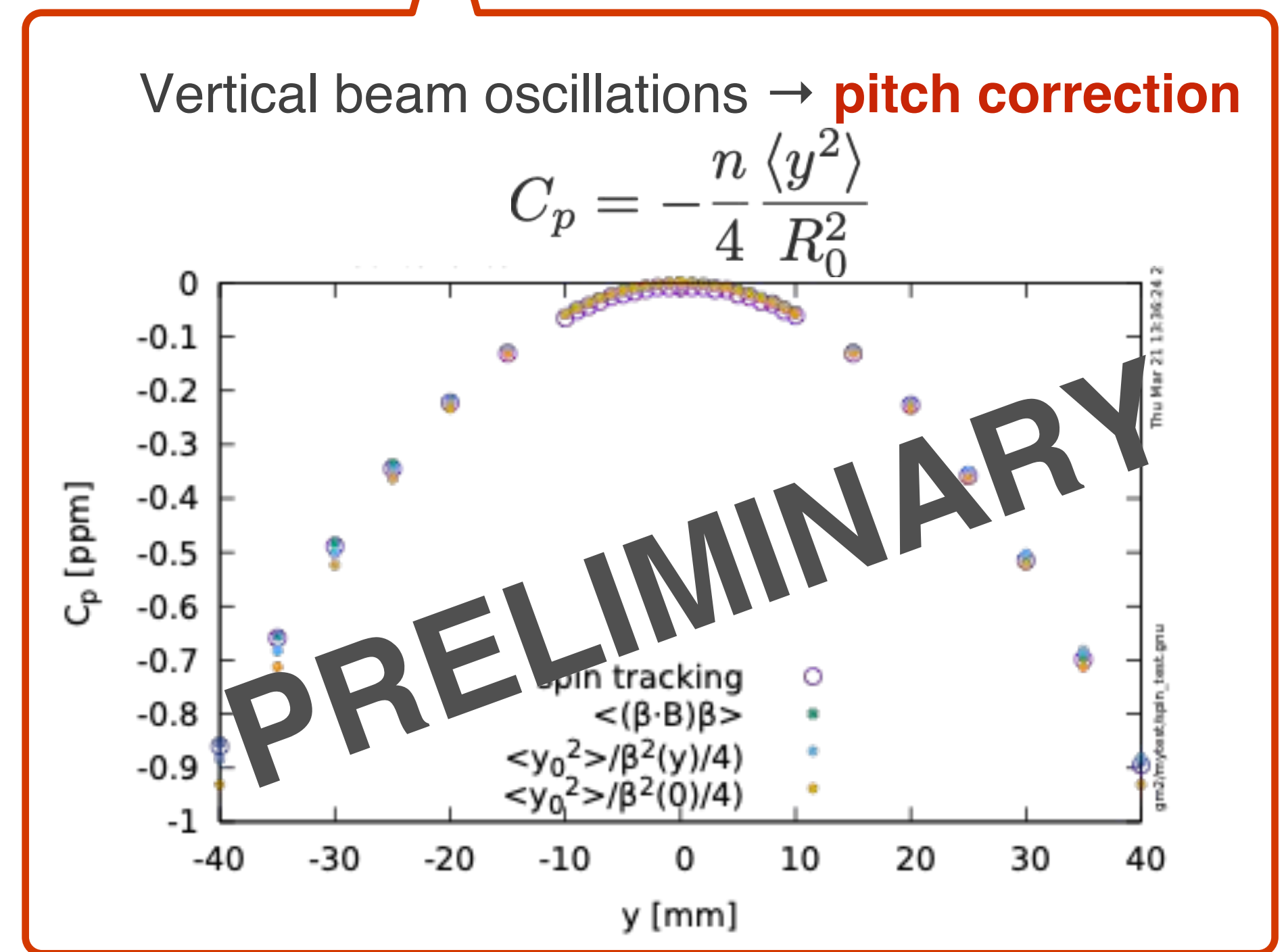
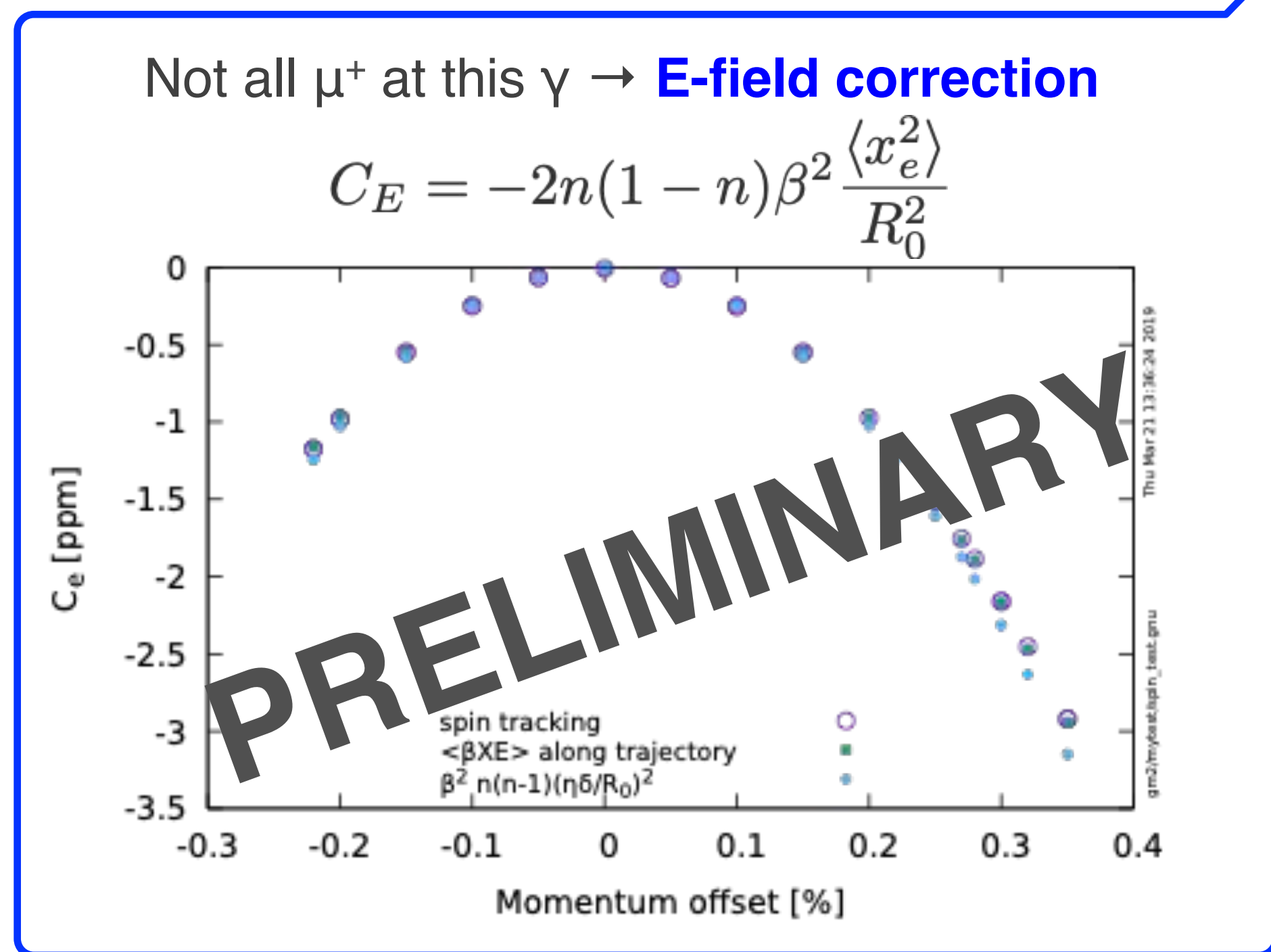
Beam Dynamics Corrections



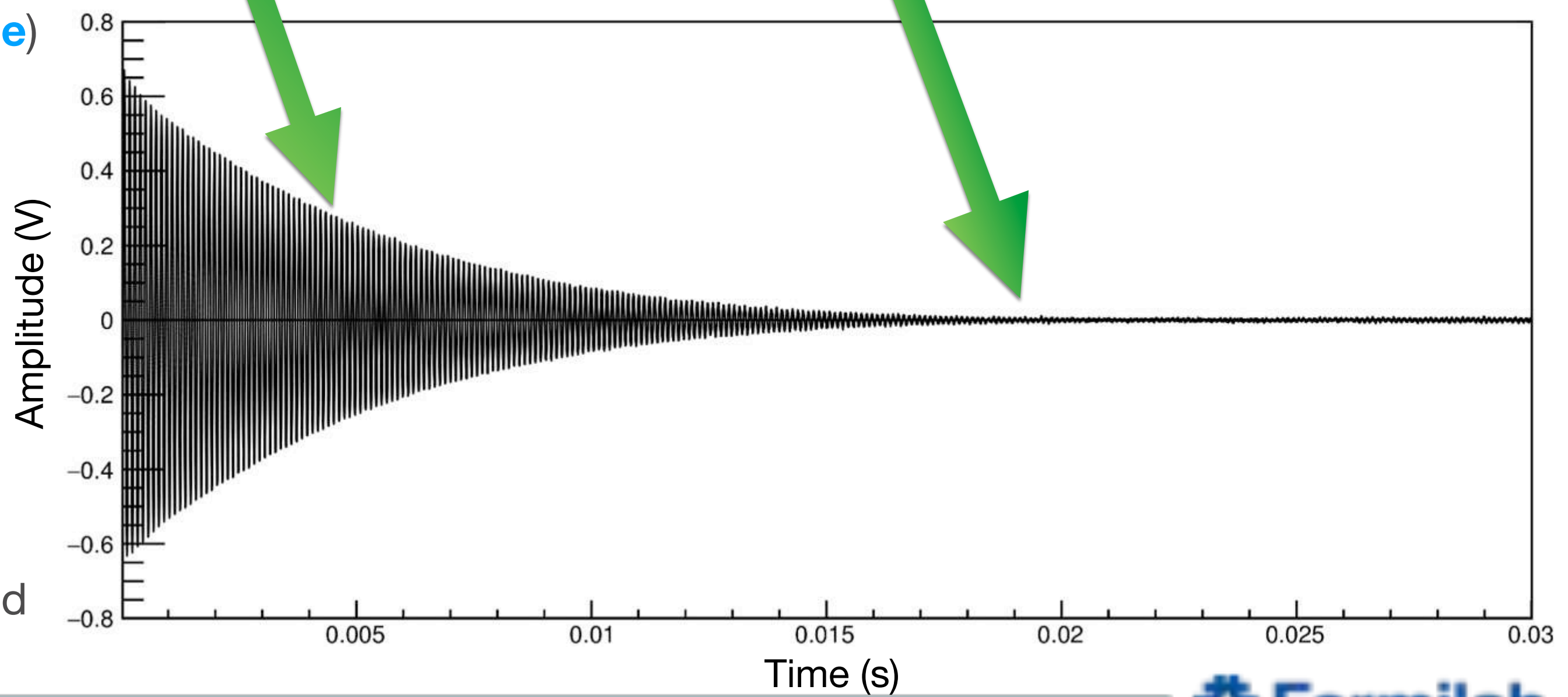
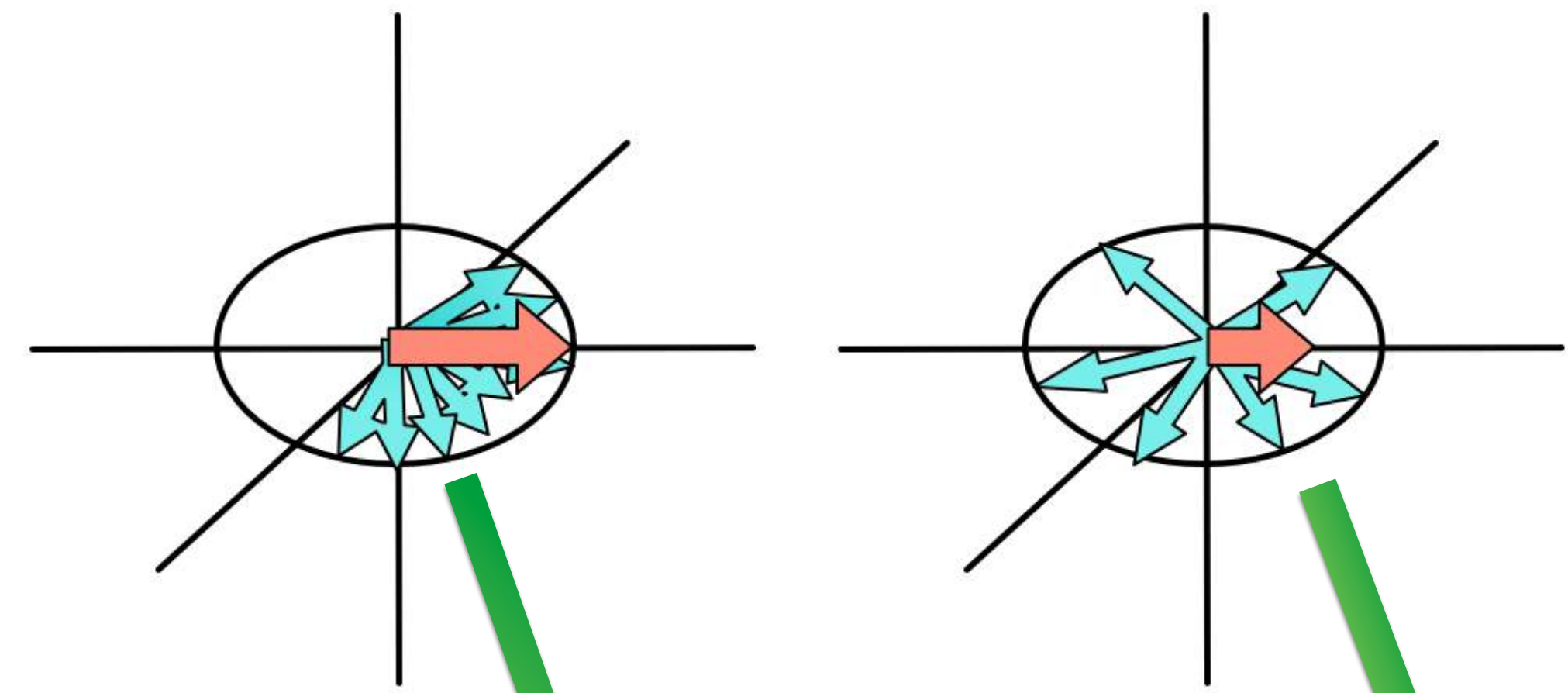
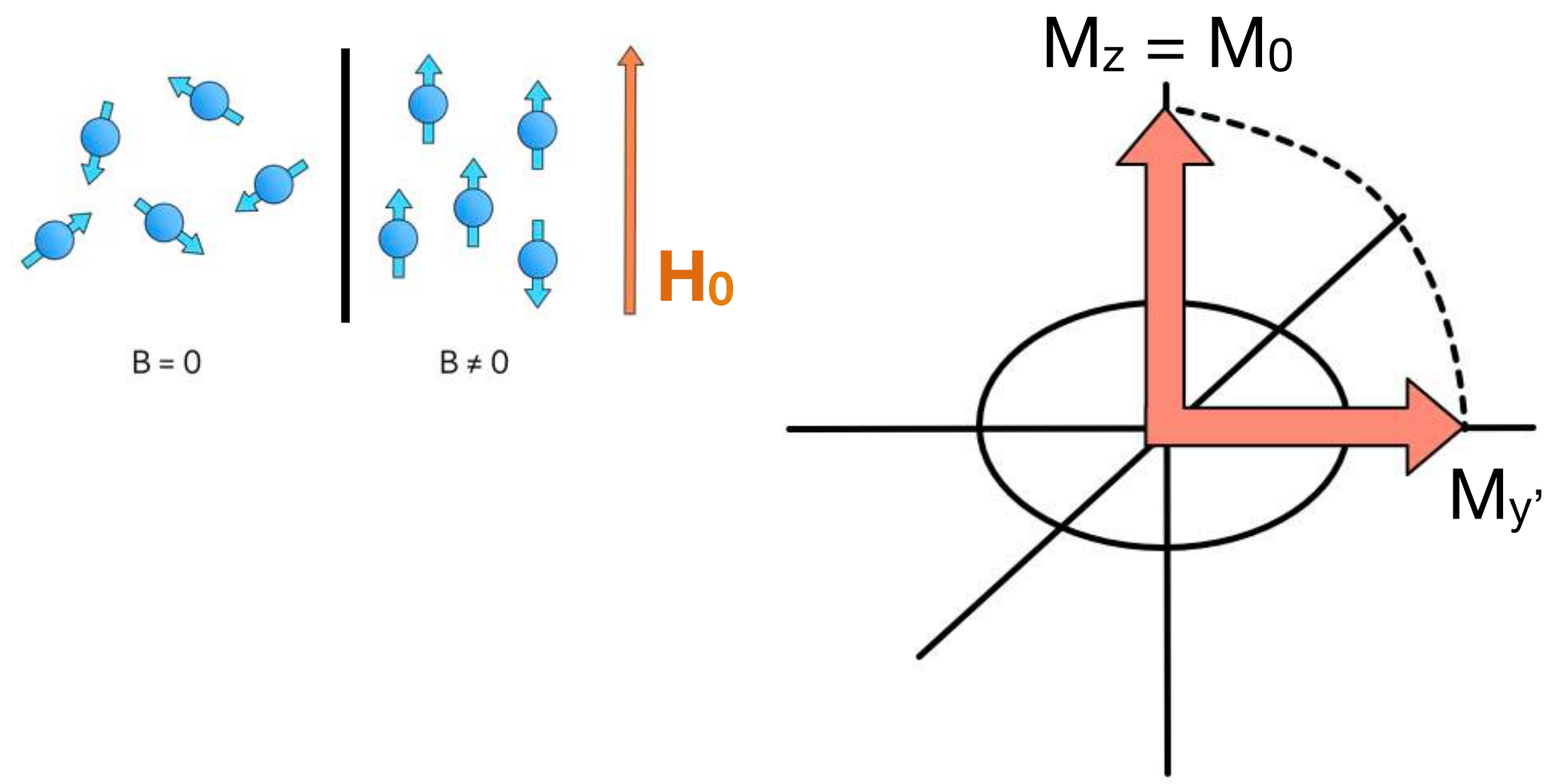
- Full expression for ω_a :

$$\vec{\omega}_a = \vec{\omega}_S - \vec{\omega}_C = -\frac{e}{mc} \left[a_\mu \vec{B} - \left(a_\mu - \frac{1}{\gamma^2 - 1} \right) \vec{\beta} \times \vec{E} - a_\mu \left(\frac{\gamma}{\gamma + 1} \right) (\vec{\beta} \cdot \vec{B}) \vec{\beta} \right]$$

- Choose $\gamma = 29.3$ ($p_\mu = 3.094$ GeV/c)



Pulsed Nuclear Magnetic Resonance



- Apply an RF pulse for a short time to the sample at Larmor frequency — tips spins perpendicular to external B field (**$\pi/2$ pulse**)
- Spin precession induces an EMF in the pickup coil
 - So-called **Free-Induction Decay (FID)**
- Decay of signal driven by:
 - Spin-spin interactions (dephasing) (pure T_2)
 - Field inhomogeneities (T_2^*)
 - Simultaneously, spins relax back to alignment with holding field (spin-lattice relaxation, T_1)

Magnetic Circuits

$$\mathcal{E} = \oint \vec{f}_s \cdot d\vec{\ell} = V = IR$$

Can write a similar equation for magnets

$$\mathcal{F} = \oint \vec{H} \cdot d\vec{\ell} = NI$$

Magnetomotive Force (mmf)

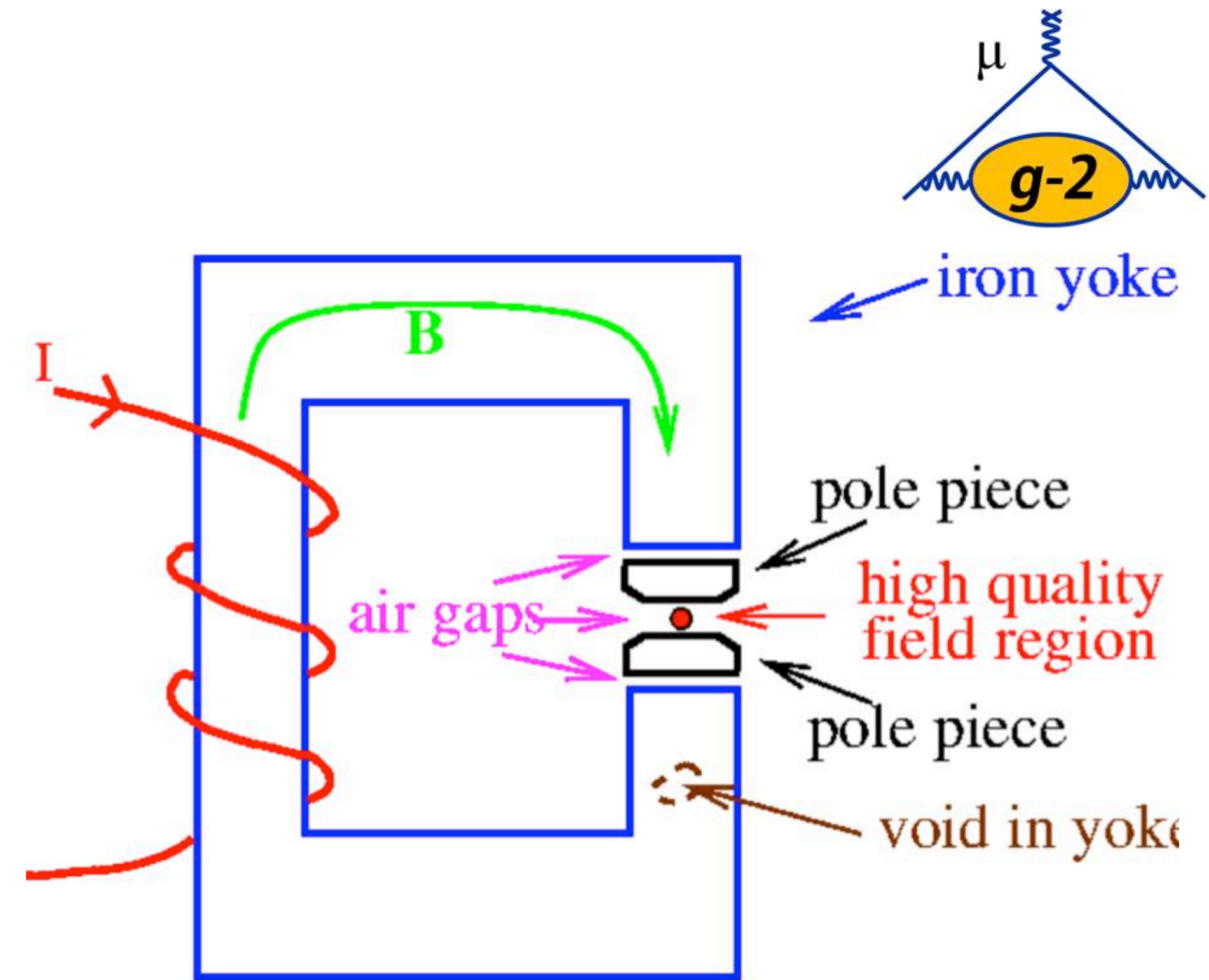
$$\vec{B} = \mu_0 (1 + \chi_m) \vec{H} = \mu \vec{H}$$

Rewrite H in terms of B

$$\Phi = \vec{B} \cdot \vec{A} = \mu \vec{H} \cdot \vec{A}$$

Consider magnetic flux

$$\Phi \int \frac{dl}{\mu A} = \mathcal{F} \Rightarrow \mathcal{R} = \int \frac{dl}{\mu A} = \frac{\mathcal{F}}{\Phi}$$



Magnetic Reluctance

- Analogous to resistance in an electrical circuit

$$V = IR \Leftrightarrow \mathcal{F} = \Phi \mathcal{R}$$

- Current flows along a path of least resistance while field lines will take a path of least reluctance
- While the emf drives electric charges (Ohm's Law), the mmf "drives" magnetic field lines (Hopkinson's Law)

Magnet Anatomy

- For E821, Gordon Danby had a brilliant magnet design



B = 1.45 T (~5200 A)

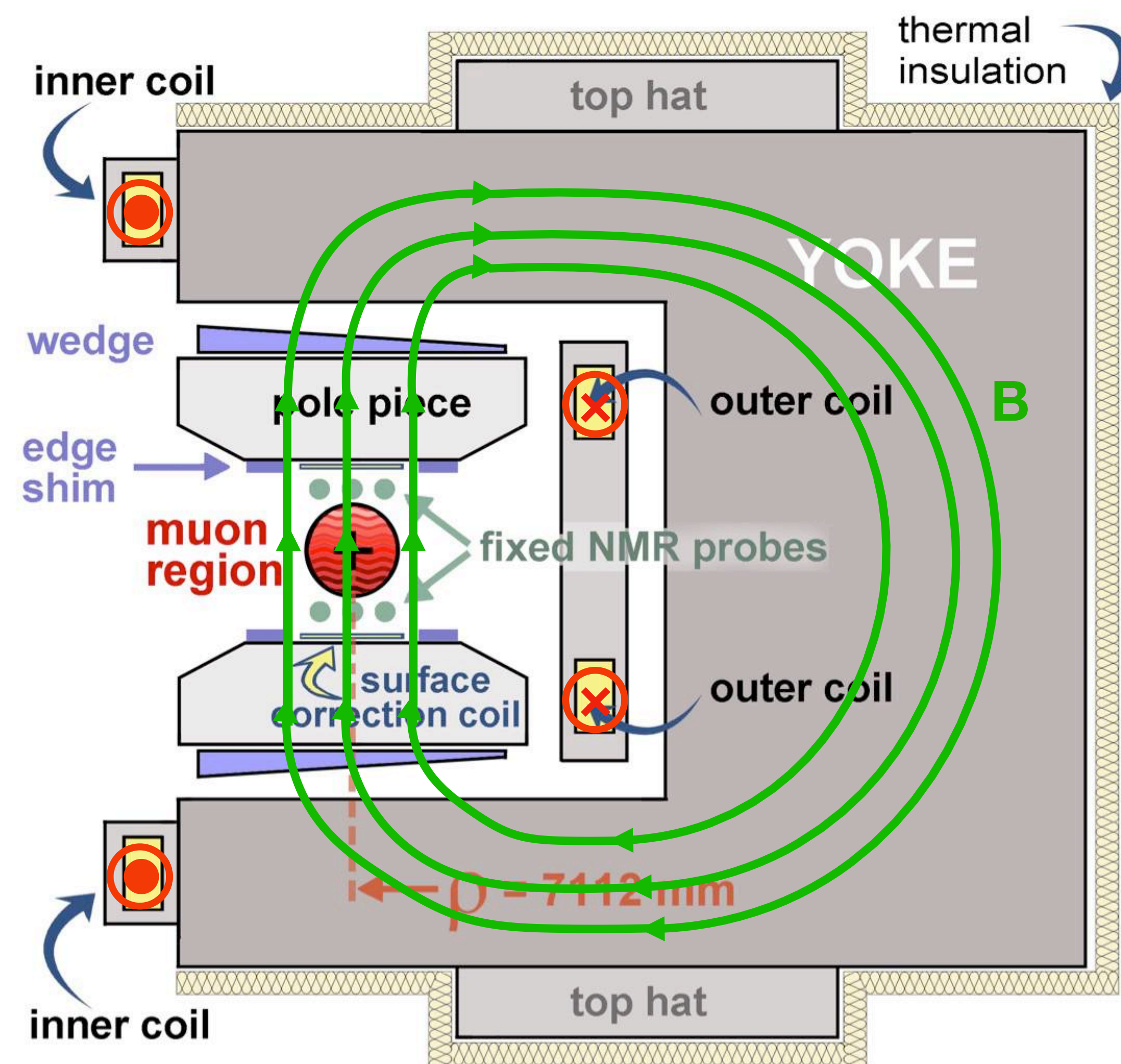
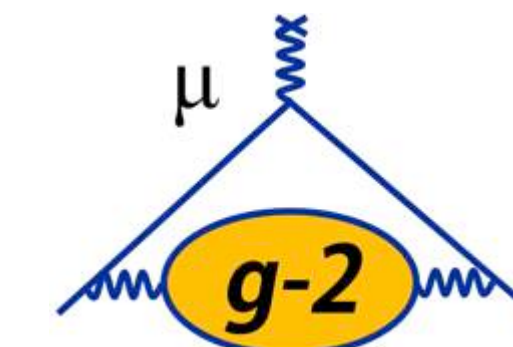
- Non-persistent current: fine-tuning of field in real time

12 C-shaped yokes

- 3 upper and 3 lower poles per yoke
- 72 total poles

Shimming knobs

- Pole separation determines field: pole tilts, non-flatness affect uniformity
- Top hats (30 deg effect, dipole)
- Wedges (10 deg effect, dipole, quadrupole)
- Edge shims (10 deg effect, dipole, quadrupole, sextupole)
- Laminations (1 deg effect, dipole, quadrupole, sextupole)
- Surface coils (360 deg effect, quadrupole, sextupole,...)

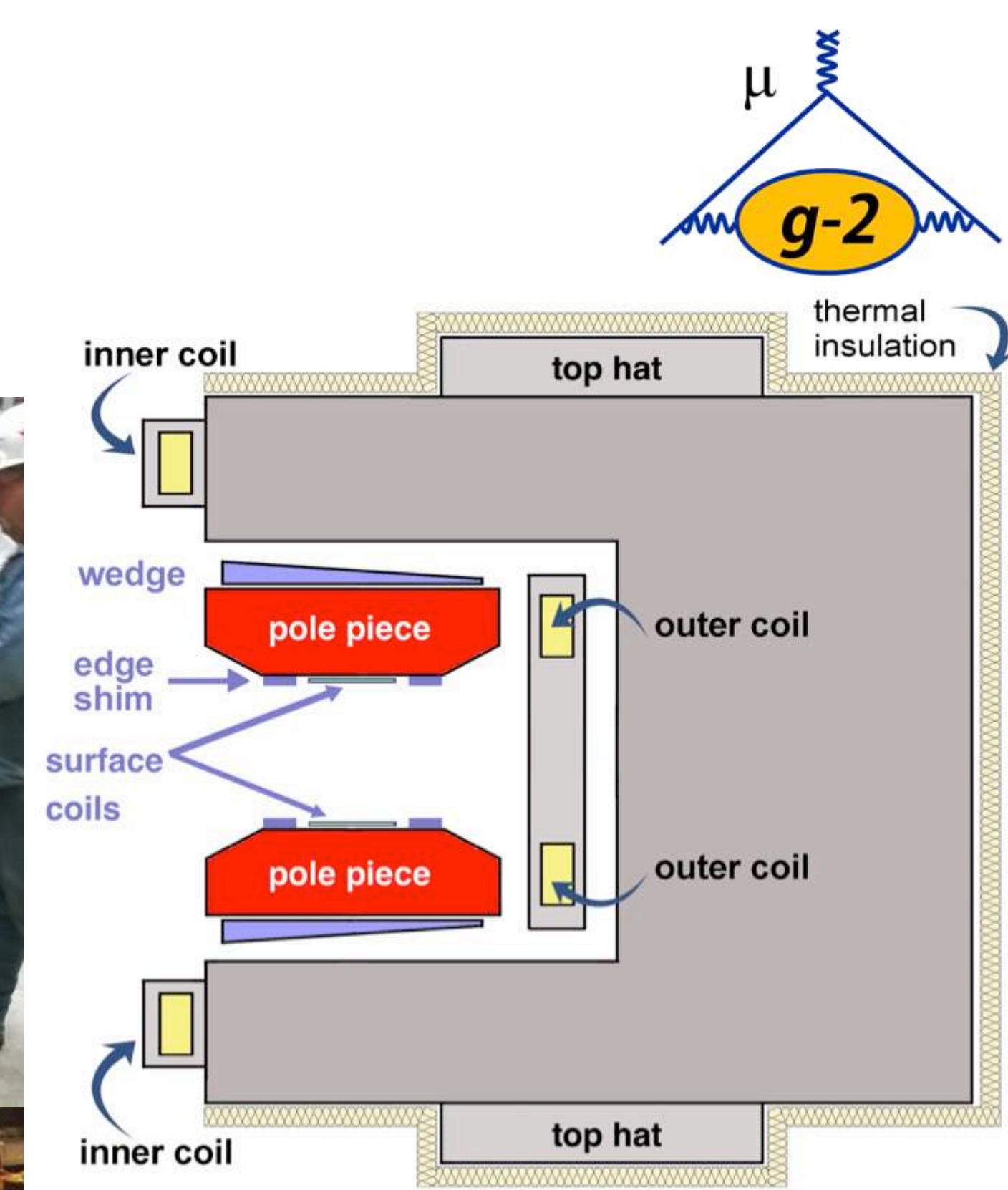
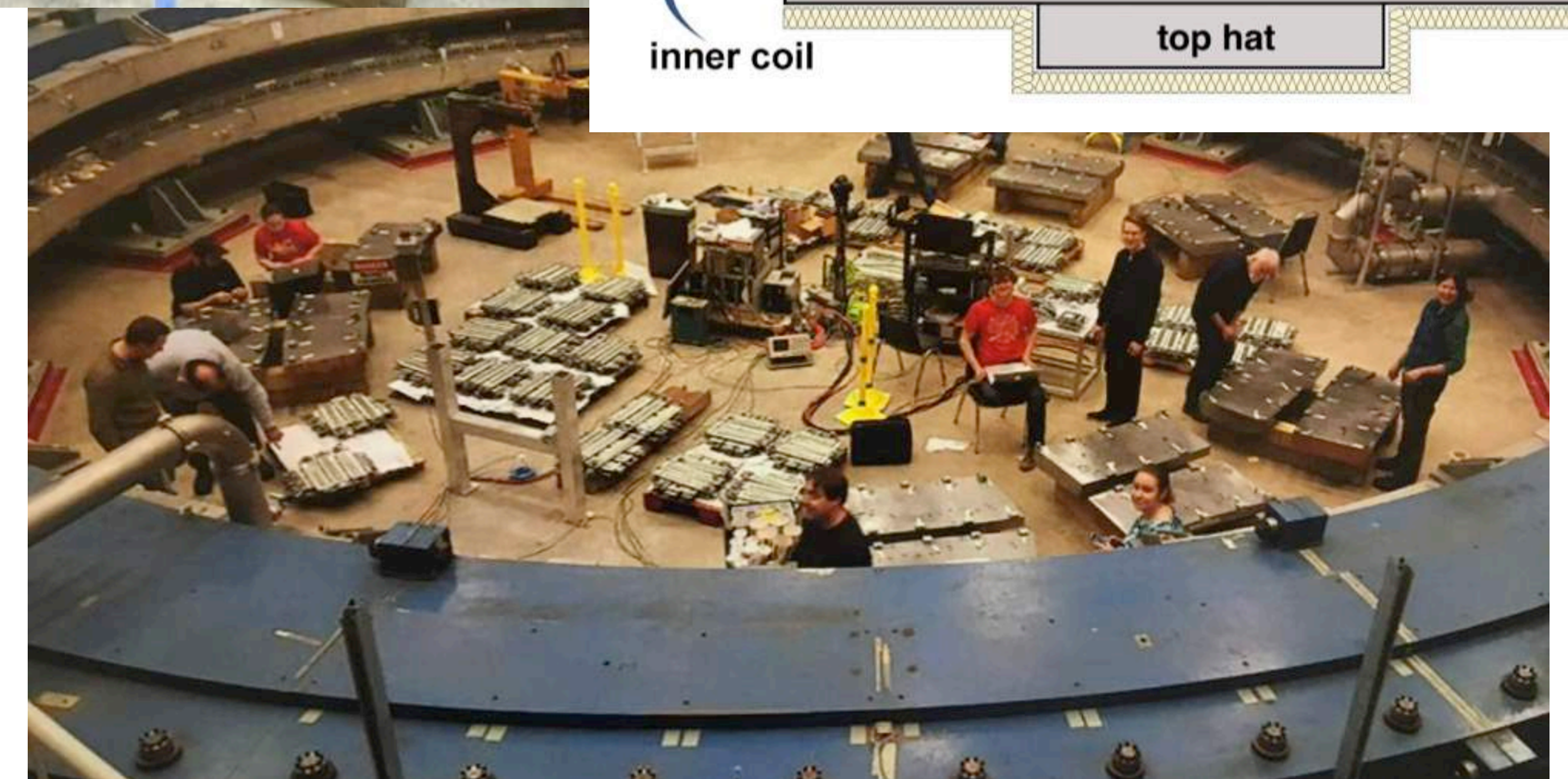


Current direction indicated by red markers



Optimizing the Dipole Moment

- Want to optimize the vertical component of the field
- Step and tilt discontinuities in pole surfaces yield large variations in the field
- To reduce/remove such effects, make adjustments to pole feet, which changes the magnet gaps and tilts
 - Use 0.001 – 0.010” thick shims
 - Requires removal of poles from the ring
- Informed by a computer model that optimizes the pole configurations
 - Requires global continuity between pole surfaces
 - Allows only three adjacent poles to be moved at a time (preserves alignment)



Minimizing the Quad, Sext, Octu

Calibrated shimming knobs

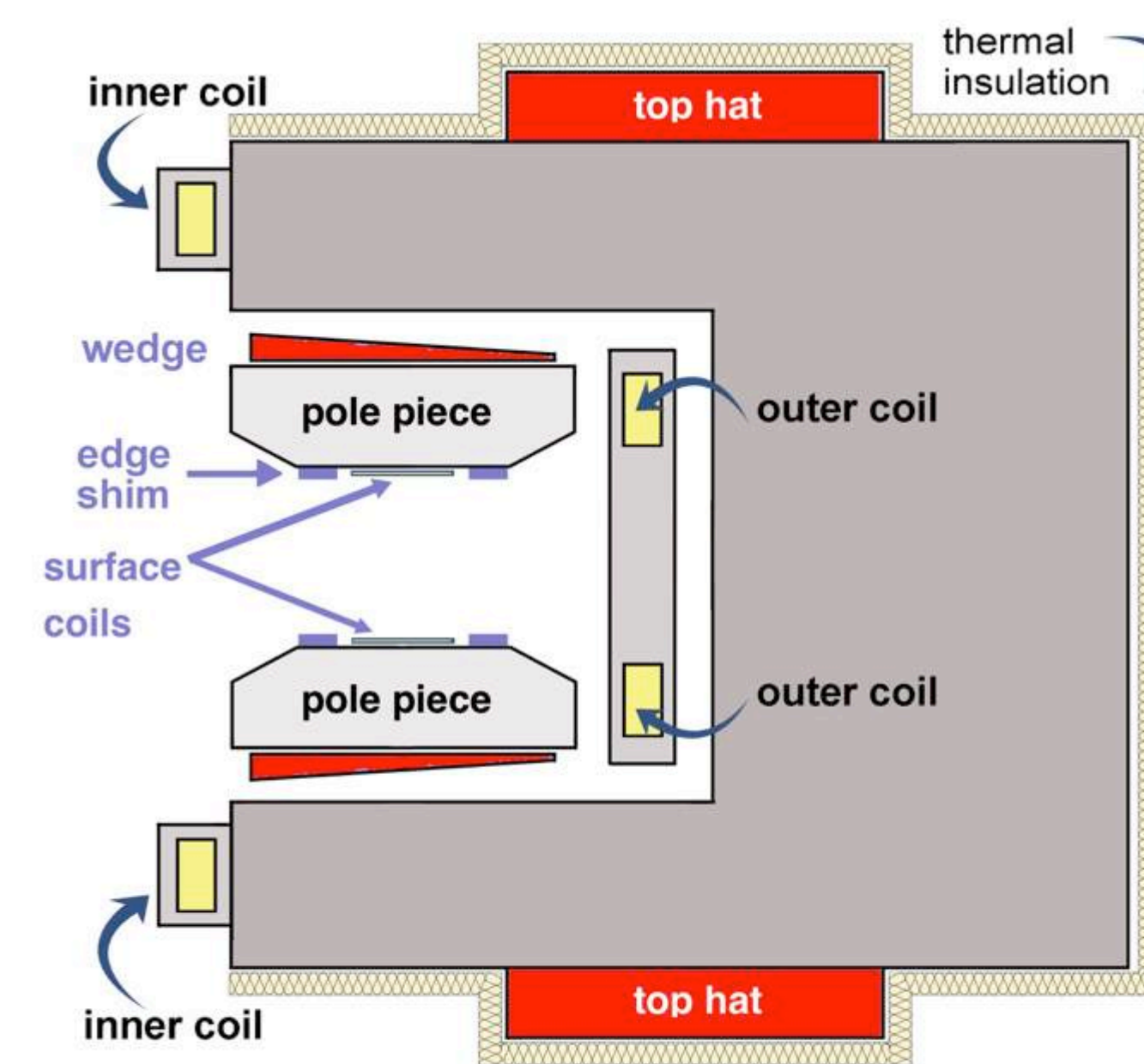
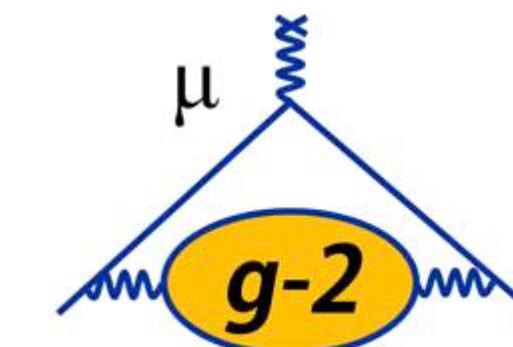
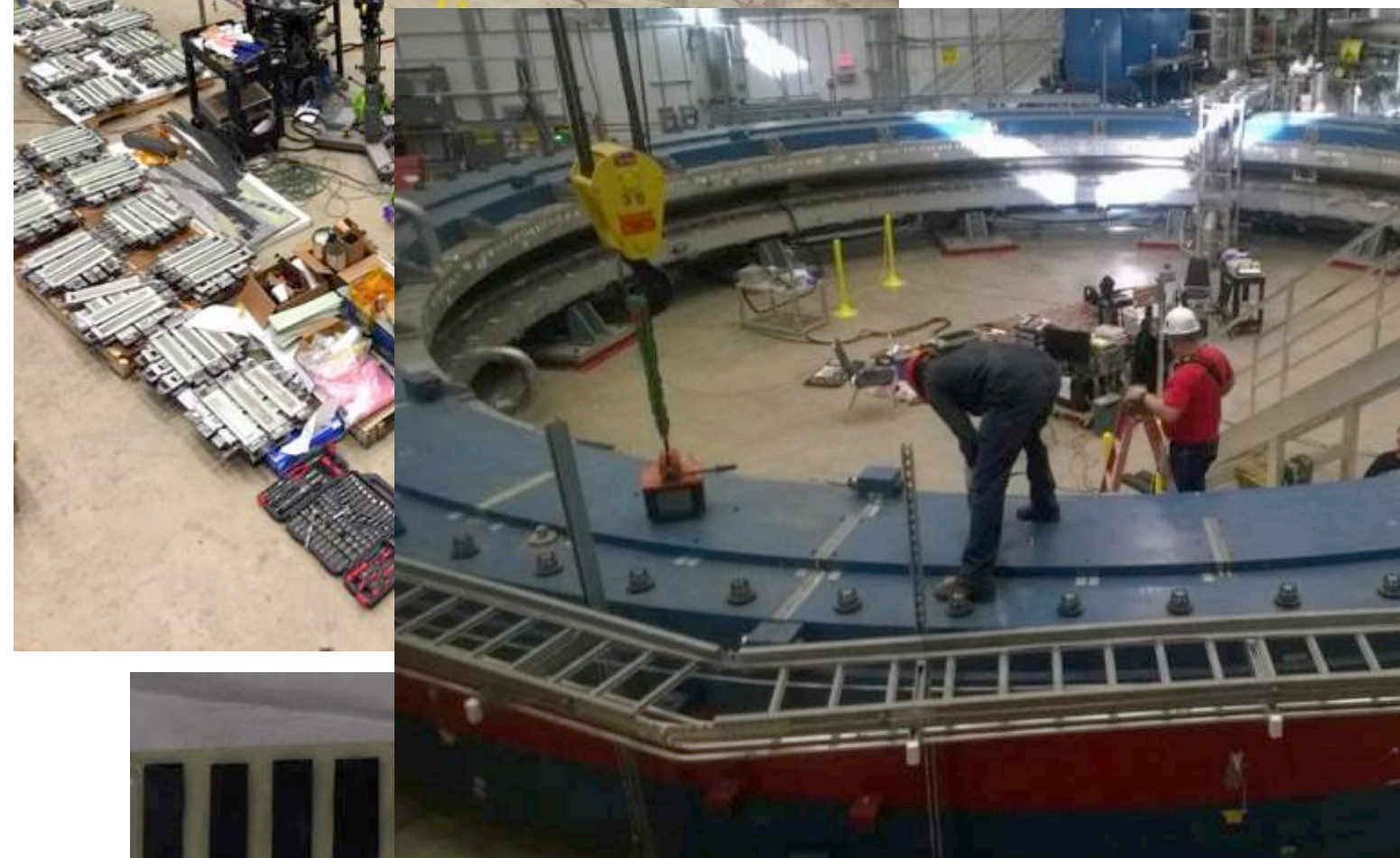
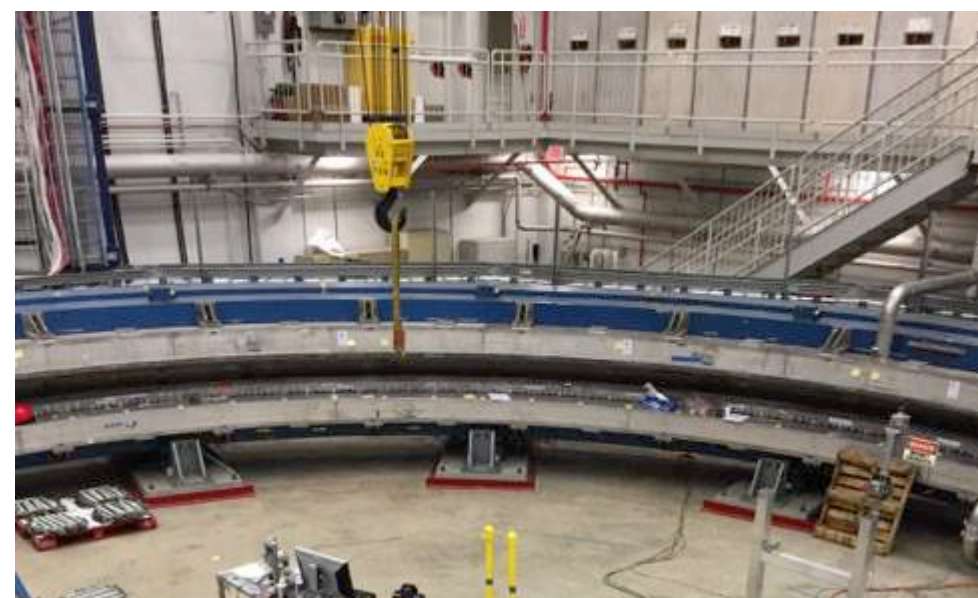
- 48 top hats
- 864 wedges
- ~8400 iron foils (on pole surfaces)

Coarse tuning: top hat & wedge adjustments (dipole, quadrupole)

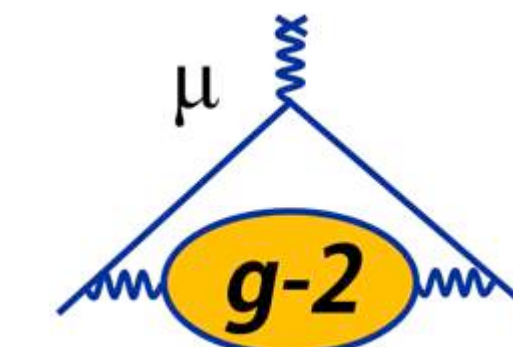
- Least-squares fit to field maps predicts top hat and wedge positions

Fine tuning: iron foils (quadrupole, sextupole,...)

- Modeled as saturated dipoles in 1.45 T field
- Computer code predicts foil width (mass) distribution to fill in the valleys of the field map

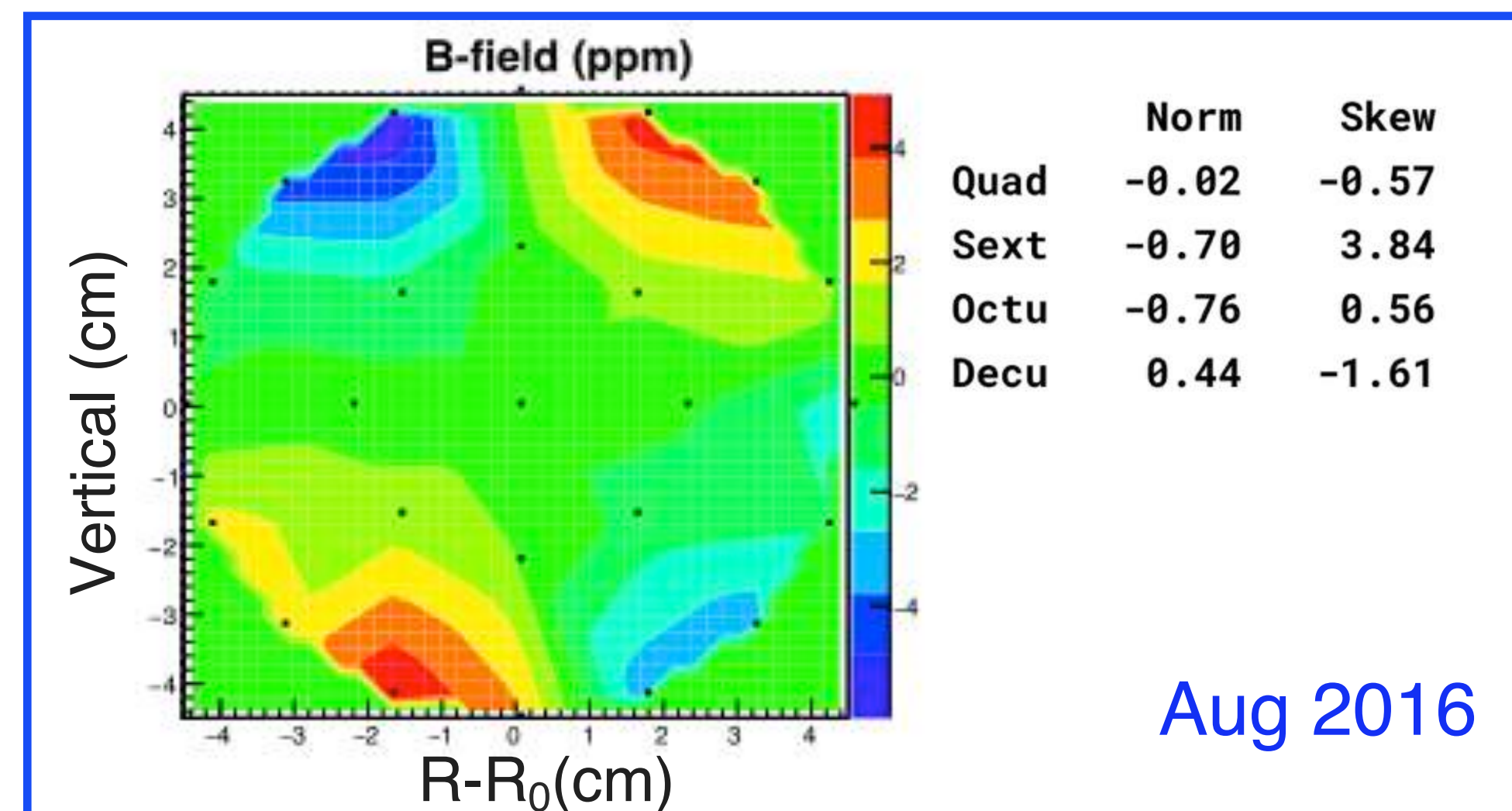
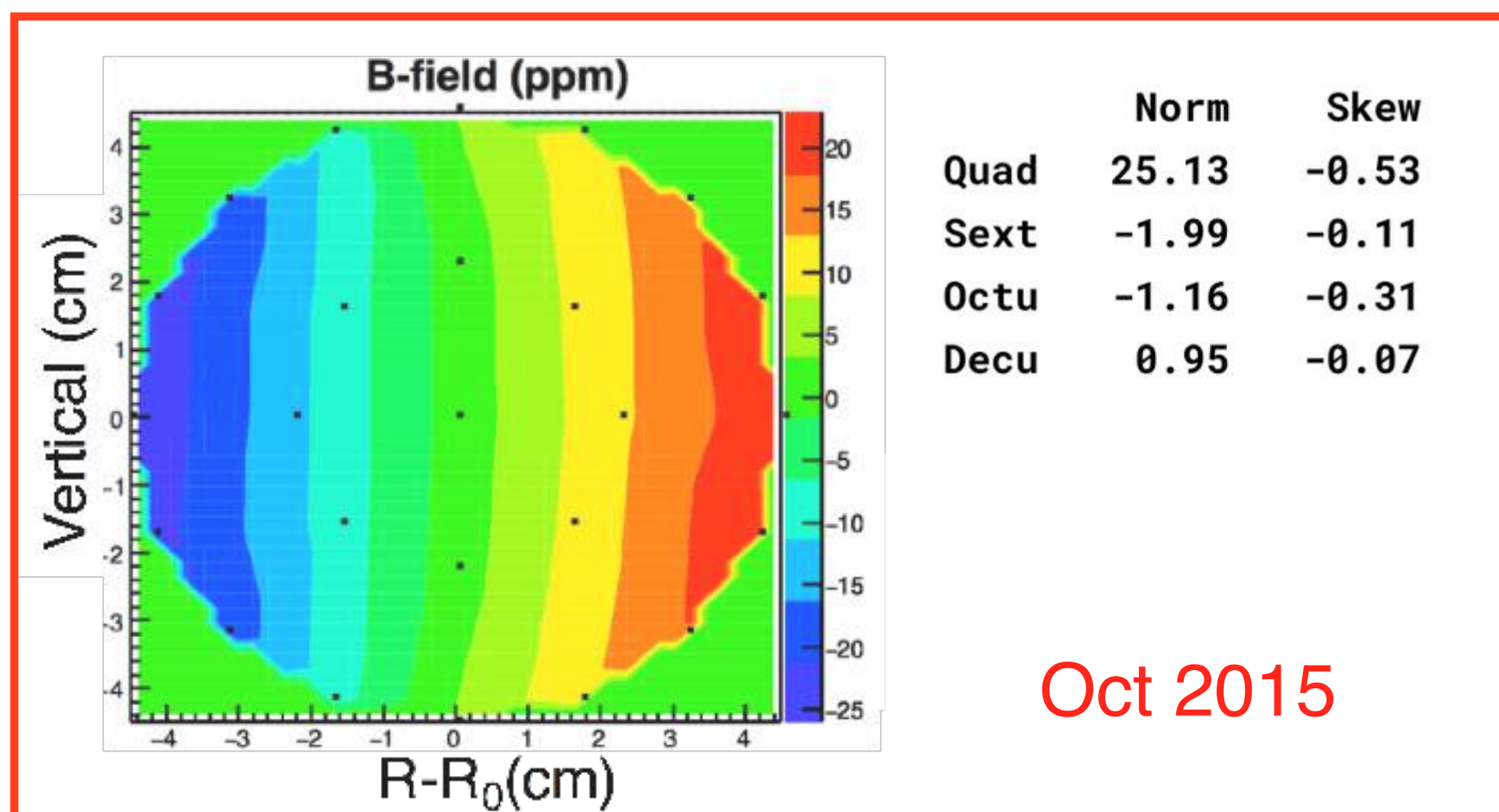
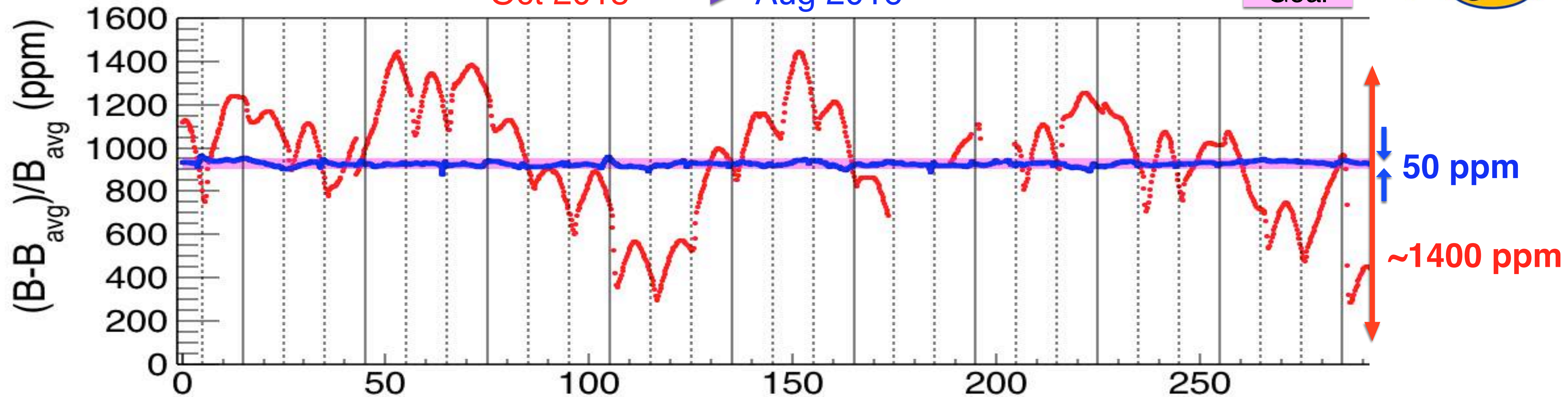


Rough Shimming Results



Oct 2015 → Aug 2016

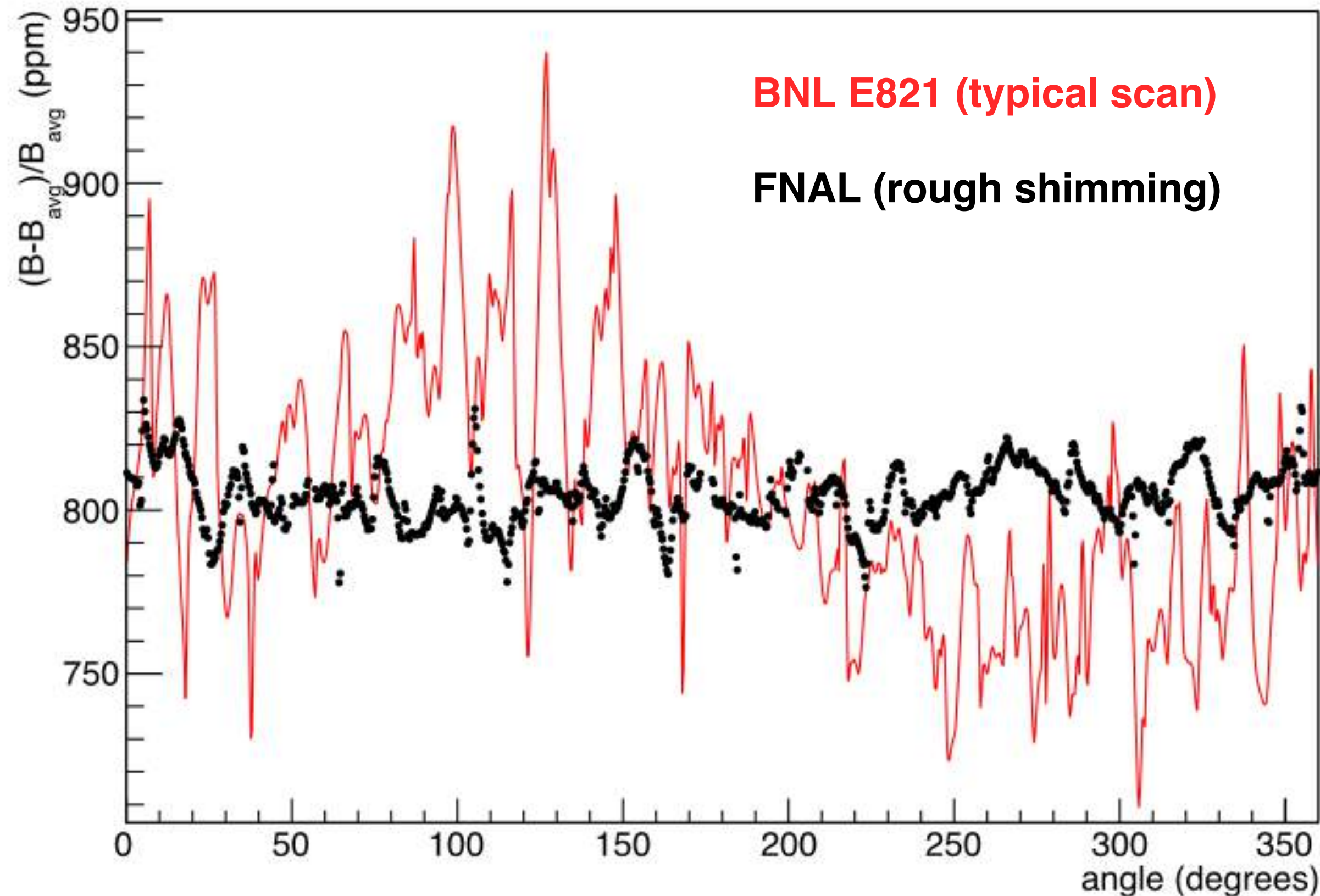
Goal



Magnetic Field Comparison: BNL 821 and FNAL E989



Dipole Vs Azimuth



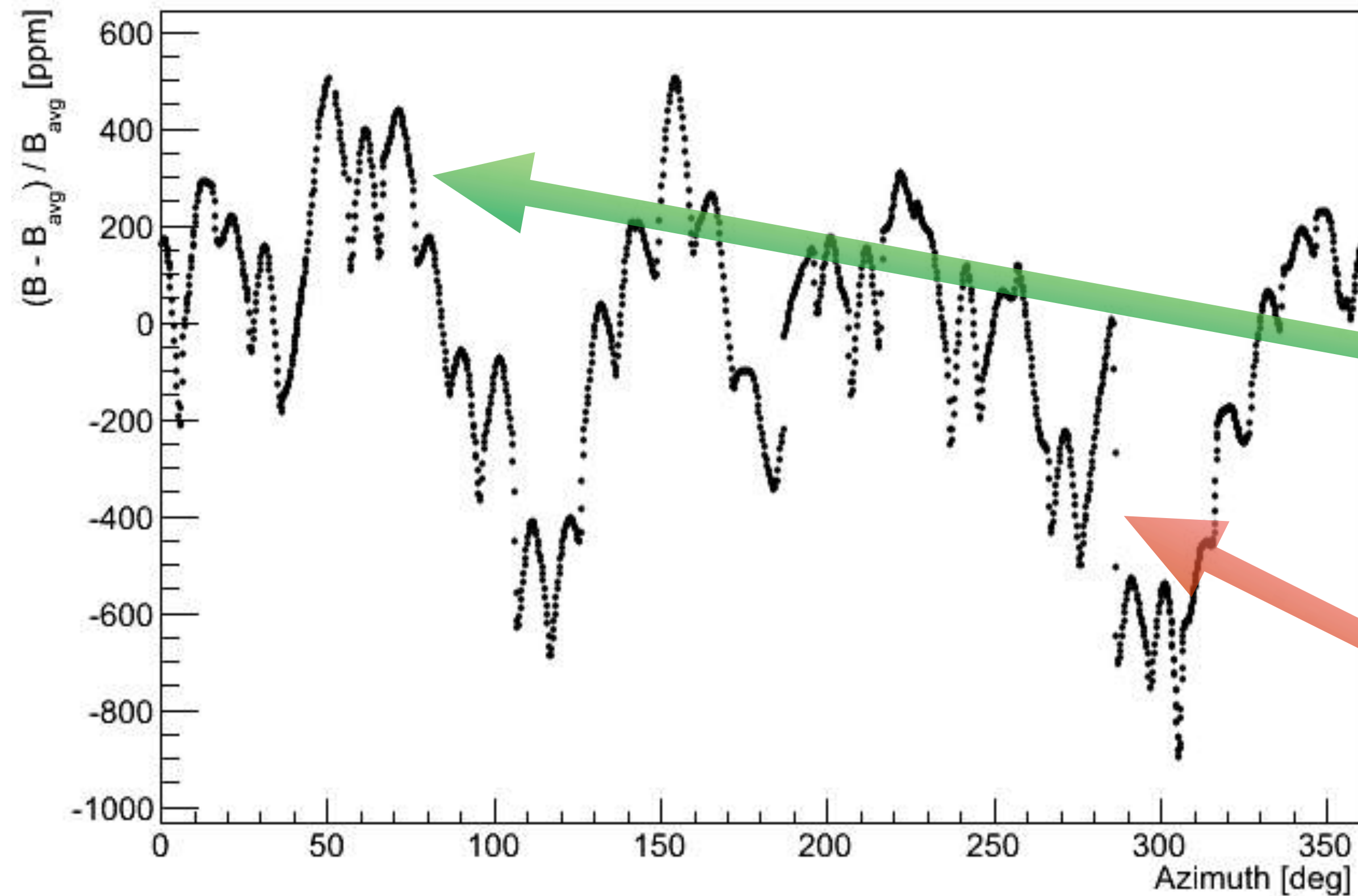
- Laminations very successful in reducing field variations

- **BNL E821: 39 ppm RMS (dipole), 230 ppm peak-to-peak**
- FNAL rough shimming: 10 ppm RMS (dipole), 75 ppm peak-to-peak

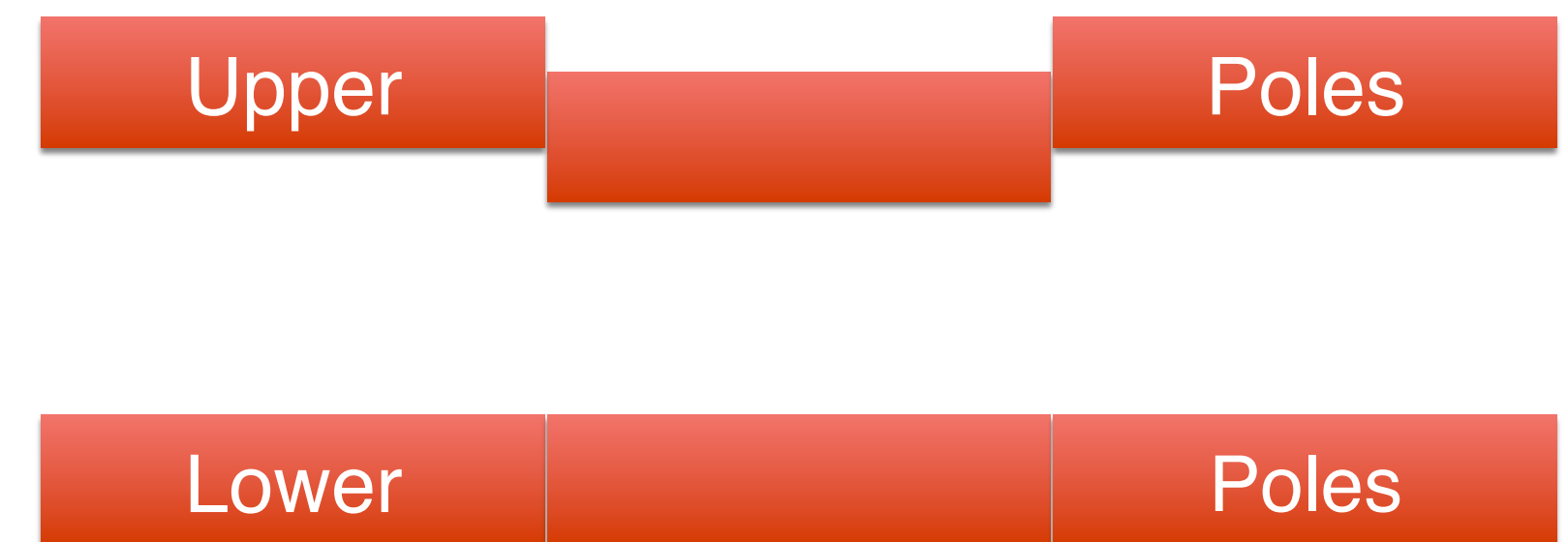
Magnetic Field Variations



First Magnetic Field Map, Oct 14 2015



- Gradual drift from materials, pole gap changes
- 36 pairs of poles \rightarrow 10-degree structure
- Pole shape:
- Pole-to-pole discontinuities

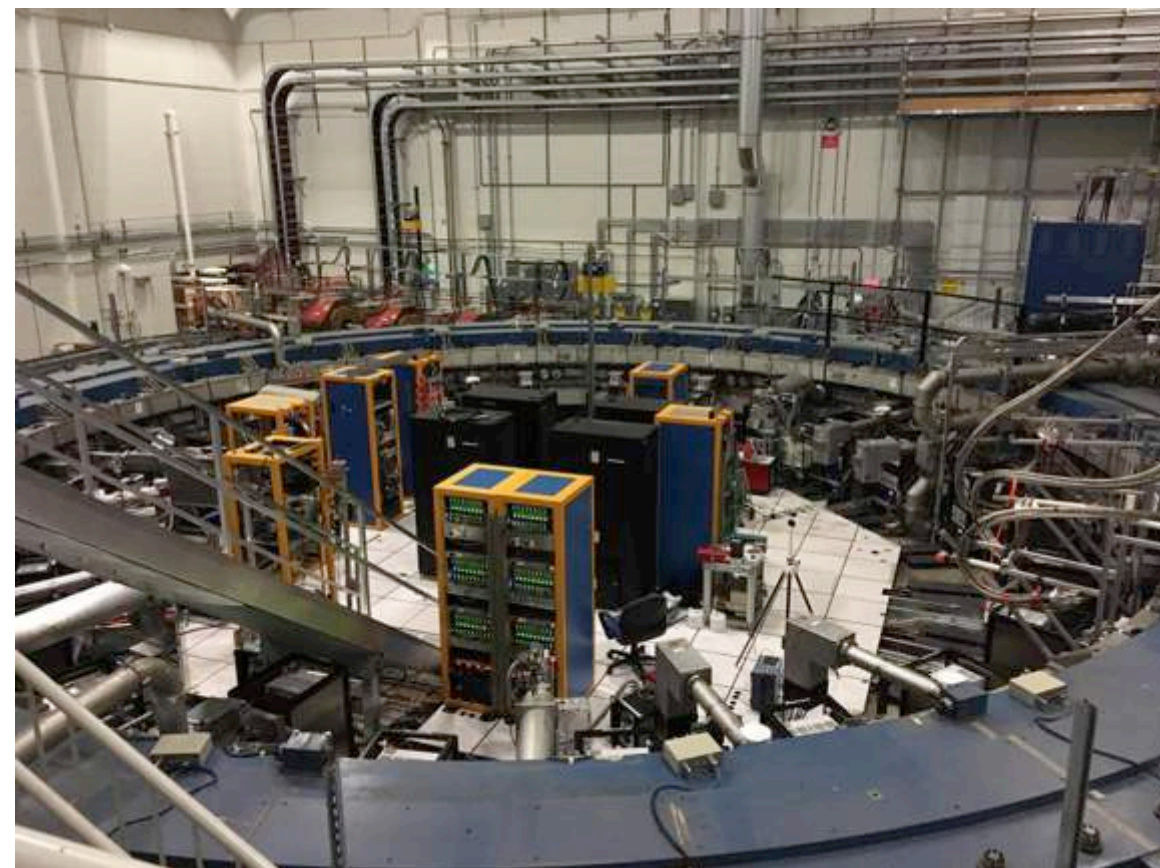


Auxiliary Field Systems



Surface Correction Coils

- Continuous PCB traces going around the ring on pole surfaces
- 100 concentric traces on upper poles, 100 on lower poles
- Programmable range: ± 20 ppm on the field
- Used to cancel higher-order multipole moments in the magnetic field (on average)



Power Supply Feedback

- Programmable current source with a range of ± 5 ppm on the field
- Uses data from **fixed probe** system to stabilize the field at a specified set point



Fluxgates

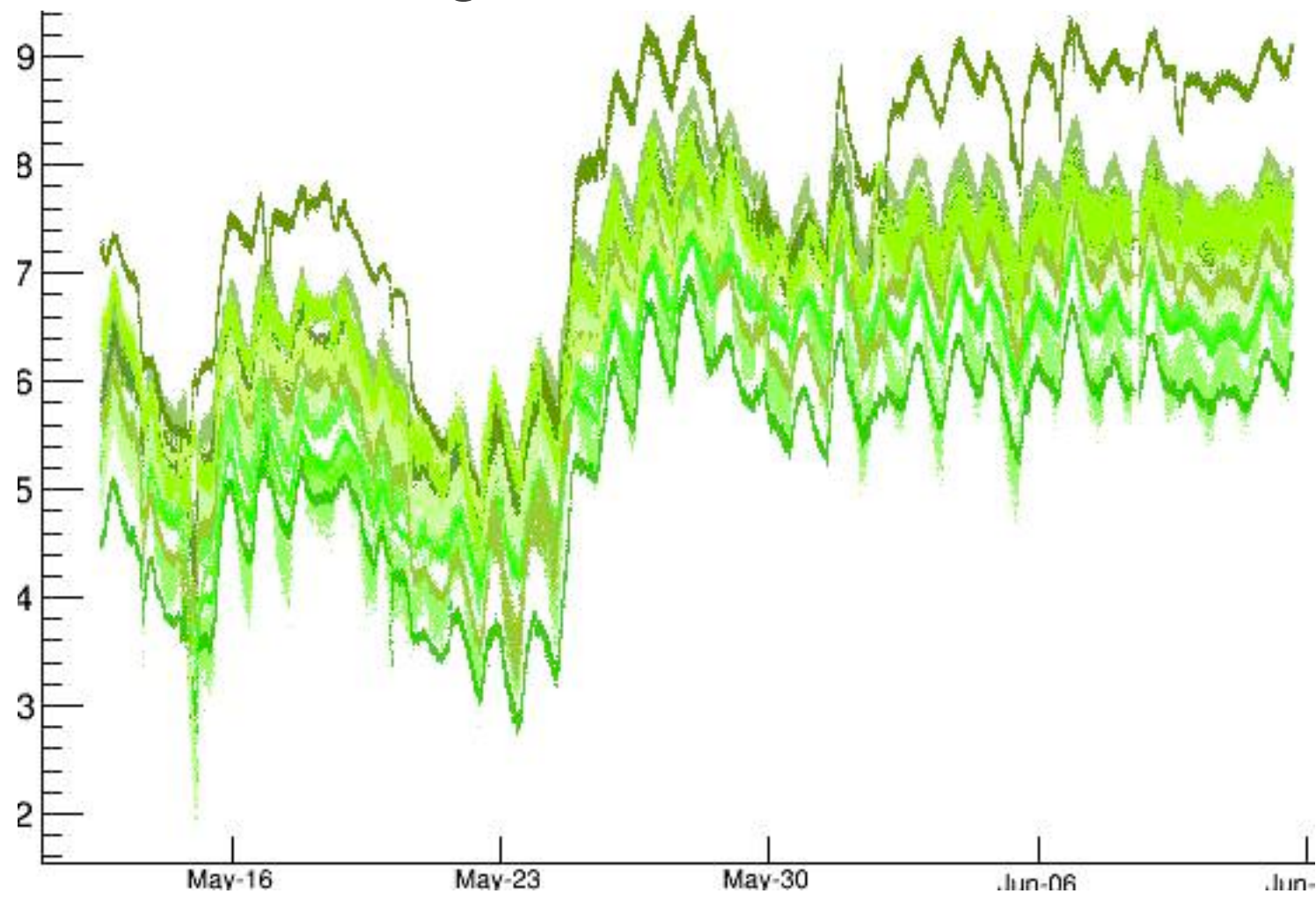
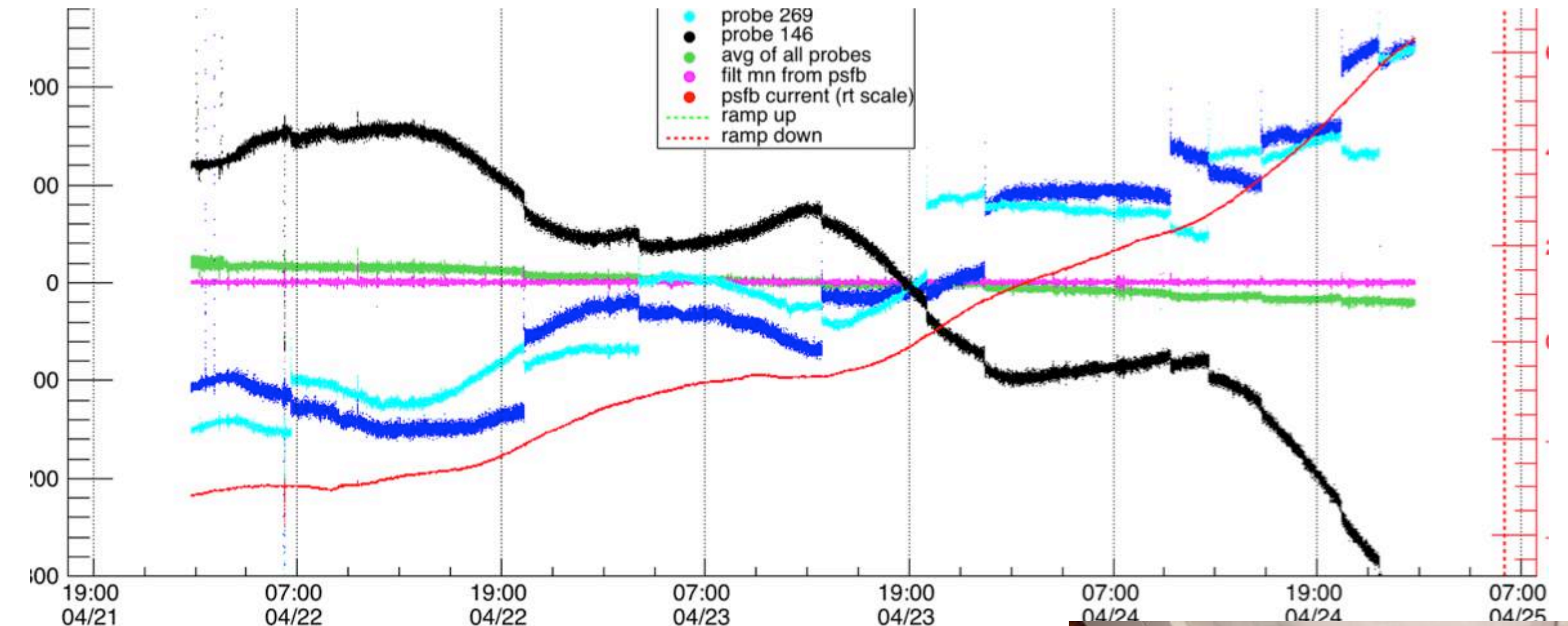
- Measure (x,y,z) components of transient fields in the hall
- Sensitive down to 10^{-9} T (DC or AC) fields
- Bandwidth up to 1 kHz



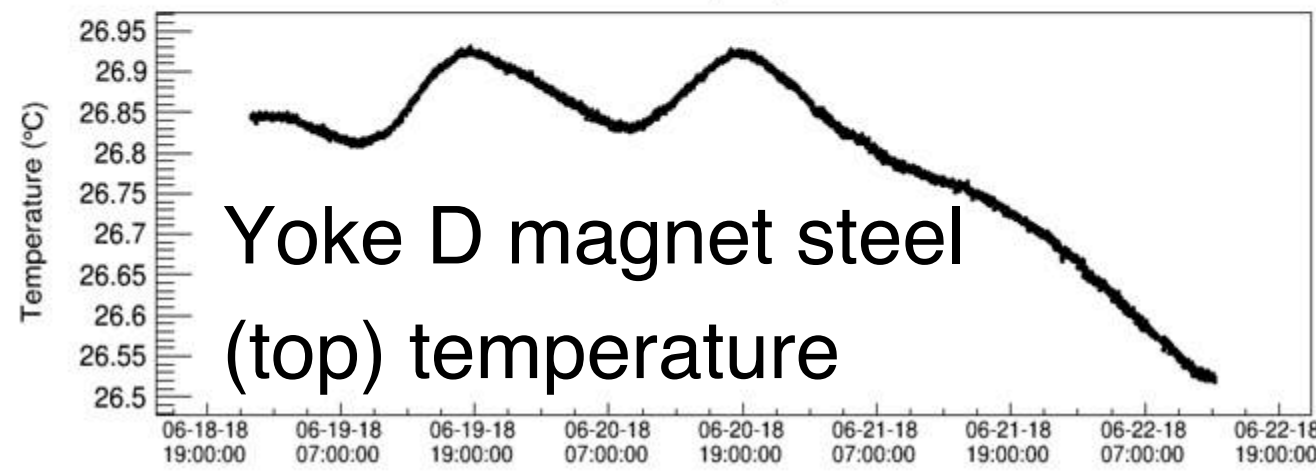
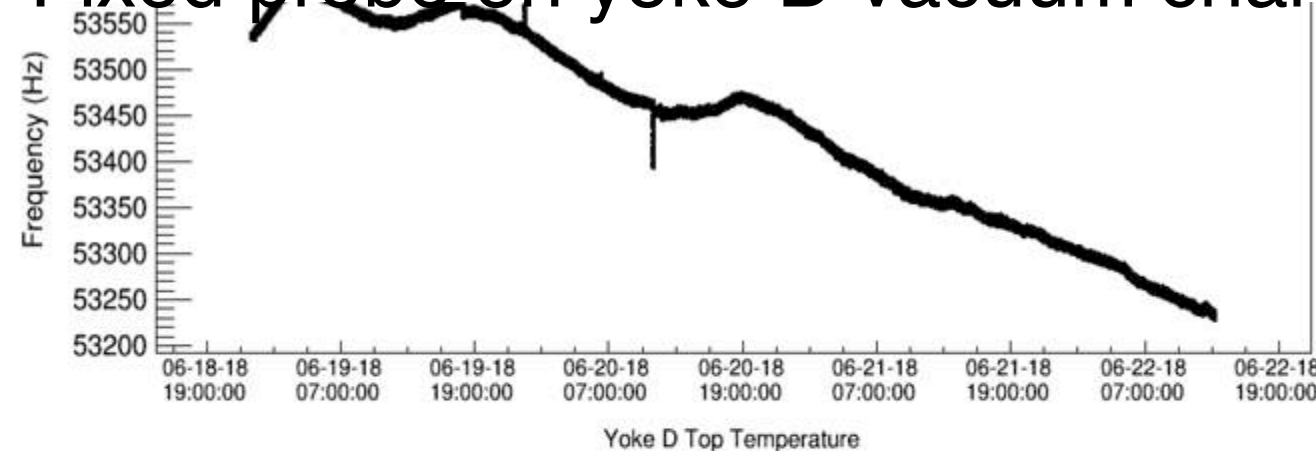
Magnet Insulation



- Temperature variations in the hall affect the quality of the magnetic field
 - Observed ~ 20 ppm/deg C effects on the dipole moment during the run
 - Also affects ability to track higher-order multipoles
- Two main issues
 - Large changes in average temperature over time (2–3°C)
 - Differential changes across the magnet ($\sim 3^\circ\text{C}$)
- Two-pronged solution:
 - Improved cooling system in the hall
 - Install fiberglass insulation blanket on magnet steel



Fixed probe on yoke D vacuum chamber (top)



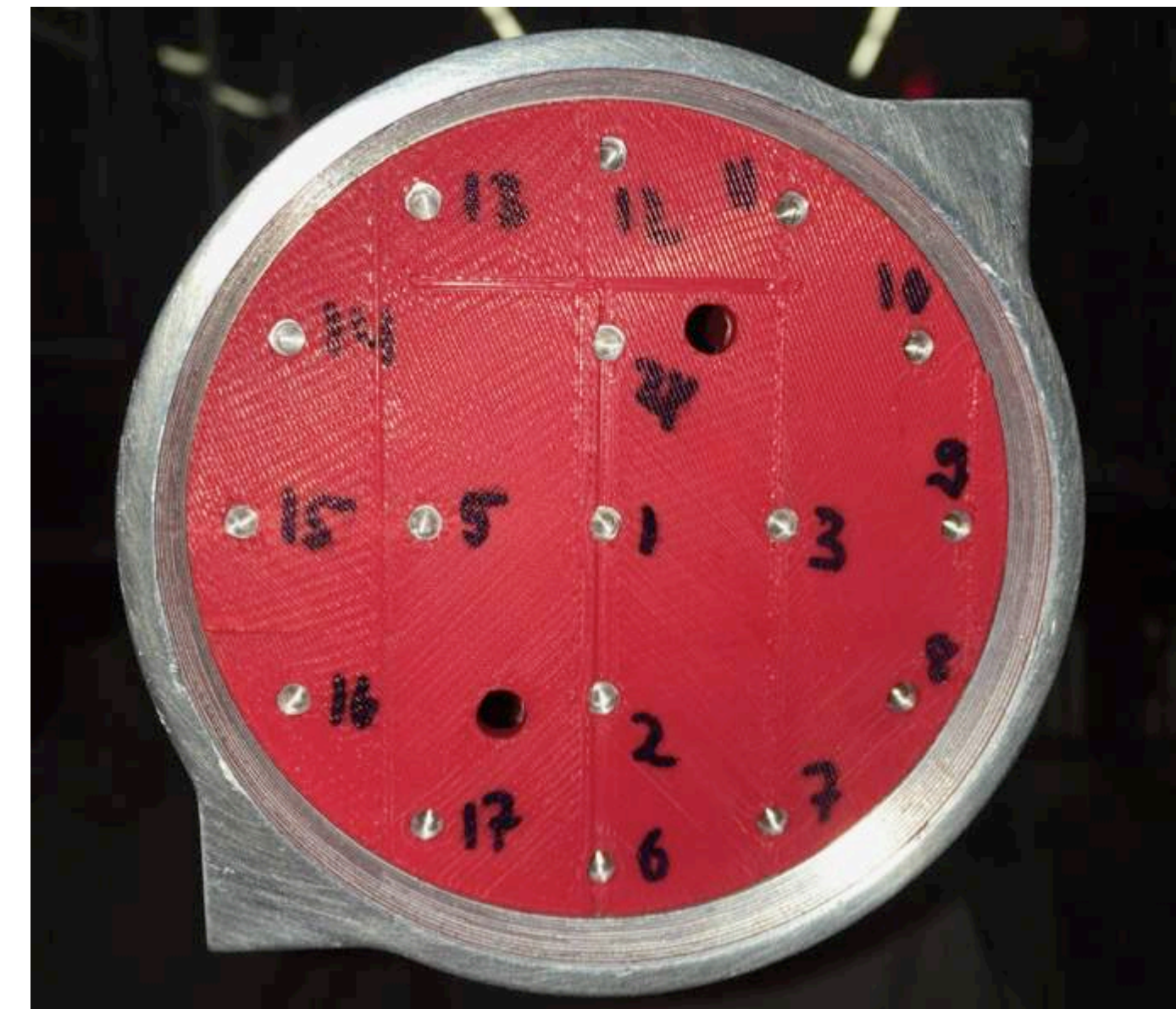
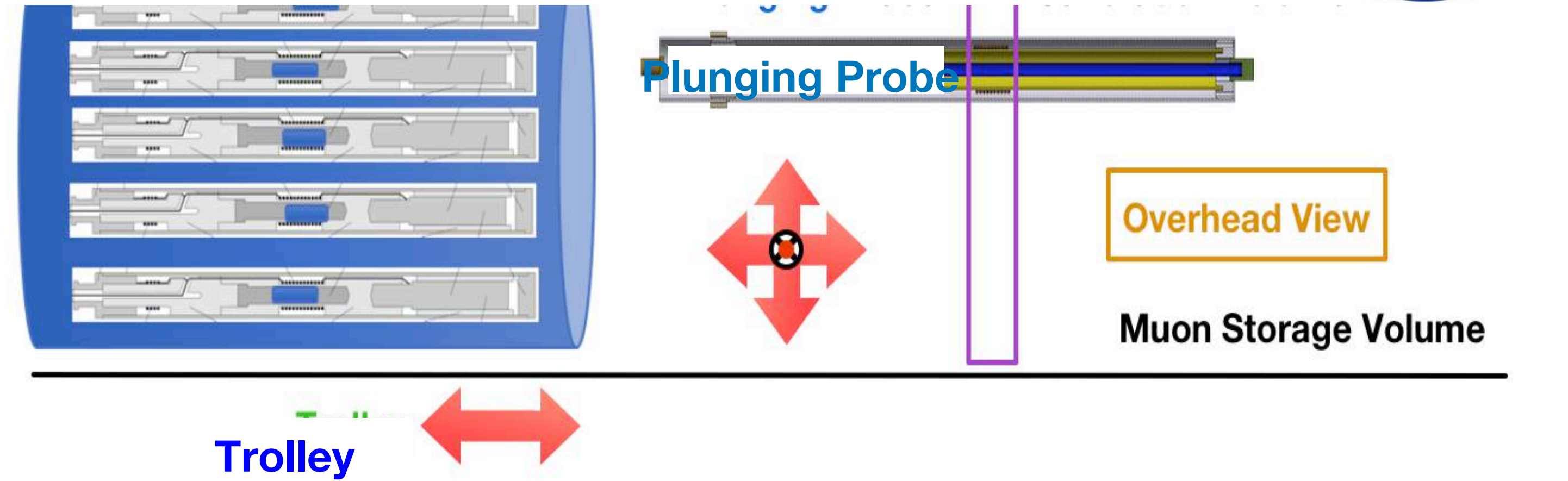
Installed blankets this past summer



Calibrating the Trolley

Procedure

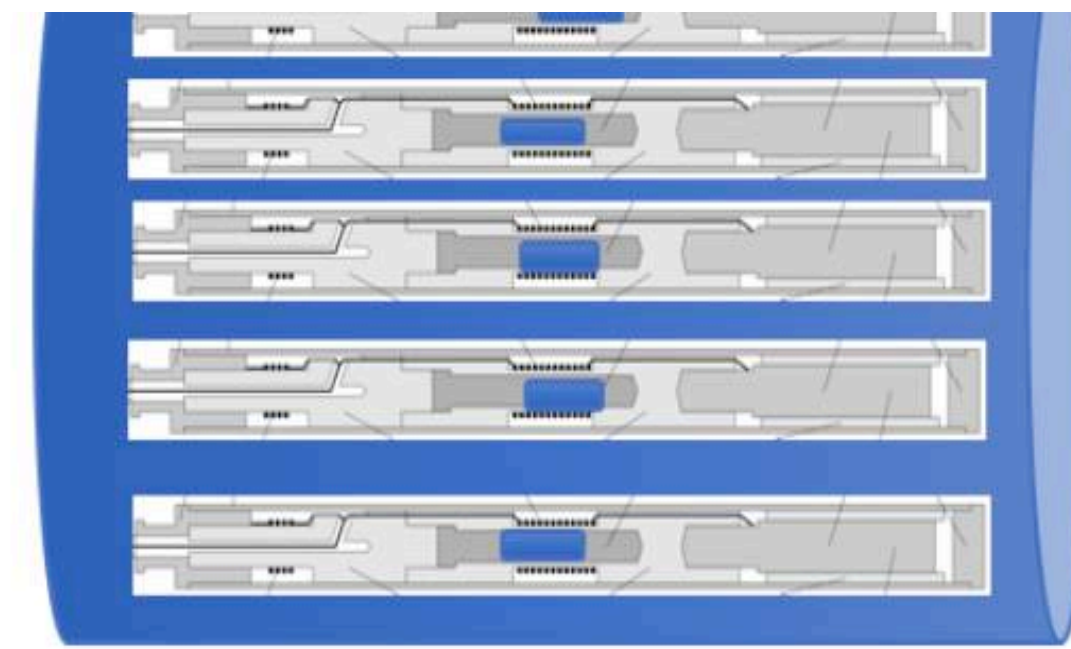
- Select **trolley** probe to calibrate



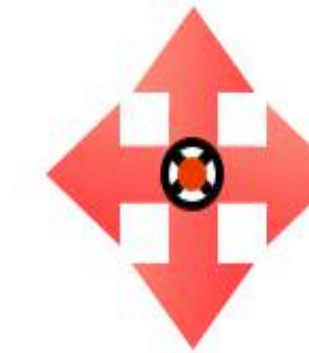
Calibrating the Trolley

Procedure

- Select **trolley** probe to calibrate
- Impose a **known gradient** across the trolley; compare to **bare field B_0** . Define $\Delta B = B(I \neq 0) - B(I = 0)$

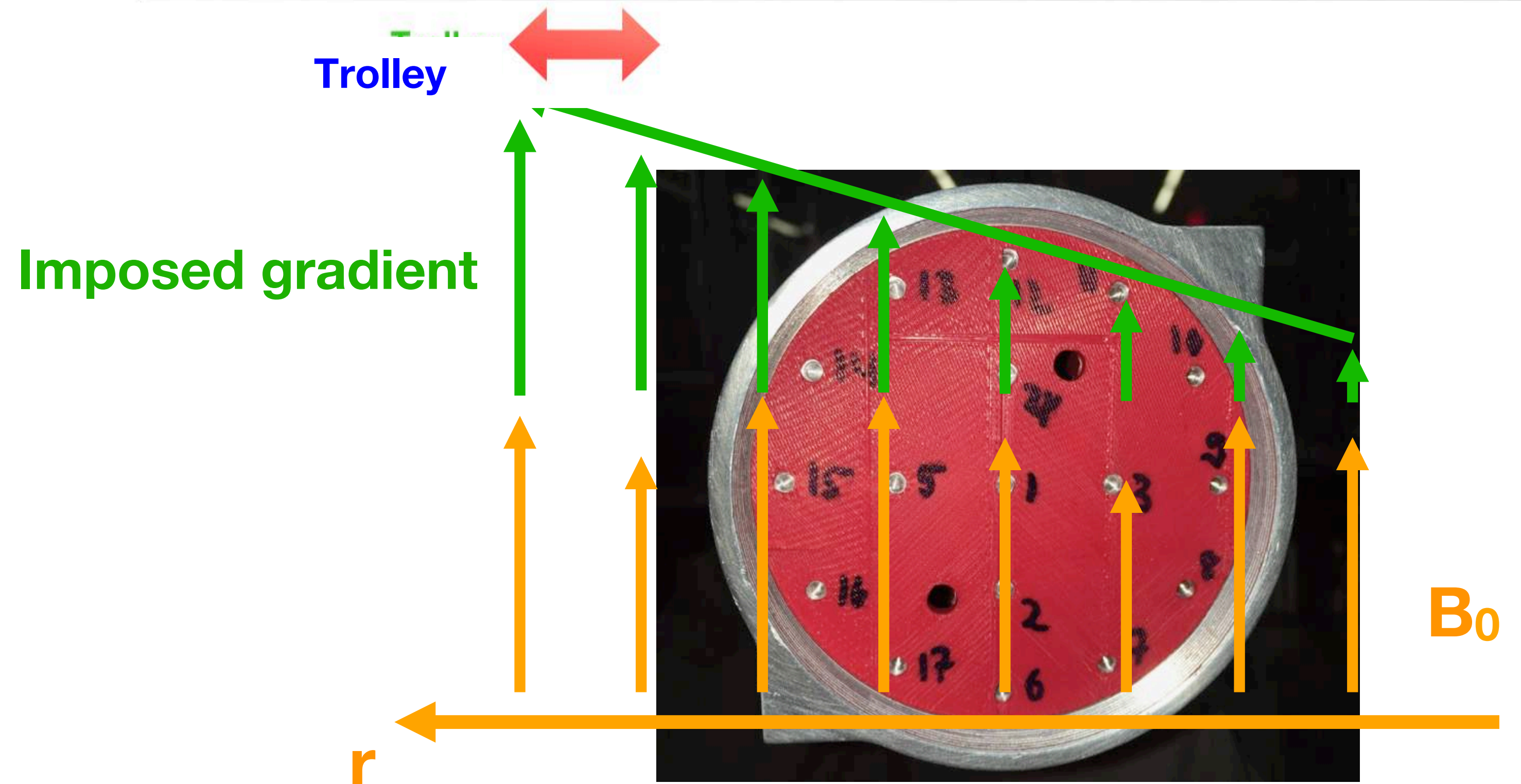
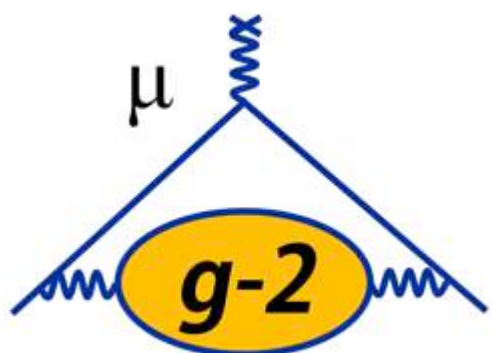


Plunging Probe



Overhead View

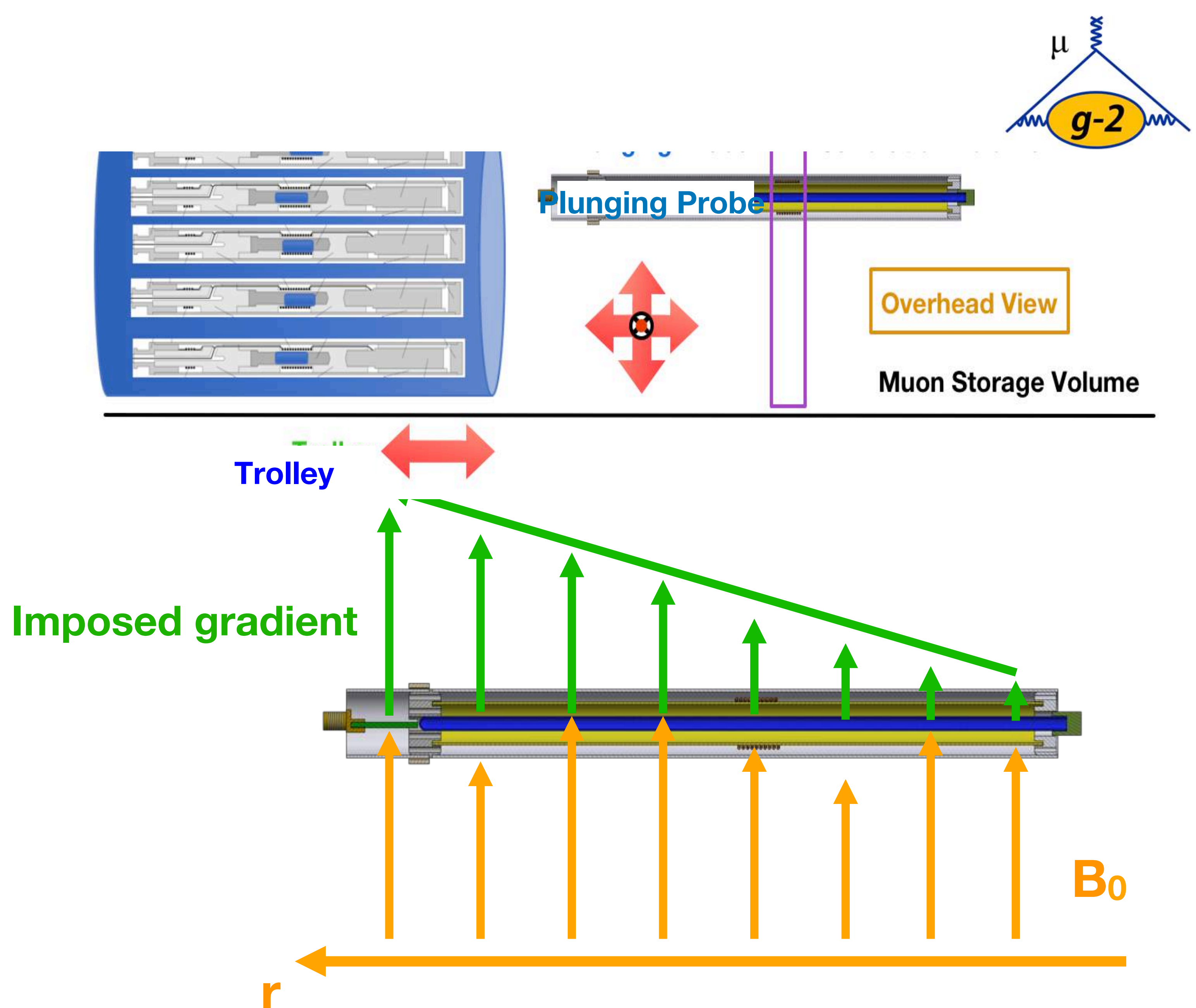
Muon Storage Volume



Calibrating the Trolley

Procedure

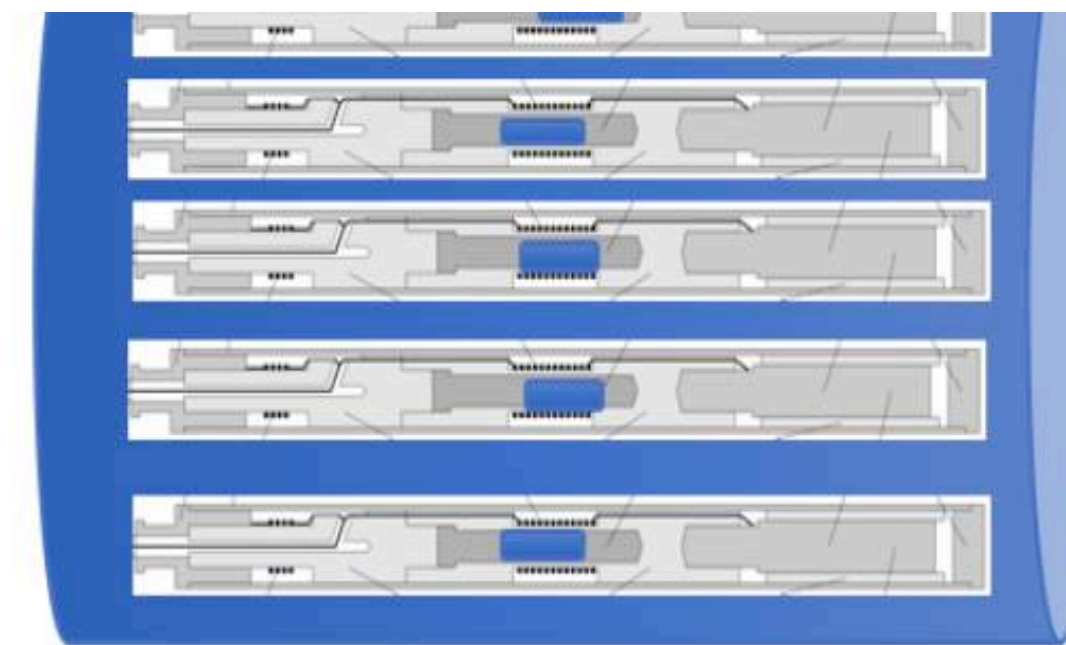
- Select **trolley** probe to calibrate
- Impose a **known gradient** across the trolley; compare to **bare field B_0** . Define $\Delta B = B(l \neq 0) - B(l = 0)$
- Unique ΔB for each **trolley** probe gives position
- Move **plunging probe** into volume; measure ΔB and determine distance to move **plunging probe**



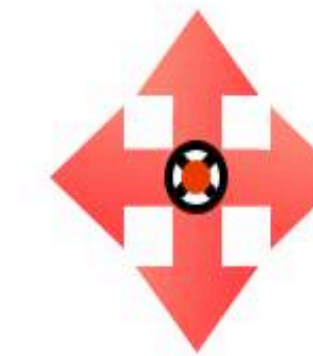
Calibrating the Trolley

Procedure

- Select **trolley** probe to calibrate
- Impose a **known gradient** across the trolley; compare to **bare field B_0** . Define $\Delta B = B(I \neq 0) - B(I = 0)$
- Unique ΔB for each **trolley** probe gives position
- Move **plunging probe** into volume; measure ΔB and determine distance to move **plunging probe**
- Iterate until **plunging probe** ΔB matches **trolley** probe ΔB
- Perform for radial, vertical, azimuthal coordinates



Plunging Probe



Overhead View

Muon Storage Volume

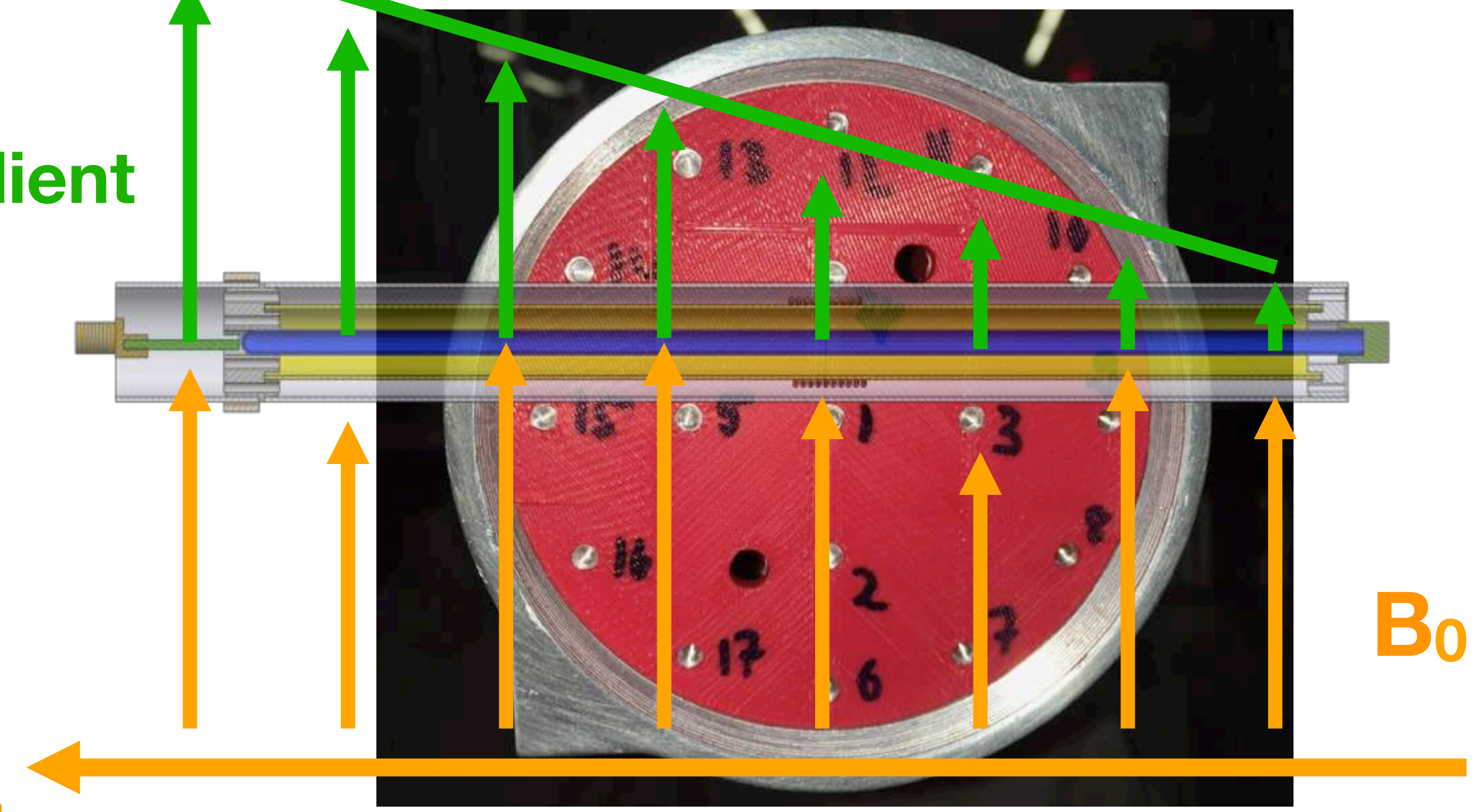


Imposed gradient

Trolley

r

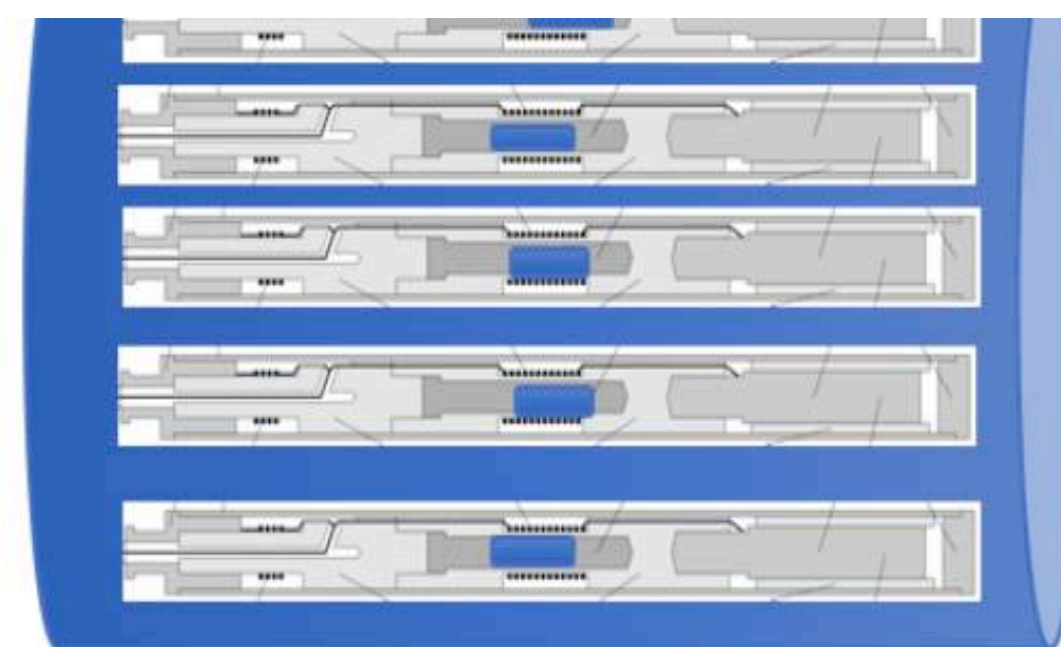
B_0



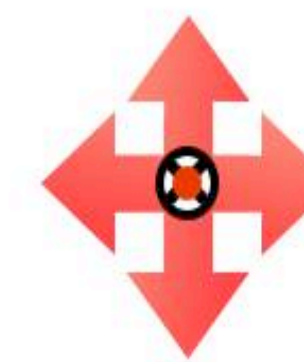
Calibrating the Trolley

Procedure

- Select **trolley** probe to calibrate
- Impose a **known gradient** across the trolley; compare to **bare field B_0** . Define $\Delta B = B(I \neq 0) - B(I = 0)$
- Unique ΔB for each **trolley** probe gives position
- Move **plunging probe** into volume; measure ΔB and determine distance to move **plunging probe**
- Iterate until **plunging probe** ΔB matches **trolley** probe ΔB
- Perform for radial, vertical, azimuthal coordinates
- Shim the field to be highly uniform, and measure using the **PP** and the **trolley** (rapid swapping)

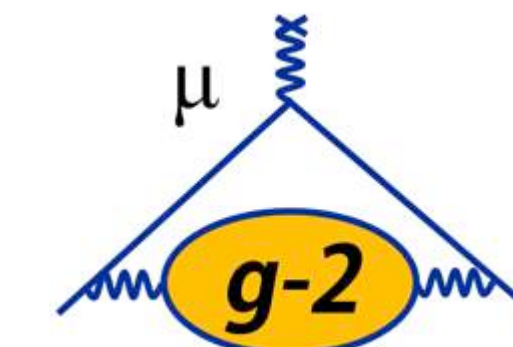


Plunging Probe

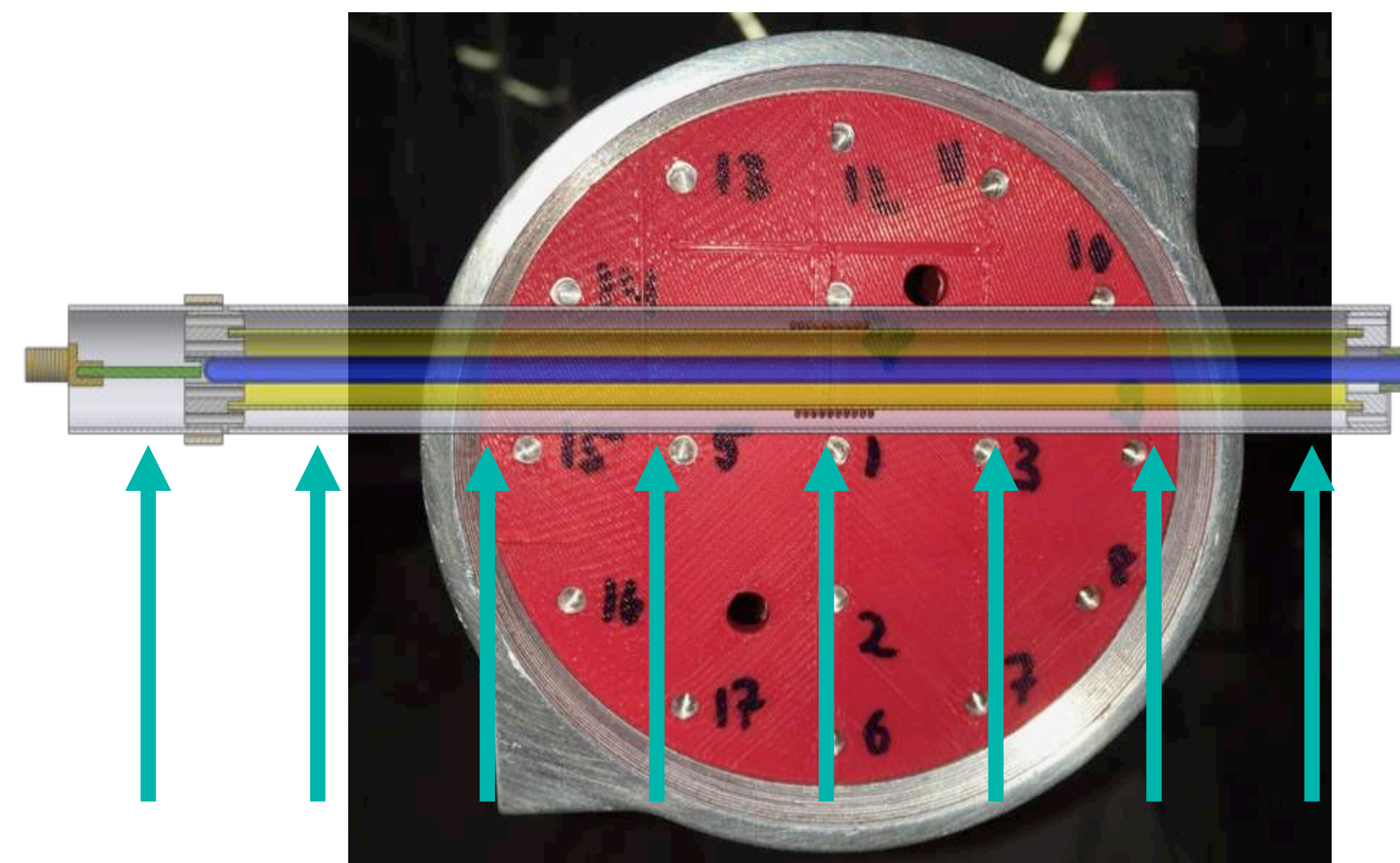


Overhead View

Muon Storage Volume



Trolley



B_s

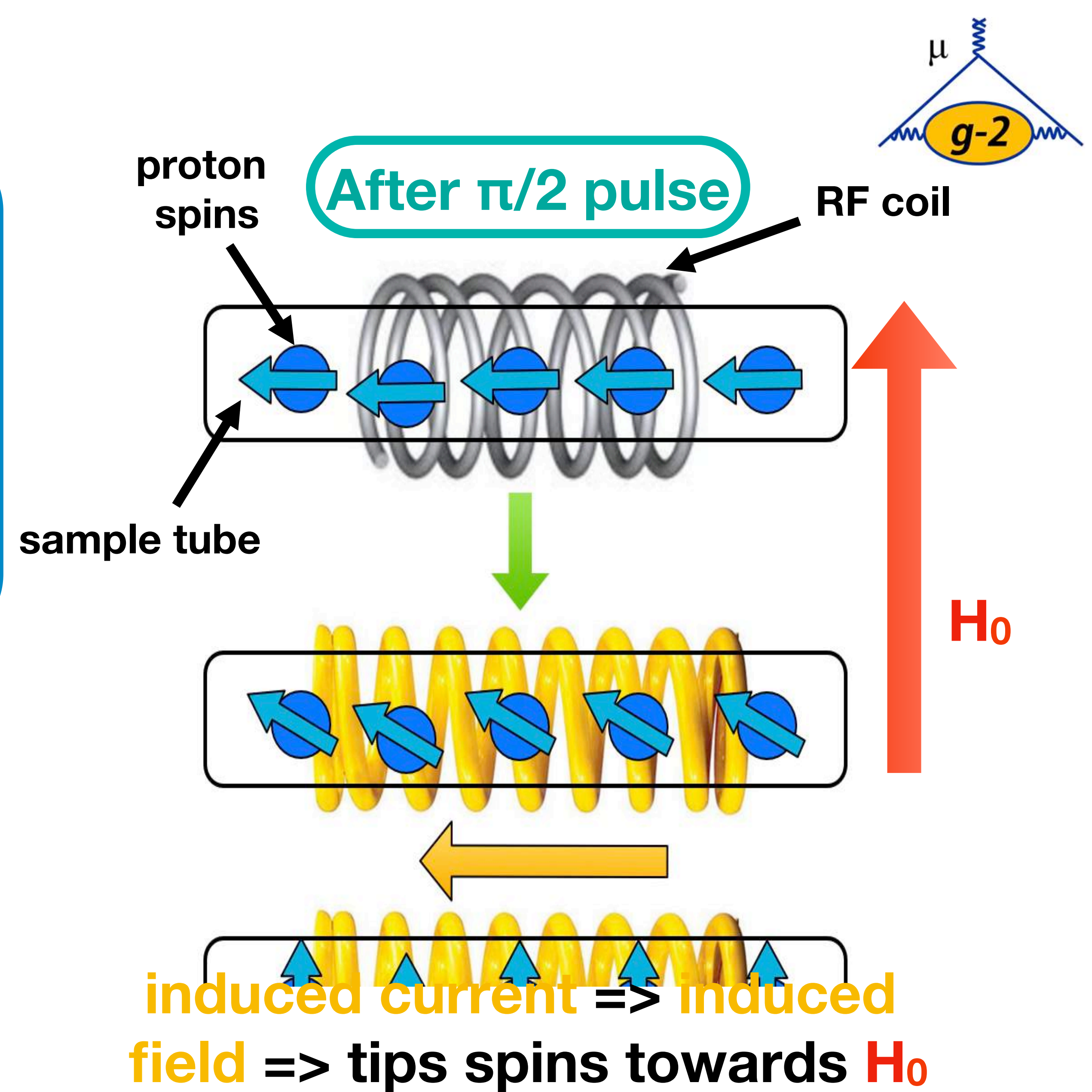
Radiation Damping

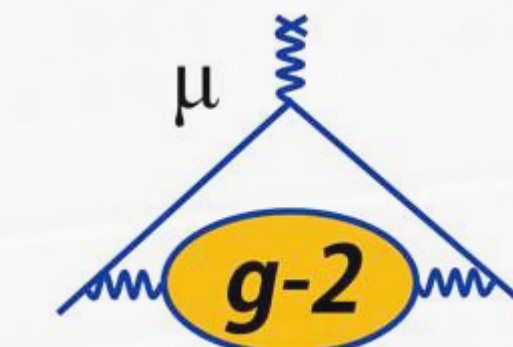
What is it?

- Precessing spins induce emf in pickup coil; this in turn generates an alternating magnetic field that **acts to rotate spins back towards the main field**
- **Size of effect:** $\delta_{RD} \sim [(f_0 - f_L)/f_0] \eta Q M_z(t)$
 - f_0 = resonant frequency of circuit; f_L = Larmor frequency
 - η = filling factor; Q = quality factor of circuit
 - $M_z(t)$ = magnetization of sample

How to quantify?

- Use coils to produce a longitudinal field
 - Precise control over main field to mimic damping effect
- Vary $\pi/2$ pulse \Rightarrow vary $M_z(t)$ \Rightarrow changes δ_{RD}





Muon g-2 at JPARC

3 GeV 333 uA proton beam from MUSE H-line at JPARC

Graphite target
(20 mm)

Surface muons

Ultra Cold μ Source

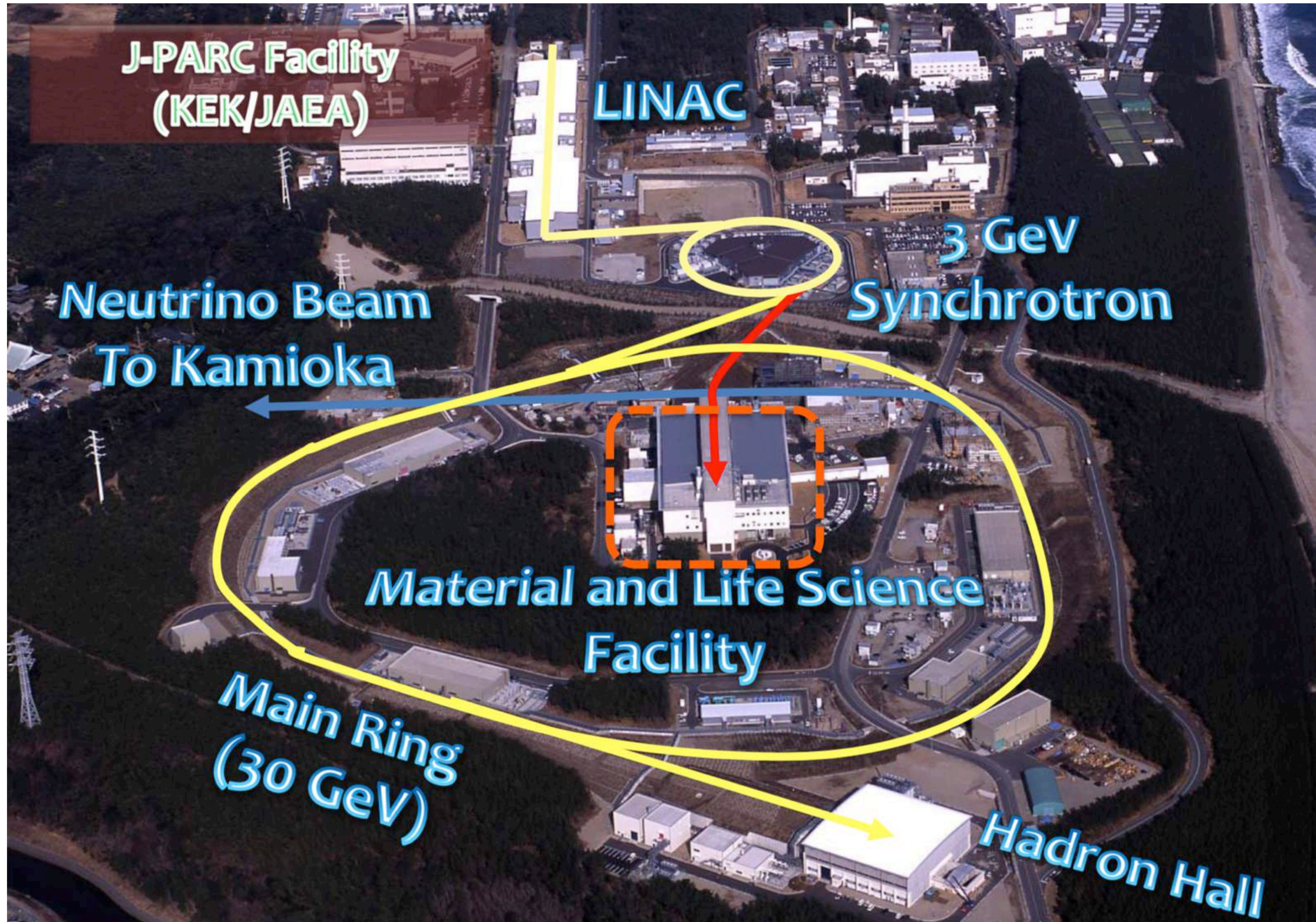
Muon LINAC (300 MeV/c)

Muon storage

g-2/EDM storage magnet



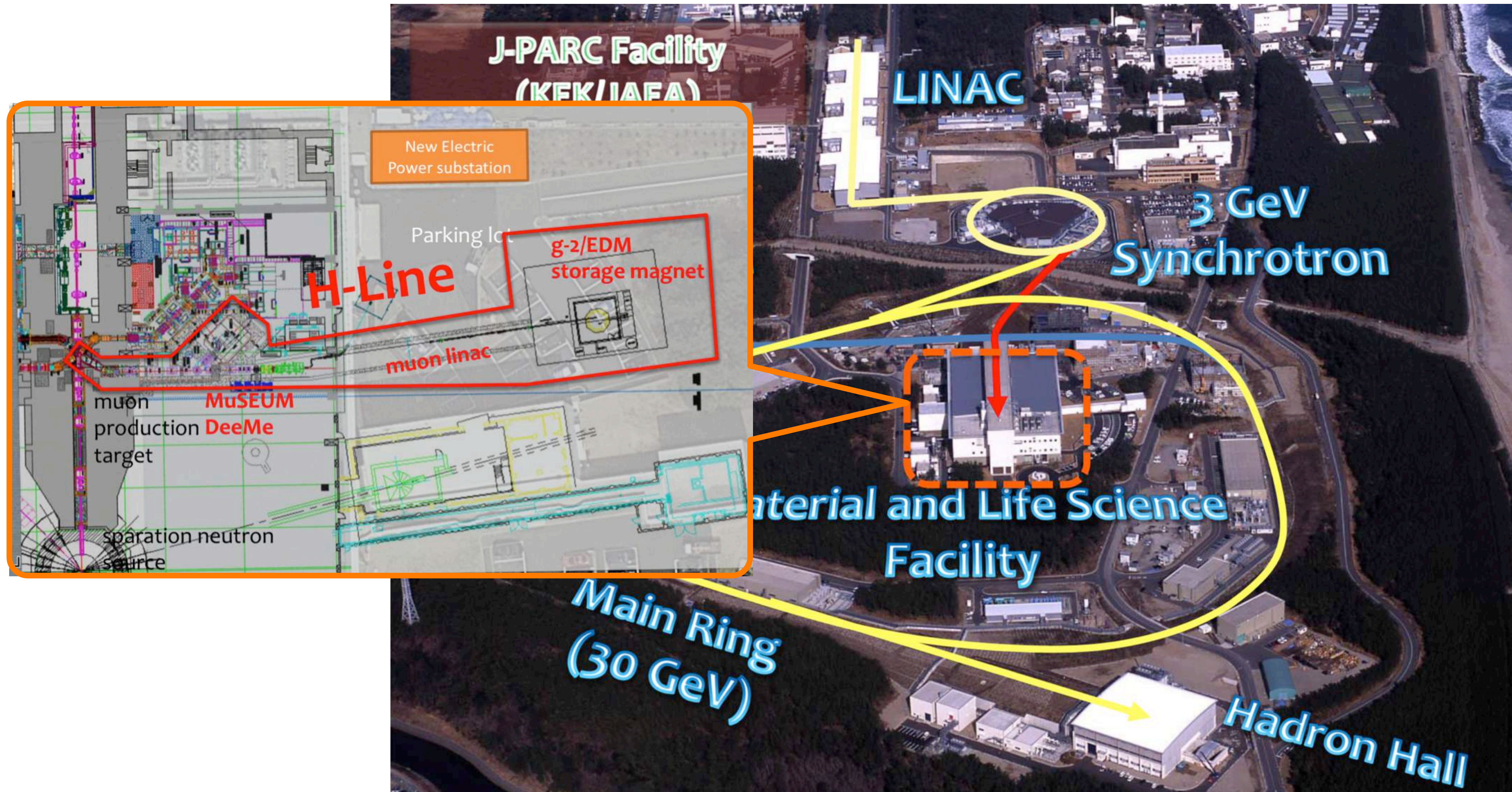
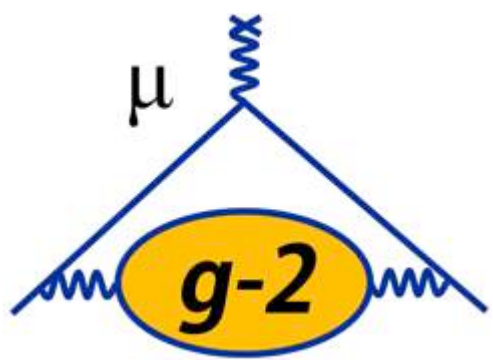
JPARC Facilities



Images from Tsutomu Mibe



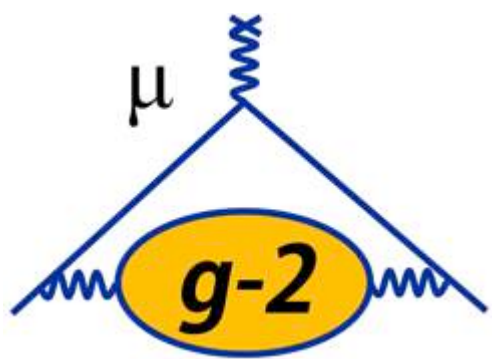
JPARC Facilities



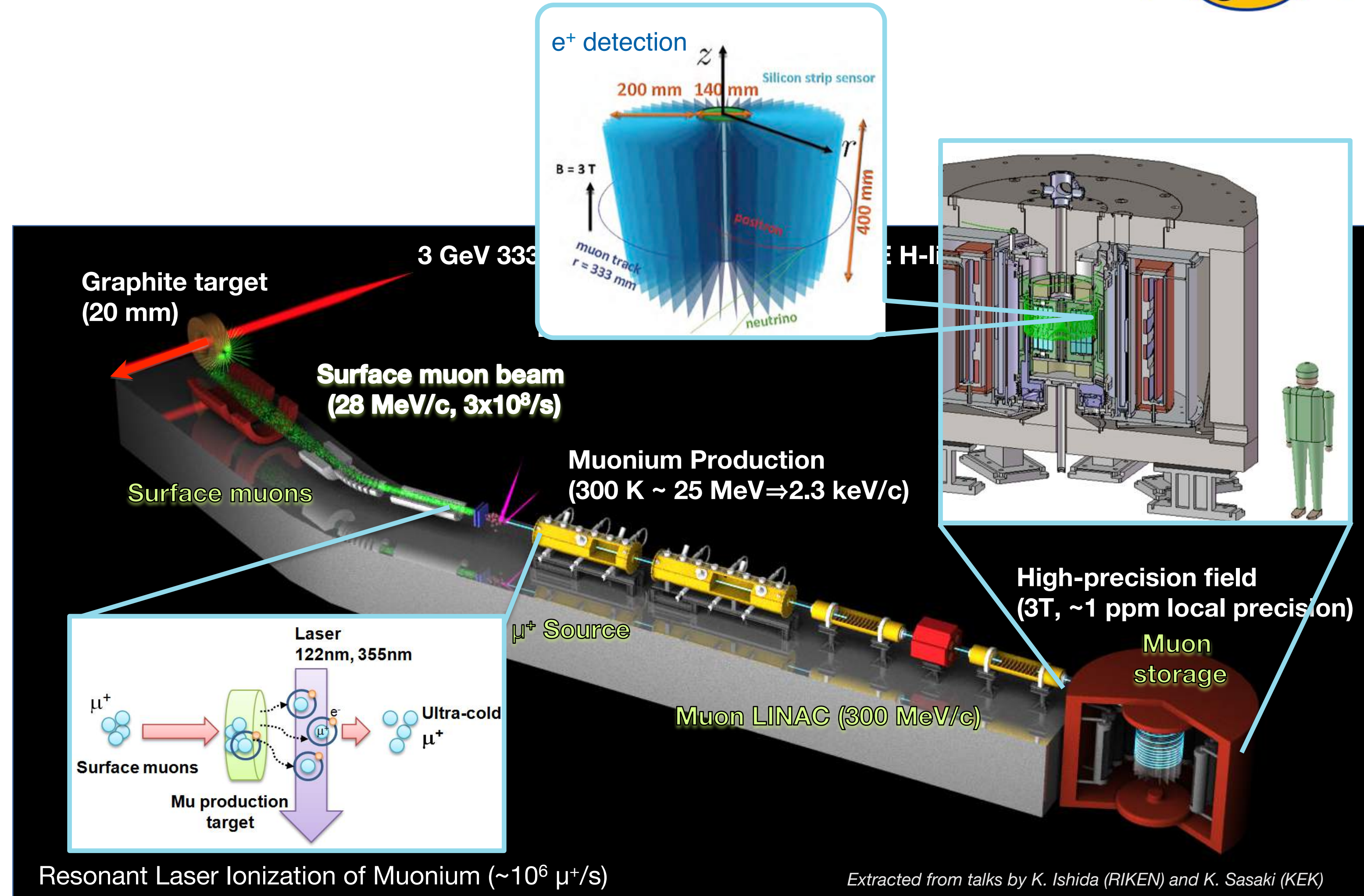
Images from Tsutomu Mibe



The Muon g-2 Experiment at JPARC



- New experiment being prepared in Japan
- Features
 - **Low-emittance muon beam**
 - 40 silicon **high-resolution tracking** vanes
 - **High-uniformity storage field** (~ 1 ppm)
- Different technique \rightarrow different systematics
 - Excellent cross-check against E989 at FNAL

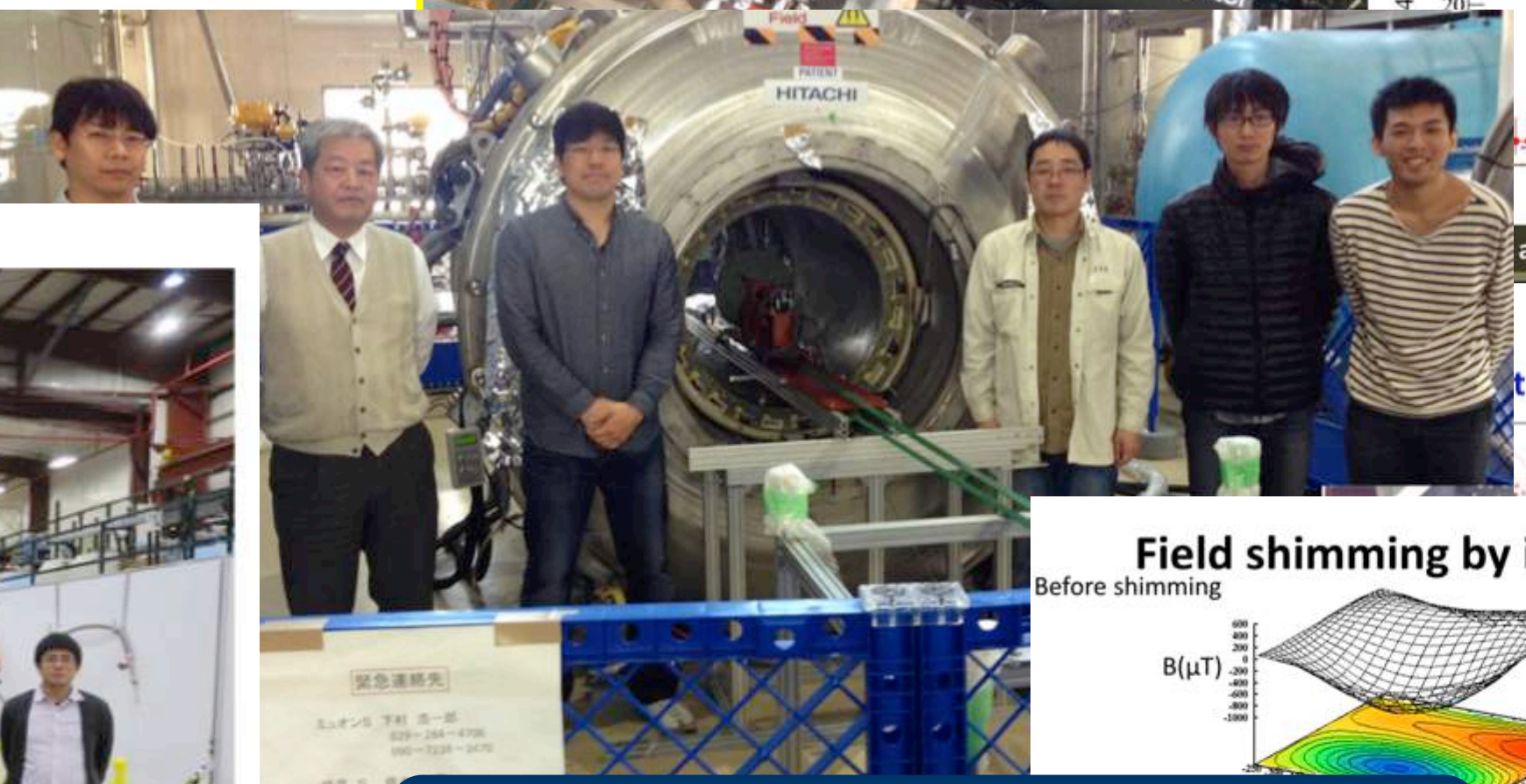
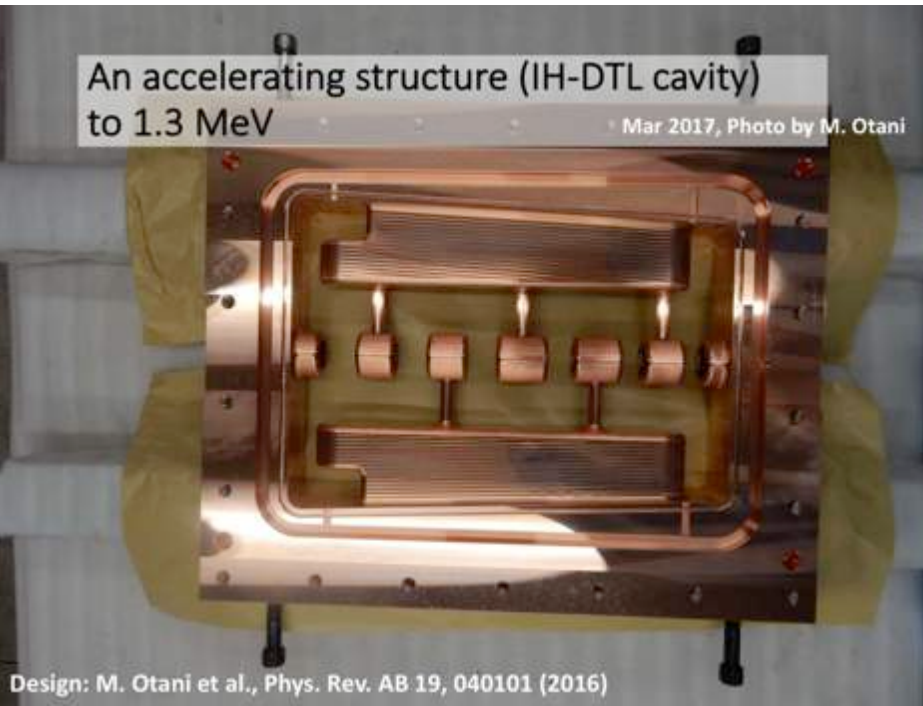
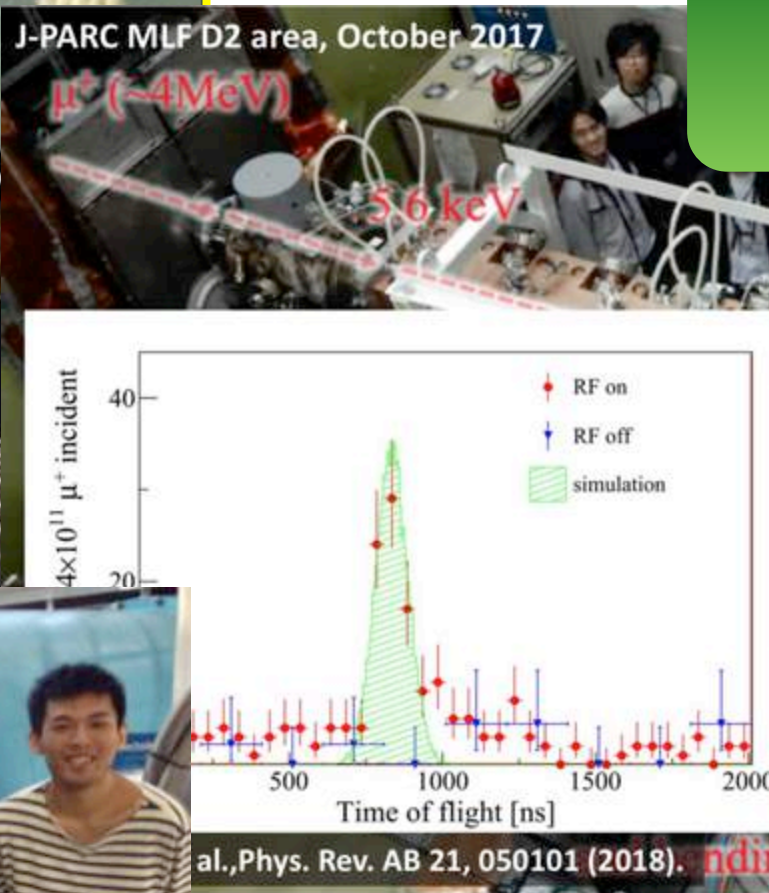
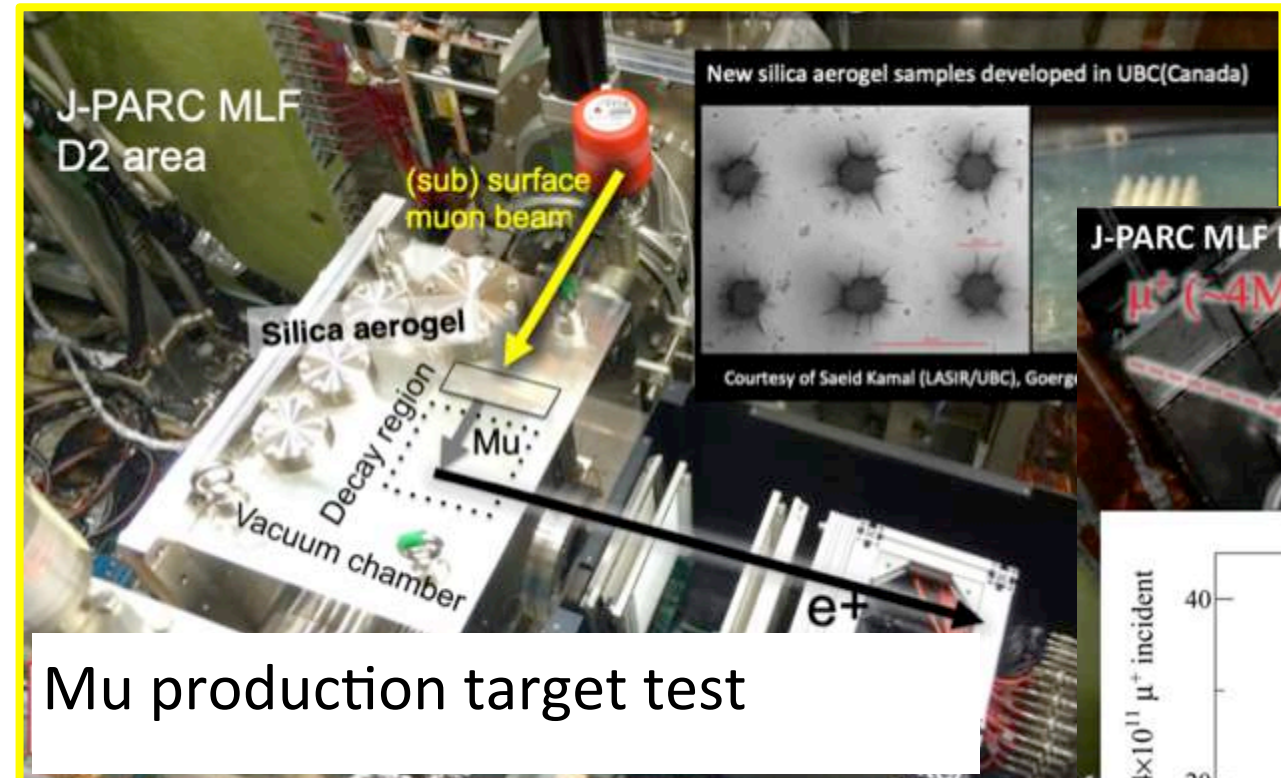


The Muon g-2 Experiment at JPARC: Current Status

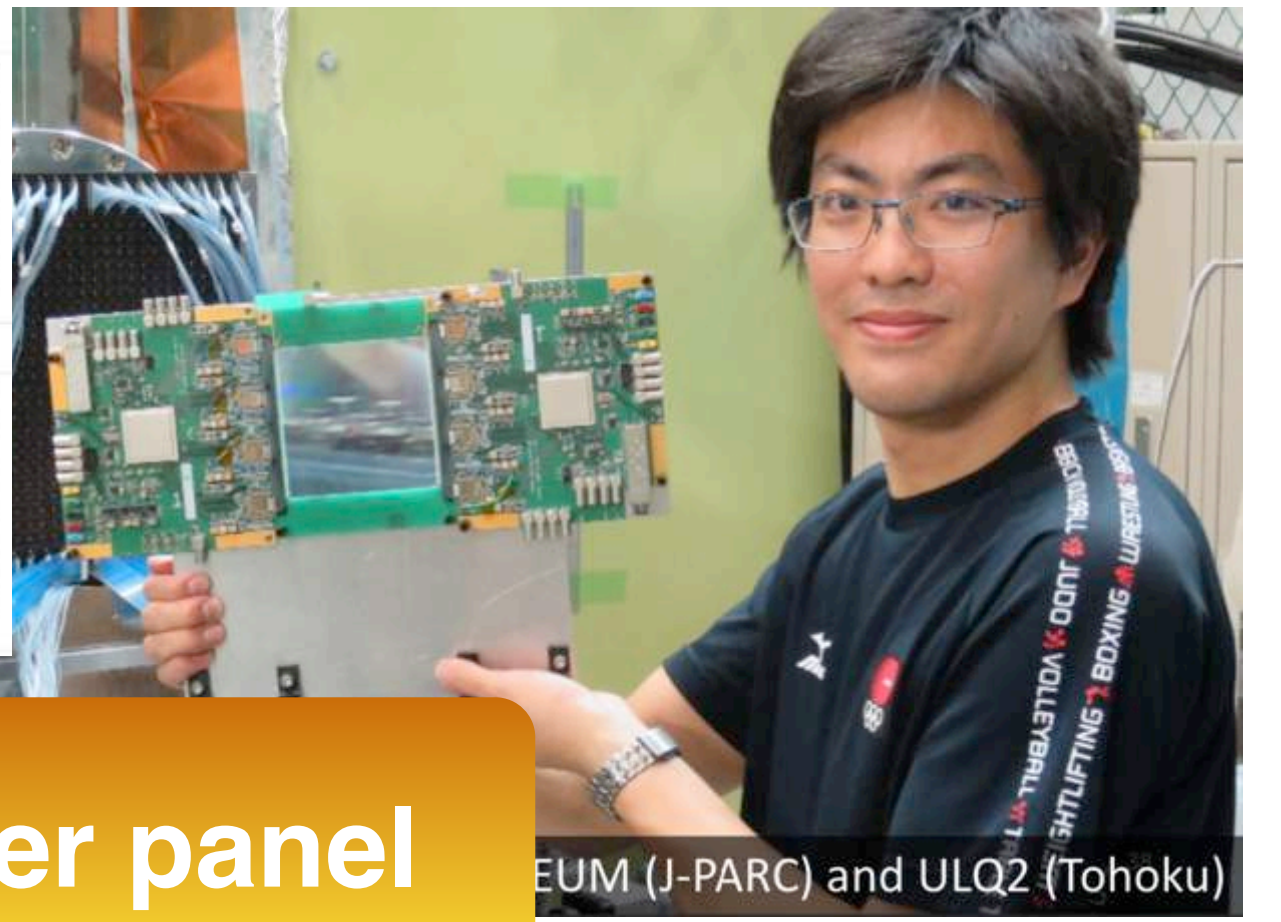
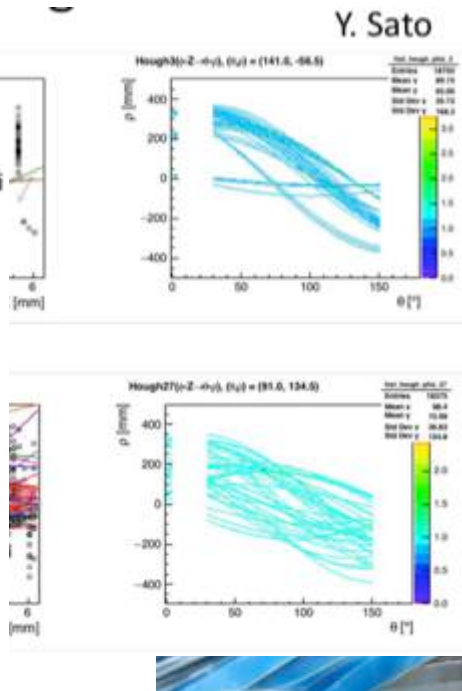
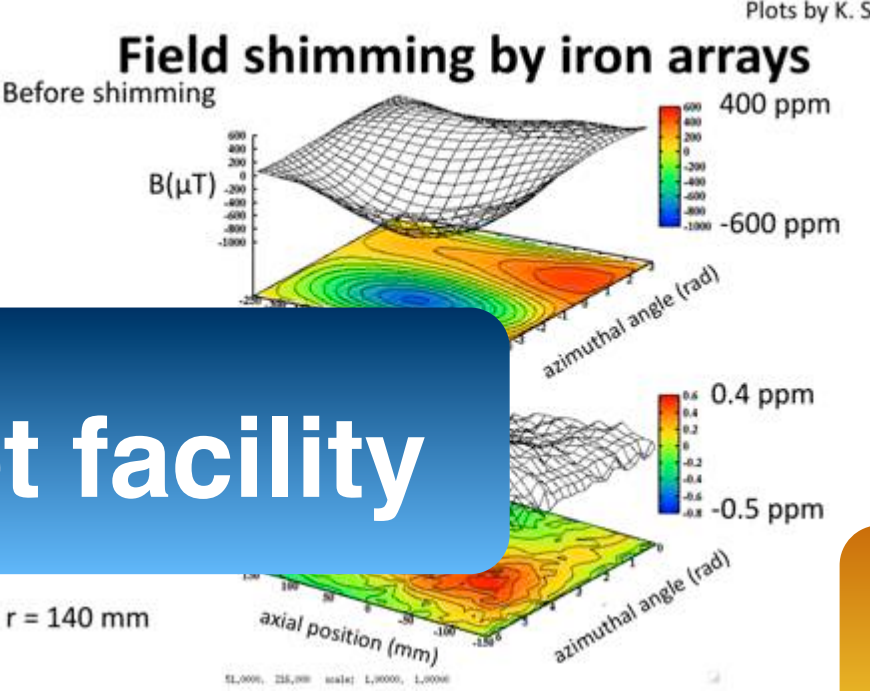


- Various systems are progressing forward
 - **Beamline**
 - **e⁺ trackers**
 - **Magnetic field**

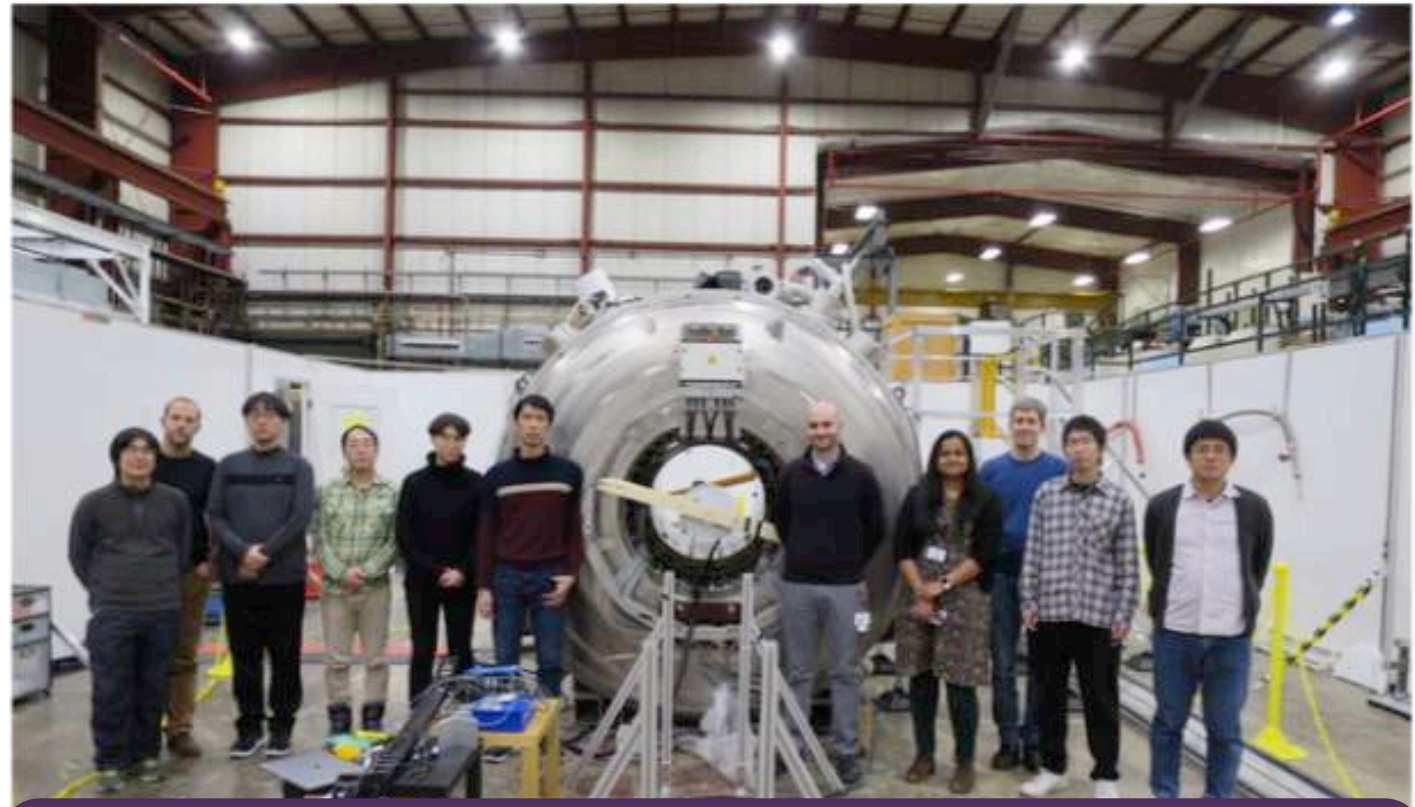
μ⁺ accelerator tests



Test magnet facility



e⁺ tracker panel

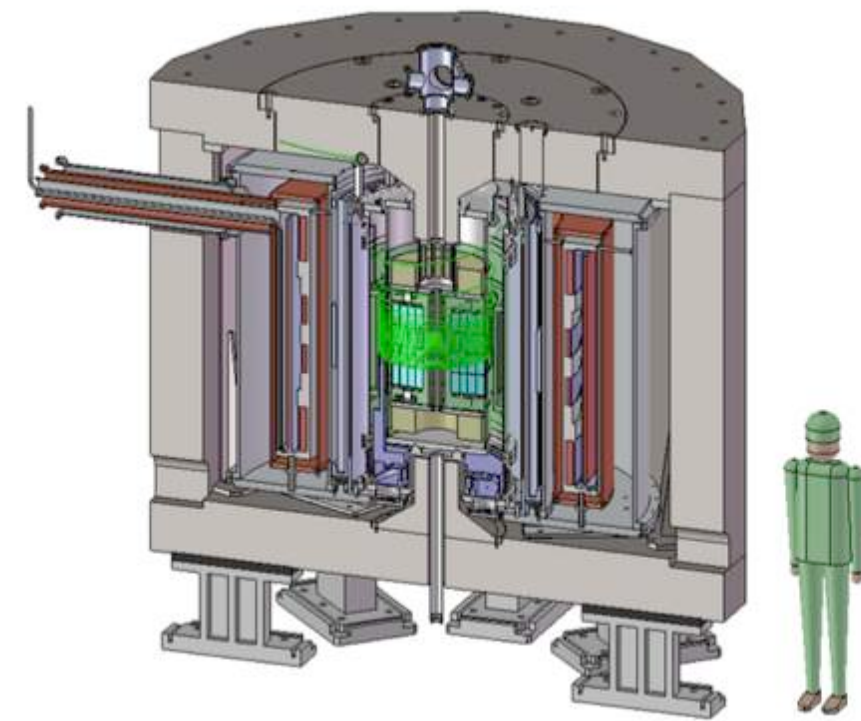
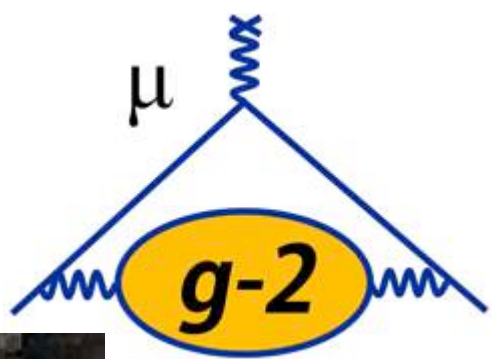


Cross Calibration at ANL Feb 2019

Images from Tsutomu Mibe (KEK)

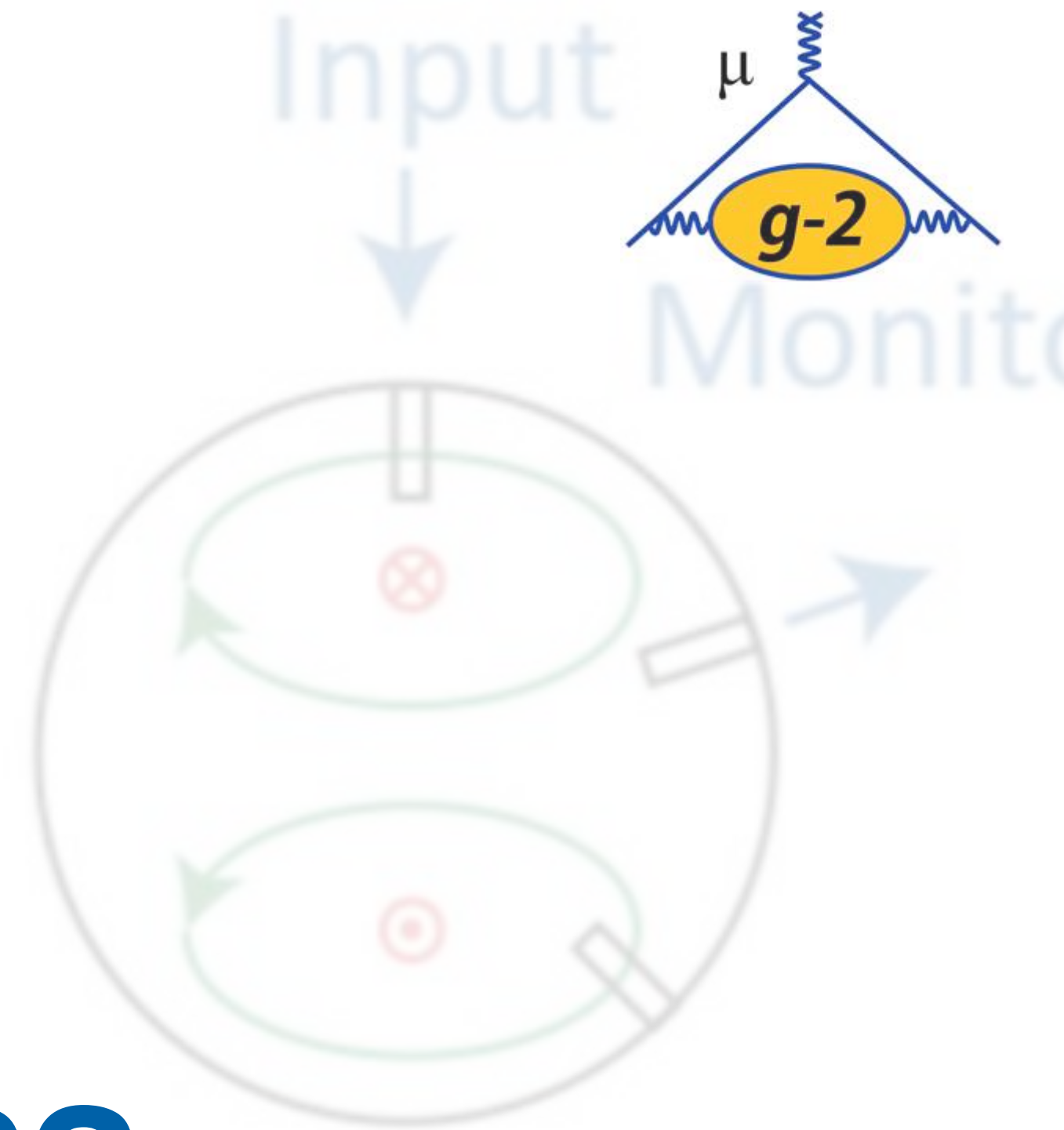
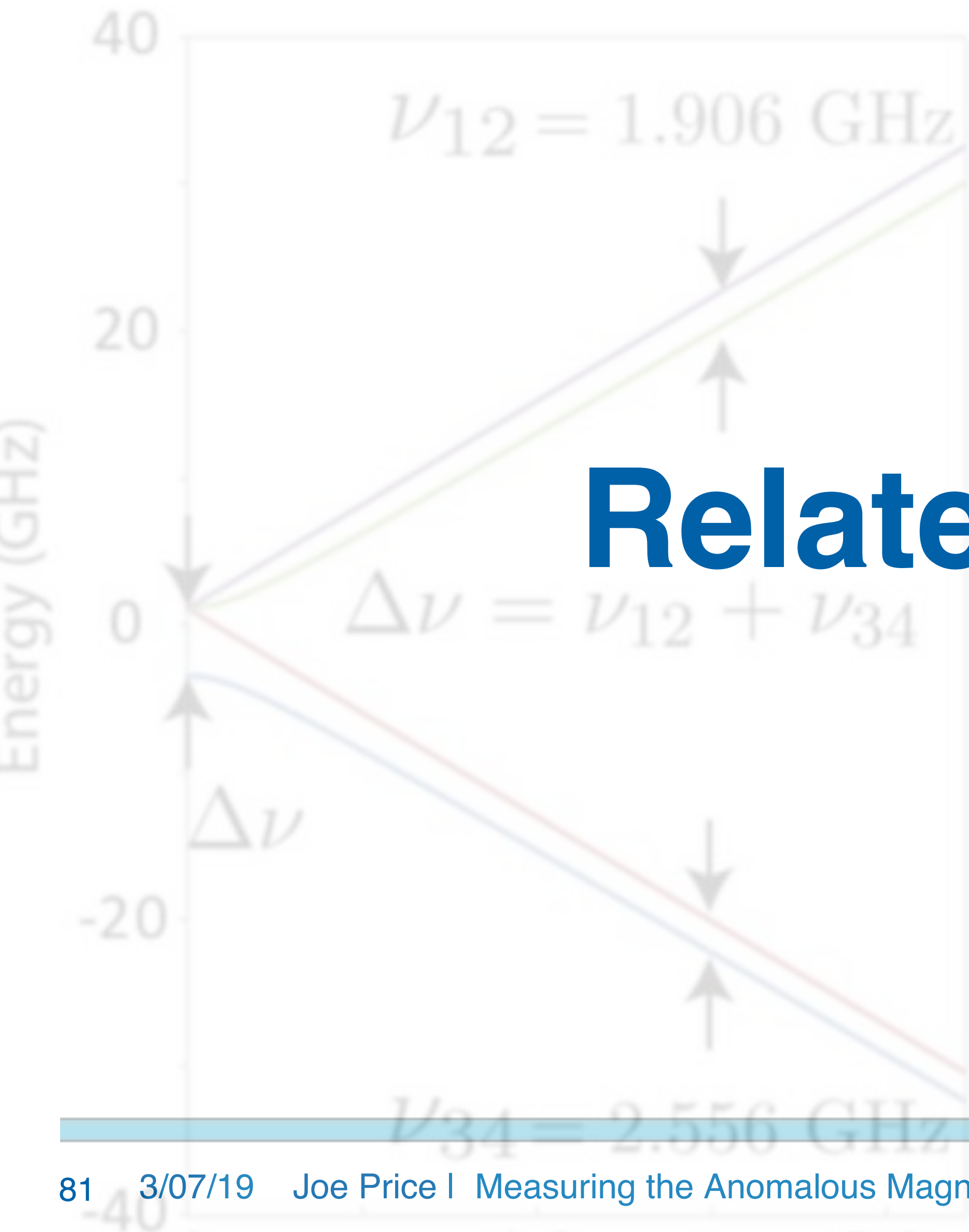


Muon g-2 Experiment Comparison



Parameter	E34 @ JPARC	E989 @ Fermilab
Beam	High-rate, ultra-cold muon beam ($p = 300 \text{ MeV}/c$)	High-rate, magic-momentum muons ($p = 3.094 \text{ GeV}/c$)
Polarization	$P_{\text{max}} = 50\text{-}90\%$ (spin reversal possible)	$P \approx 97\%$ (no spin reversal)
Magnet	MRI-like solenoid ($r_{\text{storage}} = 33 \text{ cm}$)	Storage ring ($r_{\text{storage}} = 7 \text{ m}$)
B-field	3 Tesla	1.45 Tesla
B-field gradients	Small gradients for focusing	Try to eliminate
E-field	None	Electrostatic quadrupole
Injection	Spiral + kicker ($\sim 90\%$ efficiency)	Inflector + kicker ($\sim 5\%$ efficiency)
Positron detector	Silicon vanes for tracking	Lead-fluoride calorimeter
B-field measurement	Continuous wave NMR	Pulsed NMR
Current sensitivity goal	450 ppb	140 ppb

Related Muon Physics



Ingredients to Extracting a_μ

- Recall the expression for a_μ :

$$a_\mu = \frac{\omega_a}{\tilde{\omega}_p} \frac{\mu_p}{\mu_e} \frac{m_\mu}{m_e} \frac{g_e}{2}$$



Ingredients to Extracting a_μ



- Recall the expression for a_μ :
- m_μ/m_e value based on muonium hyperfine theory:

$$a_\mu = \frac{\omega_a}{\tilde{\omega}_p} \frac{\mu_p}{\mu_e} \frac{m_\mu}{m_e} \frac{g_e}{2}$$

$$\Delta\nu_{\text{Mu}}(\text{Th}) = \frac{16}{3} c R_\infty \alpha^2 \frac{m_e}{m_\mu} \left(1 + \frac{m_e}{m_\mu}\right)^{-3} + \text{higher order terms}$$

- Equate theory to experiment, treat m_μ/m_e as a free parameter, obtain m_μ/m_e to 22 ppb



Ingredients to Extracting a_μ

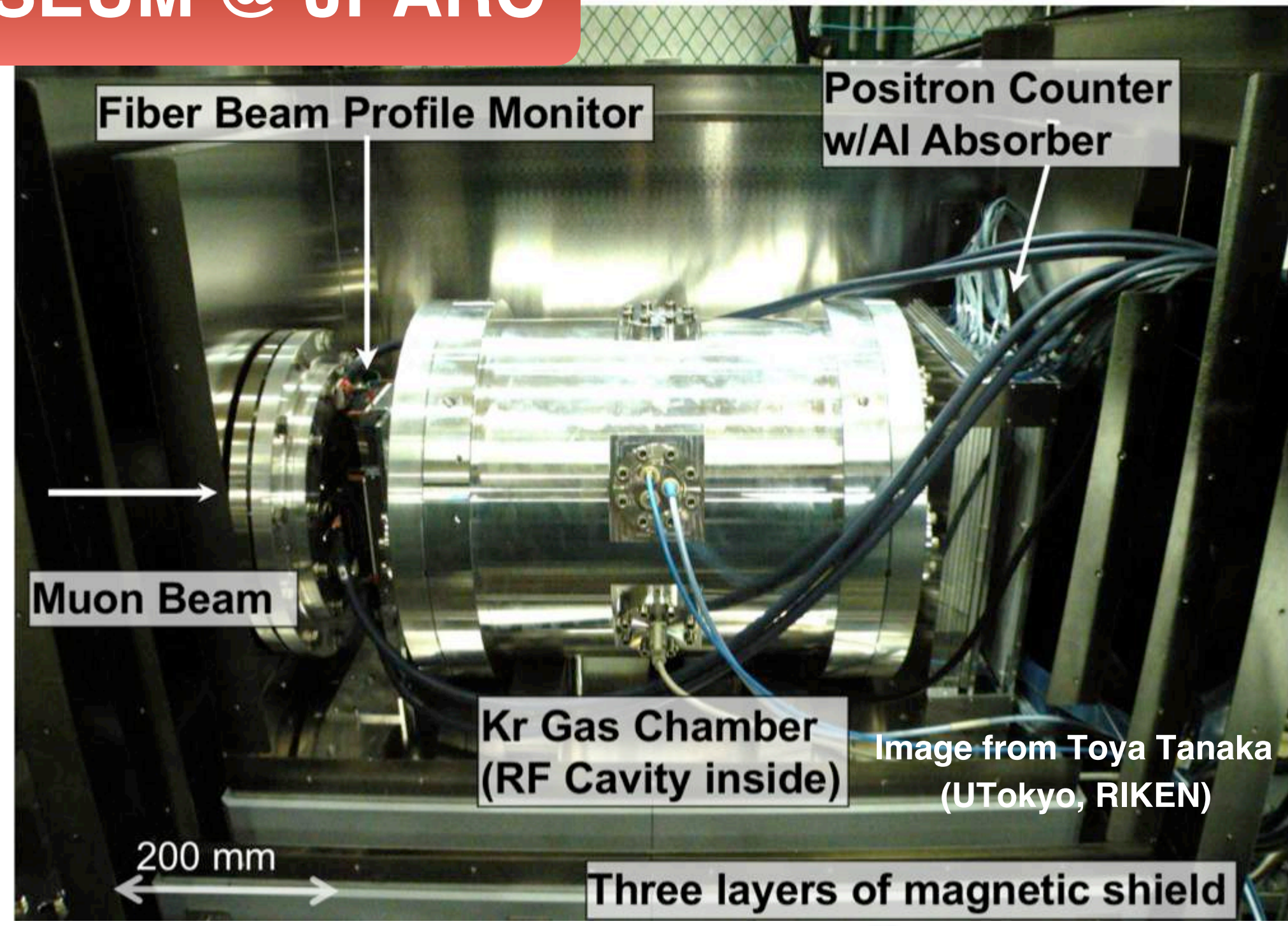
- Recall the expression for a_μ :
- m_μ/m_e value based on muonium hyperfine theory:

$$a_\mu = \frac{\omega_a}{\tilde{\omega}_p} \frac{\mu_p}{\mu_e} \frac{m_\mu}{m_e} \frac{g_e}{2}$$

$$\Delta\nu_{\text{Mu}}(\text{Th}) = \frac{16}{3} c R_\infty \alpha^2 \frac{m_e}{m_\mu} \left(1 + \frac{m_e}{m_\mu}\right)^{-3} + \text{higher order terms}$$

MuSEUM @ JPARC

- Equate theory to experiment, treat m_μ/m_e as a free parameter, obtain m_μ/m_e to 22 ppb
- Muonium hyperfine splitting at JPARC** aims to improve precision by a factor of 10 for μ_μ/μ_p to $\ll 120$ ppb





Ingredients to Extracting a_μ

- Recall the expression for a_μ :
- m_μ/m_e value based on muonium hyperfine theory:

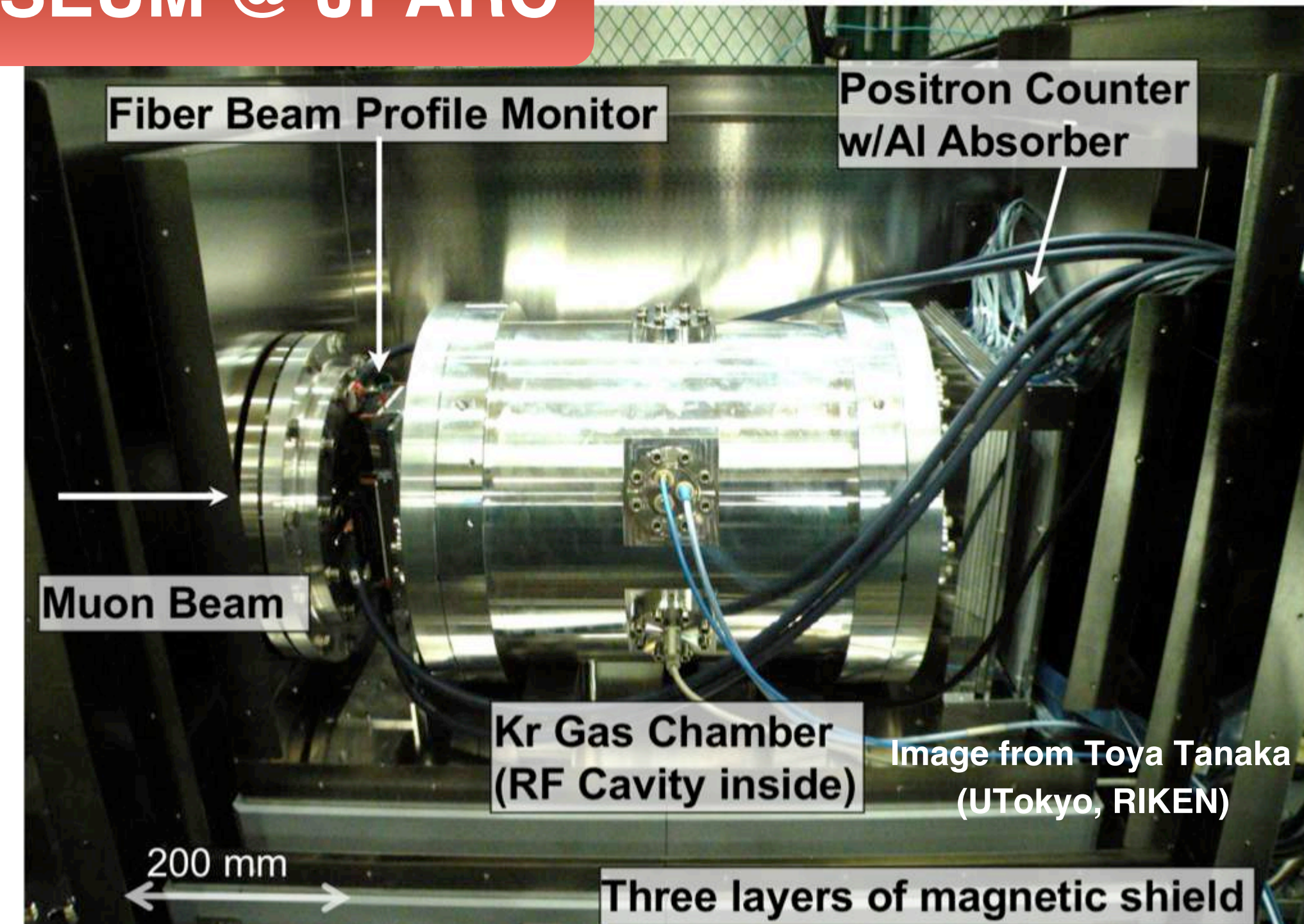
$$a_\mu = \frac{\omega_a}{\tilde{\omega}_p} \frac{\mu_p}{\mu_e} \frac{m_\mu}{m_e} \frac{g_e}{2}$$

$$\Delta\nu_{\text{Mu}}(\text{Th}) = \frac{16}{3} c R_\infty \alpha^2 \frac{m_e}{m_\mu} \left(1 + \frac{m_e}{m_\mu}\right)^{-3} + \text{higher order terms}$$

MuSEUM @ JPARC

- Equate theory to experiment, treat m_μ/m_e as a free parameter, obtain m_μ/m_e to 22 ppb
- Muonium hyperfine splitting at JPARC** aims to improve precision by a factor of 10 for μ_μ/μ_p to $\ll 120$ ppb
- Allows extraction of a_μ **independent of theory**:

$$a_\mu = \frac{\omega_a / \tilde{\omega}_p}{\mu_\mu / \mu_p - \omega_a / \tilde{\omega}_p}$$



EDM measurement at FNAL



- Precession plane tilts towards center of ring
- Causes an increase in muon precession frequency
- Oscillation is 90° out of phase with the a_μ oscillation
- 10 x improvement to current limit expected

